Investigating the molecular mechanisms underlying paternal effects of obesity on the sperm epigenome, the developing placenta, and the transmission of metabolic disorders

By
Anne-Sophie Pépin

Department of Pharmacology and Therapeutics
Faculty of Medicine and Health Sciences

McGill University, Montreal

March 2023

A thesis submitted to McGill University in partial fulfillment of the requirements of the degree of Doctor of Philosophy in Pharmacology and Therapeutics

Table of Contents

Thesis Format

This thesis is in manuscript format which conforms to the “Guidelines for Thesis Preparation” of the Faculty of Graduate Studies and Research at McGill University. The thesis consists of four chapters and the manuscripts are presented in the order of which they were published or submitted for publication. Chapter 1 provides a general introduction and overview of the relevant literature of this thesis. A subsection of Chapter 1 (section X.3.7) has been incorporated in a textbook chapter (Do chromatin dynamics in spermatogenesis have implications for fertility and epigenetic inheritance?, 3rd edition of Andrology Handbook, American Society of Andrology, 2023, in press). Chapter 2 is a manuscript published in the journal *Molecular Metabolism* [1]. This study assessed the inter- and transgenerational effects of paternal diet-induced obesity in combination with germline-specific overexpression of a histone modifying enzyme, their impact on offspring metabolic health and on the sperm epigenome. Chapter 3 of this thesis is a manuscript currently under revision (*eLife*, manuscript #06-09-2022-RA-eLife-83288), which has also been uploaded as a preprint (DOI: https://doi.org/10.1101/2022.08.30.503982). In this chapter we assessed the consequences of diet-induced obesity on the sperm epigenome, the placental transcriptome and cellular composition. Lastly, Chapter 4 includes a general discussion of the thesis.

Abstract

Worldwide obesity rates have drastically increased over the past 50 years, at rates that cannot be attributed to genetic factors alone. Other known factors contributing to obesity risks include diet, energy imbalance, the microbiome, and environmental stressors during the *in-utero* and preconception development. Most preconception health research has historically revolved around maternal factors, whereas the paternal influence on future generations health has received less attention. Importantly, both epidemiological studies and animal models have provided compelling evidence that a father's environment can impact his children's metabolic health. Whether paternally-induced phenotypes can have transgenerational effects remains subject of debate. The mechanisms underlying the paternal transmission of non-genetic information is still poorly understood, but likely involve epigenetic inheritance. In terms of paternal obesity (non-genetic) transmission, research investigating the mechanisms has only focused on DNA methylation and non-coding RNA as sperm-mediated factors, whereas the role of sperm histones and their modifications has been underexplored. Recent advances in sequencing technologies and biochemical methods have provided us with the unprecedented opportunity to study the unique chromatin profiles in sperm.

In this thesis, I provide a better understanding on the paternal contribution to future generations metabolic health. As such, in Chapter 2, we used a diet-induced obesity (DIO) model to assess whether obesity alters the sperm chromatin at the level of histone modifications. We combined this DIO model with a genetic model of epigenetic inheritance, where males overexpress the histone demethylase KDM1A specifically in the germline. We aimed to determine whether multiple epimutation-inducing factors could result in cumulative epigenetic changes in sperm associated with more severe phenotypes in the next generations, which could reflect the increasing rates of obesity worldwide. We identified sperm histone H3 lysine 4 tri-methylation (H3K4me3) as a metabolic sensor for paternal obesity and showed that DIO in combination with germline KDM1A overexpression resulted in cumulative aberrant sperm H3K4me3 profiles and more severe and transgenerational phenotypes in offspring. Obesity-sensitive epigenetic regions occurred at genes critical for embryonic development. Lastly, this chapter alluded to the intriguing possibility that paternally-induced aberrant sperm epigenetic profiles

could impact placenta development. Consequently, in Chapter 3 I aimed to assess whether paternal diet-induced obesity could impact placental functions. This study revealed that obesity-associated sperm epimutations were linked to aberrant gene expression and cellular composition in the placenta. These effects were comparable with that of hypoxic placentas – a condition previously linked to intrauterine growth restriction and increased adult-onset obesity risk.

Collectively, these studies support an important role for paternal preconception health and the sperm epigenome for proper placenta development and functions, as well as future generations metabolic health. The sperm chromatin appears to be a sensor of paternal metabolic and reproductive health, and a potential predictor for pregnancy outcomes and offspring phenotypes. More studies are warranted to better understand the molecular mechanisms that induce these obesity-associated epigenetic changes, to determine whether these effects are reversible, and to dissect the molecular events during embryogenesis and fetal development that are at the origin of paternally-induced maladaptive programming of metabolic and complex diseases.

Résumé

Les taux d'obésité dans le monde ont considérablement augmenté au cours des 50 dernières années, à des rythmes qui ne peuvent être attribués qu'à des facteurs génétiques. D'autres facteurs possibles comprennent l'alimentation, le déséquilibre énergétique, le microbiote et l'environnement durant le développement *in utero* et préconceptionnel. La recherche sur la santé préconceptionnelle a souvent porté sur les facteurs maternels, tandis que l'influence paternelle sur la santé des générations futures a reçu moins d'attention. Pourtant, plusieurs études épidémiologiques et modèles animaux ont fourni des preuves convaincantes que le père peut influencer la santé métabolique de ses enfants. Si les phénotypes induits par le père peuvent avoir des effets transgénérationnels reste un sujet de débat. Les mécanismes de transmission de l'information paternelle non génétique sont encore mal compris, mais impliquent probablement un héritage épigénétique. En termes de transmission paternelle de l'obésité, les recherches portant sur les mécanismes (non génétiques) se sont jusqu'à présent concentrées sur la méthylation de l'ADN et l'ARN non codante comme facteurs médiés par les spermatozoïdes, alors que le rôle des histones spermatiques et leurs modifications a été sous-exploré. Les progrès récents des technologies de séquençage et de méthodes biochimiques nous ont fourni l'opportunité sans précédent d'étudier les profils uniques de chromatine du sperme.

Dans cette thèse, j'ai cherché à mieux comprendre la contribution paternelle à la santé métabolique des générations futures. Ainsi, dans le chapitre 2, nous avons utilisé un modèle d'obésité induite par l'alimentation (OIA) pour évaluer si l'obésité altère les modifications des histones des spermatozoïdes. Nous avons combiné ce modèle OIA avec un modèle génétique d'hérédité épigénétique, où les mâles transgéniques surexpriment l'histone déméthylase KDM1A spécifiquement dans la lignée germinale. Nous avons cherché à déterminer si de multiples facteurs pouvaient entraîner des changements épigénétiques cumulatifs du sperme, et des phénotypes plus prononcés dans les prochaines générations. Nous avons identifié la triméthylation de l'histone H3 lysine 4 (H3K4me3) du sperme comme un capteur métabolique de l'obésité et avons montré que l'OIA chez les mâles transgéniques entraînait des profils H3K4me3 cumulatifs aberrants de sperme, et des phénotypes plus graves et transgénérationnels chez la

progéniture. Des régions épigénétiques sensibles à l'obésité se sont produites au niveau de gènes critiques pour le développement embryonnaire. Enfin, ce chapitre a éludé la possibilité que les profils épigénétiques aberrants de spermatozoïdes induits par le père puissent avoir un impact sur le développement du placenta. Par conséquent, dans le chapitre 3, j'ai cherché à évaluer si l'obésité induite par l'alimentation paternelle pouvait avoir un effet sur les fonctions placentaires. Cette étude a révélé que les épimutations du sperme étaient associées à une expression génique et à une composition cellulaire aberrantes du placenta. Ces effets étaient comparables à ceux de placentas hypoxiques - une condition liée à une restriction de croissance intra-utérine et à un risque accru d'obésité à l'âge adulte.

Collectivement, ces études soutiennent un rôle important pour la santé paternelle avant la conception et l'épigénome du sperme, pour le bon développement du placenta, ainsi que pour la santé métabolique des générations futures. La chromatine du sperme semble être un capteur de la santé métabolique et reproductive paternelle, et un prédicteur potentiel des phénotypes de la progéniture. D'autres études sont nécessaires pour mieux comprendre les mécanismes qui induisent ces changements épigénétiques associés à l'obésité, pour déterminer si ces effets sont réversibles, et pour disséquer les événements moléculaires au cours du développement fœtal qui sont à l'origine de la programmation inadaptée de maladies métaboliques.

Acknowledgments

I would first like to thank my supervisor, Dr. Sarah Kimmins, for taking a chance on me on this large-scale study, providing me with numerous amazing opportunities, technical, financial and mental support, resources, and for being such a good mentor. I am grateful for the experience I gained throughout these years and owe that largely to you!

None of this work would have been possible without the extensive time Christine Lafleur has put to help me with what we have called “high-throughput testing” of the animals, as well as valuable guidance and insights from Dr. Vanessa Dumeaux. It was a pleasure to work with you both and I learned a great deal and have grown both professionally and personally by interacting with you.

I would also like to acknowledge and thank the current and former Kimmins lab members for answering my many questions and providing their support; Dr. Deepak Tanwar, Eliza Zahirovic, Dr. Rose Gherawi, Dr. Ariane Lismer, Dr. Romain Lambrot, Dr. Marie-Charlotte Dumargne, Shannon Aldridge, Dr. Keith Siklenka and Janice Ou. Special shout out to Ariane for the running lessons and for being a great travel/conference buddy, as well to Deepak for introducing me to bioinformatics and being a great model for “good computer work practices”!

Many thanks to my thesis advisory committee members, Dr. Jacquetta Trasler, Dr. Jason Tanny and Dr. Thomas Duchaine, for their valuable and continuous feedback throughout the years and for your mentorship. Jason and Jacquetta: it was great to interact with you at these meetings, but also at conferences, departmental meetings and events and through PHAR 565. I am grateful for your continuous support, for genuinely caring about my success, and for your constant encouragement. I truly felt supported.

A special thanks to Dr. Moshe Szyf, Dr. David Cheischvili, and current and past members of the Szyf lab for contributing to my interest in research and my passion for Epigenetics.

Huge thanks to the past and present Win4Science committee and community members. Thank you for allowing me to grow through this initiative and providing me with a support system where I have felt like “home” since the beginning. It was a pleasure to see the initiative grow and to work alongside with all of you, Dr. Lisa Munter, Dr. Maureen McKeague, Ms. Bobbi Bidochka, and everyone that has been involved in this initiative.

I want to acknowledge past members of the Graduate Association of Pharmacology and Therapeutics Students (GAPTS). This association has been an integral part of my PhD as I have served on this council for 4 years. I am grateful for the opportunity to grow and learn via this involvement, but also for being surrounded with amazing colleagues and friends. I will keep great memories of my time on GAPTS and all the fun activities and events throughout the years.

I would like to mention the scientific networks I have had the chance to be part of and to participate and present at their scientific meetings: CEEHRC, SSR, CRRD, RQR, GRC, CFAS, ESHRE, GdR, CNPRM, DOHaD, the department of Pharmacology, and the Faculty of Medicine and Health Sciences. These scientific societies and research groups have provided me with networking opportunities, travel grants, presentation awards and valuable exposure to cutting-edge research.

A million thanks to the friendships I have developed with amazing people I had the chance to meet throughout my time at McGill. My *pharmily*: Dr. Ryan Martin, Dr. Thomas Nardelli, Dr. Jennifer Chen, Dr. Jace Jones-Tabah, Daniel Sapozhnikov, Dr. Morgan Foret, Dr. Kyla Bourque, Heather Fice, Sarah MacKinnon, Andrew Bayne, Courtney Smith, Marika Arsenault, Jessica Massé, Hayley Lippiatt, James Gauthier. You have made my time in the department more enjoyable than I could have expected. I will keep precious memories of our time together – from life hardships to good times. I thank you for helping me to grow, for your constant support and encouragement. I hope we will keep in touch and wish you all the best! Thank you Morgan for your friendship, your support and the comfort you have brought me.

People I had the chance to work with on various projects or extracurricular activities that have become mentors to me: Dr. Terry Hebert, Dr. Aimee Ryan, Dr. Alba Guarné, Dr. Lisa Munter, Dr. Maureen McKeague. Thank you for your patience, your mentorship, your positivity (and devil's advocate role at times!), and for pushing me always to improve. I have learned a great deal by interacting with you all. Special thanks to Maureen for being such a caring, thoughtful and inspiring mentor. Thank you for always having my back, you're amazing!

I had the pleasure to build and launch a new student association for the School of Biomedical Sciences called the Biomedical Interdisciplinary Student Association (BISA).

I want to thank the BISA founding members, Caitlin Anderson, Hossein Poorhemati and Alexandra Mircescu, for being the best team I could have wished for, with whom I have had the pleasure to work in. We went through some difficult times and faced many challenges, but I am really proud of what we have built and accomplished together throughout these years during the pandemic. I hope that we get to work together again, this project with you really showed me how a successful team can operate. Thank you!

A special mention to the Sloboda team including Dr. Deborah Sloboda, Patrycja Jazwiec, Christian Bellissimo, Dr. Kate Kennedy, and Violet Patterson. It was great to collaborate with you and interact with you in different settings, and see your work evolve. Thank you for your insights, feedback, kindness… and importantly, your samples!!!

A special mention to the pillars of our department (past and present administrative staff members): Tina Tremblay, Chantal Grignon, Anna Cuccovia, Nadee Buddhiwickrama, Cathy Shang Kuan, Bobbi Bidochka, and Lara Vani Palladini. Thank you for your hard work and for always being there for our students. You are amazing!

I also wanted to thank the overall Department of Pharmacology. I have had such formative years since 2013 in this department and it is difficult to leave this place behind! I could not have hoped for a more vibrant, dynamic, welcoming, and inspiring work environment. I am grateful for the culture of always wanting to improve our department, from social activities, societal issues, to facilities, student space, and education. This environment is filled with ambitious scientists, supportive mentors and inspiring individuals. I am proud to have been part of this department, and I hope to join back in the near future. Thank you!

Lastly, I wanted to thank my family and childhood friends. Thanks to my parents and sister for believing in me, supporting me over the years, for being patient for my constant worries and frequent absences. Thanks to Audrey-Ann, Chloe, Layina, Magalie, Noemie, Laurence, Maude, Elodie, Boris; my faithful friends, I am so grateful to have maintained these relationships over the years and I feel so lucky that we can always pick up where we left off no matter how much time has passed. Thanks to you Audrey for being there since Day 1 and for being the most understanding human being I have known. Love you all.

Acknowledgments (Chapter 2)

We thank the team at the McGill University Small Animal Research Unit, Genome Quebec Innovation Centre for performing the sequencing, and Dr. Deborah M. Sloboda (McMaster University) for advice on metabolic phenotyping methods. This research was funded by the Canadian Institute of Health Research (CIHR) grants to SK (358654 and 350129).

Acknowledgments (Chapter 3)

We thank the team from Genome Quebec for the sequencing of the ChIP-seq experiment, and the team from the Applied Genomics Innovation Core of the McGill Genome Centre for the sequencing of the RNA-seq experiment. This study was funded by the Canadian Institutes of Health Research grants to Dr. Sarah Kimmins (DOHaD Team grant 358654 and Operating 350129) and grants to Dr. Deborah M. Sloboda (CIHR Team grant 146333; Operating 175293).

5.1 Sources of Funding

These studies were funded by the Canadian Institutes for Health Research (CIHR #358654, #350129, #146333, and #175293).

The doctoral candidate is a recipient of scholarships from the McGill University Centre for Research in Reproduction and Development, the Desjardins Foundation, and the J. P. Collip scholarship for Medical Research from the McGill University Faculty of Medicine and Health Sciences. She has also received travel stipend awards from the Centre for Research in Reproduction and Development, the Canadian, Epigenetics, Environment and Health Research Consortium, the *Réseau Québécois en Reproduction*, and the McGill University Faculty of Medicine and Health Sciences.

Contribution of Authors

6.1 Chapter 1 (Section X.3.7): Epigenetic landscape establishment and programming during spermatogenesis

(In press: Do chromatin dynamics in spermatogenesis have implications for fertility and epigenetic inheritance?, 3rd edition of Andrology Handbook, American Society of Andrology, 2023)

A subset of section X.3.7 from Chapter 1 has been incorporated in a textbook chapter. The doctoral candidate wrote the chapter and Sarah Kimmins edited the portion that has been submitted for publication.

6.2 Chapter 2: Sperm histone H3 lysine 4 tri-methylation serves as a metabolic sensor of paternal obesity and is associated with the inheritance of metabolic dysfunction

(Published: *Molecular Metabolism*, May 2022)

The doctoral candidate developed the model, conducted the animal studies, laboratory experiments, bioinformatics data analysis, and generated all figures and tables included in the manuscript. Christine Lafleur and Romain Lambrot assisted with the animal studies, Vanessa Dumeaux provided guidance and assistance for bioinformatics data analysis. Sarah Kimmins conceived, designed, funded and guided the study. The manuscript was written by the doctoral candidate and Sarah Kimmins and was edited by Vanessa Dumeaux.

6.3 Chapter 3: Paternal obesity alters the sperm epigenome and is associated with changes in the placental transcriptome and cellular composition

(Under revision: *eLife*, Manuscript #06-09-2022-ISRA-eLife-83288, preprint available on bioRxiv: https://www.biorxiv.org/content/10.1101/2022.08.30.503982v1)

Tissue samples were collected in the laboratory of Deborah M. Sloboda at McMaster University by Patrycja A. Jazwiec. The doctoral candidate conducted the laboratory experiments, developed methodology, curated data, performed the bioinformatics data analysis, and generated all figures included in the manuscript. Vanessa Dumeaux provided guidance for bioinformatics and statistical analyses. Sarah Kimmins provided supervision and conceptualization of the project. The manuscript was written by the doctoral candidate and Sarah Kimmins, and was reviewed and edited by Vanessa

Dumeaux, Deborah M. Sloboda and Patrycja A. Jazwiec. The study was funded by Sarah Kimmins and Deborah M. Sloboda.

List of Abbreviations

17ß-HSD: 17-beta hydroxysteroid dehydrogenase

1C: One-carbon

5hmC: 5-hydroxymethylcytosine

5mC: 5-methylcytosine

8-oxo-G: 8-oxoguanine

AgRP: Agouti-related protein

ANOVA: Analysis of variance

ARC: Arcuate nucleus

ART: Assisted reproductive technologies

AUC: Area under the curve

BMI: Body mass index

BMP: Bone morphogenetic protein

Bp: Base-pair

BSA: Bovine serum albumin

BTB: Blood-testis-barrier

CCK: Cholecystokinin

CDP: Cytidine diphosphate

ChIP-seq: Chromatin immunoprecipitation followed by sequencing

CNS: Central nervous system

CRH: Corticotropin-releasing hormone

CVD: cardiovascular disease

CON: Control

CUT&Tag: Cleavage Under Targets and Tagmentation

CUT&RUN: Cleavage Under Targets and Release Using Nuclease

DALY: Disability-adjusted life years

DDT: Dichlorodiphenyltrichloroethane

DEG: Differentially expressed gene
DEXA: Dual x-ray absorptiometry
DIO: Diet-induced obesity
DMR: Differentially methylated region
DNA: Deoxyribonucleic acid
DNAme: DNA methylation
DNMT: DNA methyltransferase
DOHaD: Developmental Origins of Health and Disease
DTT: Dithiothreitol

E: Embryonic day
EDC: Endocrine disrupting chemical
EPC: Ectoplacental cone
EXE: Extraembryonic ectoderm

FA: Fatty acid
FD: Folate deficient
FFA: Free fatty acid
FSH: Follicle-stimulating hormone

GBP: Gastric bypass
GDNF: Glial cell derived neurotrophic factor
GEO: Gene Expression Omnibus
GI: Glycemic index
GLP-1: Glucagon-like peptide-1
GlyT: Glycogen trophoblast
GnRH: Gonadotropin-releasing hormone
GO: Gene ontology
GTT: Glucose tolerance test
GWAS: Genome-wide association studies
gWAT: Gonadal white adipose tissue

H3K4me3: Histone H3 lysine 4 tri-methylation
H3K27me3: Histone H3 lysine 27 trimethylation
H4R3me2: Histone H4 arginine 3 dimethylation
HDL: High-density lipoprotein
HFCS: high-fructose corn syrup
HFD: High-fat diet
HIF1-α: Hypoxia-induced factor 1 alpha
HOMA-IR: Homeostatic model assessment of insulin resistance
HPA: Hypothalamic-pituitary-adrenal (axis)

IHTG: Intrahepatic triglyceride
IHW: Independent hypothesis weighting
IL-1 β: Interleukin-1 beta
IL-6: Interleukin-6
ITT: Insulin tolerance test
IUGR: Intrauterine growth restriction
IVF: In vitro fertilization

KDM1A: Lysine-specific histone demethylase 1A

LDL: Low-density lipoprotein
LH: Luteinizing hormone
lncRNA: Long non-coding RNA
LPD: Low-protein diet
LSD1: Lysine-specific histone demethylase 1A

MBP: Methyl-CpG-binding protein
MC1R: Melanocortin 1 receptor
MC4R: Melanocortin 4 receptor
MeCP2: Methyl-CpG-binding protein 2

microCT: Micro computed tomography
miRNA: MicroRNA
mRNA: Messenger RNA
mWAT: Mesenteric white adipose tissue

NAFLD: Non-alcoholic fatty liver disease
NASH: Non-alcoholic steatohepatitis
NCBI: National Centre for Biotechnology Information
ncRNA: non-coding RNA
NEM: N-ethylmaleimide
NIH: National Institutes of Health
NMR: Nuclear magnetic resonance
NPY: Neuropeptide Y

OGG1: Oxoguanine glycosylase 1
OS: Oxidative stress
OXM: Oxyntomodulin

PBAT: Post-bisulfite adaptor tagging
PBS: Phosphate-buffered saline
PC: Phosphatidylcholine
PCA: Principal component analysis
PE: Phosphatidylethanolamine
PEMT: Phosphatidylethanolamine N-methyltransferase
PERMANOVA: Permutational multivariate analysis of variance
PGC: Primordial germ cell
piRNA: Piwi-interacting RNA
PND: Postnatal day
POHaD: Paternal Origins of Health and Disease
POMC: Pro-opiomelanocortin
PPAR: Peroxisome proliferator activated receptors

PTM: Post-translational modification
PVN: Paraventricular nucleus
PYY: Peptide YY

RNA: Ribonucleic acid
RNA-seq: RNA sequencing
ROS: Reactive oxygen species

SAH: S-adenosylhomocysteine
SAM: S-adenosylmethionine
SAT: Subcutaneous adipose tissue
scBS: Single-cell bisulfite sequencing
SEMA3A-G: Sematophorins class 3 A-G
SGP: Slow growth period
sncRNA: Small non-coding RNA
SNP: Single nucleotide polymorphism
snRNA: Small nuclear RNA
SpT: Spongiotrophoblast
SRA: Sequencing Read Archive
SSC: Spermatogonial stem cell
SynT: Syncytiotrophoblast

T2D: Type 2 diabetes
T2T: Telomere-to-telomere
TE: Trophectoderm
TET: Ten-eleven translocation
TF: Transcription factor
TG: Transgenic
TGC: Trophoblast giant cell
TNF-α: Tumour necrosis factor alpha
TP: Transition protein

tRF: transfer RNA-derived fragment
TRH: Thyrotropin-releasing hormone
TSC: Trophoblast stem cell
tsRNA: Transfer RNA-derived small RNA
TSS: Transcription start site

UCP-1: Uncoupling protein-1

VAT: Visceral adipose tissue
VLDL: Very low-density lipoprotein

WAT: White adipose tissue
WES: Whole-exome sequencing
WHO: World Health Organization
WT: Wildtype

List of Figures

Figures from XI Chapter 1

Figures from XII Chapter 2

Supplemental figures from XII Chapter 2

Figures from XIV Chapter 3

Supplemental figures from XIV Chapter 3

Figures from XV Chapter 4

List of Tables

Tables from XII Chapter 2

10.1 Obesity and metabolic syndrome etiology

Obesity rates have drastically increased within the past four decades, with 39% of the world adult population being overweight and 13% being obese as of 2016 [2]. Alarmingly, children and adolescents have also experienced a global rise in obesity prevalence with a seven-fold increase between 1975 and 2016 [3]. These rates are projected to maintain an upward trend in all age groups with an estimated prevalence of 45% (39-52%) of overweight individuals and 16% (13-20%) of obese individuals, as of 2050 [4]. This health condition has become a problem not only for developed countries, but for low- and middle-income countries as well, with global obesity prevalence now exceeding rates of underweight individuals [2].

Obesity is defined based on the body mass index (BMI; kg/m^2), with a BMI<18.5 considered underweight, a BMI between 18.5 and 25 considered normal, a BMI>25 considered overweight, and a BMI>30 considered obese. An elevated BMI globally accounts for a large fraction of a plethora of noncommunicable and chronic diseases such as type 2 diabetes (T2D), cardiovascular and cerebrovascular diseases, hypertension, and certain cancer types [5–7]. Excess weight is also a predictor for conditions that negatively impacts an individual's life quality, such as osteoarthritis and sleep apnea [8,9]. Furthermore, obese individuals are at heightened risk for severe forms of communicable diseases, as exemplified during the COVID-19 pandemic [10–12]. Consequently, obesity and its comorbidities are among the leading causes of global premature deaths and disability-adjusted life years (DALYs) [5,13,14]. This obesity epidemic and its associated comorbidities therefore represent a huge burden for the healthcare system, even more so in the context of an aging population, especially since obesity rates are not expected to drop in the coming years [15]. A deeper understanding on the molecular mechanisms underlying the causes, progression, and impacts of obesity and how to prevent this condition, could help alleviate the consequences it has worldwide and reduce its use on health care resources.

Body weight is regulated via complex and interconnected neuronal, hormonal, and metabolic pathways, balancing energy (Figure 1, from [16]). Hedonic (reward/craving) and homeostatic (hunger or satiety) signals from the periphery are integrated within the central nervous system (CNS) to promote food-seeking behaviours [17–19]. Highly palatable foods

promote the release of dopamine via the mesolimbic dopamine pathway, driving hedonic feeding behaviours [20–23]. In contrast, homeostatic pathways regulate feeding behaviour to maintain physiological needs [17,24,25]. One such signalling pathway regulating energy homeostasis involves the hypothalamic melanocortin circuit, which is comprised of hormone- and peptide-responsive neurons located in the arcuate nucleus (ARC) that project to melanocortin 4 receptor (MC4R)-expressing neurons in the paraventricular nucleus (PVN) [26]. These ARC hypothalamic neurons either express orexigenic neuropeptides (neuropeptide Y or NPY; agouti-related protein, AgRP) or the anorexigenic (appetite-suppressing) neuropeptide precursor pro-opiomelanocortin (POMC) [27]. PVN neurons integrate these orexigenic and anorexigenic signals to modulate physiological and metabolic responses via the release of thyrotropin-releasing hormone and corticotropin-releasing hormone (TRH and CRH, respectively) [26]. Peripheral hormones associated with a fed state act on POMC neuron receptors to promote POMC release, and on NPY neuron receptors to suppress NPY/AgRP signalling [28]. These anorexigenic-inducing hormones include leptin (produced by adipocytes proportional with fat mass), insulin (secreted by pancreatic beta islets proportional to blood glucose levels), and estradiol (secreted by the gonads and by aromatase-expressing peripheral organs such as adipose tissue, brain, bone, placental syncytiotrophoblast, and skin fibroblasts) [27–31]. Other anorexigenic hormones that are released post-prandially from cells located in the gastrointestinal system include peptide YY (PYY_{3-36}), cholecystokinin (CCK), oxyntomodulin (OXM), and glucagon-like peptide-1 (GLP-1) [28,32]. In contrast, the peptide hormone ghrelin is produced by the stomach in a fasting state and acts to stimulate the production of NPY/AgRP and promote food intake [33]. When exposed to obesogens, these key hormones and neurotransmitters are all subject to modifications that can result in aberrant energy balance, thereby increasing risk for elevated body weight and associated comorbidities.

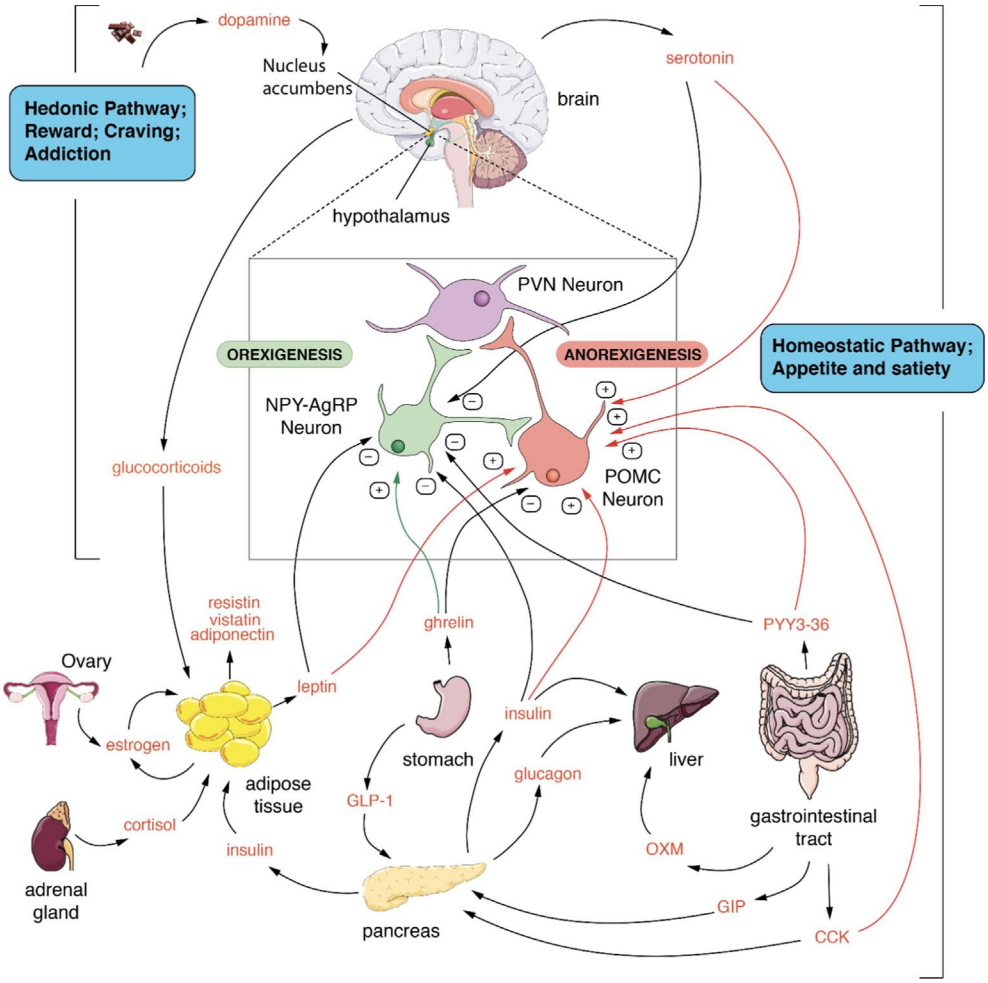

Figure 1: Hormonal and neuronal control of body weight.

Figure obtained from [16], Copyright (2022), with permission from Elsevier.

Obesity is a complex health condition with multifactorial origins, for which numerous risk factors likely have interacting or additive effects. This condition results from genetic factors, an obesogenic environment, (epi)genetic-environmental interactions, *in utero* programming, and parental preconception health. These factors will be further discussed in the next subsections.

10.1.1 Genetic factors

Obesity can be classified into two distinct genetic categories: monogenic and polygenic obesity. Monogenic obesity manifests early, is typically severe, rare, and caused by a single mutation, and follows Mendelian patterns as mode of heredity. In contrast,

polygenic obesity (or common obesity) results from many interacting polymorphisms of small but additive effects. Although monogenic and polygenic obesity show distinct phenotypic, genetic and etiology characteristics, they share common underlying biology, involving genes of similar pathways, mainly impacting the regulation of food intake via satiety, hunger and hedonic signals within the CNS. [34,35]

The first genes linked to body weight were identified in the *ob* and *db* mouse lines. Mutations in the *ob* and *db* genes (later identified as encoding leptin, and leptin receptor, respectively) result in hyperphagia and severe obesity and were found to be due to leptin deficiency [36–39]. In the Agouti mouse model, obesity resulted from ectopic and constitutive expression of the agouti peptide, an antagonist for melanocortin 1/4 receptors (*Mc1r* and *Mc4r*) which are key mediators for the anorectic effects of leptin [40–43]. These discoveries demonstrated the first evidence for hormonal and neuronal basis of body weight and feeding behaviour regulation, and prompted the search for genetic drivers underlying human interindividual variations in body weight, adiposity and metabolic status, beginning in the early 1990s.

Early attempts to identify genes causing monogenic obesity were made by examining individuals with severe obesity along with their family members with the use of Sanger sequencing, restricted to a set of candidate genes. These investigations led to the discovery of severe obesity-inducing mutations in leptin and its receptor associated with leptin deficiency, and in key components of the melanocortin system such as *PCSK1*, *MC4R* and *POMC* [44–50]. Technical advances and increased accessibility in unbiased genetic screening approaches such as whole-exome sequencing (WES) have identified novel causative mutations such as genes encoding class 3 sematophorins (SEMA3A-G) [51]. Sematophorin signalling drives the development of hypothalamic neurons of the energy homeostasis-regulating melanocortin circuit [51].

In the search for genetic variants driving polygenic obesity, candidate gene studies were initially performed. For over a decade, variants from previously identified genes were assessed to test their association with obesity traits, yielding only six variants identified with reproducible outcomes [52–57]. Next, genome-wide linkage approaches were introduced and revealed over 300 loci with potential links with obesity traits. However, the replicability of these identified loci has been limited and no causal gene has been

successfully mapped to these candidate loci [58]. These approaches were constrained by low genome coverage, small sample size, and limited replicability. Advances in sequencing technologies and the introduction of genome-wide association studies (GWAS) led to a significant progression in the discovery of genes associated with obesity traits. GWAS have now identified over 1,000 genes associated with various obesity traits, such as BMI, body fat mass, body fat percentage, fat-free mass, adipose tissue imaging, and leptin levels [59–65]. Some examples are shown in Figure 2 [66]. Important challenges to note in the gene discovery for polygenic obesity are the pleiotropic effects of transcription factors involved which can impact expression of several target genes; the epistasis nature of genes involved where one gene can affect another gene's expression or action; and gene-environment interactions. Given the multifactorial nature of obesity etiology, several GWAS studies have included demographic and environmental factors in their analyses [67–70]. These studies have identified 12 loci showing gene-by-environment interactions, whereby certain non-genetic factors can have attenuating or exacerbating effects on genetic variant-associated obesity risk. These studies highlighted the complexity of obesity traits etiology, with numerous interacting genetic and non-genetic factors involved.

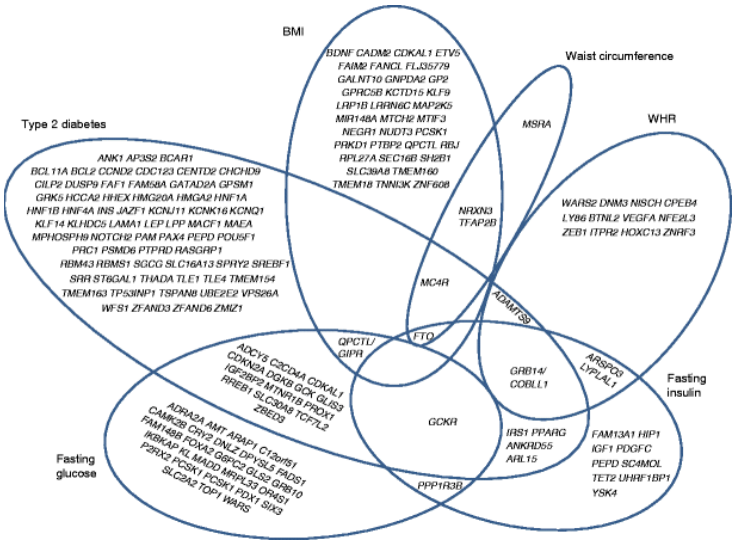

Figure 2: Venn diagram showing the overlap of identified loci associated with various metabolic traits related to obesity and metabolic syndrome.

Figure obtained from [66], Copyright (2014) with permission from Springer Nature.

Although the advances in high-throughput sequencing technologies, computational tools and regulatory regions mapping have allowed for a better understanding of the regulatory pathways involved in obesity and identified numerous associated loci, the main challenge remaining is the translation of the genomic regions into meaningful functional biology via follow-up analyses. For example, most of the GWAS-identified variants loci map to regulatory elements at non-coding or intergenic regions in the genome – potentially at enhancer regions or alternative promotes – posing a particular challenge in determining the underlying biological mechanism explaining their role in obesity risk. Furthermore, most GWAS have been biased with sample population overrepresented with European ancestry. However, obesity-related loci have been identified in cohorts of African, Asian, Hispanic and other ancestry background, with associations consistent across ancestries [71–74]. Using the newest version of the human reference genome recently presented by the Telomere-to-Telomere (T2T) Consortium, now covering gapless assemblies of all autosomal chromosomes, future studies will likely be able to identify novel obesity-associated genetic variants [75].

Although there clearly is a strong genetic component underlying risks for obesity and associated comorbidities, genetic studies describe heritability estimates ranging from 10% and 30% to 70% [76–79]. Consequently, the rapid and drastic rise in global obesity rates observed within the past four decades cannot be attributed to genetic factors alone. Nevertheless, the remaining unexplained heritability can be attributed to non-genetic factors which can also strongly contribute to interindividual variability in BMI and obesity risks. These environmental factors are discussed in the next subsections.

10.1.2 Obesogens and the obesogenic environment

Obesity can also result from an imbalance in energy expenditure and energy consumption. Such imbalance has been exemplified by the recent pandemic-related drastic changes in behaviour, such as the increased implementation of remote working during the past three years due to ongoing lockdowns, sedentary lifestyles, and reduction of exercise with sporadic sports centres closure. These behavioural changes have resulted in sharp increase in self-reported weight gain and increased obesity prevalence in USA among all age group [80,81]. Before the COVID-19 pandemic, the rise in obesity

prevalence can be partly attributed to behavioural changes observed worldwide throughout the past century due to industrialization, urbanization and Westernization phenomena [4,13,82–88]. These phenomena are characteristic of the modern world, particularly in Western countries, associated with behavioural changes leading to an imbalance in energy consumption and expenditure.

At the beginning of the 20th century, approximately 10 percent of the global population lived in cities [87]. Since then, urbanization has spread in both developed and developing countries, with now over 50% of the world population living in cities, and these numbers are projected to increase to two thirds by 2050 [87,89]. Urbanization comes with various changes in dietary habits, and a shift towards a more sedentary lifestyle [87,89,90]. For example, this phenomenon leads to greater food supply and access, and increased fast-food availability, thereby altering food consumption patterns with higher caloric intake [4]. Urbanization is also associated with reduced physical activity, given the increase in computer-based activities both at work as well as during leisure time, and with the use of cars as means of transport being preferred over means of transport associated with more energy spending, such as public transport, walking, or biking. Importantly, physical activity and exercise are beneficial as they can have preventative effects on obesity due to increased energy expenditure. Furthermore, metabolites produced upon exercise have been shown to suppress feeding [91]. The recent finding that BMI values have increased at the same rate in rural and urban area in low- and middle-income countries further highlights the contribution of other factors driving the obesity epidemic [88].

Dietary factors strongly influence an individual's BMI, and food consumption trends have also greatly evolved within the past 50 years. Improved agricultural practice and productivity have led to increased food availability along with increased food diversity and reduced seasonal dependence [87]. The use of sweeteners has drastically increased during the 1900s and since then their composition has shifted from glucose-based to high-fructose corn syrup (HFCS) and sucrose [92–95]. Additionally, the westernization of lifestyles favours a reduction in home cooking, increased consumption of convenience food and snacks [82,96–98]. Persuasive marketing of the food industry also strongly influences dietary habits by promoting large meal portions, snaking, and normalizing the consumption of soft drinks, candies and fast food on a weekly or even daily basis [98,99]. Other overall

changes observed in dietary habits include an increased consumption in sugar and fat, energy-dense, low-fibre and animal-source food [4]. Consequently, these shifts in dietary trends have resulted in an overall increase in the daily caloric intake, concomitant with the global rise in obesity prevalence [96].

Of note, although caloric intake influences energy imbalance, the sources of calories such as macronutrient distribution and other food properties play an important role in obesity etiology, weight loss and body weight maintenance [100–102]. Food properties that must be taken into consideration in this paradigm include energy densities, glycemic index, satiety value, macronutrient composition, taste, metabolic response elicited upon consumption, the types of fats or carbohydrates consumed, the amount of fibres, and more [100]. The glycemic index (GI) is a numerical value that reflects the blood glucose levels elicited following consumption of a specific food, relative to pure glucose as reference [103]. A low GI food (≤ 55) will slowly and steadily release glucose, whereas a high GI food (≥ 70) will result in rapid and high postprandial blood glucose, which is associated with glucose homeostasis impairments and metabolic disturbances [102,104]. The satiety value reflects the degree a food reduces hunger or appetite [105]. It is thought that foods with high-energy density but low satiety value, such as diets high in fat, are prone to facilitate overconsumption [106]. In contrast, high-protein diets provide high satiety levels and facilitate energy consumption control [107]. Certain types of sugars are associated with impaired glucose metabolism such as fructose [108–110]. Fructose bypasses the main rate-limiting and enzymatically-regulated step of glycolysis, resulting in uncontrolled production of glucose and other molecules, and excess energy flux [111]. The amount of fibres in food is associated with lower GI, greater satiety value (due to delayed gastric emptying and increased production of satiating gut hormones), as well as lower energy density [112]. Due to its properties, dietary fibres have been shown to provide a wide range of health benefits, with protective effects for certain complex diseases such as obesity, coronary heart disease, stroke, hypertension, diabetes, and gastrointestinal diseases [112].

Aside from dietary factors, many environmental chemicals have been shown to have obesogenic effects. These compounds are classified as obesogens, with biological properties promoting obesity by increasing white adipose tissue mass *in vivo*. To date, about 50 compounds have been identified with obesogenic properties, and most of these

chemicals are commonly found in our environment such as in dust, water, processed food from additives, food packaging, cosmetics, furniture, electronics, pesticides, plasticizers, sweeteners, medications and household products [113,114]. Obesogens can elicit their obesogenic effects and act directly on adipocytes, affecting stem cell commitment or differentiation into adipocytes, the size and number of adipocytes, and adipocyte triglyceride storage. Some of these compounds are endocrine disrupting chemicals (EDC), meaning that they can disrupt hormone levels or actions and modulate endocrine pathways [115]. Obesogens can also act on critical organs such as the brain, liver, pancreas, gastrointestinal system, muscles and adipose tissue, to modulate physiological pathways involved in appetite control, metabolism and energy homeostasis [113,116–119]. Other obesogens can elicit their obesogenic actions via other mechanisms such as by acting on specific target receptors, or via intermediate events such as inflammatory processes and oxidative stress. These compounds do not necessarily induce obesity alone, but rather interact with and exacerbate the effects of various factors on weight gain, such as dietary composition, energy balance and metabolism.

Biological agents such as the microbiome can impact the bioavailability of nutritional metabolites and small molecule intermediates involved in metabolic processes. The host microbiome is comprised of bacteria, viruses and fungi residing in symbiosis within the gut, more specifically in the small and large intestine, and in the colon. These resident bacteria play critical roles in homeostasis, maintaining the gut, brain, metabolic and immune physiological health [16,120]. With advances in next-generation and high-throughput sequencing, the microbiome has recently received increased attention in the research community. The microbiome content is highly variable throughout one's life, and studies have described associations with microbiota signatures and various health conditions, including obesity [120,121]. Some diets high in fat or in fructose have been shown to alter gut barrier integrity and absorption capacity, promoting increased capacity for energy harvest and thereby contributing to excess energy stores [122–125]. Likely contributing to the low-grade metainflammation of metabolic disease, it was reported that pro-inflammatory bacteria are enriched in T2D microbiomes at the expense of anti-inflammatory bacteria [122,125–133]. Although the causal role of the microbiome in obesity onset remains a subject of debate, it is clear that dysbiosis is part of the obesity and

metabolic syndrome phenotype, and influences the progression and perpetuation of these diseases [134].

Taken together, numerous factors including genetics as well as lifestyle, diet and environmental exposures throughout a person's lifetime can interact and influence their risk to develop obesity and associated co-morbidities. These factors can be of particular importance during critical periods of development, which are discussed in the next subsection.

10.1.3 The *in utero* and preconception environment

10.1.3.1 Developmental Origins of Health and Disease (DOHaD)

Although the global rise in obesity rates has been largely causally linked to behavioural changes related to post-natal diet and physical activity during a life course, the focus of research on obesity etiology has now shifted towards considering early life factors [135,136]. This shift was prompted by a report published almost 40 years ago, linking increased heart disease mortality rates in the years of 1968-78, and infant mortality in 1921-25 [137]. It was therefore speculated that poor living conditions such as nutrition in early life increases risk for chronic diseases in adulthood [137]. Following these speculations, documented feeding practices and birth weights from babies in the early 1900s revealed an association between small birth weight and increased risk for complex diseases including T2D, hypertension and coronary heart disease [138–140]. Since then, similar observations have been drawn from cohorts in Africa, northern Europe, North and South America, and Asia [141–145]. Additionally, a number of epidemiological studies with historical food supply data and birth weights found that individuals born from *in utero* exposure to famine, as well as their children, were at heightened risk to develop chronic diseases, mental health and neurological disorders in adulthood [141,146,155–163,147–154]. A U-shaped relationship has also been described between birth weight and BMI, where weights of < 2,500 g and > 3,500 g at birth were associated with increased risk to obesity in adulthood [164,165]. Furthermore, the growth trajectory after birth seems to be of particular importance for metabolic programming. Indeed, maternal stress or poor nutrition during pregnancy resulting with low birth weight and rapid postnatal weight gain – also called catch-up growth – has been linked to metabolic dysfunction in adulthood [166,167].

Collectively, these studies suggested that the *in-utero* environment represents a critical window of development that can program maladaptive responses to affluent food availability, with specific timing of exposures resulting in varying degrees of phenotypes, including obesity, hypertension, dyslipidemia, insulin resistance, and impaired glucose metabolism [168–172]. This so-called “Barker’s Hypothesis” paved the way for research avenues on the concept of the Developmental Origins of Health and Disease (DOHaD) [136,173,174]. Importantly, the developing gonads are also susceptible to *in utero* insults, consequently with far-reaching implications for the health of the next generation(s) – potentially leading to inter- or transgenerational effects.

The mechanistic basis of DOHaD in humans has been difficult to study with large, complex and longitudinal cohorts. The underlying mechanism is thought to involve adverse influences of various environmental and extrinsic factors during development that could result in permanent physiological and metabolic changes in the developing fetus, which could in turn lead to increased predisposition to adult-onset non-communicable diseases. During development, organisms adapt to external signals such as nutrition and stress, by adjusting their phenotype and metabolic trajectory to match their environment. These effects can be maladaptive and result in the thrifty phenotype (where low birth weight is associated with increased risk for complex diseases in adulthood), particularly if there are discrepancies between the intrauterine and postnatal environments [175,176].

Animal models of undernutrition and overnutrition have been helpful in providing insights on the underlying mechanisms of metabolic programming. Consistent with epidemiological data, maternal caloric restriction, diet-induced obesity models, and low-protein diets in rodents have been linked to low birth weight, lower nephron numbers associated with elevated blood pressure, as well as reduced pancreatic beta-islets proliferation, size and vascularization [177–183]. Consequently, catch-up growth poses excess metabolic demand on limited beta-cell mass thereby impairing metabolic functions. Supporting the detrimental effects of mismatched perinatal versus postnatal environments, postnatal caloric restriction of rodents born from intrauterine growth restriction protects from obesity [184,185]. Additionally, the effects of obesogenic diets are more pronounced in animals born from undernourished mothers [186]. In terms of stress models, maternal stress has been associated with offspring elevated blood pressure,

glucose intolerance, and altered stress response in adulthood [187–189]. Because the hypothalamic-pituitary-adrenal (HPA) axis has strong impact on metabolism and the vasculature, the stress response is thought to be involved in maternal stress-induced hypertension and altered metabolism [190,191]. Indeed, intrauterine stress results in reduced glucocorticoid receptor density in the hypothalamus, leading to long-term upregulation of the HPA axis and thereby impair blood pressure regulation and glucose metabolism [192,193]. Both intrauterine stress and nutritional programming inducing fetal maladaptation and adult-onset phenotypes are thought to also involve epigenetic mechanisms, with aberrant epigenetic patterns in various tissues upon *in utero* insults [194–198].

The term epigenetics – with the Greek prefix *epi* that stands for “on top of” or “in addition to” – refers to the biochemical features that associate with DNA and influence gene expression. First, these epigenetic factors include histone proteins within the chromatin, which are organized as nucleosomes whereby the DNA is wrapped around histone octamers (pairs of histones H2A, H2B, H3 and H4). Histone proteins can bear post-translational modifications which impact DNA compaction and association with DNA-binding proteins [199,200]. Second, the most well-studied epigenetic factor is DNA methylation (DNAme), where methyl groups are found (generally) at the 5th position of cytosines. DNAme regulates gene expression via the recruitment of proteins repressing gene expression, or by preventing the binding of transcription factors to DNA [201]. Third, another layer of epigenetic factors are non-coding RNAs (ncRNAs), which are RNA molecules that are not translated into proteins, but instead are involved in a number of biological processes including RNA splicing and gene regulation [202]. While the genome encodes information within the DNA sequence, the epigenome dictates the spatio-temporal characteristic of gene expression. Consequently, epigenetic profiles vary across cell types, they are dynamic throughout development, cellular differentiation, and maturation, and under varying conditions. Importantly, aberrant epigenetic signatures have been associated with nearly any known disease or health status, including infertility and obesity.

10.1.3.2 Paternal preconception health and long-term consequences on the next generations

Most of the focus of DOHaD research has historically revolved around maternal factors, and their impact on the *in-utero* and postnatal development are well recognized. In contrast, until recently, the influence of paternal factors on offspring metabolic health has largely been unexplored. Indeed, this is partly because childbearing people directly expose the developing fetus during gestation, and the baby during breastfeeding. In contrast, men were initially thought to only provide genetic material at fertilization via their sperm. However, epidemiological studies have highlighted the intriguing possibility that ancestral exposures could have generational impacts, with a paternal germ line non-genetic transmission of phenotypes (reviewed in [203]). For example, an epidemiological study conducted in a small municipality named Överkalix in Northern Sweden, revealed sex-specific associations between grandparent's diet during the pre-pubertal period – also called the slow growth period (SGP) – and grandchildren longevity [204]. Additionally, the ALSPAC study showed that sons from fathers with a smoking onset during the SGP were more likely to become obese [205]. Since then, cumulative data support a link between paternal preconception factors such as advanced age, vitamin D levels, smoking, phthalates exposure, stress, and BMI, with poor embryo quality, and offspring increased risk to develop elevated BMI, asthma, and autism [205–213]. Several studies identified epigenetic changes in various tissues, associated with paternally-induced offspring outcomes. While some of these epidemiological studies have been criticized due to relatively low sample sizes and suboptimal statistical testing approaches, the growing evidence from human data and animal models have made it clear that a father's environment before conception can impact pregnancy outcomes and offspring health [203,214–218].

From a mechanistic point-of-view, the paternal contribution in DOHaD had previously not received much attention, due to the misconception that sperm only provides genetic material and does not encode any paternal preconception environmental information via epigenetic marking. In fact, despite a number of reprogramming steps throughout spermatogenesis (described in detail in a later section), mature spermatozoa do contain some epigenetic information that could be transmitted to the embryo after

fertilization and potentially impact development [219–223]. This knowledge highlights the possibility that factors impacting men's reproductive and overall health could have implications for the metabolic and reproductive health of the next generation(s). Exactly how paternal information including diet, lifestyle, environmental exposures, and health status, can be at the origins of offspring disease, still warrants further investigation. Furthermore, whether these effects can persist over multiple generations remains a topic of debate. The phenomenon of intergenerational and transgenerational epigenetic inheritance, as well as the potential underlying molecular mechanisms, will be further discussed in a later section.

10.2 Pathophysiological and molecular changes in obesity

Obesity results in excess weight gain concomitant with excessive fat accruement and is associated with a health condition called metabolic syndrome [224,225]. Incidentally, the worldwide increase in obesity rates is concomitant with an increase in metabolic syndrome incidence [226]. Metabolic syndrome is defined by the co-occurrence of multiple risk factors for atherosclerotic cardiovascular disease (CVD), such as central obesity (high waist circumference), elevated blood glucose (hyperglycemia), elevated plasma insulin (hyperinsulinemia), hypertension, and dyslipidemia including elevated triglycerides, reduced levels of high-density lipoprotein (HDL), and elevated low-density lipoprotein (LDL) [227]. This shared pathophysiology among patients with metabolic syndrome puts them at particularly greater risk for CVD and T2D [228,229]. Some of these key characteristics of obesity and how they impact organs physiology will be discussed in this section.

10.2.1 Adipose tissue biology in obesity

A key hallmark of obesity includes accumulation and dysfunction of white adipose tissue (WAT). Excessive fat accruement can have systemic impacts on the metabolism and basic functions of multiple organs. Adipose tissues are highly dynamic, and they adapt to changes in weight. For example, weight loss will result in decreased adipocyte size, whereas weight gain causes hyperplasia (increased number of fat cells) and hypertrophy (increased fat cell size) [230,231].

There are four distinct types of adipocytes: brown, beige, white and pink [232]. They differ in cell-surface marker expression, functions, and metabolic activity [233]. While white adipocytes store energy in the form of intracellular lipid droplets, brown adipocytes are involved in thermogenesis and energy expenditure processes [234,235]. Healthy white adipocytes are small in size, numerous in numbers, highly vascularized, they contain low numbers of macrophages with anti-inflammatory characteristics, they secrete adiponectin, are sensitive to insulin levels, and have low lipolytic activity [236]. In contrast, upon obesity, unhealthy white adipocytes show increased secretion of leptin, but decreased secretion of adiponectin, they increase in size, show increased lipolytic activity, with reduced blood vessel density, increased infiltrating macrophages with pro-

inflammatory characteristics, and decreased sensitivity for insulin [237]. Brown adipocytes have a limited capacity for lipid storage, are highly vascularized, and contain a high number of mitochondria, conferring their brown colour [238]. Their functional capacity for heat generation and energy expenditure is due to the expression of uncoupling protein-1 (UCP-1) which uncouples respiration from ATP synthesis towards thermogenesis [234]. Beige adipocytes reside within white adipose tissues and are involved in cold-induced thermogenesis [234]. Pink adipocytes appear from pregnancy up to post lactation in breast tissue [239]. The level of impact adipose depots can have on metabolic health depends on the location of the fat deposit.

There are three main adipose depots in rodents and humans: subcutaneous adipose tissue (SAT), visceral adipose tissue (VAT), and ectopic fat [16]. These fat deposits can have divergent effects on metabolic syndrome etiology based on their biological functions (for example: blood drainage sites and metabolic activity) [240,241]. Adipose tissue distribution manifests in a sexual dimorphism manner. In general, women tend to carry more total body fat compared to men, and harbour more SAT and less visceral adipose depot than their male counterparts - likely as a result of hormonal differences across sexes [242–244].

SAT represents the largest adipose deposit of all three [241]. In humans, the two main subcutaneous depots are divided in the upper-body region (abdominal depot), and in the lower body (gluteofemoral depot; buttocks and thighs). In contrast, in mice, the two main subcutaneous pads are located in the anterior and posterior regions, with the posterior pad (also called inguinal fat pad) corresponding to the human gluteofemoral depot [245]. Because the blood drains from the SAT site into the systemic circulation, its cytokines and triglyceride loads are diluted within the circulation before it reaches key metabolic organs such as the liver. Although excess SAT accruement is associated with increased risk to develop metabolic syndrome, it requires at least over 10 kg of excess SAT in order to induce metabolic disturbances. For these reasons, accumulation of this fat depot (pear-shaped obesity) confers relatively less metabolic impairments compared to other adipose tissues [246–250].

In contrast, VAT accruement (apple-shaped or central obesity) strongly correlates with insulin resistance, glucose metabolism impairments and T2D, both in humans and in

mice [251–253]. The mesenteric fat pad in mice is thought to be the most analogous to human intra-abdominal depot, both in terms of location and biology [245]. This adipose depot is in the abdominal cavity including the omentum and mesentery, and therefore drains into the portal circulation, directly exposing the liver with its cytokines and triglyceride content. For this reason, the portal vein hypothesis states that increased adiposity deposition will result in excess free fatty acid flux via portal and systemic circulation [254–257]. Additionally, the adipocytes within VAT are thought to be more metabolically and lipolytically active thereby contributing more strongly to circulating free fatty acid (FFA) levels in comparison with SAT [258]. This adipose deposit is also more innervated and vascularized than SAT [241,257]. Consequently, VAT is thought to be particularly damaging for metabolic health, with only an excess two kg of VAT associated with metabolic disease [259].

The fat deposit that is thought to be the most metabolically harmful and a strong predictor for metabolic disease is ectopic fat [260]. In ectopic fat, lipids are not stored in WAT, but instead within organs such as the liver, skeletal muscle or the pancreas. As little as 0.25 kg of fat accumulation within the liver can induce insulin resistance [261]. Hepatic fat accumulation can also result in a condition called non-alcoholic fatty liver disease (NAFLD), while fat accumulation in the pancreas impairs insulin secretion [262].

During obesity, the reduced capacity of adipocytes to store lipids result in enhanced lipolytic activity thereby releasing excess FFAs, and inflammatory factors. These FFAs are metabolized in the liver into triglycerides and released as very low-density lipoproteins (VLDL) in the circulation. Consequently, these effects can impact metabolic organs such as skeletal muscles, the pancreas, and the liver, resulting in ectopic lipid deposition, hyperlipidemia, pancreatic ß-cell impairments, and altered metabolic functions, such as impaired glucose metabolism, and insulin secretion and sensitivity. [240]

10.2.2 Hepatic role in obesity etiology

The liver is the main site of biochemical reactions regulating whole-body metabolic homeostasis. It plays critical roles in nearly every organ system, by interacting with endocrine and gastrointestinal systems. Its functions range from producing bile (for fat breakdown), plasma proteins, cholesterol, proteins carrying fats, immune factors, to

glucose metabolism and storing excess glucose in the form of glycogen, metabolizing drugs, clearing bilirubin, and regulating amino acid levels, and blood clotting. This organ is highly vascularized allowing for the delivery and export of nutrients, hormones, and metabolites [263]. It is supplied of blood via 2 sources: oxygenated blood is delivered through the hepatic artery, and nutrient-rich blood through the hepatic portal vein. The unique anatomy of the liver facilitates the sequential perfusion of nutrients and metabolites (see Figure 3 from [264]). Hepatocytes are positioned along blood vessels in functional units called lobules, forming different metabolic zones (periportal, intermediate, and pericentral zone) from the portal triad to the central vein [265]. This hepatic architecture phenomenon is termed metabolic zonation [266–271]. Blood flows in a unidirectional manner creating zone-specific concentration patterns of various metabolites and signalling molecules, resulting is specific hepatocyte metabolic activity accordingly [264,272]. Metabolic changes occurring following obesity can impact liver zonation and functions.

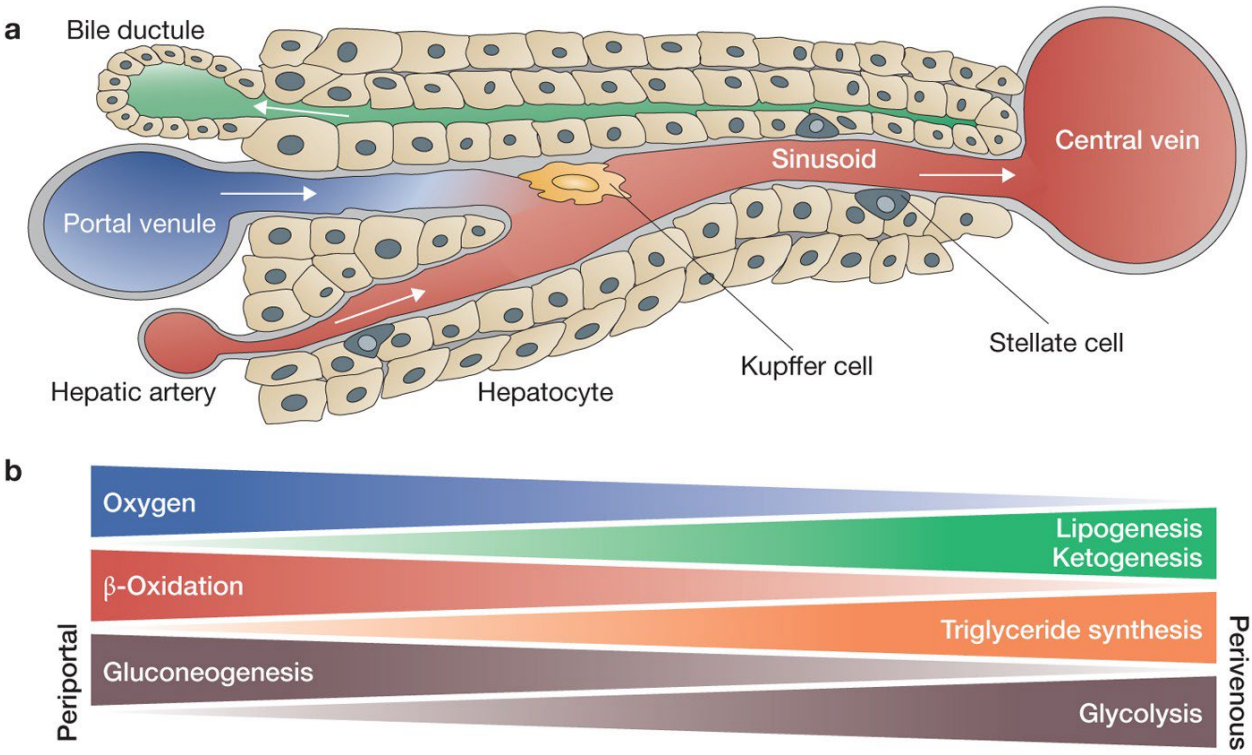

Figure 3: Blood flow, nutrient and oxygen gradients in the liver.

Figure adapted from [264] (Copyright 2016) with permission from Springer Nature.

Upon obesity, increased FFA production is associated with aberrant intrahepatic triglycerides (IHTG). IHTG develops when the uptake and synthesis of fatty acids is greater than its oxidation and secretion, and is the major cause of non-alcoholic fatty liver disease (NAFLD) [273–276]. This condition is an umbrella term that encompasses a spectrum of liver pathologies, including non-alcoholic hepatic steatosis, steatohepatitis (NASH), liver fibrosis, cirrhosis or hepatocellular cancer [277]. NAFLD is the most common chronic liver disease, concomitant with the obesity epidemic, and is found in over 60% of T2D patients [278,279].

10.2.3 Lipotoxicity

As described previously, obesity is accompanied with excess fat accruement. Adipose tissues have the capacity to expand in order to accommodate for fluctuations in energy availability. This ability is not unlimited and greatly varies across individuals, likely due to variance in adipocyte expansion capacity [280]. Indeed, adipocyte hypertrophy is associated with dyslipidemia, impaired glucose metabolism and inflammation in obese individuals. Additionally, adipocytes are smaller in size in obese individuals that do not show metabolic disturbances in contrast with metabolically compromised obese people with larger adipocytes [281]. In other words, a high prevalence of hypertrophic adipocytes in combination with low prevalence of hyperplasia reduces the threshold for adipose tissue expansion, rendering an individual more prone for metabolic syndrome. The inability of adipocytes to expand impedes the overall lipid storage capacity which results in adipose tissue dysfunction, inefficient energy storage, and systemic hyperlipidemia. Over time, hyperlipidemia causes the deposition of circulating free fatty acids in non-adipose organs such as hepatic, cardiac, skeletal muscle and pancreas tissue [282,283]. Ectopic fat deposition is accompanied with lipotoxicity, which ultimately accounts for obesity-related adverse outcomes. The accumulation of excessive body fat mass induces a constellation of metabolic disturbances and diseases. These effects include hyperinsulinemia and multi-organ insulin resistance, hyperglycemia and glucose intolerance, dyslipidemia (high plasma triglyceride and low plasma HDL-cholesterol), pancreatic ß cell dysfunction, low-grade inflammation, non-alcoholic fatty liver disease, prediabetes, type 2 diabetes, cardiovascular diseases, and more.

10.2.4 ß cell integrity and insulin resistance

Insulin is secreted by pancreatic ß islet cells and exerts its actions by binding to its receptors on target cells, activating a cascade of intracellular events. Insulin regulates circulating glucose levels via several different mechanisms that involve increasing glucose uptake by tissues, reducing circulating glucose, and increasing glucose conversion into energy storage molecules. First, insulin stimulates the uptake and use of glucose in skeletal muscle and adipose tissues, by promoting the translocation of glucose transporter-containing vesicles to the plasma membrane [284]; second, insulin also induces glycogen synthesis and inhibits glycogenolysis in skeletal muscles and liver; third, insulin inhibits gluconeogenesis in the liver, and fourth, insulin action on adipose tissue stimulates glucose uptake and inhibits lipolysis [227]. Other downstream actions of insulin signalling include the activation of endothelial nitric oxide synthase in vascular endothelial cells, the production of the vasoconstriction-inducing factor endothelin-1, and the expression of cell adhesion molecules that promote leukocyte-endothelial interaction.

Insulin resistance is characteristic of obesity and T2D, and refers to the process by which a rise in insulin levels does not result in an increased uptake of glucose by insulin-sensitive tissues [227]. In that process, cells in adipose tissues, muscles and the liver do not response properly to insulin, resulting to hyperglycemia. Ultimately, the pancreas aims at compensating via the increased production of insulin leading to hyperinsulinemia. Additionally, the deregulated action of insulin signalling results in endothelial dysfunction via imbalanced endothelial nitric oxide production, as well as vascular abnormalities, all contributing to the development of metabolic syndrome associated comorbidities such as atherosclerosis.

Pancreatic islet integrity is a critical determinant for metabolic functions in obesity. Indeed, the progressive decline of ß cell function causes a decline in proper glycemic control. In obese individuals, ß cell mass is about 50% greater than in lean individuals, but the relative ß cell volume is 50% lower due to ß cell apoptosis [285]. Several factors are thought to negatively impact ß cell function, growth, and survival. These factors include plasma glucose levels, as well as lipid mediators such as free fatty acids, long-chair acyl-CoA esters, ceramides, phosphatidic acid, diacylglycerides, and more [286]. The

glucolipotoxicity of increases in plasma glucose and lipid factors likely act synergistically, along with other metabolic stressors, to cause ß cell dysfunction.

10.2.5 Inflammation and oxidative stress in obesity

Other key hallmarks of obesity are chronic low-grade inflammation, systemic oxidative stress and damage, and immune dysfunction [287]. Adipokines produced by adipose tissues can induce the production of reactive oxygen species (ROS) thereby resulting in oxidative stress. Additionally, excess adipose tissue is associated with increased production of pro-inflammatory cytokines such as tumor necrosis factor-alpha (TNF-α), interleukin (IL)-6 and IL-1ß. These inflammatory factors impact adipose tissue biology, promote ROS production, reduce systemic anti-inflammatory cytokines, and further stimulate the production of pro-inflammatory cytokines. Obese individuals are at greater susceptibility to oxidative damage with reduced antioxidants sources such and decreased activity of superoxide dismutase, glutathione peroxidase, and catalase, and decreased levels of vitamins A, E, C, and ß-carotene [288]. Pathological increase in serum FFA levels results in increased mitochondrial oxidation and thereby elevated synthesis of free radicals, which in turn impacts cellular structures and damage [289–293].

Overall, the plethora of obesity-associated physiological changes ranging from insulin resistance, systemic inflammation, oxidative stress, altered metabolism, visceral fat accumulation, dyslipidemia, to endothelial dysfunction, all contribute to the development of metabolic syndrome and associated comorbidities. Not only do these pathophysiological hallmarks occur in metabolic tissues, but also they can compromise the integrity and functions of germ cells, which can have far-reaching implications for the next generations' health. Indeed, in humans, an elevated BMI has been linked to subfertility, with increased time to conceive, increased rates of pregnancy losses and reduced rates of fertilization in couples undergoing assisted reproductive technologies (ART), and poor semen parameters [294–299]. In animal models of high-fat diet-induced obesity, male obesity has been linked to embryo health impairments with reduced implantation and live birth rates, reduced sperm DNA integrity, and poor sperm

parameters, with elevated intracellular ROS [216,300–303]. These findings highlight the consequences of obesity that go beyond metabolic functions and reproductive health, whereby germ cells are not immune to obesity-induced damage, which implications for the next generations. The next section will dive into the cellular and molecular mechanisms involved in the production of male germ cells: spermatogenesis.

10.3 Cellular and molecular events in spermatogenesis: implications for the next generation

The process of spermatogenesis takes place in the testes, within the seminiferous tubules. The seminiferous tubules contain the developing germ cells and Sertoli cells. These convoluted tubules are surrounded by interstitial space where immune cells and steroidogenic Leydig cells reside, as well as contractile peritubular myoid cells that permit the transport of spermatozoa and testicular fluid within the tubules to the epididymis, where spermatozoa cells are stored [304]. While there are differences in terms of cellular organization within the testes and seminiferous tubules between rodents and humans, the overall cellular arrangements and components are highly similar.

Spermatogenesis is a complex process that involves dynamic chromatin remodeling, progressive cellular morphological changes, in parallel with two rounds of cell mitosis, one round of meiosis, and differentiation (reviewed in [305]). This process gives rise to haploid, fully differentiated and mature germ cells. Upon fertilization, spermatozoa provide the genetic and epigenetic material necessary to produce a totipotent zygote which will give rise to all somatic lineages, tissues, and gametes of the next generation.

The complex series of molecular events that entails spermatogenesis is tightly regulated via the reciprocal interactions between the endocrine system, germ cells, and somatic supporting cells, and is influenced by the seminiferous tubule microenvironment (see Figure 4 from [305]). Hypothalamic cells within the brain are responsible for the production of gonadotropin-releasing hormone (GnRH) which acts on gonadotropic cells located within the anterior pituitary, to induce the production and secretion of the gonadotropin follicle-stimulating hormone (FSH) and luteinizing hormone (LH) [306]. FSH and LH are released in the circulation and reach the testes where they act on FSH and LH receptors on Sertoli and Leydig cells, respectively [307–310]. Sertoli and Leydig cells produce a number of endocrine and paracrine factors, as well as chemokines, that act in a cell- and stage-specific manner. The major cell types involved, and each spermatogenesis step, will be described in the next subsections, including the cellular, hormonal, molecular, and epigenetic events involved in this process.

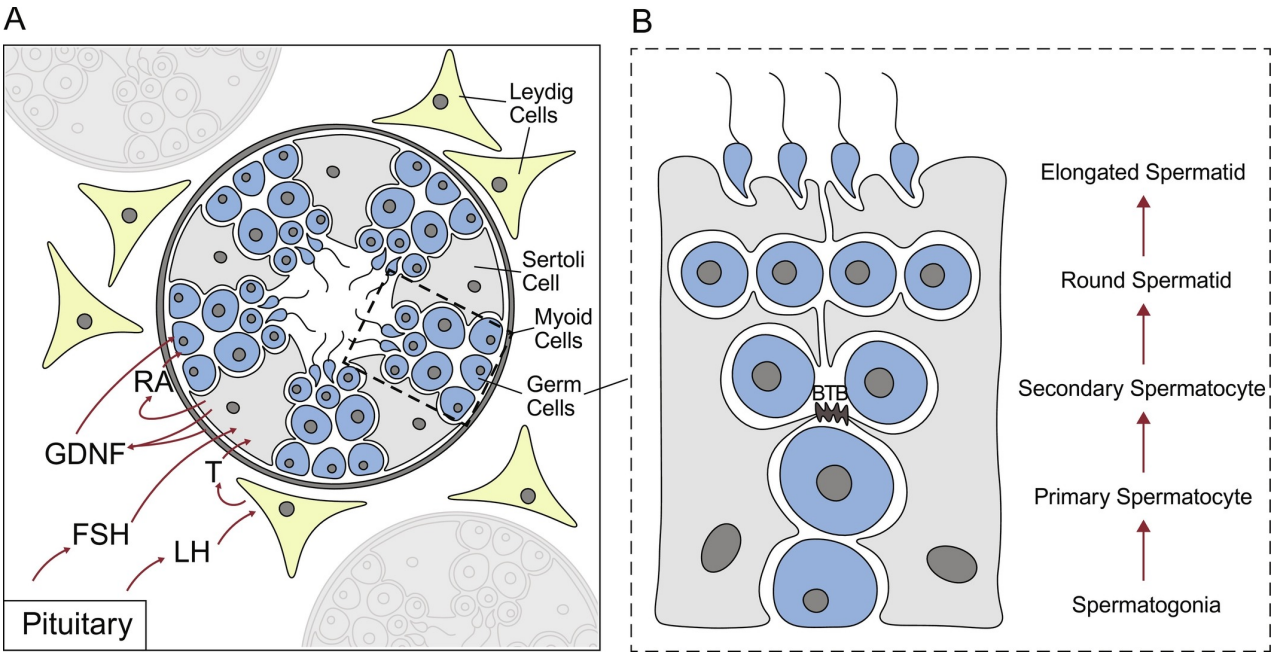

Figure 4: Schematic representation of a testis cross section including key somatic and germ cells, and paracrine and endocrine factors.

BTB, Blood-testis barrier; FSH, Follicle-stimulating hormone; GDNF, Glial cell line-derived neurotrophic factor; LH, Luteinizing hormone; RA, Retinoic acid; T, Testosterone.
Figure obtained from [305] Copyright (2019), with permission from Elsevier.

10.3.1 Spermatogenesis-supporting cells: Leydig cells and Sertoli cells

Sertoli cells, or “nurse” cells, accomplish structural, protective, immunomodulatory, and secretory roles that support the development and maturation of germ cells. Until the first wave of spermatogenesis, the predominant cell type occupying the seminiferous tubules are the Sertoli cells. Thyroid hormone and FSH-induced GDNF secretion are among the factors responsible for the rapid expansion of the Sertoli cell population during the fetal, neonatal and peripubertal periods [308–312]. Spermatogenic output is in part determined by Sertoli cell number [313].

At puberty, Sertoli cells undergo maturation, cease proliferation, and establish the blood-testis barrier (BTB) via the formation of tight junctions. This separates the interstitial blood compartment from the adluminal compartment [314–316]. This barrier prevents the passage of cytotoxic agents, and also maintains the unique composition of the adluminal environment, which is rich in androgens, estrogens, potassium, inositol, glutamic and

aspartic acid, and other regulatory factors, and poor in protein and glucose [317–319]. Furthermore, the BTB creates an immune-privileged environment whereby the immune system is prevented from mounting autoimmune reactions against sperm-specific antigens [320]. These autoimmune reactions are also prevented by immunomodulatory factors that are produced by Sertoli cells [321]. Because of the apical movement of the developing germ cells, the BTB is highly dynamic, being reformed and broken down to allow the passing of immune-identical spermatogonia through the barrier [320].

In addition to providing structural support and protection against autoimmune responses to germ cells, Sertoli cells secrete a number of regulatory molecules which are essential to support spermatogenesis. For example, they secrete the anti-Müllerian hormone, which is expressed during fetal development to inhibit the formation of the female reproductive tract. Complex proteins produced by Sertoli cells, namely inhibins and activins, act with opposing effects on FSH metabolism and secretion. Sertoli cells also support spermatogenesis by producing androgen binding proteins, which maintain the high testosterone concentration within the tubules [322].

In mice, fetal Leydig cells arise at around embryonic day (E)12.5 after Sertoli cell differentiation, forming clusters in the interstitial compartment [323]. They acquire steroidogenic capacity around E16 to produce androstenedione [324]. Because they do not yet express 17-beta hydroxysteroid dehydrogenase (17ß-HSD), fetal Leydig cells rely on Sertoli cells for the conversion of androstenedione to testosterone [325]. Adult Leydig cells are the primary source of androgens and testosterone in males [326]. Under the regulation of the hypothalamic-pituitary-gonadal axis, androgens are secreted and diffuse into the seminiferous tubules, the bloodstream and the interstitial space [327]. These hormones elicit their regulatory functions on spermatogenesis by binding the androgen receptors of Sertoli and myoid cells. Testosterone impacts spermatogenesis by facilitating meiotic progression, regulating sperm release, maintaining the BTB by promoting its assembly upon preleptotene spermatocyte transit, and regulating the separation of spermatocytes from sperm via the expression of connexin [328].

10.3.2 Myoid cells

Peritubular myoid cells are located around the seminiferous tubules providing structural support [329]. Their smooth muscle-like characteristics generate peristaltic contractions that facilitate movement of immotile spermatozoa forward throughout the seminiferous tubules up to the epididymis where they are stored. These cells secrete signalling factors such as components of extracellular matrix and growth factors that can modulate the activity of Leydig and Sertoli cells [330,331]. They also secrete GDNF which serves in the maintenance of the spermatogonial stem cells within the stem cell niche [332].

10.3.3 Male germ cell specification and sex determination

Germ line epigenetic and gene expression programs are established early in development (see Figure 5 from [333]). Beginning in the post-implantation embryo (E6), commitment of germ cells is induced by bone morphogenetic protein signals (BMP4,8b,2) arising from the extraembryonic ectoderm and visceral endoderm [334–341]. These signals lead to the expression of *Blimp1*, *Tcfap2c*, and *Prdm14*, a triad of transcription factors that facilitates germ cell specification via the repression of somatic genes including *Lim1*, *Evx1*, *Fgf8*, *Snail*, and homeobox genes [342–349]. From that stage on, the specified primordial germ cells (PGCs) express the PGC markers TNAP, SSEA1, and DPPA3, and some pluripotency genes including *Sry*, *Nanog*, and *Oct4* [350–359].

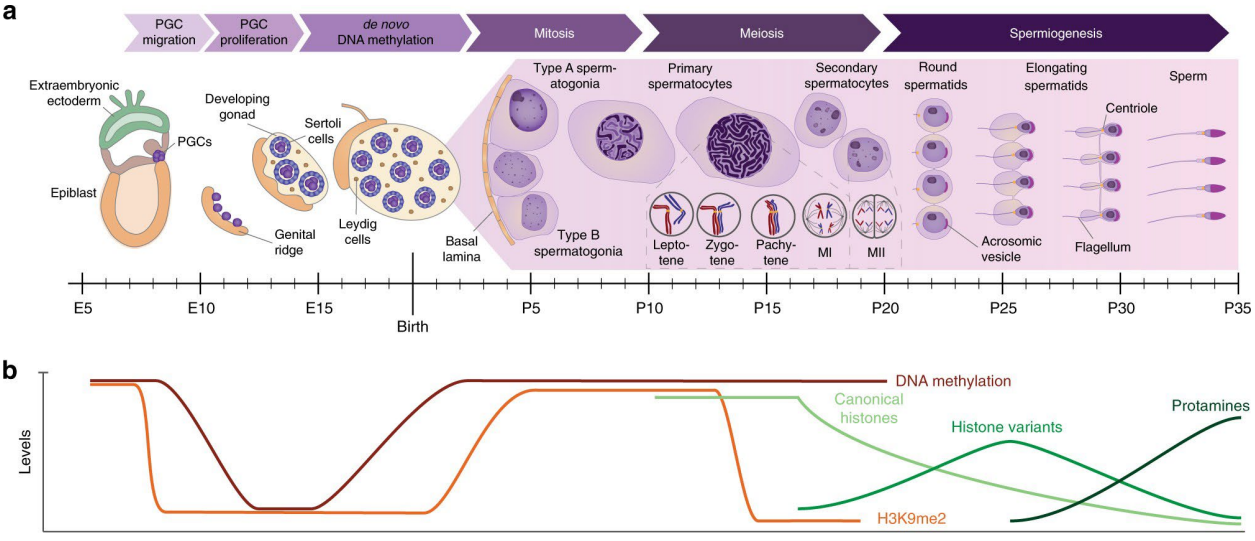

Figure 5: Male germ cell development and reprogramming of epigenetic marks throughout spermatogenesis in mice.

Figure adapted from [333] (Copyright 2017) with permission from Springer Nature.

Upon completion of PGC specification (E7.5 to E10.5), the cells proliferate and migrate through the hind gut, then to the genital ridge – the future gonad. Germ cell-soma signalling facilitate this directional migration, where germ cells express c-KIT and somatic cells paving the way to the gonad express STEEL. Mesenchyme near the genital ridges express the chemoattractant SDF-1 [360–364]. Once the PGCs have reached the gonad, they undergo several rounds of cellular divisions with incomplete cytokinesis forming germ cell clusters [365]. These germline cysts remain indistinguishable in male and female fetuses, both morphologically and molecularly, up until sex determination [366,367].

Male sex determination and testis morphogenesis begins at E11.5 with the expression of SRY within the genital ridges, which later prompts the specification of Sertoli cells [368–370]. Following Sertoli cell proliferation and cluster formation, testis cords are formed, establishing structural organization in the developing testis where germ cells and Sertoli cells are separated from the interstitium. The interstitium is comprised of Leydig cells, peritubular myoid cells, immune cells and vasculature [367,371]. Male fate commitment of the gonocytes occurs at E14.5, where cells exit the cell cycle, arrest at G0, and remain in a quiescent state up until after birth [372].

10.3.4 From primordial germ cells to the life-long supply of spermatogonial stem cells

Once primordial germ cells have migrated to the genital ridge and undergone rounds of cellular proliferation and differentiation to colonize the developing testes, there is a change in gene expression marked by downregulation of alkaline phosphatase, and upregulation of *Gcna1* [373]. The cells are then in a transient state as gonocytes [374–376]. These transitionary cells migrate to populate the seminiferous tubules at the basement membrane, and undergo differentiation into spermatogonial stem cells (SSC) or spermatogonia (for the first wave of spermatogenesis) [376]. This prepubertal first cycle of spermatogenesis is different from the subsequent adult cycles in that its rate is much faster, and a large portion of the resulting spermatogonia and pachytene spermatocytes undergo apoptosis, likely due to the newly but incompletely formed BTB [377–379]. The subsequent “regular” waves take place in a continuous and asynchronous manner and last for approximately 35 days in mice and 42-76 days in humans [380–382].

10.3.5 Spermatogenesis

Spermatogenesis involves multiple rounds of mitotic divisions and differentiation, that can be classified into 12 distinct stages in the mouse, based on cell type associations [383]. Because spermatogenesis occurs continuously, all the cell types involved can be found at any given time in an adult testis. SSCs represent about 0.02-0.03% of all testicular germ cells and are thought to represent the life-long supply of germ stem cells [384–389]. SSCs have the capacity to self-renew via asymmetrical mitotic divisions (called A_{single} spermatogonia), and can also divide symmetrically giving rise to the A_{paired} spermatogonia, which are interconnected via cytoplasmic bridges resulting from incomplete cytokinesis [304,384–390]. The A_{paired} spermatogonia go through successive rounds of mitosis with again incomplete cytokinesis, giving rise to approximately 16 bridged $A_{aligned}$ spermatogonia. Next, retinoic acid from Sertoli cells prompts the undifferentiated spermatogonia to differentiate into A1 spermatogonia which gain expression of the *cKIT* receptor [391]. Sequential mitotic division give rise to the A2, A3, A4, intermediate and B spermatogonia [392,393]. Next, type B spermatogonia undergo cellular division to produce the tetraploid primary spermatocyte, or pre-leptotene spermatocyte, which subsequently undergo meiosis [394]. This meiosis step consists of two sequential reductive cellular division giving rise to the haploid round spermatid cells [395]. This complex process requires multiple days and is further subdivided into the leptonema, zygonema, pachynema and diplonema phases [395,396]. Round spermatids next enter the spermiogenesis cycle.

10.3.6 Spermiogenesis and the production of a terminally differentiated and mature spermatozoa

The process of spermiogenesis involves a differentiation and maturation process as well as structural and morphological changes that give rise to the fully mature and differentiated spermatozoon. Round spermatids elongate, shedding a large portion of its cytoplasm which is engulfed by Sertoli cells [397,398]. Spermatids also develop specialized structures such as the flagellum and the acrosome [399]. In parallel, a drastic chromatin reorganization (further described in the next subsection) allows for the compaction of the haploid genome within the sperm head, up to a volume that represents about 5% of that

of somatic cell nucleus. Finally, sperm cells leave the testis and enter the epididymis – a long convoluted tubule. During the epidydimal transit, spermatozoa undergo maturation and progressively acquire motility and fertilizing capacity (reviewed in [400]).

10.3.7 Epigenetic landscape establishment and programming during spermatogenesis

The testis is comprised of a highly diverse and complex transcriptome, partly owing to the uniquely expressed coding and non-coding transcripts [401–404]. Many genes expressed in somatic cells make use of alternate promoters in male germ cells, have homologs that are expressed in a male germ line-specific manner, or are regulated via germ-cell specific factors [405,406]. These spermatogenic-specific transcriptomic programs permit the unique functions of male germ cells and are promoted by profound epigenetic reprogramming and chromatin remodeling during spermatogenesis.

Throughout germ cell development, cells undergo two waves of epigenetic reprogramming. The first reprogramming round occurs upon PGCs specification, where two sequential rounds of DNA methylation erasure take place (see Figure 5 from [333]). First, from E6.5 to E10.5, repression of the *de novo* DNA methyltransferases DNMT3a and DNMT3b causes passive DNA demethylation in germ cells upon replication-dependent dilution [343,407–410]. In parallel, during this rapid proliferation phase, the DNA methyltransferase DNMT1 maintains DNA methylation at maternally and paternally imprinted genes and at genes involved in meiosis [411]. A second round of DNA methylation erasure takes place in an active manner, from E10.5 to E12.5 during PGCs migration to the genital ridge, by ten-eleven translocation 1 and 2 (TET1/2) enzymes [412–414]. These enzymes catalyze the conversion of 5-methylcytosine (5mC) into 5-hydroxymethylcytosine (5hmC), and the resulting 5hmC are either cleared in a passive manner via replication, or in an active manner via base excision repair mechanisms [412,415]. By E13.5, germ cells reach their lowest DNA methylation levels, with only 4% of the genome being hypermethylated, including at some repetitive elements and intracisternal A particles (IAPs; a class of transposable elements) [416,417]. Unlike in somatic cells, hypomethylation in PGCs does not result in genome instability and ectopic expression of retrotransposons [407,418]. Maintenance of genome stability is promoted by the increasing enrichment of the repressive histone marks histone H3 lysine 27 trimethylation

(H3K27me3), and histone H2A and H4 arginine 3 dimethylation (H2A/H4R3me2), from E8.5 to E11.5 [349,419,420]. After erasure of the majority of methylated sites in the genome, *de novo* DNA methylation takes place in the male germline from E14.5 until birth to re-establish methylation profiles including at sex-specific imprinted loci with the action of DNMT3A/B and DNMT3L [421–426]. Imprinted genes (260 in mice and 228 in humans identified thus far) have monoallelic expression in a parent-of-origin manner in the next generation [427–429].

During gametogenesis, the chromatin undergoes a series of drastic waves of partial remodeling, including chromatin reorganization which includes the incorporation of histone variants and the temporary transition proteins. The majority of histones are replaced by protamines in condensing spermatids (reviewed in [305,430–432]). These gamete-specific events facilitate meiosis, germ cell morphological changes, and the progression of spermatogenesis. Ultimately, these unique processes produce a predominantly non-histone genome-packaging structure within the nucleus of the highly specialized spermatozoa.

Global reorganization in chromatin packaging takes place in post-meiotic cells where most histone proteins are replaced by nuclear sperm proteins called protamines in a stepwise process [305,430–438]. The nucleohistone-nucleoprotamine exchange begins in the round spermatids by the weakening of interactions between histones and the DNA upon histone hyperacetylation [439–441]. Histone protein eviction is followed by the accumulation of unique testis-specific histones and histone variants, which almost completely replace canonical histones [437].

In differentiating spermatogonia, the gene coding for the histone H3 variant H3t becomes active, and gradually replaces the canonical histone H3. This testis-specific variant decondenses nucleosomes [442,443]. Meiosis is marked by a sequential incorporation of transient histone variances such as H1t, macroH2A.X, H2A.Z, and H3.3 [444–447]. At the onset of meiosis in early spermatocytes, the majority of histones H2A and H2B are replaced by the co-expressed germline-specific TH2A and TH2B (or THS2B), respectively [448–451]. These variants permit the weakening of nucleosomes stability genome-wide, thereby facilitating subsequent histone eviction [452–454]. In contrast to TH2A, TH2B function is not dispensable for proper spermatogenesis progress due to

compensatory mechanisms involving H2B accumulation, and intranucleosome-destabilizing histone modifications [449,453–457]. Post-meiosis, the sex chromosomes accumulate the variant H2A.Z, and H2A.Z is subsequently replaced by H2A.B.3 at the exon-intron boundaries of active genes, likely regulating RNA splicing events [445,458]. It is thought that H2A, H2A.Z and H2A.B.3 may define spatio-temporal expression of the genes they mark. Indeed, the incorporated variant H2A.L.2 appears to regulate stage-specific transcriptomic program, by accumulating at transcriptional start sites of genes highly expressed in spermatocytes and round spermatids [459]. Additionally, H2A.B.3 marks X-linked genes that escape sex chromosome inactivation [460]. Another histone variant is the replication-independent histone H3.3, which massively replaces the canonical histone H3 on sex chromosomes during meiosis [446]. It is encoded by the *H3f3a* and *H3f3b* mouse genes, both producing identical H3.3 but functioning at different stages of spermatogenesis [446,461,462]. Interestingly, the combinations of H3.3 with macroH2A in spermatocytes and H3.3 with H2A.Z in round spermatids confer either more stable or unstable chromatin domains, respectively [463–465].

Next, most of these germline-specific histones are replaced by transition proteins [466]. The incorporation of transition proteins onto chromatin is ensured by the replacement of TH2A with the H2A.L.2 variant, promoting accessibility of H2A.L.2-contaning nucleosomes [450,467]. Transition proteins (TP1 and TP2) are small basic proteins that constitute 90% of the basic proteins present at that stage. They are important for proper sperm configuration, chromatin condensation, and DNA integrity, and both TPs appear to accomplish overlapping roles and partly compensate for each other [466]. Their assembly ultimately permits the final eviction of histones, and the incorporation of protamines. The high content of positively charged amino acids in protamines promotes the compaction of, and complex with, the negatively charged paternal genomic DNA within the small sperm head. Compared to somatic cell heterochromatin, sperm DNA is ten-fold more compact with protamines [468].

Despite the complex reprogramming and reorganization of the chromatin, the retention and establishment of epigenetic marks in sperm is not random in the genome. Most of the sperm genome is hypermethylated, with the exception of most CpG islands at promoters, and several retrotransposon families [221,469,470]. Despite the drastic histone-

to-protamine exchange, mature spermatozoa retain 1-15% of histones in mice and men, respectively [220,223,471,472]. Early studies established that histones are preferentially retained at genomic regions that are rich in CpGs and hypomethylated in the sperm of mice and men [223,472]. In contrast, subsequent studies with distinct experimental and analysis approaches suggested histones are located at gene-poor regions such as retrotransposons and intergenic regions [473–475]. It is thought that the sperm histone landscape is complex. Indeed, the gene-activating histone mark histone H3 lysine 4 trimethylation (H3K4me3) is enriched at promoters, embryonic enhancers, some retrotransposons subfamilies, and largely mutually exclusive with DNA methylation at promoters, with the exception of regions bearing intermediate and high levels of DNA methylation overlapping with H3K4me3-marked regions [1,221,476,477]. Interestingly, many of the retained canonical histones present in mature spermatozoa are enriched at key promoters and enhancers of developmental genes [220,221,472]. Importantly, histone H3K4me2 profiles are highly conserved from the spermatogonia to the mature spermatozoa, suggesting epigenetic errors could persist throughout spermatogenesis at certain sites [478]. Some developmental loci bear bivalent domains – that is, the presence of both active and repressive histone marks – which are thought to be in a poised chromatin state, an evolutionarily conserved feature in the male germline of the zebrafish and the mouse [220,223,473,479–481].

These findings on the epigenetic landscape of mature spermatozoa and its evolutionary conservation, suggest sperm packages paternal information that could be transmitted to the next generation and be instructive for developmental processes. This so-called process of paternal epigenetic inheritance will be further discussed in the next subsection.

10.4 Paternal epigenetic inheritance and the transmission of obesity and metabolic syndrome

Globally, one in six couples experience infertility, with nearly half of cases being attributed to male factors [482]. Male infertility is intertwined with environmental factors and health status, such as toxicant exposures, diets, and obesity. Of note, elevated BMI and obesity have been linked to negative impacts on semen parameters and sperm functions, male fertility, and seminal plasma composition [294,295,483–487]. Importantly, these paternal environmental conditions not only impact sperm function, they can also influence pregnancy outcomes and offspring health [488–491]. Exactly how paternal exposures can influence offspring health is still poorly understood. The underlying molecular mechanisms are likely to involve sperm-mediated transmission of environmentally-sensitive epigenetic regions. The studies on which this thesis is based aimed to address this gap in knowledge in the context of paternally-transmitted metabolic dysfunction.

In order for a paternal environmental factor to induce phenotypes in the next generation(s) via epigenetic inheritance: (1) the exposure must induce epigenetic alterations in the developing sperm; (2) these environmentally-induced epigenetic changes must escape reprogramming and be retained in the fully differentiated and mature sperm; (3) this epigenetic information must be transmitted to the embryo and escape embryonic epigenetic reprogramming; and (4) the sperm-transmitted epimutations must perturb gene expression in the developing embryo or fetus (Kimmins, unpublished). The following subsections will cover the evidence for the phenomena of paternal epigenetic inheritance, with a focus on the transmission of paternally-induced obesity in the next generation(s).

10.4.1 Evidence paternal factors are associated with metabolic disturbances and obesity phenotypes in offspring (POHaD)

10.4.1.1 Epidemiological studies

Several of the foundational studies establishing the concept and research field of DOHaD have suggested that prepubertal nutritional conditions are associated with sex-specific and transgenerational phenotypes through the male line. For example, historical datasets from the Överkalix northern Sweden region, revealed that paternal grandfather's good

food access was linked to increased diabetes and all-cause mortality in grandchildren. Moreover, paternal poor, and maternal good nutritional exposure was associated with cardiovascular disease mortality in their children [204,492,493]. Some of these findings have been recently replicated with a larger dataset from the Uppsala Multigeneration Study, where paternal grandfather's good food supply could predict male grandchildren's all-cause mortality including cancer, but not diabetes nor cardiovascular mortality [494,495]. The lack of congruence and reproducibility across these studies is likely due to differences in methodological approaches involving different factors being taken into account, the smaller sample sizes from the initial study, and differences in procedure for cause-of-death recording given data across studies come from different years. Nevertheless, since then other studies have drawn associations between paternal and children metabolic health. For example, children born from two overweight or obese parents are more likely to become overweight than children from none or one overweight parent [496]. Paternal body fat has been associated with a daughter's changes in body fat before puberty [497]. Additionally, excessive BMI gains from childhood to adulthood in parents is associated with an elevated BMI and risk for obesity in offspring [498]. Despite these studies, an important challenge with human data is to exclude genetic, epigenetic, cultural, and ecological factors of inheritance, and separate maternal and paternal factors [214]. Therefore, it poses a challenge to provide evidence for true (paternal) epigenetic inheritance and draw conclusions regarding whether effects occur inter- or transgenerationally in humans.

10.4.1.2 Animal models

Animal models have been useful to dissect the paternal contribution to offspring health, given the possibility to use inbred strains in strictly controlled environments. The diet-induced obesity (DIO) model consists of feeding rodents with an obesogenic diet such as diets high in fat, which induce obesity and recapitulate symptoms that are characteristic of the metabolic syndrome [499]. This DIO model was established and characterized over 30 years ago, and has since been a valuable tool to study the interplay between diets, obesity development, progression, and the underlying mechanisms [499–503].

The first report of paternal non-genetic and intergenerational transmission of metabolic disturbances in mammals was shown using a DIO model in Sprague-Dawley

rats [504]. Paternal chronic high-fat diet (HFD) consumption led to impaired insulin sensitivity and glucose tolerance, pancreatic ß-islets dysfunction with altered gene expression and DNA methylation in F_1 female offspring [504]. Since then, numerous studies have replicated the findings that paternal HFD impacts offspring metabolic functions. Studies have additionally linked paternal DIO with offspring increased adiposity, elevated body weight, metabolic dysfunction including elevated glucose and insulin blood levels, blood leptin levels, elevated blood pressure, aberrant whole-body energy metabolism, glucose intolerance, reduced insulin sensitivity, differential hepatic, adipose, and pancreatic islet gene expression, and more [504,505,514–517,506–513]. Similar cardiometabolic phenotypes have been observed in offspring associated with a wide range of paternal factors such as a paternal low-dose streptozotocin-induced prediabetes, low-protein or caloric restriction diets, age, smoking, and chemical exposures (reviewed in Eberle, Kirchner, Herden, & Stichling, 2020). While it has become evident from these models that paternal exposures lead to increased risk to develop various health conditions in the next generations, elucidating how paternal non-genetic information can influence offspring phenotype would help understanding the underlying molecular mechanisms and determine whether these effects are preventable.

10.4.2 Evidence paternal environmental factors alter the sperm epigenome

The non-genetic transmission of paternally-induced phenotypes is thought to occur via epigenetic inheritance mechanisms whereby paternal factors influence epigenetic information encoded in mature germ cells to impact offspring development and health. The next subsections describe the current state of knowledge regarding how paternal exposures alter the sperm epigenome at the level of DNA methylation patterns, RNA content and histone modifications, respectively.

10.4.2.1 DNA methylation

DNA methylation (DNAme) is the most well-studied epigenetic mark, and has been associated with various health conditions, disease states and environmental exposures, in a wide range of different tissues [519]. More specifically, in the context of obesity-associated sperm epimutations, in humans, comparing sperm from lean versus obese individuals revealed differentially methylated regions (DMRs) at genes involved in the

central nervous system development and functions [520]. Importantly, these DMRs were no longer detected following bariatric surgery-induced weight loss, suggesting the potential reversibility of these epigenetic changes. In rodent models, obesity and HFD have been linked to altered global DNAme profiles in germ cells [506,521]. Additionally, some of these models have detected changes at specific DMRs, including at retrotransposons, satellite repeats, insulin signalling genes, and imprinted genes [508,521,522]. The obesity-associated DNAme patterns previously detected could impact offspring development and contribute to paternally-induced phenotypes across generations.

10.4.2.2 Non-coding RNA

Although the vast majority of the mammalian genome is transcribed at varying levels, some genomic regions do not code for proteins [202,523–525]. These non-protein-coding sequences are transcribed in molecules termed non-coding RNAs (ncRNAs), which serve a number of biological functions [526–528]. For example, ncRNAs are involved in gene expression regulation by altering the stability and translation of messenger RNAs (mRNAs), they modulate chromatin function, and interfere with signalling factors. Ultimately, their functions impact gene expression, and aberrant ncRNA expression or action are involved in a number of diseases [202,529].

While the sperm is transcriptionally inactive, it does carry various RNA species, such as messenger RNAs (mRNAs), long non-coding RNAs (lncRNAs), as well as several small non-coding RNA (sncRNA) subtypes such as small nuclear RNA (snRNA), piwi-interacting RNA (piRNA), microRNA (miRNA), transfer RNA-derived fragments (tRFs). PiRNAs are mainly expressed in the germline [530]. This class of ncRNA is involved in regulating the expression of coding genes, and its role in maintaining genomic stability by repressing repetitive elements has been shown to be evolutionarily conserved [531,532]. The role of piRNAs in epigenetic inheritance has been described in *C. elegans* and *Drosophila*, suggesting that alterations in this class of sperm RNA abundances could potentially have an impact on development [533,534].

In the context of obesity, aberrant abundance of specific miRNAs, piRNAs, tRFs, and snRNAs has been linked to elevated BMI in humans [520]. In DIO mouse models, changes in sperm-borne RNA content was detected in sires fed a HFD, which was linked to intergenerational metabolic disturbances in the F_1 generation [506,508,509,513,517,535].

Importantly, zygotic injection of isolated testes or sperm total RNA, or of a subset of sperm transfer RNA-derived small RNAs (tsRNAs) from HFD-fed males conferred metabolic disorders in offspring [513,517]. RNA modifications have also been found to carry an additional layer of epigenetic information, as an injection of unmodified RNA fractions did not induce these offspring metabolic phenotypes [514,536–538]. These studies suggest sperm RNA is impacted by diets inducing obesity and could contribute to offspring metabolic health.

10.4.2.3 Histone modifications

Most of the focus of research on the underlying mechanisms of epigenetic inheritance has been concentrated on assessing DNA methylation profiles and RNA content in sperm to link paternal factors and offspring phenotypes. Indeed, it was thought that sperm-borne histone modifications were unlikely to be involved in the phenomenon of paternal epigenetic inheritance, given that most histones are evicted from the paternal genome during spermiogenesis and replaced by protamines [431,436]. It has now become clear that the remaining of histones in mature sperm are not retained randomly, but instead serve critical functions for proper spermatogenesis progression and embryonic development [219–222]. Nevertheless, a few studies have assessed whether paternal factors can impact sperm nucleosome positioning and histone modifications.

In the context of obesity, to date and to the best of my knowledge, only one study has profiled sperm histone methylation to link paternal diet-induced obesity with offspring metabolic disturbances in mammals [539]. Although authors claim to detect diet-associated changes in H3K4me1 enrichment, the study only shows comparison across two samples (one sample per experimental group), with changes that appear to occur globally in the genome, suggesting the detected differential H3K4me1 enrichment may only be driven by differences in library sizes. Additionally, the sequencing data is not publicly available, making it impossible to assess the quality of the data. One study has profiled testicular germ cells H3K9me2 enrichment upon low-protein diet feeding, but this was assessed using targeted approaches, restricting the analysis to a few sites and therefore lacking genome-wide information [540]. In another mouse model, folate deficiency was found to be associated with reduced global levels of H3K4me1, H3K9me1, and H3K9m3 in sperm as assessed by Western blot [541]. In humans, sperm samples collected in lean versus obese

men revealed no changes in nucleosome positioning [520], but whether the enrichment of specific histone modifications are altered in sperm in association with BMI values has yet to be assessed.

Because of the lack of studies assessing diet-induced changes in sperm histone modification enrichment, this thesis will focus on exploring the potential role of this epigenetic mark in the molecular mechanisms underlying paternal epigenetic inheritance of obesity. The next subsections highlight the rationale behind the importance to study the implication of histone modification in sperm the transmission of paternally-induced phenotypes.

10.4.3 Evidence sperm histones are important for offspring health

Following the emerging interest in the field of paternal epigenetic inheritance, it remained unclear whether retained canonical histones in sperm and their modifications served any functions or whether they were remnants of incomplete histone-to-protamine exchange. This latter hypothesis was challenged by the intriguing findings that histones are not retained randomly in the genome, but instead are conserved across mammalian species, they are enriched at genes important for spermatogenesis, and importantly at developmental loci, and genes involved in metabolism and cellular processes [220,221,472,542].

While histone modifications in sperm have been overlooked in the field of paternal epigenetic inheritance research, evidence suggests they serve critical roles for proper embryonic development and offspring health. A foundational study using a genetic model of epigenetic inheritance, where males overexpressed the lysine-specific histone demethylase 1A (LSD1 or KDM1A) enzyme specifically in the developing germline, demonstrated for the first time that sperm-borne histone methylation is critical for offspring health [543]. Indeed, the genetic model generated males that have an altered sperm epigenome at the level of histone H3K4me2 and H3K4me3, and that sire offspring with a wide range of developmental abnormalities, reduced survivability, with phenotypes that persisted transgenerationally. KDM1A overexpression in the developing male germline was associated with differential gene expression in two-cell embryos that corresponded with sperm regions bearing differentially enriched H3K4me2 [543]. Further supporting the role of paternal histones for proper embryonic development, is the finding that sperm

H3K4me loss disrupts paternal pronucleus zygotic genome activation [544]. Additionally, embryos derived from spermatids that have not undergone histone-to-protamine exchange, develop less frequently to adulthood than embryos derived from sperm, suggesting a reduced developmental potential for spermatid cells [545,546]. Spermatid-derived embryos also show deregulation of developmental genes, which corresponds with epigenetic differences that distinguish spermatid chromatin from that of sperm [222]. These findings are in accordance with the premise that sperm is epigenetically programmed to regulate gene expression in the embryo.

10.4.4 Evidence sperm-borne histone modifications are transmitted to the embryo

Whether paternal histones are fully reprogrammed shortly after fertilization, or whether they persist to alter embryonic gene expression was unresolved. This open question was purportedly addressed in a report using ultra-low input chromatin immunoprecipitation followed by sequencing (ChIP-seq) protocols on pre-implantation embryos derived by crossing two distinct parental mouse strains, allowing for discrimination of paternal or maternal alleles. The authors claimed H3K4me3 peaks from the paternal allele were fully depleted after fertilization [547]. However, a re-analysis of their data revealed an error in their normalization of paternal reads. Correcting this error revealed that a subset of H3K4me3 regions in sperm are transmitted and retained from the pronucleus stage zygote throughout pre-implantation embryo development [476]. Further evidence supporting the transmission of sperm histones and retention beyond fertilization is the detection of histone H3.3 in the paternal pronucleus of the zygote, a variant that is enriched in sperm [544,548,549]. Although this has yet to be demonstrated in humans, the enrichment of the gene-activating histone mark H3K4me3 in sperm at genes expressed in the pre-implantation embryo, is in accordance with a potential transmission in the human embryo [221].

More recently, a paternal folate deficiency model further supported the transmission of sperm H3K4me3 to alter embryonic gene expression. Feeding males with a folate deficient diet was associated with offspring developmental abnormalities, and induced differential H3K4me3 enrichment in sperm, with 64% of these aberrant epigenetic regions persisting in the 8-cell embryo, of which half showed the same directionality

change from the sperm to the embryo [477]. Furthermore, altered sperm H3K4me3 profiles were associated with the differential gene expression in the 8-cell embryo. This study demonstrated that diet-induced changes in sperm H3K4me3 are transmitted to the embryo, involving paternally-induced intergenerational phenotypes. Collectively, these findings show transmission of sperm H3K4me3 to the embryo, and that some regions bearing H3K4me3 persist during early chromatin remodeling in the embryo.

While there is now evidence that diet-induced obesity can alter the sperm epigenome, exactly how these paternally-inherited epimutations can impact development throughout and program offspring maladaptive metabolic phenotypes *in utero* remains unclear. Additionally, whether these effects can span multiple generations – resulting in transgenerational epigenetic inheritance – remains an open question.

10.4.5 Intergenerational versus transgenerational inheritance

10.4.5.1 Definition

The concept of intergenerational and transgenerational epigenetic inheritance refers to the non-genetic transmission of phenotypes, with inheritance spanning one or multiple generations. Such effects are termed 'transgenerational' when an environmental stimulus to one directly exposed individual (F_0) induces phenotypes to the subsequent *unexposed* generations. Paternal and maternal *transgenerational* epigenetic inheritance therefore differ in that they can be characterized as such when the F_2 and F_3 generations are phenotypically affected, respectively [550,551]. Indeed, in order for a paternal exposure to result in transgenerational effects, the F_2 generation must show a phenotype, given that the F_1 offspring and its germ cells arise from the exposed sperm (F_0). In contrast, the mother will directly expose the fetus (F_1) during gestation, as well as the developing germ cells of the fetus that will give rise to the next generation (F_2) for that reason maternal transgenerational inheritance occurs at the F_3 generation. The next subsections will highlight evidence and mechanisms on the phenomenon of transgenerational epigenetic inheritance in various organisms.

10.4.5.2 Examples of transgenerational inheritance in mammals: epigenetic mechanisms and gaps in knowledge

10.4.5.2.1 In rodents

One of the first examples of transgenerational epigenetic inheritance in mammals was described in mice with endogenous metastable epialleles – variably expressed alleles in isogenic individuals. The viable yellow agouti (A^{VY}) and the Axin fused ($Axin^{Fu}$) alleles are classical models, which arise from the random insertion of an intracisternal A particle (IAP) retrotransposon upstream or inside a gene, controlling its expression in an epigenetic-dependent manner [41,552,553]. The A^{VY} insertion occurs upstream of the *Agouti* murine gene, a gene that promotes the production of yellow pigment in follicular melanocytes, and act on melanocortin receptors to inhibit leptin anorectic effects. The epiallele insertion resulted in constitutive and ectopic Agouti expression, causing yellow fur, obesity and tumorigenesis in these mice, with variable degrees of the phenotypes related to the degree of DNA methylation at the IAP locus. These effects were shown to be maternally transmitted – but not paternally – and this parent-of-origin effect is thought to arise from differences in IAPs epigenetic reprogramming between the male and female germline, and across paternal and maternal genome after fertilization [551]. Similarly, the $Axin^{Fu}$ IAP metastable epiallele occurs within an intron of the *Axin* gene, which encodes the axin protein which plays roles in embryonic axis formation. Consequently, $Axin^{Fu}$ mice show tail kinks, with variable severity of the kink in the tail depending on the state of methylation at the IAP [554]. Both the A^{VY} and $Axin^{Fu}$ models showed transgenerational transmission of phenotypes.

More recently, another genetic model of transgenerational epigenetic inheritance has been established. A hypomorphic mutation in the methionine synthase reductase (Mtrr) enzyme – responsible for utilizing methyl groups generated in the folate cycle – showed transgenerational transmission of congenital malformations over five generations through either maternal grandparents [555]. These effects were associated with differentially methylated regions (DMRs) in F_0 sperm that did not persist in offspring (F_1-F_2) embryos, placentas, and somatic tissue [556]. Some of the sperm DMRs corresponded with altered somatic gene expression in F_2 embryos and adult livers and F_1-F_3 embryos, including that of *Hira* – a histone chaperone – which was considered a reflection of transcriptional

memory of the associated germline DMR. It remains to be determined how misexpression of *Hira* persists across generations through the sperm. A proposed mechanism was through altered histone methylation, given that embryonic stem cells are enriched for H3K4me3 at the DMR genomic location. It was also speculated that aberrant sperm epigenetic patterns could be reprogrammed and then stochastically re-established, which would explain inter-individual variability in the phenotypes observed.

In terms of transgenerational responses to environmental or nutritional exposures, previous studies have focused on models of over- or under-nutrition, endocrine-disrupting chemical exposure, stress, and drug-induced diabetes [521,557–560]. These studies detected exposure-associated changes in sperm at the level of DNA methylation and non-coding RNA content, but the contribution of these marks in the non-genetic transmission of phenotypes remains ill-defined. Indeed, the implication of DNA methylation in sperm in the transmission of diet-induced phenotypes has been challenged, given that stochastic variation appeared to show a greater contribution to the sperm methylome than that associated with dietary treatment [561]. Additionally, several studies detecting sperm DMRs failed to detect corresponding epigenetic or transcriptomic alterations in offspring tissue [541,562]. In terms of the acquisition of aberrant RNA content in sperm, this is thought to occur through the transfer of RNA cargoes from somatic to germ cells via extracellular vesicles in the epididymis (also called epididymosomes) [538]. While it was demonstrated that RNA-carrying vesicles can fuse with and transfer RNA molecules to sperm cells *in vitro*, it remains to be confirmed whether this occurs in the epididymis *in vivo* [563]. The mechanism by which this RNA-mediated transmission could occur transgenerationally also remains unresolved. Further contributing to the confusion and controversy in this field of research, some studies state detecting paternally-induced transgenerational effects, when solely the F_1 generation was being assessed, permitting only intergenerational characterization [564]. Consequently, the evidence for transgenerational epigenetic inheritance is scarce and these exposure studies remain to be independently replicated. It is also still unclear how sperm-borne epigenetic alterations can be transmitted over multiple generations.

10.4.5.2.2 In humans

Transgenerational inheritance of phenotypes in humans – as highlighted in previous sections of this chapter – have been described in several epidemiological studies, linking grandparental nutritional states with heightened risk for complex diseases. While these studies paved the way for the DOHaD and transgenerational inheritance research fields, demonstrating transgenerational epigenetic inheritance mechanisms in humans is difficult. Indeed, such retrospective epidemiological studies are confounded by cultural and ecological factors. These studies have received tremendous attention through media coverage but have also been criticized given the important claims made with limitations in study design and statistical approaches used. First, the sample sizes were relatively small, especially for such epidemiological studies. Additionally, authors claimed to observed sex-specific effects, but it appeared that these effects were not hypothesized *a priori*, and instead arose from the results [204]. Additionally, there were many parameters assessed, implying high number of multiple testing with small sample size. In other words, these studies involve small sample sizes, hypotheses that are not predefined and instead are established after results are generated, and excessive multiple testing [214]. Better designed studies with larger sample size, and independent validations would be required to provide more convincing evidence of the phenomenon in humans.

10.4.5.3 Challenges and gaps in knowledge

Collectively, whether transgenerational inheritance can have an epigenetic basis in mammals – especially in humans – remains controversial. Proving such phenomenon in humans is extremely challenging, especially with current reliance on retrospective studies with confounding factors that are impossible to rule out. Additionally, studies describing epigenetic inheritance effects in mammals often show inter- rather than transgenerational effects, or do not exclude a genetic basis initiating the heritability of phenotypes.

In order to prove such transgenerational epigenetic inheritance mechanism in mammals, genetic, cultural and ecological confounding factors must be ruled out. This can only be achieved by using isogenic animal models in strictly controlled environment. The use of *in vitro fertilization* (IVF) should be used in order to rule out any intrauterine or semen factors, and instead ensure exclusive gametic transmission. Nevertheless, it is

worth mentioning that IVF has been linked to epigenetic changes which could potentially impact the findings [565,566]. Lastly, to show proof-of-concept that a specific epigenetic mark plays a causal role in the transmission of phenotypes, the specific mark should be manipulated to show that the effect is lost when the mark is erased/removed, and that the effect is gained once the mark is reintroduced. With non-coding RNA, this can be done via microinjection of RNA molecules in the zygote, as has been previously performed in paternal high-fat diet and stress models [514,557,567]. For histone modifications and DNA methylation epigenetic marks, epigenome editing methods using CRISPR-dCas9 systems can be leveraged [568]. However, these methods can be challenging especially if more than one locus is being targeted at once. Overall, true transgenerational epigenetic inheritance mechanisms are extremely challenging to prove in mammals, and even more so in humans.

10.4.6 Potential role of the placenta in the developmental origins of paternally-induced phenotypes

The placenta is an extraembryonic tissue that is critical for proper fetal development as it functions to deliver nutrients and oxygen to, and remove metabolic waste from, the fetus, produce pregnancy-associated hormones, synthesize glycogen and cholesterol, regulate the maternal immune system to prevent the rejection of the allogeneic fetus, and more. This temporary organ arises from the trophectoderm upon the first cell fate decision between the inner-cell mass and trophoblast lineages established early in development by the blastocyst stage [569]. Post-implantation, trophoblast cells invade the maternal decidua to remodel the vasculature which facilitates the flow of maternal blood to the placenta and thereby the fetus [570,571]. This transient organ is fully formed at embryonic (E)14.5 day in mice and 10 to 12 weeks in humans [572].

The mature mouse placenta can be divided into three major functional regions – the decidua, the junctional zone and the labyrinth. The junctional zone is located directly beneath the decidua and is comprised of cells that serve endocrine and metabolic functions, including trophoblast giant cells, spongiotrophoblasts, and glycogen cells

[573,574]. The labyrinth lies beneath the junctional zone, and its architecture permits to maximize surface area for efficient exchange between the maternal and fetal blood [575,576].

Placenta function can influence the development of specific embryonic organ systems. Indeed, gene knockouts that induce placental defects are significantly more prone to exhibit abnormal brain, heart and vascular system development, in comparison with knockouts that do not impact placentation [577]. Such influence may occur through placenta production of various factors including neurotransmitters, hormones, and growth factors [578,579]. For example, the placenta produces serotonin, dopamine, epinephrine, and norepinephrine, which have been postulated to influence brain functions [580]. Importantly, changes in placental serotonin production may put the fetus at greater risk to develop neurobehavioral disorders such as autistic spectrum disorders and anxiety-like behaviours.

Placental abnormalities can be classified as structural, implantation, and functional anomalies. These placental defects can impact decisions related to delivery methods and timing, but also result in complications that can be fatal for both the mother and the fetus, such as serious hemorrhage, and fetal growth restriction (FGR). FGR can result from placental insufficiency, whereby the placenta fails to deliver sufficient oxygen and nutrients to the fetus. This placental complication can result from various maternal chronic conditions such as pregnancy-induced hypertension, as well as due to idiopathic causes. Intrauterine growth restriction (IUGR) occurs in approximately 10% of pregnancies, and babies born from IUGR can suffer from a number of neonatal metabolic, hematological, and cognitive disturbances. A deprived intrauterine environment is also associated with low birth weight, which can set the postnatal trajectory for rapid catch-up growth. This catch-up growth process has been linked both in humans and animal models with an imbalanced accumulation in lean versus fat mass and a transition from insulin sensitivity to resistance [581–585]. These early life growth trajectories increase the risk to develop T2D, coronary heart disease, hypertension, and stroke, in adulthood [585,586].

The placenta is of particular interest to study in the context of paternal preconception health. Indeed, the paternal genome is thought to strongly contribute to placental development. Early experimental evidence suggested that the paternal and maternal genome exert divergent but complementary potential for inner cell mass and

trophectoderm development. This was recognized through studies with manipulated mouse embryos, whereby embryos derived from two paternal genomes showed greater developmental potential for the trophoblast lineage than embryos generated with two maternal genomes [587–591]. Further supporting a strong contribution of the paternal genome is the finding that paternally expressed genes are enriched in the placenta [592]. Moreover, paternal factors have been linked to adverse pregnancy outcomes and placental dysfunction. In humans, recurrent pregnancy loss and preeclampsia – a form of placental insufficiency – have been linked to poor semen parameters and paternal metabolic syndrome status, respectively [593,594]. In animal models, advanced paternal age as well as paternal preconception toxicant exposure or folate deficiency, have been associated to alterations in placental gene expression and methylation profiles [541,595,596]. In the context of paternal obesity, paternal high-fat diet alters blastocysts cell allocation ratios to the inner cell-mass versus the trophectoderm lineage [489,491]. More recently, paternal high-fat diet was shown to impact placental functions, with elevated hypoxia and altered vasculature, characteristics of placental insufficiency [597].

Because the placenta plays such critical roles in supporting fetal growth, with implications for adult-onset complex disease risk, and because increasing evidence hint towards a paternal contribution to placental integrity and functions, it suggests this organ represents an important site of action for paternally-induced intergenerational transmission of phenotypes. This possibility will be addressed and further explored in the third chapter of this thesis.

10.5 Research goals and scope of the thesis

The previous sections have highlighted the negative consequences the rapid rise in obesity rates has had on the healthcare system with obesity being associated with numerous adverse health conditions, particularly in the context of an aging population. This condition therefore remains a health priority to tackle due to its prevalence reaching epidemic levels, with rates that are not expected to decrease. Given genetic factors alone cannot fully explain the sharp rise in obesity rates globally, it is also possible that a cumulation of potentially interacting factors, such as behavioural changes surrounding eating patterns and energy expenditure, obesogens exposure, *in utero* programming, as well as generational exposures, could contribute to this obesity epidemic. Consequently, there are implications for parental health status and the non-genetic transmission of complex disease to future generations. Importantly, paternal environmental factors in preconception health have received considerably less attention in public health and there is a lack of public awareness on how men can impact the health of their children. Although little is known on the exact paternal contribution to preconception health, it is clear that a father's environment plays a crucial role in offspring health. Mechanistically, it is known that diets associated with obesity alter the epigenome, including that of the sperm at ncRNA and DNAme. It remains unclear whether diet-induced obesity can also alter sperm histone post-translational modifications (PTMs). More scientific effort is required to focus on identifying molecular mechanisms underlying paternal origins of health and disease (POHaD), identify molecular signatures that could predict pregnancy outcomes including obstetrical complications, translate mechanistic findings to the clinic, and act to limit further spread of noncommunicable diseases.

In light of these knowledge gaps, within the scope of this thesis, I aimed to address these issues through the following aims:

1. Investigate whether paternal obesity can lead to inter- or transgenerational heightened risk to complex disease, and whether these effects are sex-specific.
2. Examine whether diets associated with obesity alter the sperm epigenome at the level of histone modifications.

3. Using a genetic model of epigenetic inheritance combined with a diet-induced obesity model, assess whether there can be cumulative impacts of paternal stressors on the sperm epigenome and on offspring metabolic health.
4. Assess whether there are environmentally-sensitive epigenetic regions in sperm that could impact embryonic or fetal development to program paternally-induced maladaptive responses in the next generation.
5. Interrogate whether paternal obesity influences placenta development, and can be associated with cellular compositions and altered gene expression.

Chapter 2: Sperm histone H3 lysine 4 tri-methylation serves as a metabolic sensor of paternal obesity and is associated with the inheritance of metabolic dysfunction

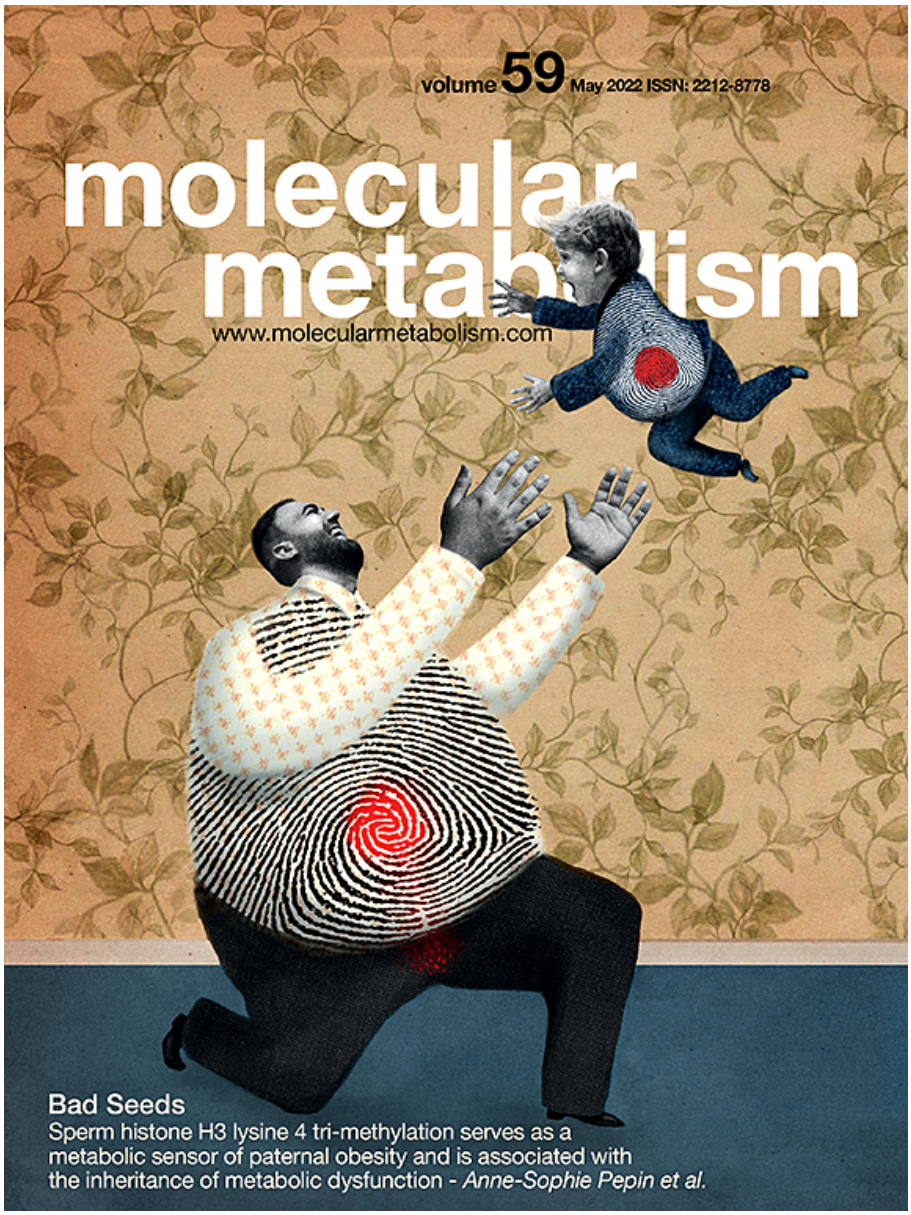

Pepin, A.-S., Lafleur, C., Lambrot, R., Dumeaux, V., Kimmins, S., 2022. Sperm histone H3 lysine 4 tri-methylation serves as a metabolic sensor of paternal obesity and is associated with the inheritance of metabolic dysfunction. Molecular Metabolism 59: 101463, Doi: https://doi.org/10.1016/j.molmet.2022.101463.

11.1 Abstract

Objective: Parental environmental exposures can strongly influence descendant risks for adult disease. How paternal obesity changes the sperm chromatin leading to the acquisition of metabolic disease in offspring remains controversial and ill-defined. The objective of this study was to assess (1) whether obesity induced by a high-fat diet alters sperm histone methylation; (2) whether paternal obesity can induce metabolic disturbances across generations; (3) whether there could be cumulative damage to the sperm epigenome leading to enhanced metabolic dysfunction in descendants; and (4) whether obesity-sensitive regions associate with embryonic epigenetic and transcriptomic profiles. Using a genetic mouse model of epigenetic inheritance, we investigated the role of histone H3 lysine 4 methylation (H3K4me3) in the paternal transmission of metabolic dysfunction. This transgenic mouse overexpresses the histone demethylase enzyme KDM1A in the developing germline and has an altered sperm epigenome at the level of histone H3K4 methylation. We hypothesized that challenging transgenic sires with a high-fat diet would further erode the sperm epigenome and lead to enhanced metabolic disturbances in the next generations.

Methods: To assess whether paternal obesity can have inter- or transgenerational impacts, and if so to identify potential mechanisms of this non-genetic inheritance, we used wild-type C57BL/6NCrl and transgenic males with a pre-existing altered sperm epigenome. To induce obesity, sires were fed either a control or high-fat diet (10% or 60% kcal fat, respectively) for 10-12 weeks, then bred to wild-type C57BL/6NCrl females fed a regular diet. F_1 and F_2 descendants were characterized for metabolic phenotypes by examining the effects of paternal obesity by sex, on body weight, fat mass distribution, the liver transcriptome, intraperitoneal glucose, and insulin tolerance tests. To determine whether obesity altered the F_0 sperm chromatin, native chromatin immunoprecipitation-sequencing targeting H3K4me3 was performed. To gain insight into mechanisms of paternal transmission, we compared our sperm H3K4me3 profiles with embryonic and placental chromatin states, histone modification, and gene expression profiles.

Results: Obesity-induced alterations in H3K4me3 occurred in genes implicated in metabolic, inflammatory, and developmental processes. These processes were associated with offspring metabolic dysfunction and corresponded to genes enriched for

H3K4me3 in embryos and overlapped embryonic and placenta gene expression profiles. Transgenerational susceptibility to metabolic disease was only observed when obese F_0 had a pre-existing modified sperm epigenome. This coincided with increased H3K4me3 alterations in sperm and more severe phenotypes affecting their offspring.

Conclusions: Our data suggest sperm H3K4me3 might serve as a metabolic sensor that connects paternal diet with offspring phenotypes via the placenta. This non-DNA-based knowledge of inheritance has the potential to improve our understanding of how environment shapes heritability and may lead to novel routes for the prevention of disease. This study highlights the need to further study the connection between the sperm epigenome, placental development, and children's health.

Summary sentence: Paternal obesity impacts sperm H3K4me3 and is associated with placenta, embryonic and metabolic outcomes in descendants.

11.2 Introduction

The prevalence of obesity and type II diabetes is growing globally at rates indicating that environment rather than genes is the principal driver. Exposures to high-fat diet, toxicants or micronutrient deficiency can impact our health and that of future generations [518,598–600]. Only now are we beginning to identify mechanisms linking these exposures to parental and offspring health. One connection between environment and health is the epigenome. The epigenome refers to the biochemical content associated with DNA that impacts gene expression and chromatin organization. Uncovering how genomic information is organized and regulated through epigenetic processes to control gene expression and cell functions in the next generation is still in a nascent stage. We and others have shown that errors in epigenomic profiles in sperm can be induced by environmental exposure to toxicants such as those in insecticides and plastics, obesity, and poor diet [477,520,541,562,601,602]. We recently demonstrated that these epigenome changes at the level of chromatin can be transmitted via sperm to alter embryonic gene expression, development, and offspring health [477]. Historically, parental health and fertility have focused predominantly on the mother, although it is clear a father's health and lifestyle can also impact his children's health. How epimutations in sperm functionally impact the embryo urgently require elucidation to prevent transmission of disease from father to offspring.

Metabolic disease including obesity and type II diabetes can in part be attributed to genetic factors with a 5-10% increased risk [76]. The remaining risk is attributable to environmental-epigenetic interactions including potentially those of our ancestors. This possibility is supported by epidemiological and animal studies. Transgenerational effects are suggested by studies in humans that linked the food supply of grandfathers to obesity and cardiovascular disease in their grandchildren [204,603,604]. However, the ability for diet to induce transgenerational effects in animal models remains controversial and requires more in depth studies addressing the underlying molecular mechanisms [493,543,605]. To date, studies using mice to assess the impact of diet and obesity in relation to the sperm epigenome, have focused on the DNA methylome and non-coding RNA (ncRNA) as the potential sperm-borne mediators of metabolic disease [513,517,562–564,606,607]. The role of

sperm chromatin in the non-genetic inheritance of metabolic disorders is unknown. In human and mouse sperm, histone H3 lysine 4 trimethylation (H3K4me3) localizes to genes involved in metabolism and development [477,608,609]. Moreover, sperm H3K4me3 can be altered by folate deficiency and influences embryonic development and gene expression [476,543]. This association of histone modifications in sperm with offspring phenotypes has since been confirmed in other mouse models [610,611]. Based on these observations, we hypothesized that sperm H3K4me3 may serve as a metabolic sensor that is implicated in the paternal transmission of obesity-associated disease in offspring.

A focus of this study was to identify whether paternal obesity impacts the F_1-F_2, and if so, to identify potential mechanisms of this non-genetic inheritance. In our transgenic (TG) mouse model of epigenetic inheritance, male mice overexpress the histone demethylase KDM1A specifically in spermatogenesis, resulting in sperm with alterations in H3K4me2 and me3. Of note, only H3K4me3 has been implicated in transgenerational inheritance in this mouse model [476]. Therefore, as sperm H3K4me3 is responsive to paternal folate deficiency [477], and has been implicated in transgenerational inheritance [476], we targeted this mark in sperm to probe in response to paternal obesity and as a potential mediator of inheritance. In this study, we aimed to: 1) assess the impact of high-fat diet (HFD) induced paternal obesity on sperm H3K4me3 and its association with metabolic dysfunction across generations, and 2) determine if descendants of obese TG sires with a previously altered sperm epigenome would show more severe metabolic dysfunction. To address these aims, we used wildtype (WT), or the germline specific KDM1A-overexpressing TG mice, in combination with a diet-induced obesity model. These TG sires have descended from males that have an altered sperm epigenome and whose ancestors had compromised health (see Materials and Methods for details). This TG model is used to represent an at-risk population that may be more susceptible to poor health when challenged with obesity. Here, we demonstrate that a paternal high-fat diet induces F_0 obesity and metabolic dysfunction in the F_1. Remarkably, transgenerational phenotypes were only observed in descendants of obese KDM1A TG males, and this was associated with enhanced alterations in H3K4me3 enrichment in obese TG sperm. This suggests that the risk of transgenerational disease transmission may be greater if an

ancestor has had prior exposures that cause pre-existing damage to the sperm epigenome. Concordant with the metabolic phenotypes observed in offspring, obesity-induced alterations in sperm H3K4me3 occurred at genes involved in development, placenta formation, inflammatory processes, glucose and lipid metabolic pathways. These sperm altered H3K4me3 regions persist in the embryo and placenta, supporting a role for sperm H3K4me3 in paternal origins of adult-onset metabolic disorders.

11.3 Materials and Methods

11.3.1 Resource availability

11.3.1.1 Lead contact

Further information and requests for resources and reagents should be directed to and will be fulfilled by the Lead Contact, Sarah Kimmins (sarah.kimmins@mcgill.ca).

11.3.1.2 Materials availability

This study did not generate new unique reagents.

11.3.1.3 Data and code availability

The sperm H3K4me3 ChIP-Seq and liver RNA-Seq data generated in this study are available at the following GEO accession number: GSE178096.

11.3.2 Experimental model and subject details

11.3.2.1 Animals

All animal procedures were carried out in accordance with the guidelines of the Faculty Animal Care Committee of McGill University, Montreal. For the wildtype line (WT), C57BL/6NCrl 8-week old males and 6-week old females were purchased from Charles Rivers Laboratory and were allowed one week of acclimation before breeding. For the KDM1A transgenic line (TG), mice were generated as previously described [543], with the same genetic background as the wildtype line. The F_0 TG mice used in this study were from the 11th generation. The earlier generations of mice in this KDM1A TG had severe developmental abnormalities, pre-implantation loss and early post-natal death [543]. Over time we have selected against the severe phenotype by breeding the mice that survive and are normal. Single males were housed with two females to generate the F_0

generation. All animals were given access to water and food *ad libitum* and were maintained on a controlled light/dark cycle.

11.3.3 Methods details

11.3.3.1 Diet experiments and animal breeding

The low-fat control diet (CON; D12450J) and high-fat diet (HFD; D12492) were obtained from Research Diets, and selected based on the matched amounts of sucrose, vitamin mix and folate. Diets' macronutrients composition are listed in Table S1. Males of the F_0 generation were generated from at least 7 different sires per group. F_0 males were weaned at 3 weeks of age and randomly assigned to either a CON or HFD. The number of animals per group, per sex and per generation, used for all metabolic characterization tests can be found in Table S2. Total body weights were monitored weekly. Cumulative caloric intake was recorded weekly by weighting pellets from the food hopper and calculated as kilocalorie per animal. The diet intervention spanned 10-12 weeks followed by 2 weeks of metabolic testing (at 4 months of age), 1 week of rest and 1-2 weeks of breeding with 7-week old C57BL/6NCrl females. Females used for breeding were housed with males overnight (1-2 females per male) and removed the following morning. This was repeated until a vaginal plug was detected, 3 nights per week for a maximum of 2 consecutive weeks. A limitation worth noting is that despite these precautions the females were exposed for a maximum of 6 nights to the HFD pre-pregnancy during this breeding period. However the impacts of this exposure are minimal as female mice require several weeks (~5-8 weeks) before significant weight gain on a HFD [612].

Litter sizes (number of pups per litter) were recorded, and sex ratios (ratio of male pups over total number of pups) were calculated for all litters generated and can be found in Tables S3 and S4, respectively. The same timeline was used to generate the F_1 and F_2 animals. All females used for breeding and all F_1 and F_2 were fed a regular chow diet (2020X Teklad rodent diet, Envigo). All animals were sacrificed at 22 weeks (±2 weeks) by carbon dioxide asphyxiation under isoflurane anesthesia.

11.3.3.2 Metabolic testing

Assessment of metabolic parameters was conducted at 4 months of age within 2 consecutive weeks according to the standard operating procedures of the National

Institutes of Health (NIH) Mouse Metabolic Phenotyping Center [613]. For the glucose tolerance test, animals were fasted overnight for 15 hours (± 1 hour) starting at 6:00PM with free access to water. Blood glucose was measured before and 15, 30, 60 and 120 minutes following an intraperitoneal injection of 2 g/kg of a 20% glucose solution (D-glucose, G7021, Sigma Aldrich) with one drop of blood from the tail-tip using a glucometer (Accu-Chek Aviva Nano). For the insulin tolerance test, animals were fasted for 6 hours (± 1 hour), starting at 9:00AM with free access to water. Blood glucose was measured before and 15, 30, 60 and 120 minutes following an intraperitoneal injection of 1 IU/kg insulin (Insulin solution, I9278, Sigma Aldrich), with one drop of blood from the tail-tip using a glucometer (Accu-Chek Aviva Nano). The area under the curves (AUCs) for the tolerance tests were calculated using the trapezoidal rule (GraphPad Prism, version 8). For the baseline blood glucose levels, blood glucose levels were measured after an overnight fasting of 15 hours (± 1 hour) with one drop of blood from the tail-tip using a glucometer (Accu-Chek Aviva Nano).

11.3.3.3 Tissue collection

At necropsy, mice were dissected to collect adipose tissue (gonadal and mesenteric white adipose depots; gWAT and mWAT, respectively) and a liver lobe (left lateral lobe or *lobus hepatis sinister lateralis* for RNA-sequencing). All tissues were weighed, transferred to a clean tube, snap frozen in liquid nitrogen and stored at -80°C until subsequent downstream experiments. Cauda epididymides were weighed and immediately used for sperm isolation.

11.3.3.4 Sperm isolation

Spermatozoa were isolated from paired caudal epididymides [614,615]. Cauda epididymides were cut into 5 mL of freshly-prepared Donners medium (25 mM $NaHCO_3$, 20 mg ml^{-1} BSA, 1 mM sodium pyruvate, 0.53% vol/vol sodium DL-lactate in Donners stock) and gently agitated to allow to swim out for 1 hour at 37°C. The solution was passed through a 40-µm cell strainer (Fisher Scientific, #22363547) and washed three times with phosphate-buffered saline (PBS). The swim out and the cleaning steps remove 99% of contaminating somatic cells which is visually confirmed and has been validated in our prior studies [476,477,543,608,614,615]. The sperm pellet was cryopreserved in freezing medium

(Irvine Scientific, cat. #90128) and kept in a -80°C freezer until the chromatin immunoprecipitation experiment.

11.3.3.5 RNA-Sequencing and library preparation

RNA extraction was performed using the RNeasy Mini Kit (Qiagen, cat. #74104) following the manufacturer's protocol with slight modifications. In brief, 15-20 mg of liver lobes were cut on dry ice using a sterile scalpel and Petri dish. Samples were lysed in 350 µL of a denaturing buffer (*Buffer RLT* with beta-mercaptoethanol) and homogenized with homogenizer pestles. Lysates were centrifuged at maximum speed for 3 minutes and the supernatants transferred to a clear tube. Ethanol (50%) was added to lysates to promote selective binding of RNA molecules to the silica-based membrane when applied to the spin columns. To avoid genomic DNA contamination, an additional DNase digestion was performed. Finally, membranes of the spin columns were washed twice with 500 µL of *Buffer RPE* and total RNA was eluted using 30 µL of RNase-free water. Libraries were prepared and sequenced at the *Génome Québec Innovation Centre* with single-end 50 base-pair (bp) reads on the illumina HiSeq 4000 and paired-end 100 bp reads on the illumina NovaSeq 6000 S2 sequencing platforms.

11.3.3.6 ChIP-Sequencing and library preparation

Chromatin immunoprecipitation was performed as we have previously described [614,615]. In brief, spermatozoa samples in freezing media were thawed on ice and washed with 1 mL phosphate-buffered saline. For each sample, two aliquots of 10 µL were used to count spermatozoa in a hemocytometer under microscope, and 10 million spermatozoa were used per sample (n=5 sample per group). Sperm chromatin was decondensed in 1 M dithiothreitol (DTT; Bio Shop, #3483-12-3) and the reaction quenched with N-ethylmaleimide (NEM). Samples were lysed in lysis buffer (0.3 M sucrose, 60 mM KCl, 15 mM Tris-HCl pH 7.5, 0.5 mM DTT, 5 mM $McGl_2$, 0.1 mM EGTA, 1% deoxycholate and 0.5% NP40). An MNase enzyme (15 units; Roche, #10107921001) was added to aliquots containing 2 million spermatozoa in an MNase buffer (0.3 M sucrose, 85 mM Tris-HCl pH 7.5, 3 mM $MgCl_2$ and 2 mM $CaCl_2$), for exactly 5 minutes at 37°C. The digestion was stopped with 5 mM EDTA. Samples were centrifuged at maximum speed for 10 minutes, and the supernatants of aliquots from each sample were pooled back together. Each tube was supplemented with a protease inhibitor to obtain an 1X solution (complete Tablets

EASYpack, Roche, #04693116001). Magnetic beads (DynaBeads, Protein A, Thermo Fisher Scientific, #10002D) were pre-blocked in a 0.5% Bovine Serum Albumin (BSA, Sigma Aldrich, #BP1600-100) solution for 4 hours at 4°C and then used to pre-clear the chromatin for 1 hour at 4°C. Pulling down of the pre-cleared chromatin was performed with the use of magnetic beads that were previously incubated with 5 µg of antibody (Histone H3 Lysine 4 trimethylation; H3K4me3; Cell Signaling Technology, cat. #9751) for 8 hours at 4°C. Immunoprecipitation of the chromatin with the beads-antibody suspension was performed overnight at 4°C. Beads bound to the chromatin were subjected to a 3-step wash, one wash with Washing Buffer A (50 mM Tris-HCl pH 7.5, 10 mM EDTA, 75 mM NaCl) and two washes with Washing Buffer B (50 mM Tris-HCl pH 7.5, 10 mM EDTA, 125 mM NaCl). The chromatin was eluted in 250 µL of Elution Buffer (0.1 M $NaHCO_3$, 0.2% SDS, 5 mM DTT) by incubating the beads twice (2 x 125 µL) shaking at 400 rpm for 10 minutes at 65°C, vortexing vigorously and transferring the chromatin elute in a clean tube. The eluted chromatin was finally treated with 5 µL of RNase A (Sigma Aldrich, #10109169001) by shaking in a thermomixer at 400 rpm for 1 hour at 37°C, and then with 5 µL of Proteinase K (Sigma Aldrich, #P2308) overnight at 55°C. DNA was extracted and purified using the *ChIP DNA Clean and Concentrator kit* (Zymo Research, #D5201) using the manufacturer's protocol, eluted with 25 µL of the provided elution buffer. Size selection of the mononucleosomes (147 bp) was performed with the use of Agencourt AMPure XP beads (Beckman Coulter, #A63880). Libraries were prepared in-house using the Ultra-low Input Library kit (Qiagen; #180495). Libraries were sequenced with single-end 50 bp reads on the illumina HiSeq 4000 sequencing platform (n=5 samples per experimental group).

11.3.3.7 Pre-processing

11.3.3.7.1 Liver RNA-Sequencing data

All samples were processed with the same parameters with the exception of those sequenced on the NovaSeq platform to adapt for paired-end sequencing and sequencing read length. Reads were trimmed using *Trim Galore* (version 0.5.0, parameters for HiSeq: --phred33 --length 36 -q 5 --stringency 1 -e 0.1; parameters for NovaSeq: --paired --retain_unpaired --phred33 --length 36 -q 5 --stringency 1 -e 0.1) [616]. Trimmed reads were aligned to the *Ensembl* Genome Reference Consortium mouse reference 38 (GRCm38)

primary assembly using *hisat2* (version 2.1.0, parameters: -p 8 --dta) [617]. Aligned files with SAM format were converted to binary SAM format (BAM) and sorted by genomic position using *SAMtools* (version 1.9) [618]. Transcripts were assembled and gene abundances calculated using *Stringtie* (version 2.1.2, parameters: -p 8 -e -B -A) [619].

11.3.3.7.2 Sperm ChIP-Sequencing data

Sequencing reads were trimmed using *Trimmomatic* on single-end mode to remove adapters and filter out low-quality reads (version 0.36, parameters: 2:30:15 LEADING:30 TRAILING:30) [620]. Trimmed reads were aligned to the *Mus Musculus* mm10 genome assembly using *Bowtie2* (version 2.3.4) [621]. Unmapped reads were removed using *SAMtools* (version 1.9) [618], and those with 3 mismatches or more were filtered out using *Perlcode*. BAM coverage files (BigWig) were generated using *deeptools2 bamCoverage* function (version 3.2.1, parameters: -of bigwig -bs 25 -p 20 --normalizeUsing RPKM -e 160 --ignoreForNormalization chrX) [622].

11.3.3.7.3 Other publicly available ATAC-Sequencing or ChIP-Sequencing datasets

Raw files were downloaded from the National Centre for Biotechnology Information (NCBI) using the Sequencing Read Archive (SRA) Toolkit for 2-cell H3K4me3 ChIP-Seq [623] (GEO: GSE73952), MII oocyte H3K4me3 ChIP-Seq [547] (GEO: GSE71434), sperm ATAC-Seq [471] (GEO: GSE79230), 4-cell and morula ATAC-Seq [624] (NCBI SRA: SRP163205), TE H3K4me3 ChIP-Seq [623] (GEO: GSE73952), and placenta H3K4me3 ChIP-Seq [625] (GEO: GSE29184). Files were pre-processed as described above for the sperm H3K4me3 ChIP-Sequencing with slight modifications to adapt for datasets with paired-end reads and for different sequencing read lengths.

11.3.3.7.4 Other publicly available RNA-Sequencing data

Raw files for 4-cell and morula [624] (NCBI SRA: SRP163205), TE [623] (GEO: GSE73952), and placenta [626] (NCBI SRA: SRP137723) RNA-Seq were downloaded from NCBI using the SRA Toolkit. Files were pre-processed as described above for the liver RNA-Sequencing with slight modifications to adapt for datasets with paired-end reads and for different sequencing read lengths.

11.3.3.7.5 Paternal allele 2-cell embryo ChIP-Sequencing data

Raw files for 2-cell H3K4me3 ChIP-Seq [547] (GEO: GSE71434) were downloaded from NCBI using the SRA Toolkit. These datasets from mouse 2-cell embryos were generated

by crossing males and females of different strains, permitting the assignment of reads to the paternal-specific allele. *SNPsplit* (version 0.3.2) was used to build a reference genome with PWK_PhJ single nucleotide polymorphism (SNPs) masked [627]. Reads were aligned to the generated PWK_PhJ SNPs N-masked reference genome using *Bowtie2* (parameters: -p 10 -t -q -N 1 -L 25 -X 2000 --no-mixed --no-discordant). Aligned files with SAM format were converted to binary SAM format (BAM) and sorted by genomic position using *SAMtools (*version 1.9) [618]. *SNPsplit* (version 0.3.2) was used to assign reads to either the paternal (PWK_PhJ) or the maternal (C57BL/6) genome based on SNPs origin. BAM coverage files (BigWig) were generated using *deeptools2 bamCoverage* function (parameters: -of bigwig -bs 25 -p 20 --normalizeUsing RPKM -e 160 --ignoreForNormalization chrX).

11.3.4 Quantification and statistical analysis

11.3.4.1 Visualization and statistical analyses for metabolic characterization

Visualization of the metabolic characterization data was performed using Jupyter Notebook (version 6.0.1) with Python (version 3.7.4), with the use of the following packages: *seaborn* (version 0.9.0) [628], *numpy* (version 1.17.2) [629], and *panda* (version 0.25.2) [630]. The *pyplot* and *patches* modules were loaded from the *matplotlib* library (version 3.4.2) [631]. Statistical analyses were conducted using GraphPad Prism 8. For all tests, a p-value less than 0.05 was considered significant. To assess main effects of time, diet or genotype, and diet-genotype interactions, for the blood glucose curves of the glucose and insulin tolerance tests, and for cumulative energy intake and growth trajectories during the diet intervention, 3-way ANOVA with Geisser-Greenhouse correction was used. Significance for individual time points was tested using multiple t-test with a Holm-Sidak correction. For total body weight, mesenteric and gonadal white adipose tissue weight, baseline blood glucose and the area under the curve for the glucose and insulin tolerance tests, main effects of diet, genotype, and diet-genotype interactions were assessed using 2-way ANOVA. To assess significance for pairwise comparisons of interest, normality was assessed by D'Agostino and Pearson's test to determine whether parametric or nonparametric statistics should be conducted. For parametric tests, an F-test was used to determine whether equal variance can be

assumed. The unpaired t-test or the Welch's t-test was used accordingly. For nonparametric tests, the Mann-Whitney test was used. Litter sizes and sex ratios were analyzed by 2-way ANOVA to assess main effects of genotype and diet, and interaction, followed by Tukey's multiple comparisons test.

11.3.4.2 Bioinformatics analysis

All bioinformatics analyses were conducted using R version 4.0.2 [632].

11.3.4.3 Liver RNA-Sequencing data

Transcripts with a mean count below 10 were filtered out, conferring a total of 27,907 and 45,992 detected expressed transcripts in samples sequenced on the illumina HiSeq and NovaSeq platforms, respectively. The samples tended to cluster by RNA Integrity Number (RIN), which was corrected for in the differential analysis (Fig. S3B). Differential expression analysis was conducted using *DESeq2* (version 1.28.1) [633], by including sample's RIN value and group in the design formula. Independent hypothesis weighting (IHW, version 1.16.0) was used to correct for multiple testing and prioritization of hypothesis testing based on covariate (i.e. the means of normalized counts) [634]. IHW calculates weight for each individual p-value and then applies the Benjamini-Hochberg (BH) procedure to adjust weighted p-values [635]. Finally, we used the Lancaster method to perform a gene-level analysis at single transcript resolution (*aggregation* package, version 1.0.1) [636]. Lancaster applies aggregation of individual transcripts p-values to obtain differentially expressed genes while capturing changes at the transcript level. Genes with a Lancaster p-value below 0.05 were considered significant.

For data visualization, transcript counts were normalized using variance stabilizing transformation without the use of blind dispersion estimation (i.e. with parameter *blind=FALSE*) [633]. This transformation approach translates data on a $\log_2$ scale, allows correction for library size and removes the dependence of the variance on the mean (heteroscedasticity). Variance-stabilized transcript counts were corrected for RIN values using *limma's removeBatchEffect* function (version 3.44.3) [637]. Pearson correlation heatmaps were generated using the *corrplot* package (version 0.88) [638], with samples ordered by hierarchical clustering. Principal component analysis was performed using *DEseq's plotPCA* function, with RIN values and sexes labeled. Heatmaps of differentially expressed genes were generated with the *Pheatmap* package (version 1.0.12) [639], with

transcripts ordered by k-means clustering (n kmeans=2) and samples ordered by hierarchical clustering using complete-linkage clustering based on Euclidean distance. Alluvial plots were generated with *ggplot2* (version 3.3.3) [640], and overlap of differentially expressed genes across genotypes, generations and sexes were determined by the *GeneOverlap* package (version 1.24.0) [641], which uses a Fisher's exact test to compute p-values.

11.3.4.3.1 Visualization, Semantic similarity, and Enrichment Analysis of Gene Ontology (ViSEAGO)

Gene ontology (GO) analysis was performed using the *ViSEAGO* package (version 1.2.0) [642]. Gene symbols and *EntrezGene* IDs from the *org.Mm.eg.db* database were retrieved using the *AnnotationDbi* package. GO annotations were retrieved from *EntrezGene* for the *Mus Musculus* species (ID="10090") using the *ViSEAGO EntrezGene2GO* followed by *annotate* functions. ViSEAGO uses topGO to perform GO terms enrichment tests on the sets of genes of interest (differentially expressed genes). We used the Biological Process (BP) ontology category with Fisher's exact test (classic algorithm), and a p-value below 0.01 was considered significant. Results of enrichment tests for each set of genes of interest were then merged and hierarchical clustering was performed based on Wang's semantic similarity distance and *ward.D2* aggregation criterion. Results are visualized on a heatmap where GO terms are ordered by hierarchical clustering based on their functional similarity and GO terms enrichment significance is shown as a color gradient ($-\log_{10}$ p-value) in each set of differentially expressed genes of interest.

11.3.4.4 Sperm ChIP-Sequencing data

To detect genomic regions enriched with H3K4me3 in sperm, we used *csaw* (version 1.22.1) [643] to scan the genome into windows of 150 bp. Windows with a fold-change enrichment of 4 over bins of 2,000 bp (background) were considered enriched. Enriched regions less than 100 bp apart were merged for a maximum width of 5,000 bp, conferring a total of 30,745 merged enriched regions. Counts in enriched regions were normalized using TMM normalization followed by *ComBat's* correction for batch effects (*sva* package, version 3.36.0) [644,645]. Spearman correlation heatmaps and MA-plots were generated using raw and normalized counts at enriched regions using *corrplot* (version 0.88) [638], and *graphics* packages, respectively.

Principal component analysis was conducted on normalized counts in enriched regions, by comparing WT HFD vs WT CON (effect of diet in WT), TG HFD vs TG CON (effect of diet in TG), and WT CON vs TG HFD (combined effects of genotype and HFD). Based on visual assessment of the separation of samples according to dietary or genotype groups along Principal Component 1 (PC1; x axis) or 2 (PC2; y axis), the top 5% regions contributing the PC of interest were selected. Permutational multivariate analysis of variance (PERMANOVA) was conducted to determine whether variation is attributed to dietary/genotype group, using the *adonis* function (*vegan* package, version 2.5-7) [646]. Euclidean distances were used as a metric, 999 permutations were performed, and a $p<0.05$ was considered significant. The directionality change in enrichment was identified based on the positive (up-regulated regions) and negative (down-regulated regions) log_2 fold change values of the median of normalized counts using *gtools' foldchange2logratio* function. Regions with increased and decreased enrichment for each comparison of interest were visualized using *Pheatmap* (version 1.0.12) [639]. Regions distance relative to transcription start site (TSS) were annotated and visualized using the package *chipenrich* (version 2.12.0) [647]. Gene ontology analysis was performed using *topGO* (version 2.40.0) for genes with increased or decreased H3K4me3 enrichment at the promoter region for each comparison of interest. We used the Biological Process (BP) ontology category with Fisher's exact test *weight01Fisher* algorithm [648], and a p-value less than 0.05 was considered significant. Genomic regions with deH3K4me3 were annotated using *annotatr* (version 1.14.0) [649] including CpG annotations and basic genes genomic features. Upset plots were generated using *UpsetR* (version 1.4.0) [650], by ordering each set by frequency and displaying 12 sets. Z-scores were calculated using *regioneR's overlapPermTest* (version 1.20.1) which performs a permutation test (n=1,000 permutations) to assess whether a set of regions is significantly enriched to a specific genomic feature compared to genomic regions from the whole genome [651]. Genome browser snapshots were generated using *trackplot* [652].

To assess linear trends associated with the cumulative exposure of KDM1A overexpression and high-fat feeding in sperm, we ran *DESeq2* (version 1.28.1) on the top 5% regions contributing to Principal Component 2 (PC2; n=1,538 regions) associated with sample separation when comparing WT CON and TG HFD normalized counts. In the

design formula, we included sample's batch information, and assigned a numerical value for each sample based on their group category (WT CON=1, WT HFD=2, TG CON=2, TG HFD=3). Independent hypothesis weighting (IHW) was used to correct for multiple testing and prioritization of hypothesis testing based on covariate (i.e. the means of normalized counts) [634]. Median of normalized counts were used to depict the increased and decreased trend of significant regions (adjusted p-value less than 0.2) across groups recoded on a numerical scale as defined above.

11.4 Results

11.4.1 Paternal obesity induces metabolic phenotypes in a sex-specific manner that are enhanced in KDM1A F_1 and F_2 transgenic descendants

11.4.1.1 Impact of paternal obesity on offspring bodyweight and fat accruement

Beginning at weaning until 20 weeks, inbred C57BL/6NCrl control mice (WT), or KDM1A heterozygous transgenics (TG) were fed either a calorie-dense high-fat diet (HFD; 60% kcal fat), or a sucrose- and vitamin-matched control diet (CON; 10% kcal fat) (Fig. 1A-C and Table S1). Table S2 provides the animal numbers by sex, generation, and genotype for metabolic characterization. In the 2-4 weeks post-weaning, F_0 males on the HFD consumed more calories and gained significantly more weight than CON males irrespective of genotype (Fig. S1A-B). These effects persisted throughout the diet intervention (Fig. S1A-C), with TG HFD males weighing the most at 4 months (Fig. S1C$_i$). This trend continued in the TG male F_1 and F_2 descendants (fed regular chow), with weights being significantly more than the F_1 and F_2 of TG CON and WT HFD (Fig. S1C$_{ii\text{-}iii}$). Indicating sex-specific responses to paternal obesity, in female descendants the changes in body weight and fat deposition differed from males (Fig. S1C-E). To assess fat accruement, we measured visceral mesenteric and gonadal white adipose tissue (mWAT and gWAT, respectively). All male (F_0) on the HFD accumulated more mWAT compared to CON males, with no genotype effect (Fig. S1D$_i$). Male and female F_1 offspring sired by WT HFD or TG HFD had increased mWAT fat mass compared to WT CON and TG CON (Fig. S1D$_{ii}$ and S1D$_{iv}$, respectively). Strikingly, mWAT stores were greater in TG HFD F_1 and F_2 males and females compared to WT HFD descendants (Fig.

$S1D_{ii-v}$). Gonadal fat depots in F_0 males were not impacted by the HFD (gWAT; Fig. $S1E_i$), while male WT HFD F_1 showed increased gWAT, and TG HFD F_1 did not (gWAT; Fig. $S1E_{ii}$). Like for body weight and mWAT, male and female F_2 TG HFD had increased gWAT in comparison to WT HFD (Fig. $S1E_v$). Overall analysis of body weight and fat accruement revealed sex-specific responses in descendants with transgenerational effects of paternal obesity being detected only in the TG HFD descendants of both males and females.

Figure 1

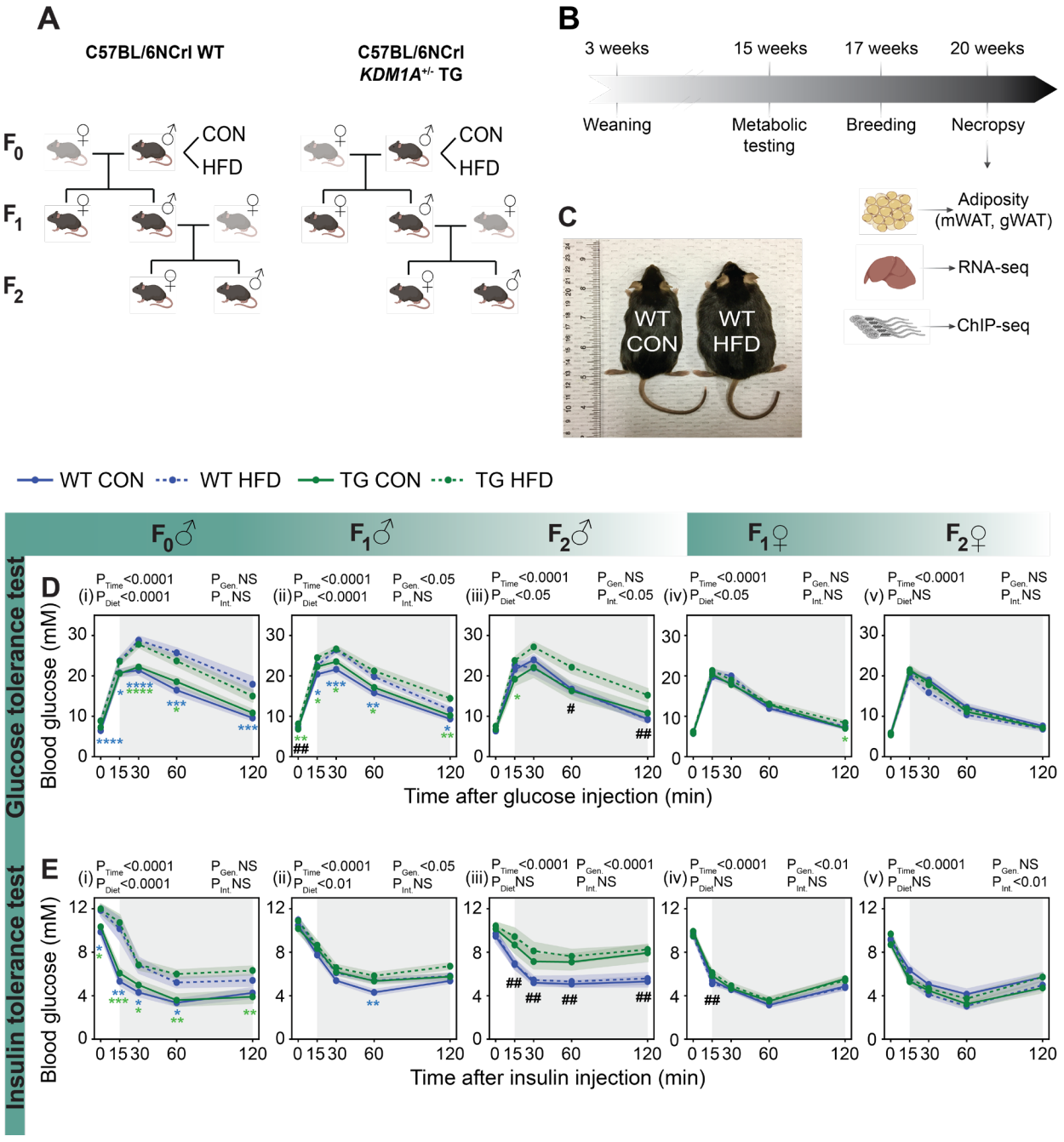

Figure 1: Paternal obesity induces transgenerational metabolic phenotypes in a sex-specific manner that are enhanced in KDM1A descendants.

A) Experimental mouse model depicting breeding scheme and generations studied. Male C57BL/6NCrl (WT) and KDM1A$^{+/-}$ transgenics (TG, C57BL/6NCrl) were fed either a control diet (CON) or high-fat diet (HFD) from weaning for 10-12 weeks, then mated to 8-week-old C57BL/6NCrl females fed a regular chow diet (CD). Animals studied per experimental group: F_0 (n=15-25 males), F_1 (n=28-49 per sex) and F_2 (n=8-21 per sex). Created with BioRender.com. B) Experimental timeline for metabolic testing and downstream experiments performed for each generation (F_{0-2}). Metabolic profiles were measured after the diet intervention at 15 weeks of age and included: baseline blood glucose, and intraperitoneal glucose and insulin tolerance tests (ipGTT and ipITT, respectively). Visceral adipose depots were weighed (mWAT: mesenteric white adipose tissue and gWAT: gonadal white adipose tissue) and the left lateral lobe of the liver used for RNA-sequencing (RNA-seq). Sperm from cauda epididymides were used for chromatin immunoprecipitation followed by sequencing (ChIP-seq), targeting histone H3 lysine 4 tri-methylation (H3K4me3). Created with BioRender.com. C) Age-matched male mice fed either a control (left) or a high-fat diet (right) for 12 weeks. D) Glucose tolerance test. Blood glucose levels before and after (shaded in grey) an intraperitoneal glucose injection, after overnight fasting (15 ±1 hour) at 4 months of age in F_0 males (i), F_1 males (ii), F_2 males (iii), F_1 females (iv) and F_2 females (v). E) Insulin tolerance test. Blood glucose levels before and after (shaded in grey) an intraperitoneal insulin injection, after a 6-hour (±1 hour) fasting at 4 months of age in F_0 males (i), F_1 males (ii), F_2 males (iii), F_1 females (iv) and F_2 females (v). Results are shown as mean ± SEM. Significance for main effects of diet, genotype, time, and for diet-genotype interactions are shown above each graph. NS, not significant (P>0.05). Significance for pairwise comparisons are shown as the following: *P<0.05, **P<0.01, ***P<0.001, ****P<0.0001 (in blue; WT CON vs WT HFD, in green; TG CON vs TG HFD) and $^{\#}$P<0.05, ##$_{P<0.01}$ (WT HFD vs TG HFD). Obtained from [1] (Copyright 2022) with permission from Elsevier.

11.4.1.2 Impact of paternal obesity on glucose homeostasis

Next, we assessed glucose metabolism and insulin sensitivity by glucose tolerance (GTT), and insulin tolerance tests (ITT). These were conducted following the standard operating procedures of the NIH Mouse Metabolic Phenotyping Center [613]. First, we assessed the effects of the HFD on fasting blood glucose. Consumption of a HFD resulted in elevated baseline glucose in male (F_0) WT HFD and TG HFD in comparison to WT CON and TG CON, respectively (Fig. S2Ai). Male TG HFD descendants (F_1), but not WT HFD descendants had significantly elevated fasting blood glucose (Fig. S2A$_{ii}$). In contrast, the glycemic status of all descendant females (F_1 and F_2) did not differ between groups

(Fig. S2A$_{iv-v}$). The same animals used to assess baseline glucose were then given an intraperitoneal glucose challenge and the rate of glucose disposal measured. Analysis of GTT data showed that F_0 WT HFD and TG HFD were glucose intolerant following glucose injection in comparison to F_0 CON males (Fig. 1D$_i$). Indicating that there were intergenerational effects of paternal obesity, elevated glucose levels persisted across the GTT time-course for the F_1 WT and TG HFD males (Fig. 1D$_{ii}$). Interestingly, glycemic response impairments persisted in the F_2 generation of male descendants of TG HFD only (Fig. 1D$_{iii}$). Although fat measures were impacted in female F_1 and F_2 HFD, they did not exhibit glucose impairment (Fig. 1D$_{iv-v}$). Analysis of the area under the curve (AUC) for the GTT was consistent with the male and female glycemic responses shown in the glucose curves (Fig. S2B$_{i-v}$). In line with the observed glycemic responses, the insulin tolerance test and the corresponding AUC demonstrated that male F_0 WT HFD and TG HFD were insulin insensitive (Fig. 1E$_i$ and S2C$_i$). Analysis of the AUC indicated that F_1 WT HFD and F_1 TG HFD were insulin insensitive (Fig. S2C$_{ii}$). Like the glucose tolerance test, there were more pronounced impairments revealed by the ITT for the F_1 TG HFD in comparison to the F_1 WT HFD and only the F_2 TG HFD showed impaired insulin sensitivity (Fig. 1E$_{iii}$ and Fig. S2C$_{ii-iii}$). Like the GTT, there was no indication of insulin impairment in female HFD F_1 nor F_2 (Fig. 1E$_{iv-v}$ and Fig. S2C$_{iv-v}$).

To summarize, the effects of paternal high-fat diet on glucose homeostasis were sex-specific; male descendants had impaired glucose homeostasis, whereas females did not. Taken together, the assessments of weight and metabolic testing indicate that the TG descendants had enhanced responses to paternal obesity in comparison to WT descendants.

11.4.2 Paternal obesity was associated with altered liver gene expression in the F0-F1 with unique genes being differentially expressed in KDM1A descendants (F1-F2)

Obesity contributes to pathophysiological changes in gene expression in the liver [653]. To determine whether the altered metabolic status of HFD sires and their descendants (F_1-F_2) was associated with differential gene expression in the liver, we performed RNA-sequencing on the left lateral lobe (*lobus hepatis sinister lateralis*) of adult mice (F_0-F_2). Sequencing quality was high with RNA profiles having a Pearson correlation coefficient >

0.8 (Fig. S3A). Interestingly, principal component analysis of sequencing data revealed distinct hepatic transcriptomic profiles between males and females that was independent of experimental group and genotype (Fig. S3C). We compared hepatic transcriptome profiles by diet, sex, genotype and generation using a gene-level analysis at single-transcript resolution [636]. As expected, obesity was associated with differential liver gene expression. Liver from obese F_0 WT males showed differential expression of 2,136 genes in comparison to non-obese F_0 WT males (Fig. 2A, Lancaster $p<0.05$). Similarly, when comparing obese F_0 TG to non-obese F_0 TG, 1,476 genes were differentially expressed (Fig. 2B, Lancaster $p<0.05$). Of these differentially expressed genes (DEGs), 448 were commonly altered by obesity in both the F_0 WT and F_0 TG ($p<0.0001$; Fig. 2_i). To identify which genes were altered due to genotype, we compared WT obese to TG obese and identified 524 DEGs, suggesting that obesity had a unique effect in TG mice due to an interaction between diet and genotype (Fig. 2C, Lancaster $p<0.05$).

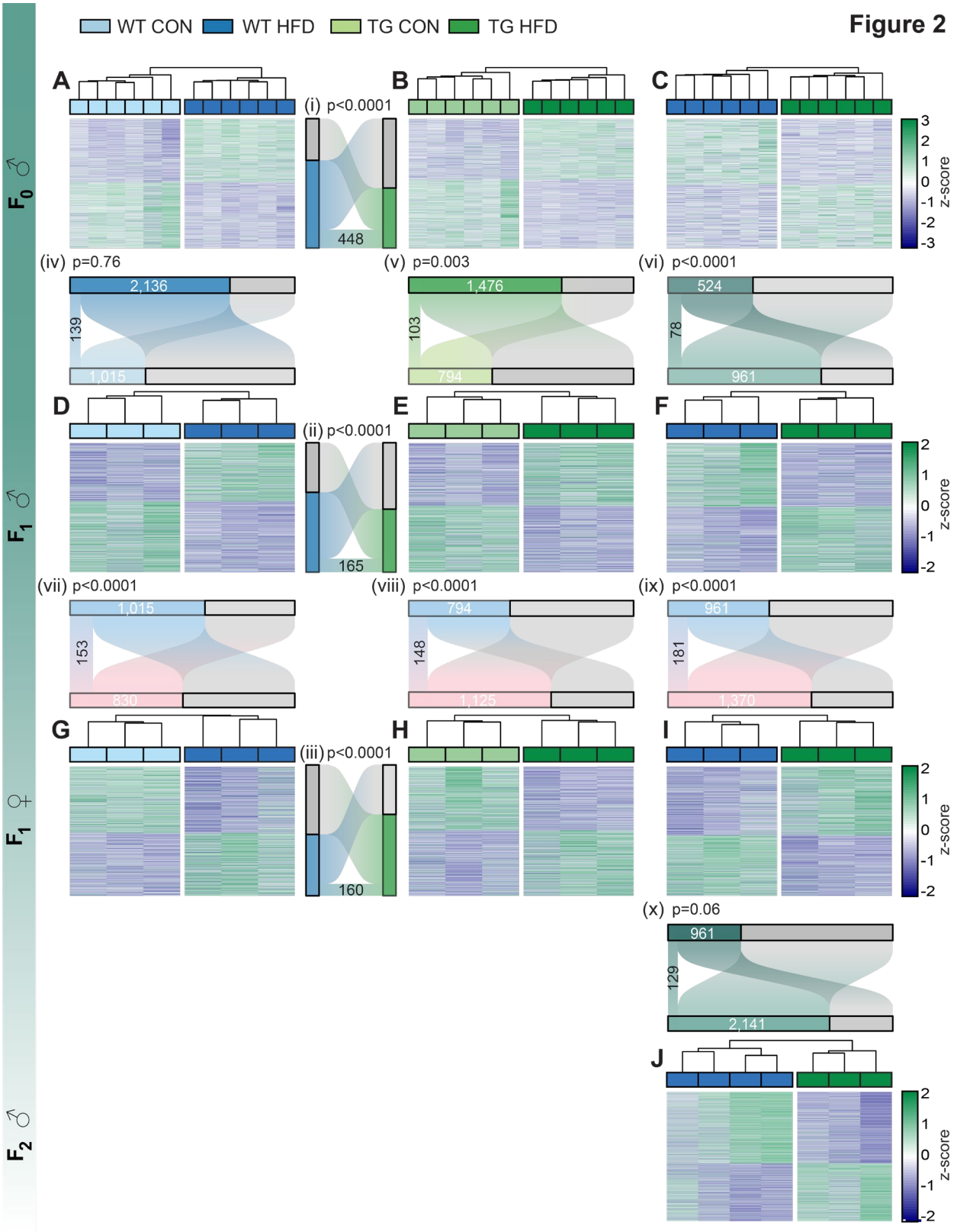

Figure 2: Paternal obesity is associated with altered gene expression in the livers of the F_0-F_2.

A-J) Heatmaps of normalized expression values scaled by row (z-score) for transcripts that code for differentially expressed hepatic genes (Lancaster p-value<0.05) for each comparison assessed across sex and generation. Individual transcripts (rows) are ordered by k-means clustering and samples (columns) are arranged by hierarchical clustering, using complete-linkage clustering based on Euclidean distance. F_0 WT CON vs WT HFD males (A), F_0 TG CON vs TG HFD males (B), F_0 WT HFD vs TG HFD males (C), F_1 WT CON vs WT HFD males (D), F_1 TG CON vs TG HFD males (E), F_1 WT HFD vs TG HFD males (F), F_1 WT CON vs WT HFD females (G), F_1 TG CON vs TG HFD females (H), F_1 WT HFD vs TG HFD females (I), and F_2 WT HFD vs TG HFD males (J). i-x) Alluvial plots depicting frequency distributions of significant (colored boxes) and non-significant (grey boxes) genes for each comparison and their overlap across genotype (i-iii), across F_0 and F_1 males (iv-vi), across F_1 males and females (vii-ix) and across F_1 and F_2 males (x). Significance of overlap between differentially expressed genes lists was calculated by Fisher's exact test. P-values are included for each comparison above the respective alluvial plot. Obtained from [1] (Copyright 2022) with permission from Elsevier.

To determine if the effects of paternal obesity on liver function were intergenerational, we compared the liver transcriptome of male and female F_1. In comparison to F_1 WT CON and TG CON males, livers of F_1 WT HFD and TG HFD, showed differential expression of 1,015 and 794 genes (Fig. 2D and Fig. 2E, respectively, Lancaster p<0.05). A total of 165 DEGs overlapped between F_1 WT and TG (p<0.0001; Fig. 2_{ii}). Of the DEGs between the WT CON and HFD in the F_1, 139 were the same deregulated genes as identified in the F_0 WT CON vs HFD males (p=0.76; Fig 2_{iv}). Similarly, there were 103 shared transcripts identified as differentially expressed between the F_1 TG CON vs HFD, that were also altered in the F_0 TG CON vs HFD (p=0.003; Fig 2_{v}). This suggests that a common set of genes maintain dysfunction as a consequence of direct exposures to obesity and these changes are maintained in the F_1 despite being fed a regular diet. When comparing genes altered by genotype in the F_1 (WT HFD vs TG HFD), 961 were significantly altered (Fig 2F, Lancaster p<0.05), with 78 overlapping DEGs between the F_0 and the F_1 (p<0.0001; Fig 2_{vi}). Demonstrating intergenerational (F_0-F_1) inheritance of metabolic dysfunction at the level of the liver, the metabolic regulators *Btg1* [654], *Cd300lg* [655], *FoxP4* [656], and *E4f1* [657], were differentially expressed in the livers of the obese F_0 and their WT descendants. The overlap in deregulated genes between the F_0 and F_1 indicates that the metabolic phenotypes generated by the paternal HFD persist intergenerationally despite the F_1 being fed a regular chow diet.

The last comparisons in liver transcriptomes were between the F_1 male and female. Despite the female F_1 having no metabolic phenotype detected by our measures, there was significantly altered gene expression in the livers of F_1 female offspring of WT HFD vs WT CON sires (830; Fig 2G, Lancaster $p<0.05$). Of these, 153 were in common with the F_1 male WT HFD sired offspring ($p<0.0001$; Fig 2_{vii}). Likewise, the F_1 female sired by TG HFD had 1,125 DEGs in comparison to females sired by TG CON (Fig. 2H, Lancaster $p<0.05$) with 148 in common with F_1 male TG HFD sired offspring ($p<0.0001$; Fig. 2_{viii}). Of these altered transcripts, 160 were in common between F_1 female descendants of WT HFD and TG HFD ($p<0.0001$; Fig. 2_{iii}). Like the F_1 male TG HFD offspring, there were unique transcripts altered in F_1 female TG HFD offspring (1,370; Fig. 2I, Lancaster $p<0.05$), with 181 differentially expressed in both F_1 males and females ($p<0.0001$; Fig. 2_{ix}). These may reflect genes impacted by genotype regardless of sex. An interesting finding from the F_2 phenotyping was those transgenerational metabolic effects of the HFD were only detected in the male descendants of TG. Therefore, we only profiled F_2 male livers by RNA-seq. This analysis revealed differential expression of 2,141 genes between the F_2 WT HFD and TG HFD (Fig. 2J, Lancaster $p<0.05$) with 129 overlapping with the F_1 WT HFD vs TG HFD males ($p=0.06$; Fig 2_x). We identified 12 genes that showed transgenerational deregulated expression across the F_0-F_2, (WT HFD vs TG HFD), including *Eno3* which has been implicated in glycogen storage [658,659], *Med23* which regulates insulin responsiveness [660], and *Prmt1* an epigenetic regulator implicated in liver glucose metabolism [661–663]. The number of differentially expressed genes increased every generation in comparisons between the WT HFD and the TG HFD (F_0=524, F_1=961, F_2 = 2,141). This sustained deregulated gene expression in the livers of TG HFD F_2, matches the enhanced metabolic phenotypes observed in only F_2 TG HFD males, but not in the F_1 WT HFD.

11.4.3 Paternal diet-induced obesity disrupts gene expression in functional processes that differ between genotypes, sexes and generations

To gain insight into the physiological implications of obesity-induced altered hepatic transcriptomes, we used a gene ontology (GO) approach combined with functional similarity clustering to compare processes in the liver impacted by diet across genotype

and sex, and those impacted by genotype across generation (Fig. 3A-C, Supplemental files 1-3 and Table S5-7) [642]. Interactive heatmaps that facilitate in-depth probing of the gene frequency and the -$\log_{10}$ p-value of enriched GO terms within each cluster are found in Supplemental files 1-3. The non-interactive heatmaps are shown in Fig. 3. Overall, there were similar processes altered by obesity in F_0 WT and TG livers, including lipid, amino acid, and small molecule metabolism (Fig. 3A, Supplemental file 1 and Table S5; clusters 1-5), homeostasis and environmental responses (clusters 8-10), and cellular differentiation and signalling (clusters 11-13). However, the gene frequency (# of genes annotated to that process) within processes differed by genotype.

When the altered functional pathways in F_1 WT CON vs WT HFD were compared between males and females, there were clear impacts of paternal obesity on the liver biological pathways of offspring, and these differed by sex (Fig. 3B, Supplemental file 2 and Table S6). Reflecting sex differences, a greater number of GO terms related to inflammation (cluster 4), and cell cycle, differentiation and signalling regulation (clusters 10-11) were significantly enriched in males compared to females. Of note, genes involved in the regulation of proinflammatory cytokines were particularly enriched in males but not females (clusters 4). This concurs with the more severe phenotypes observed in the males. Conversely, genes involved in DNA/RNA biosynthesis, transcription factors and telomere activity (clusters 1-3), and macromolecule and nitrogen metabolism (cluster 5) were more enriched in females. Interestingly, pathways associated with chromatin and cellular organization and protein metabolism (clusters 8-9) were enriched by paternal obesity in both sexes.

Next, we compared the intergenerational and transgenerational effect of the interaction between the KDM1A transgene with obesity in terms of differences in process enrichment across generations (Fig. 3C, Supplemental file 3 and Table S7). When comparing $F_{0\text{-}2}$ WT HFD with $F_{0\text{-}2}$ TG HFD, there was an increase in the number of significantly enriched GO terms across generations (F_0 male=79; F_1 male=118; F_1 female=159; F_2 male=206; Supplemental file 4). Enriched categories included functions related to inflammation and environmental response (clusters 3-5), metabolic processes (clusters 11-14), and chromatin remodelling and transcription (clusters 17-19). These enriched pathways in hepatic differentially expressed genes might reflect the interaction

between obesity and the KDM1A transgene in the F_0 sperm associated with the uniquely more severe and transgenerational phenotypes in TG HFD descendants (Fig. 3C).

Figure 3

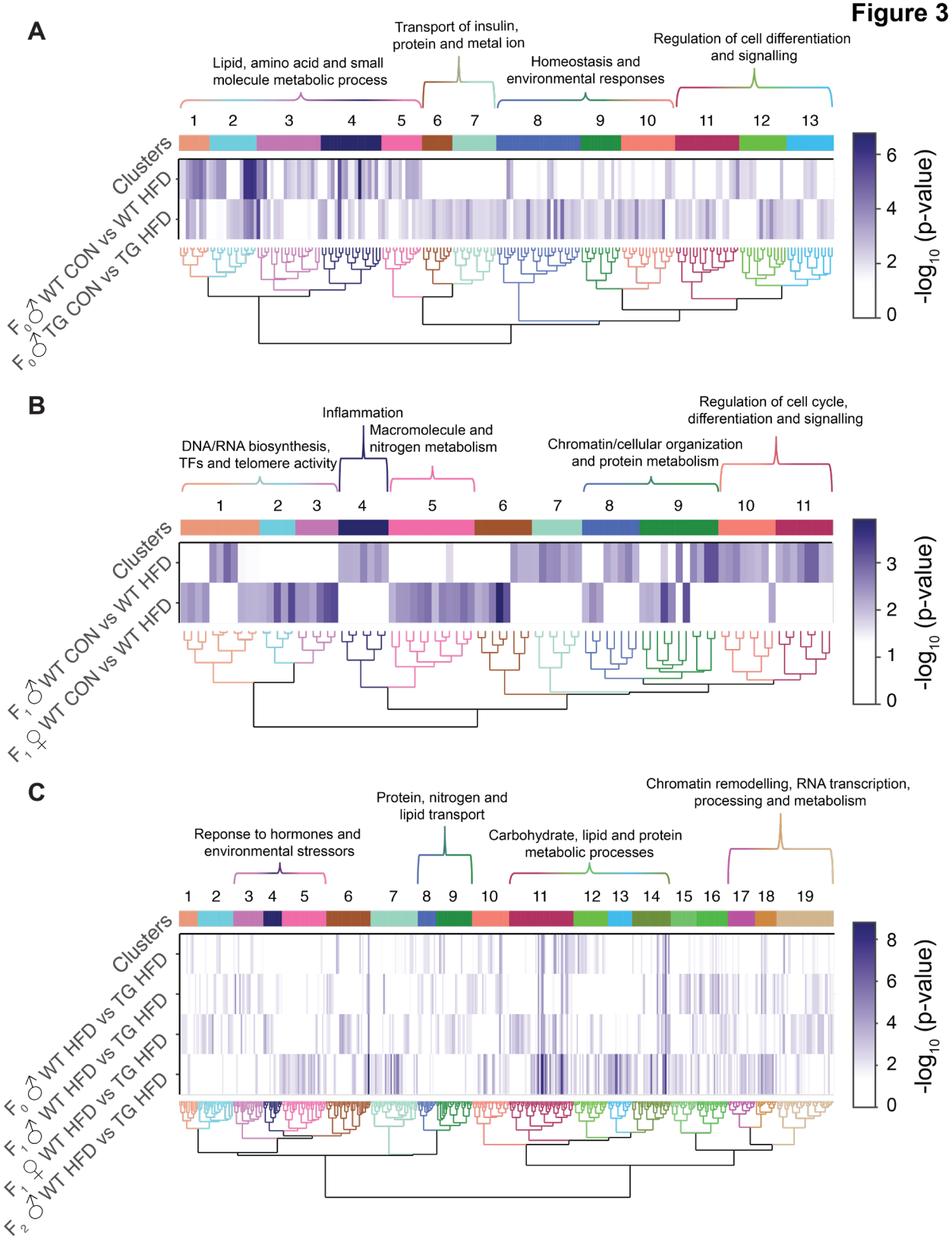
A
Lipid, amino acid and small molecule metabolic process
Transport of insulin, protein and metal ion
Homeostasis and environmental responses
Regulation of cell differentiation and signalling
1 2 3 4 5 6 7 8 9 10 11 12 13
Clusters
F0 ♂ ○ WT CON vs WT HFD
F0 ○ ♂ TG CON vs TG HFD
-log10 (p-value)
6 4 2 0
B
DNA/RNA biosynthesis, TFs and telomere activity
Inflammation
Macromolecule and nitrogen metabolism
Chromatin/cellular organization and protein metabolism
Regulation of cell cycle, differentiation and signalling
1 2 3 4 5 6 7 8 9 10 11
Clusters
F1 ♂ ○ WT CON vs WT HFD
F1 ♀ × WT CON vs WT HFD
-log10 (p-value)
3 2 1 0
C
Reponse to hormones and environmental stressors
Protein, nitrogen and lipid transport
Carbohydrate, lipid and protein metabolic processes
Chromatin remodelling, RNA transcription, processing and metabolism
1 2 3 4 5 6 7 8 9 10 11 12 13 14 15 16 17 18 19
Clusters
F0 ♂ ○ WT HFD vs TG HFD
F1 ♂ ○ WT HFD vs TG HFD
F1 ♀ × WT HFD vs TG HFD
F2 ♂ ○ WT HFD vs TG HFD
-log10 (p-value)
8 6 4 2 0

Figure 3: Obesity-induced hepatic transcriptome disturbances show functional similarities across genotype, sex and generation.

A-C) Heatmaps of significant gene ontology (GO) terms clustered by functional similarity, comparing enriched biological functions for each comparison of interest across genotype (A), sex (B) and generation (C). Columns represent enriched GO terms which are ordered by hierarchical clustering based on Wang's semantic similarity distance and *ward.D2* aggregation criterion. Each row represents a comparison of interest for which enriched GO terms were annotated based on the list of significant genes. The color gradient depicts the GO term enrichment significance (-log10 p-value). Interactive versions of these figures can be found in Supplemental files 1-3 and the complete listsof significantly enriched GO terms can be found in Tables S5-7. Obtained from [1] (Copyright 2022) with permission from Elsevier.

11.4.4 Obesity in combination with germline expression of the KDM1A transgene increases differential enrichment of sperm H3K4me3 at genes involved in metabolism and development

We hypothesized that the sperm epigenome at the level of H3K4me3 would be altered by obesity and that this effect would be enhanced in KDM1A TG males with pre-existing alterations in sperm H3K4me3. To test these hypotheses, we performed native chromatin immunoprecipitation followed by deep sequencing (ChIP-seq) targeting histone H3K4me3, using sperm from individual WT or TG males fed either a CON or HFD (N=5 per experimental group, on average 33.3 million reads per sample with an alignment rate of 97%; Table S8). H3K4me3 localized to 30,745 genomic regions, with a Spearman correlation coefficient of 0.98 between samples (Fig. 4A and Fig. S4). Principal component analysis of H3K4me3 profiles revealed a clear separation of samples according to dietary treatment within genotype groups (Fig. 4B-C). WT samples separated along Principal Component 1 (PC1) with 37.41% of variance attributed to diet (Fig. 4B; PERMANOVA, permutation-based p=0.01). TG samples separated on PC1 with 32.68% of the variability, with diet as the second source of variance (PC2), at 25.56% (Fig. 4C; PERMANOVA, permutation-based p = 0.009).

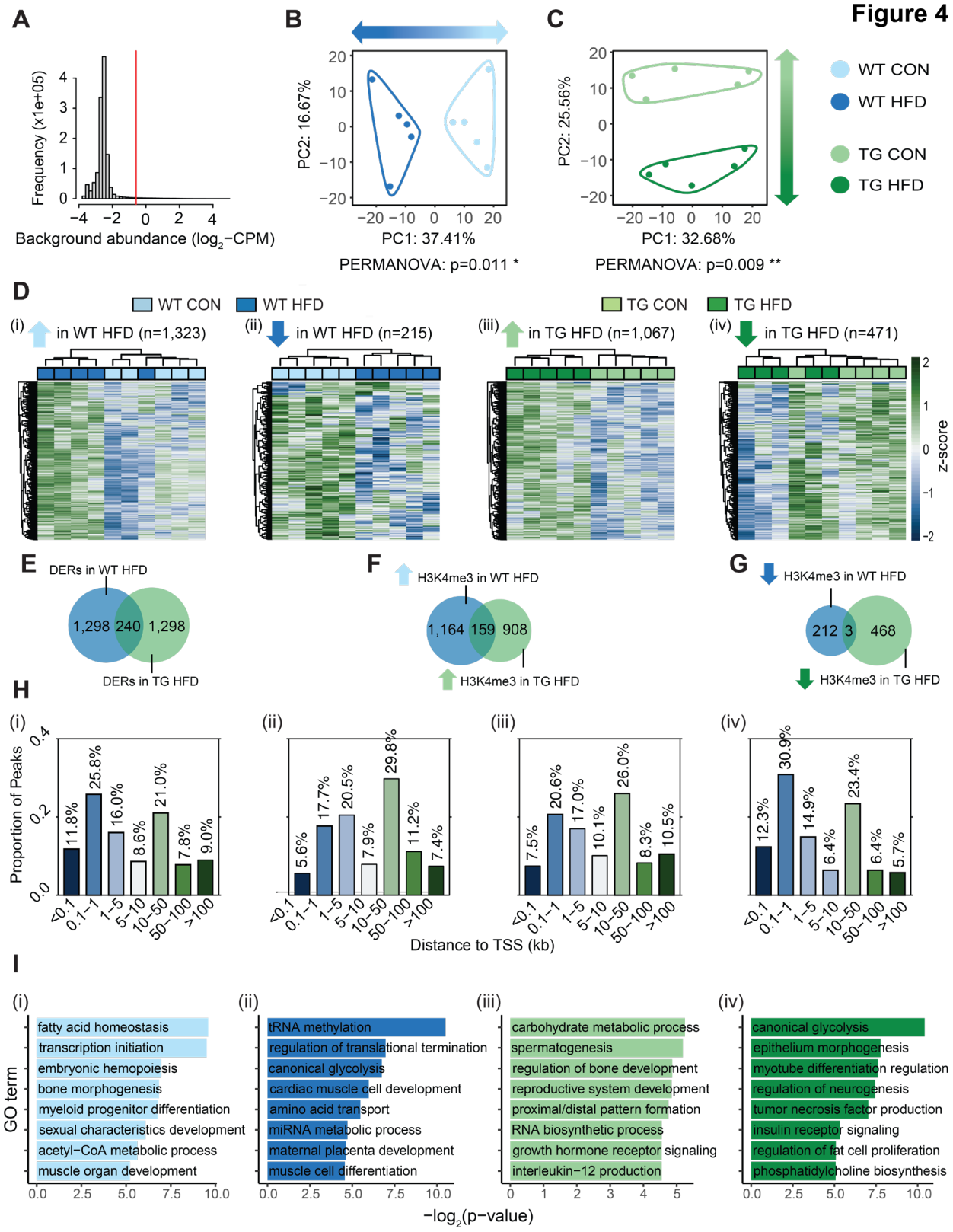

Figure 4: Genomic location, directionality change and functions of regions with altered H3K4me3 enrichment by obesity

A) Histogram showing frequency distributions of read abundances in 150 bp windows throughout the genome. Windows with an abundance below log2(4) fold over background bins of2,000 bp were filtered out as indicated by the vertical red line. Enriched regions less than 100 bp apart weremerged for a maximum width of 5,000 bp, conferring a total of 30,745 merged enriched regions. Reads were counted in merged enriched regions and normalized counts were used for downstream analyses. (seeMaterial and Methods) B-C) Principal component analysis on normalized counts at merged enriched regions comparing WT CON vs WT HFD (B) and TG CON vs TG HFD (C). The top 5% regions contributingto separation of samples along Principal Component 1 (in B; PC1; x axis) or PC2 (in C; y axis) were selected. The PERMANOVA p-values indicating significance associated with dietary treatment are includedunder each PCA plot. D) Heatmaps of log2 normalized counts of deH3K4me3 regions in sperm with increased enrichment in WT HFD (i; n=1,323), decreased enrichment in WT HFD (ii; n=215), increased enrichment in TG HFD (iii; n=1,067) and decreased enrichment in TG HFD (iv; n=471) in each group. Samples (columns) and regions (rows) are arranged by hierarchical clustering using complete-linkage clustering based on Euclidean distance. Colored boxes indicate sample groups (light blue=WT CON, darkblue=WT HFD, light green=TG CON, dark green=TG HFD). E-G). Venn diagrams showing the overlap of deH3K4me3 in sperm of WT HFD (blue) and in TG HFD (green), for all detected regions (E), those gainingH3K4me3 (F) and those losing H3K4me3 (G). H) Barplots showing the distribution of altered regions basedon the distance from the TSS of the nearest gene, for regions with increased enrichment in WT HFD (i; n=1,323), decreased enrichment in WT HFD (ii; n=215), increased enrichment in TG HFD (iii; n=1,067), and decreased enrichment in TG HFD (iv; n=471). The color gradient represents the distance of the regions to TSS in kilobase. I) Gene ontology analysis of diet-induced deH3K4me3 regions at promoters with increased enrichment in WT HFD (i; n=381), decreased enrichment in WT HFD (ii; n=34), increased enrichment in TG HFD (iii; n=230) and decreased enrichment in TG HFD (iv; n=150). Barplots show 8 selected significant GO terms with their respective -log2(p-value). Tables S9-12 include the complete lists of significantly enriched GO terms. Obtained from [1] (Copyright 2022) with permission from Elsevier.

To focus our analysis on the regions most impacted by diet, we selected the top 5% differentially enriched H3K4me3 regions (deH3K4me3, n=1,538) in each genotype (PC1 in WT, PC2 in TG) (Fig. 4D$_{i-iv}$). The genome distribution analysis for specific annotations showed that obesity-sensitive H3K4me3 regions were predominantly located in CpG islands, promoters, exons, and intergenic regions (Fig. S5). To a lesser extent, deH3K4me3 also occurred at transposable elements (LINE, SINE and LTR), where epigenetic de-repression is associated with the use of alternative promoters and long- and short-range enhancers that are implicated in embryo development and pluripotency [664] (Fig. S5). Representative genome browser tracks (Fig. S5) showing enrichment gains and losses for H3K4me3 at gene promoters are shown for *Pde1c* (phosphodiesterase 1C; affects the olfactory system), *Bcdin3d* (RNA methyltransferase; highly expressed in embryonic development), *Sh2d4a* (Sh2 domain containing protein 4A; expressed during development and associated with endocrine and liver function), and *Col15a1* (collagen Type XV alpha 1; involved in cell differentiation and various system development) [665].

Next, we compared the regions of H3K4me3 that were altered by obesity, their genomic location, directionality change and functions between diets and genotype (Fig. 4). As a response to obesity, H3K4me3 enrichment gains were more predominant than losses for both F_0 WT HFD and TG HFD (Fig. 4D). In the WT HFD, 1,323 regions gained and 215 lost H3K4m3 in comparison to the WT CON (Fig. 4D$_{i-ii}$). Similarly, in the F_0 TG HFD sperm, 1,067 regions gained and 471 lost H3K4me3 in comparison to the F_0 TG CON (Fig 4D$_{iii-iv}$). Regions with deH3K4me3 in WT HFD had an 15.6% overlap (240/1,538 regions) with those of TG HFD (Fig. 4E). Of those common 240 regions, 162 had the same directionality change in both WT and TG HFD, with 159 regions with a gain and 3 regions with a reduction in H3K4me3 enrichment (Fig. 4F and Fig. 4G, respectively). The non-overlapping regions of deH3K4me3 in WT HFD and TG HFD sperm could be a consequence of genetic-epigenetic interactions where the TG mice respond uniquely to obesity as was observed in the phenotypic characterization. The proximity to the transcription start site (TSS) of the deH3K4me3 regions in sperm altered by obesity in the F_0 WT HFD and TG HFD were similar (Fig. 4H).

Next, we performed a GO enrichment analysis on promoters to gain functional insight into the genes with obesity-responsive changes in sperm H3K4me3 enrichment

and how they may relate to the developmental origin of offspring phenotypes. Notably, deH3K4me3 genes were identified in processes related to metabolism, inflammatory processes, and one-carbon cycle metabolism (Fig. 4I$_{i\text{-}iv}$; Tables S7-10). Some of the significantly enriched pathways are concordant with disturbed metabolic phenotypes of the F_0-F_2 including for example, carbohydrate metabolic processes, glycolysis, growth hormone signaling and insulin signaling (Fig 4I, Tables S7-10).

The metabolic phenotypes of WT HFD and TG HFD descendants were similar, although the $F_{1\text{-}2}$ TG HFD showed enhanced metabolic abnormalities. We hypothesized that these enhanced metabolic disturbances may relate to the greater degree of H3K4me3 alteration in F_0 sperm, the directionality of the change (gain versus loss), and the functionality of genes bearing alterations. Together these factors could lead to increased disturbances of embryonic metabolic gene expression and more profound adult disease. Interestingly, when comparing WT CON with TG HFD sperm, samples separated along PC2, with 26.69% of variance associated with genotype and diet (Fig. 5A; PERMANOVA, permutation-based p=0.006). Of the top 5% impacted regions selected (n=1,538), a greater proportion showed a gain of enrichment for H3K4me3 in TG HFD sperm in comparison to WT CON (Fig. 5B, n=1,071 regions with gains; Fig. 5C. n=467 regions with losses). We analyzed the detected regions impacted by genotype and diet (n=1,538) for differential enrichment to determine whether obesity in combination with KDM1A overexpression led to greater changes in H3K4me3 enrichment. This analysis identified 264 regions with a significant linear trend, where TG HFD sperm showed a greater degree of change in enrichment, and TG CON and WT HFD showed intermediate changes in comparison to WT CON (Fig. 5D-E, adjusted p<0.2). There were only 9 significant regions with further increase in H3K4me3 in the TG HFD (Fig. 5D), whereas 255 regions showed a greater loss of H3K4me3 enrichment in the TG HFD (Fig. 5E). Consistent with the stronger metabolic phenotypes observed in the TG HFD $F_{1\text{-}2}$, the functional analysis of the promoters showing significant linear trends (n=104) for H3K4me3 across experimental groups occurred at genes implicated in metabolic and cardiovascular disease progression (Fig. 5F, Table S13).

Figure 5

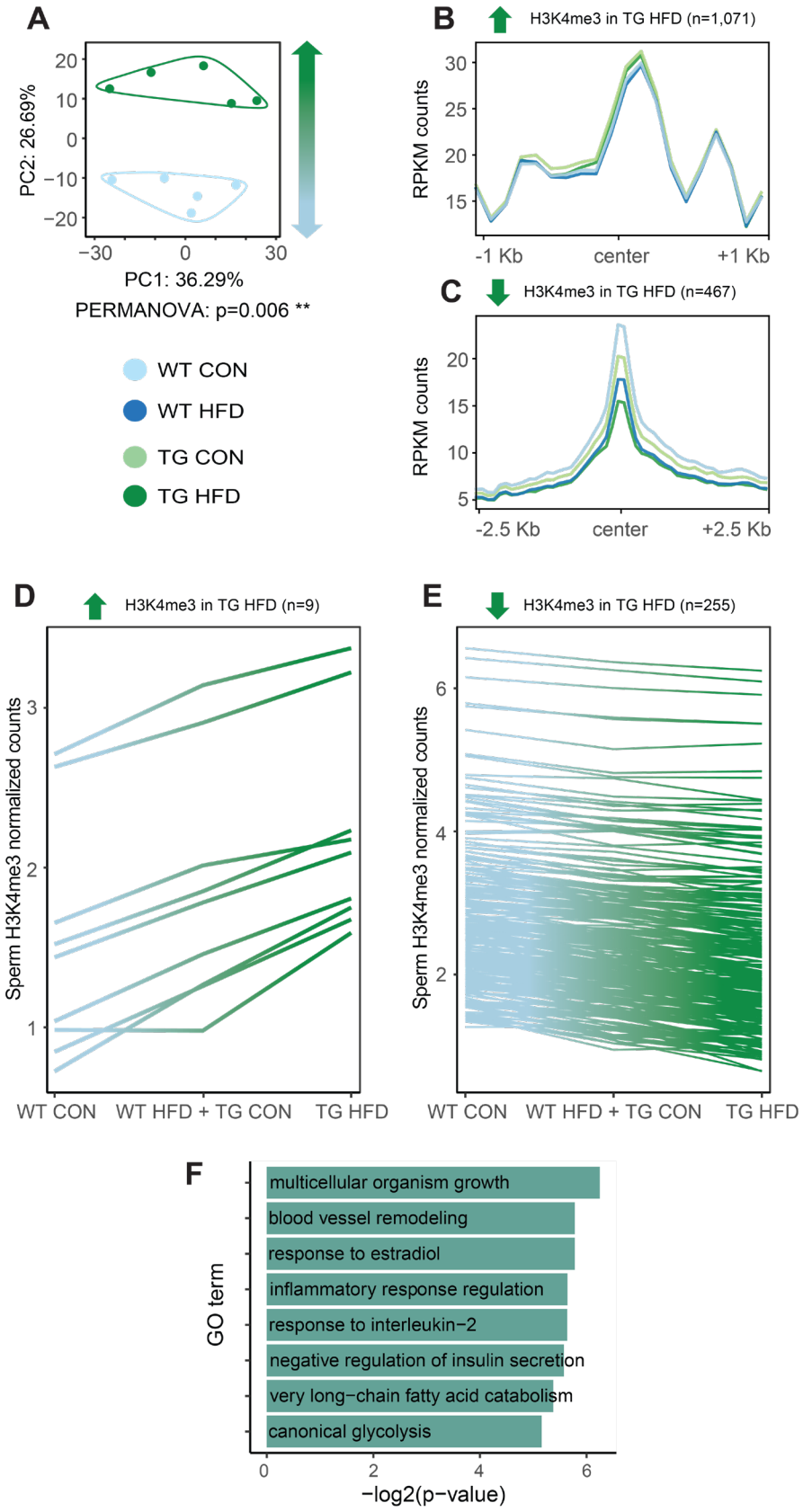
A
PC2: 26.69%
PC1: 36.29%
PERMANOVA: p=0.006 **
WT CON
WT HFD
TG CON
TG HFD
B
H3K4me3 in TG HFD (n=1,071)
RPKM counts
-1 Kb
center
+1 Kb
C
H3K4me3 in TG HFD (n=467)
RPKM counts
-2.5 Kb
center
+2.5 Kb
D
H3K4me3 in TG HFD (n=9)
Sperm H3K4me3 normalized counts
WT CON
WT HFD + TG CON
TG HFD
E
H3K4me3 in TG HFD (n=255)
Sperm H3K4me3 normalized counts
WT CON
WT HFD + TG CON
TG HFD
F
GO term
multicellular organism growth
blood vessel remodeling
response to estradiol
inflammatory response regulation
response to interleukin−2
negative regulation of insulin secretion
very long−chain fatty acid catabolism
canonical glycolysis
−log2(p−value)

Figure 5: Additive effects of KDM1A overexpression and diet-induced obesity in the sperm epigenome at the level of H3K4me3

A) Principal component analysis on normalized counts at merged enriched regions comparing WT CON vs TG HFD. The top 5% regions contributing to separation of samples along Principal Component 2 (PC2; y axis) were selected. The PERMANOVA p-value under the plot indicates significance. B-C) Profile plots of RPKM H3K4me3 counts +/- 1 kilobase around the center of regions with increased H3K4me3 (B) and +/- 2.5 kilobase around the center of regions with decreased H3K4me3 enrichment in TG HFD (C). D-E) Line plots showing the median of normalized sperm H3K4me3 counts for each experimental group at regions showing a significant trend (n=264, adjusted p-value<0.2) with a linear increase in H3K4me3 enrichment (D; n=9) or a linear decrease in H3K4me3 enrichment (E; n=255) from WT CON, WT HFD, TG CON to TG HFD groups. F) Gene ontology analysis on the regions associated with a significant linear trend at promoters (n=104). Barplots show 8 selected significant GO terms with their respective -log2(p-value). Table S13 includes the complete list of significantly enriched GO terms. Obtained from [1] (Copyright 2022) with permission from Elsevier.

11.4.5 Paternal obesity impacts sperm H3K4me3 at regions that coincide with open chromatin and gene expression in pre-implantation embryos

We recently demonstrated that sperm H3K4me3 is transmitted to the embryo and associated with gene expression [477]. We hypothesized that obesity-altered sperm H3K4me3 is transmitted and associated with chromatin accessibility in the early embryo, which in turn could influence gene expression and offspring phenotypes. To assess this possibility, we investigated the relationship between deH3K4me3 in sperm in relation to H3K4me3 in the embryo, the oocyte and open chromatin, and embryonic gene expression [471,547,623,624]. In line with a preferential paternal contribution of H3K4me3 to the 2-cell embryo, regions enriched for H3K4me3 in sperm, including those altered by obesity are not enriched in the oocyte (Fig 6A). There was a strong association between sperm H3K4me3, chromatin accessibility and embryonic gene expression at the 4-cell and morula stages (Fig. 6A-B and Fig. S6A$_i$). Strikingly, sperm H3K4me3 including obesity-sensitive regions are associated with open chromatin in pre-implantation embryos (Fig. 6A-B).

To determine the functional relationship between the H3K4me3 obesity-altered regions and embryonic gene expression, we compared these with 4-cell and morula expressed genes and performed a gene ontology analysis. Of the sperm deH3K4me3

regions overlapping promoters (n=738), 51.8% (n=382) are expressed in the 4-cell embryos, and 44.3% (n=327) are expressed in the morula embryos (Fig. S6A$_{ii}$). To gain insight into what obesity-altered H3K4me3 associated genes in sperm relate to embryonic gene expression, we performed a GO analysis on promoters with deH3K4me3 in sperm and the corresponding genes expressed in 4-cell and morula embryos (Fig. 6C$_{i-ii}$). Again, supporting a role for sperm H3K4me3 in paternal transmission of metabolic disease, gene processes that are specific to metabolism were significantly enriched (Fig. 6C$_{i-ii}$ and Tables S12-13). Taken together these findings suggest a preferential contribution of sperm H3K4me3 in the early embryo that includes obesity-sensitive regions that may be instructive of metabolic-associated gene expression and a direct route for epigenetic inheritance.

Figure 6

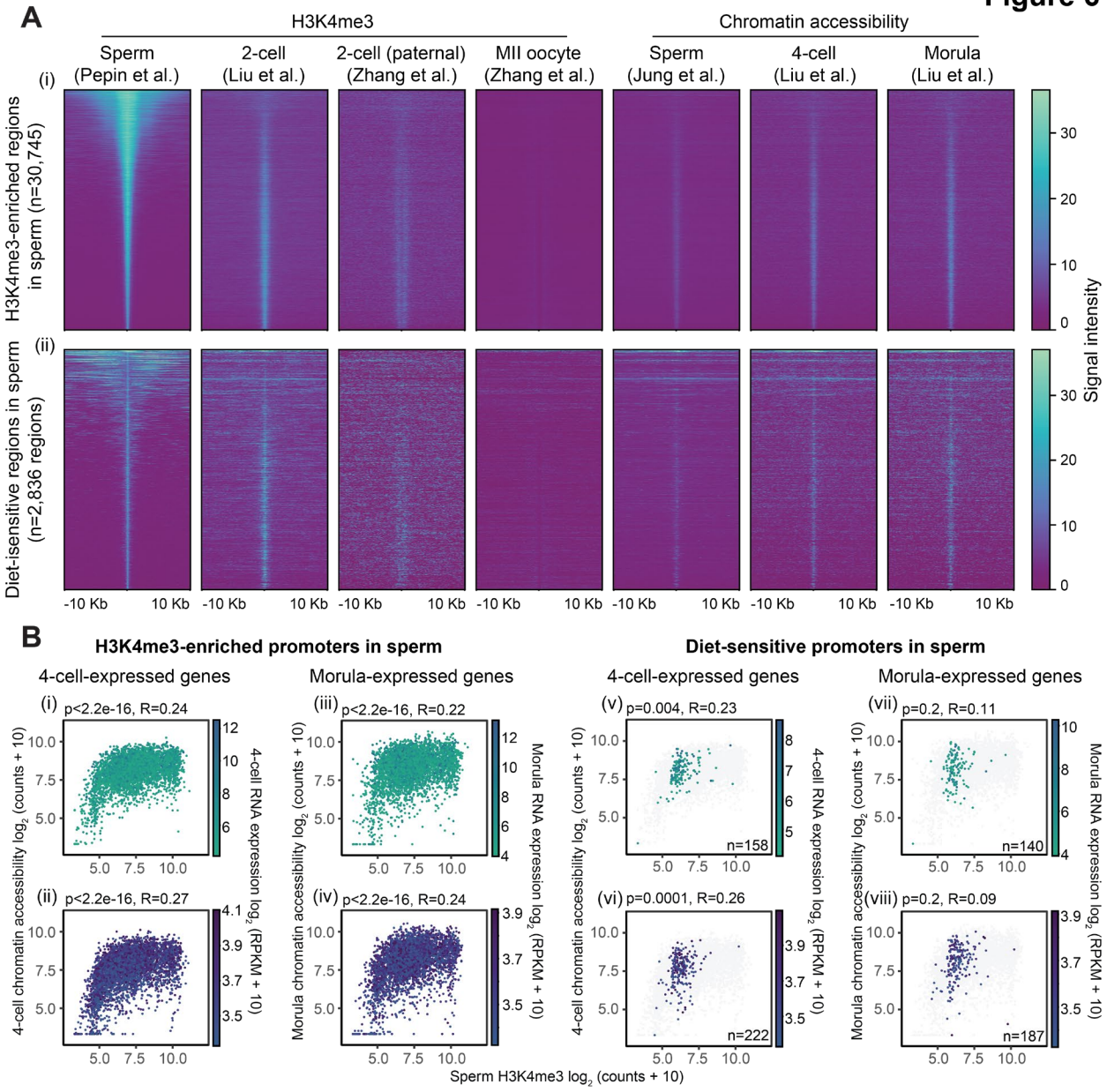
A
H3K4me3
Chromatin accessibility
Sperm (Pepin et al.)
2-cell (Liu et al.)
2-cell (paternal) (Zhang et al.)
MII oocyte (Zhang et al.)
Sperm (Jung et al.)
4-cell (Liu et al.)
Morula (Liu et al.)
(i)
(ii)
H3K4me3-enriched regions in sperm (n=30,745)
Diet-isensitive regions in sperm (n=2,836 regions)
-10 Kb
10 Kb
Signal intensity
B
H3K4me3-enriched promoters in sperm
Diet-sensitive promoters in sperm
4-cell-expressed genes
Morula-expressed genes
(i) p<2.2e-16, R=0.24
(ii) p<2.2e-16, R=0.27
(iii) p<2.2e-16, R=0.22
(iv) p<2.2e-16, R=0.24
(v) p=0.004, R=0.23
(vi) p=0.0001, R=0.26
(vii) p=0.2, R=0.11
(viii) p=0.2, R=0.09
n=158
n=222
n=140
n=187
4-cell chromatin accessibility log2 (counts + 10)
Morula chromatin accessibility log2 (counts + 10)
4-cell RNA expression log2 (RPKM + 10)
Morula RNA expression log2 (RPKM + 10)
Sperm H3K4me3 log2 (counts + 10)
C
Diet-sensitive genes
4-cell-expressed genes
canonical glycolysis
regulation of cell growth
response to oxidative stress
fatty acid homeostasis
cartilage development
muscle organ development
regulation of neurogenesis
mRNA splicing, via spliceosome
-log2(p-value)
Morula-expressed genes
translation
canonical glycolysis
transcription initiation
oxidation-reduction process
myeloid progenitor cell differentiation
carbohydrate metabolic process
histone H3 deacetylation
regulation of cell growth
-log2(p-value)

Figure 6: Sperm H3K4me3 regions sensitive to obesity occur at genes with an open chromatin stateand expressed in the pre-implantation embryo

A) Heatmaps of RPKM counts signal +/- 10 kilobase around the center of regions enriched with H3K4me3 in sperm (i; n=30,745) and regions with obesity- induced deH3K4me3 in sperm (ii; n=2,836) for H3K4me3 enrichment levels in sperm (this study), 2-cell embryo (Liu et al., 2016), 2-cell embryo on the paternal allele and MII oocyte (Zhang et al., 2016), and for chromatin accessibility signal in sperm (Jung et al., 2017), 4-cell embryo and morula embryo (Liu et al., 2019). B) Scatterplots showing H3K4me3 enrichment in sperm (x axis; log2 counts + 10), chromatin accessibility signal (y axis; log2 counts + 10; (Jung et al., 2017)) and gene expression levels (color gradient;log2 FPKM + 10; (Liu et al., 2019)) in 4-cell (i,ii,v,vi) or in morula (iii,iv,vii,viii) embryos, at either all genes with promoters enriched with H3K4me3 in sperm (i-iv) or at diet-sensitive genes (v-viii). The top row of scatterplots includes lowly-expressed genes (bottom 50%) in 4-cell (i and v) or morula (iii or vii) embryos. The bottom row of scatterplots includes highly-expressed genes (top 50%) in 4-cell (ii and iv) or morula (vi and viii) embryos. Pearson's correlation coefficients and their associated p-values are indicated above eachscatterplot, comparing H3K4me3 enrichment in sperm versus H3K4me3 enrichment in 4-cell or morula embryos. C) Gene ontology analysis of genes expressed in the 4-cell (i) or the morula (ii) embryos, overlapping with diet-sensitive promoters in sperm. Barplots show 8 selected significant GO terms with their respective -log2(p-value). Tables S14-15 include the complete lists of significantly enriched GO terms. Obtained from [1] (Copyright 2022) with permission from Elsevier.

11.4.6 HFD alters the sperm epigenome at regions instructive for placenta development

The placenta is a key extra-embryonic organ that represents the uterine-fetal interface and plays a central role in energy allocation, nutrient exchange, and developmental progression. Placental abnormalities have been linked to late onset cardiometabolic diseases, highlighting the importance of the *in utero* environment for metabolic health in adulthood [577]. Our gene ontology analysis on diet-induced deH3K4me3 regions in sperm revealed significant enrichment of genes involved in placenta development (Fig. 4I and Tables S7-10). Given the sperm epigenome influences placental gene expression [592], we were interested in the prospect that diet-induced epimutations in sperm affect placenta gene expression that could influence metabolic phenotypes across generations. To investigate this possibility, we compared the enrichment profiles of H3K4me3 in sperm, with H3K4me3 signal and gene expression data from trophectoderm (TE, the embryonic precursor of placental lineage) [623], and placenta [625,666]. Most regions enriched with H3K4me3 in sperm showed strong H3K4me3 signal in TE and placenta (Fig. 7A), with 65.9% (n=8,663) and 79.4% (n=10,434) of

H3K4me3-enriched sperm promoters (n=13,142) expressed in these tissues, respectively (Fig. S6B$_{i}$). Of the 738 deH3K4me3 regions localizing to promoters in sperm, 56.8% (n=418) were expressed in the trophectoderm, 76.8% (n=567) were expressed in the placenta, and 54.6% (n=403) were expressed in both (Fig. S6B$_{ii}$). Notably, gene ontology analysis of the shared H3K4me3 in sperm with TE and placenta revealed that there was an association with placenta function including at deH3K4me3 regions (Fig. 7B$_{i,iii}$, Tables S14 and S16). The GO analysis of the sperm H3K4me3 regions that were not common with TE and placenta were involved in spermatogenesis, fertilization and sperm function (Fig. 7B$_{ii}$ and iv, Tables S15 and S17).

Next, we compared gene enrichment of sperm H3K4me3 with low- and high-expressed genes in the TE and placenta. Suggesting an influential role of sperm H3K4me3, the highly expressed genes and to a lesser extent the lowly expressed genes in TE and placenta were positively correlated with sperm H3K4me3 (Fig. 7C$_{i-iv}$). Notably when the same comparisons were made with the deH3K4me3 there was a significant relationship with both lowly- and highly-expressed placenta genes (p=1.2e-11 and p=0.008, respectively; Fig. 7C$_{v-viii}$). These included genes implicated in altered placenta hormonal profiles and preeclampsia such as *Ldoc1*, *Dab2ip*, and *Rgs2* [667–670]. In addition, the GO analysis of TE- and placenta-expressed genes that overlap with deH3K4me3 promoters are in line with the metabolic phenotypes in offspring (Fig. 7D$_{i-ii}$, Tables S18-19). Taken together this analysis raises the possibility that obesity-induced alterations in sperm may influence embryonic and placenta gene expression to alter metabolic function of offspring.

Figure 7

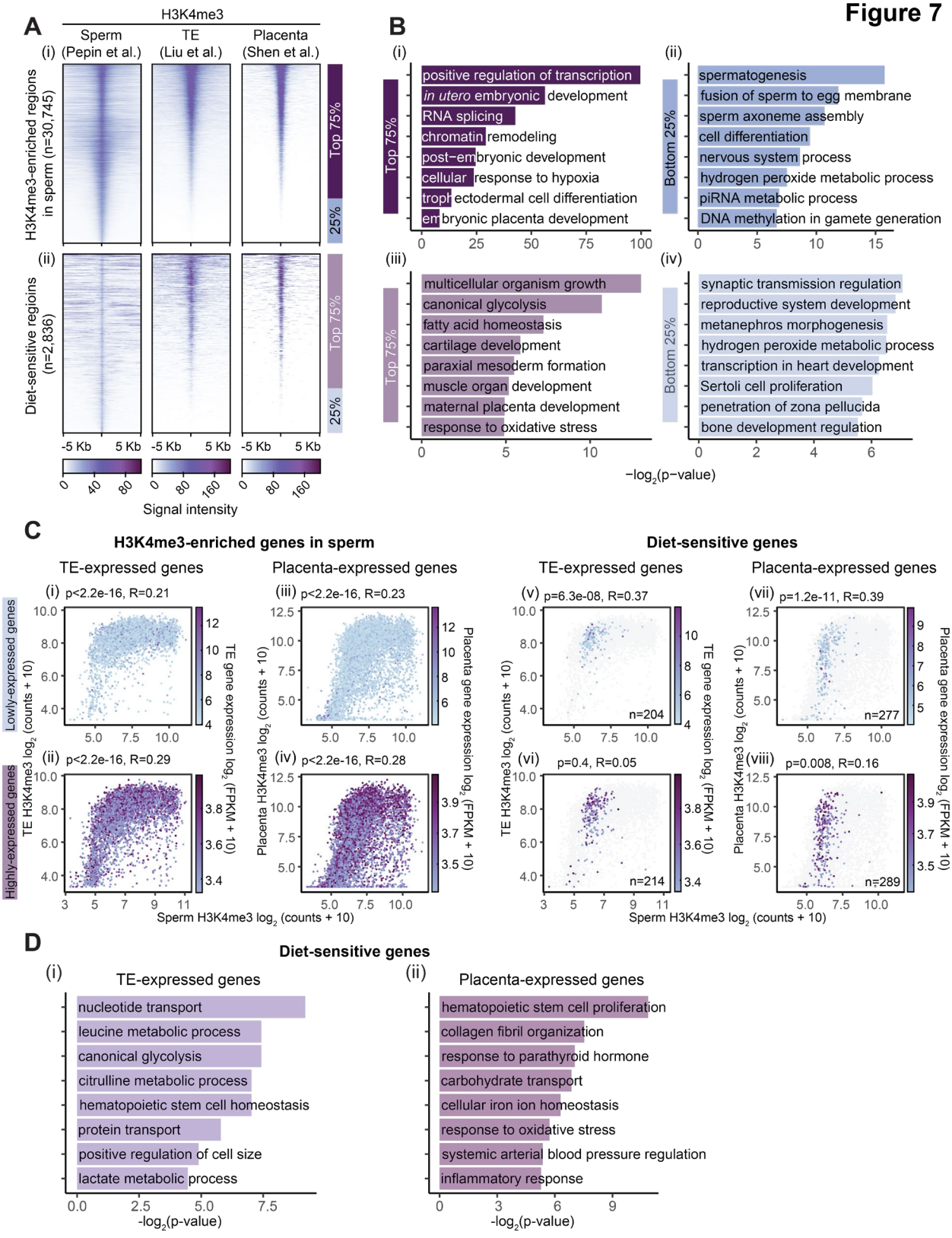

Figure 7: Obesity-induced deH3K4me3 regions overlap with genes marked by H3K4me3 and expressed in the trophectoderm and placenta

A) Heatmaps of RPKM counts signal +/- 5 kilobase aroundthe center of regions enriched with H3K4me3 in sperm (i; n=30,745) and at regions with diet-induced deH3K4me3 in sperm (n=2,836) for H3K4me3 enrichment levels in sperm (this study), trophectoderm (TE)(Liu et al., 2016) and placenta (Shen et al., 2012). B) Gene ontology analysis of regions enriched with H3K4me3 in sperm, TE and placenta (top 75% from A i) (i), regions enriched with H3K4me3 in sperm only(bottom 25% from A i) (ii), diet-sensitive regions enriched with H3K4me3 in sperm, TE and placenta (top 75% from A ii) (iii), and diet-sensitive regions enriched with H3K4me3 in sperm only (bottom 25% from A ii) (iv). Barplots show 8 selected significant GO terms with their respective -log2(p-value). Tables S16-19 include the complete lists of significantly enriched GO terms. C) Scatterplots showing H3K4me3 enrichment at promoters in sperm (x axis; log2 counts + 10), H3K4me3 enrichment (y axis; log2 counts + 10) and gene expression levels (color gradient; log2 FPKM + 10) in the trophectoderm (i,ii,v,vi; (Liu et al., 2016)) or in the placenta (iii,iv,vii,viii; (Shen et al., 2012; Chu et al., 2019)), at either all genes with promoters enriched with H3K4me3 in sperm (i-iv) or at diet-sensitive genes (v-viii). The top row of scatterplots includes lowly-expressed genes (bottom 50%) in trophectoderm (i and v) or placenta (iii or vii). The bottom row includes highly-expressed genes (top 50%) in trophectoderm (ii and iv) or placenta(vi and viii). Pearson's correlation coefficients and associated p-values are indicated above each scatterplot, comparing H3K4me3 enrichment in sperm versus H3K4me3 enrichment in the trophectoderm or placenta. D) Gene ontology analysis of genes expressed in the trophectoderm (i) or the placenta (ii), overlapping with diet-sensitive promoters in sperm. Barplots show 8 selected significant GO terms with their respective -log2(p-value). Tables S20-21 include the complete lists of significantly enriched GO terms. Obtained from [1] (Copyright 2022) with permission from Elsevier.

11.4.7 Obesity-induced sperm epigenomic and hepatic transcriptomic alterations are unrelated

In a recent study, paternal low-protein diet was associated with reduced H3K9me2 at genes in sperm and were suggested to modulate gene expression profiles in the liver [540]. We aimed to assess whether a similar association between obesity-induced deH3K4me3 in sperm would relate to differential expression in the livers of the next generation. We focused on the obesity-associated sperm deH3K4me3 at promoters in F_0 sires and their relationship to differentially expressed genes in the liver (DEGs) of F_1 males. This analysis revealed that genes with differential expression in livers (n=1,644) were by and large unrelated to genes bearing deH3K4me3 in sperm. Only 9.1% (n=67) of promoters with deH3K4me3 in sperm were differentially expressed in the liver of F_1 males sired by HFD-fed sires (Fig. S7A-B). We then asked if deH3K4me3 promoters in sperm and liver DEGs had related biological functions. Strikingly, sperm- and liver-altered genes showed few

functional similarities (Fig. S7C, Supplemental file 5 and Table S22). Functional pathways specifically enriched in deH3K4me3 promoters in sperm involved development and differentiation processes (clusters 12-15). As expected in a paternal obesity model, gene processes altered in offspring livers included: regulation of transcription and RNA splicing (clusters 1-3), protein and histone post-translational modifications (clusters 4-5), and metabolism of lipid, nitrogen and glucose (clusters 6-8). Pathways enriched in both the deH3K4me3 promoters in sperm and the DEGs in liver were involved in cell cycle, transport and signaling (clusters 16-19), and response to stress and inflammation (clusters 20-22). These commonly enriched pathways might reflect obesity-associated systemic inflammation which could affect multiple organs in a similar manner. These findings indicate that paternal obesity alters the sperm epigenome at distinct genes and functional pathways than those differentially expressed in offspring livers and fits with a developmental origin of adult metabolic dysfunction that could be related to alterations in gene expression in the embryo and placenta.

11.5 Discussion

In mammals, spermatogenesis is a highly complex cell differentiation process involving unique testis-specific gene expression programs that are accompanied by dynamic remodeling of the chromatin [305,431,671,672]. During this process, most histones are replaced by protamines to facilitate DNA compaction [431]. Interestingly, 1% of sperm histones are retained in mice and 15% in men [223,472]. Retained histones are conserved across species from mice to men and are found at the gene regulatory regions implicated in spermatogenesis, sperm function, embryo development, metabolism and routine cellular processes [220,472,542]. We have shown that in human and mouse sperm histone H3 lysine 4 dimethylation (H3K4me2) and trimethylation (H3K4me3) localize to genes involved in metabolism and development [221,477,608]. Since this tantalizing discovery we and others have suggested that histones in sperm may directly influence embryonic gene expression and contribute to the developmental origin of adult disease. The findings of this study support histones serving in this mechanism of disease inheritance.

In spermatogenesis there are dynamic changes to the sperm epigenome including histone methylation which is susceptible to alterations induced by changes in methyl

donor availability [477,541]. Diets high in fat alter epigenetic programming, likely through the alteration of cellular metabolism, which influences the availability of methyl donors and/or the activation or inactivation of chromatin modifying enzymes. In overweight and obese individuals, homocysteine is consistently elevated, and associated with reduced B12 and folate [673,674]. It follows that the obesity-induced alterations in H3K4me3 we report here could be a consequence of an altered methyl donor pool. Intriguingly, the effects of obesity on the paternal epigenome were linked with the metabolic dysfunction in the F_1 and F_2 descendants; deH3K4me3 occurred at the promoters of genes involved in fertility, metabolism, and placenta processes. Indicative of paternal transmission of sperm altered H3K4me3 as a mediator of metabolic dysfunction was the strong relationship between deH3K4me3, an open chromatin state and gene expression in embryos and placenta. However, a limitation of the study is that we did not examine H3K4me3 in sperm from the F_1 and thus whether H3K4me3 abnormalities in sperm persist in the subsequent generation is unknown. In this model of diet-induced transgenerational inheritance and in others, offspring phenotypes are likely the consequence of a complex interplay between chromatin, DNA methylation and non-coding RNA in sperm and embryos. For example, a paternal low protein diet has been shown to alter testicular germ cell activating transcription factor 7 (ATF7) binding, and this was associated with differential sperm H3K9me2 and small RNA content in spermatocytes [540]. Elucidating whether there are common molecular pathways mediating inter- and trans-generational impacts of paternal diet remains to be determined.

The enhanced metabolic abnormalities observed in the descendants of obese F_0 TG revealed an increased susceptibility to metabolic disease in the TG line. An explanation for this response is that the F_0 TG were descendants from a lineage with pre-existing alterations in the sperm epigenome due to the genetic modification causing KDM1A overexpression. This genetic stress in combination with the environmental challenge of the HFD resulted in a more severely altered sperm epigenome in comparison to the WT, with consequent enhanced offspring phenotypes. Admittedly speculative, these findings suggest that the higher incidence of poor health in at-risk populations may be attributed to generational exposures to poor diet that leads to an accumulation of sperm epigenome errors that escape reprogramming.

Notably, paternal obesity-induced transgenerational metabolic disturbances in offspring were only observed in descendants of obese TG males. The phenomenon of transgenerational inheritance has been most documented in genetic mouse models of epigenetic inheritance and studied in relation to DNA methylation patterns. These include the Avy agouti model [606,675,676], the kinky tail model ($Axin^{Fu}$ allele) [554], and in mice bearing a mutation in the *Mtrr* gene, a folate metabolism enzyme [555]. In the context of environmental challenges, paternal transgenerational inheritance has been associated with altered sperm DNA methylation when there has been gestational exposure to toxicants and undernutrition [677,678], and in a non-genetic pharmacologically-induced prediabetes model begun at weaning [521]. Taken together, this growing body of evidence indicates that transgenerational inheritance occurs under genetic influence, or when exposures coincide with developmental programming. The male F_0 mice in this study were exposed to the paternal HFD from weaning and not *in utero*, which may account for why transgenerational effects were not observed in WT HFD descendants. Another possibility is that transgenerational responses in the WT may have become detectable in older mice.

Our analysis indicates that the inherited metabolic disturbances observed in adult descendants originated early in development. In rodent models, paternal obesity and *in utero* undernutrition has been linked to altered gene expression in offspring livers and pancreatic islets with some minor links to concordant DNA methylation changes [521,678,679]. It has been suggested that diet-associated alterations in DNA methylation in sperm are retained through embryogenesis and maintained in adult tissues mediating paternally-induced phenotypes [521,678]. Consistent with these studies, altered hepatic gene expression occurred in $F_{1\text{-}2}$ offspring of obese sires. In contrast, we observed minimal overlap of genes and functional pathways between altered H3K4me3 enrichment in sperm, with those differentially expressed in F_1 livers. Instead, we demonstrate a significant overlap of obese sperm H3K4me3 profiles with the expression of metabolic-related genes in the embryo and placenta. Based on these findings, we suggest that the metabolic phenotypes we observe originate in early embryogenesis and through changes in placental gene expression.

There is a bounty of research linking maternal obesity to adverse metabolic consequences for the offspring that coincide with altered placental gene expression and function [680,681]. On the other hand, it is an emerging concept that the paternal environment including factors such as diet and age can influence placental development and function. It is known that paternally expressed genes contribute to placental growth, trophoblast invasion and insulin resistance and adiposity [491,592,682–686]. In humans, errors in epigenomic programming have been associated with gestational trophoblast disease and pre-eclampsia, but the role of the obese father in these conditions has been entirely unexplored [687,688]. Previous studies support a connection between paternal diets, obesity, and placental dysfunction as a developmental route to metabolic disease in children. For example, we have shown that a folate deficient paternal diet and altered sperm DNA methylation coincided with deregulated placenta gene expression of *Cav1* and *Txndc16* [541]. Moreover, paternal obesity in mice has been attributed to defective placental development [489,491,689]. In women, altered DNA methylation in the regulation of some genes in preeclampsia has been established. However, many genes with deregulated expression were not associated with DNA methylation raising the possibility of altered chromatin signatures leading to abnormal gene expression in this placental disorder [690]. Indeed, upregulated expression of LncRNA by increased H3K4me3 has been observed in preeclampsia placentas [691], and the levels of H3K4me3 as detected by immunohistochemistry are decreased [692]. Until now the connection between sperm chromatin and placenta function has been unexplored. Our analyses revealed that most of the obesity-altered H3K4me3 at promoters occurred at loci involved in placental development and inflammatory processes, with 56.6% and 76.8% of deH3K4me3 occurring at promoters expressed in the trophectoderm and placenta, respectively. Remarkably, deregulated expression of genes implicated in inflammation has been implicated in hypertensive disorders in pregnancy including pre-eclampsia. Hypertensive disorders in pregnancy have been associated with increased risk for developing cardiovascular disease [684]. This raises the possibility that the paternal sperm epigenome may influence maternal health during pregnancy in addition to that of the developing fetus.

As in previous studies we found that paternal obesity resulted in sex-specific differences in metabolism and fat accruement with males being more impacted. The

underlying mechanisms that lead to the greater susceptibility of males may be related to sexually dimorphic placental gene expression [693]. In support of this possibility, paternal environment (diet) influenced placental function in a sex-specific manner [489]. Alternatively, different metabolic responses in male and female offspring may be due to hormonal responses where estrogen has been shown to protect against altered glucose homeostasis [612,694].

11.6 Conclusion

In summary, we provide evidence that paternal obesity is associated with H3K4me3 signatures in sperm which could contribute to the inheritance of metabolic disease. In addition, we identified links between sperm regions bearing obesity-altered H3K4me3, with placenta and embryonic H3K4me3, and the regulation of gene expression in these tissues. Important next steps to better understand disease inheritance related to paternal obesity, sperm chromatin and placental function will be to explore this possibility using embryonic and placenta tissue from pregnancies sired by obese males. The translational validation of these findings will be important in developing intervention strategies focused on paternal factors that could impact the health of future generations [695].

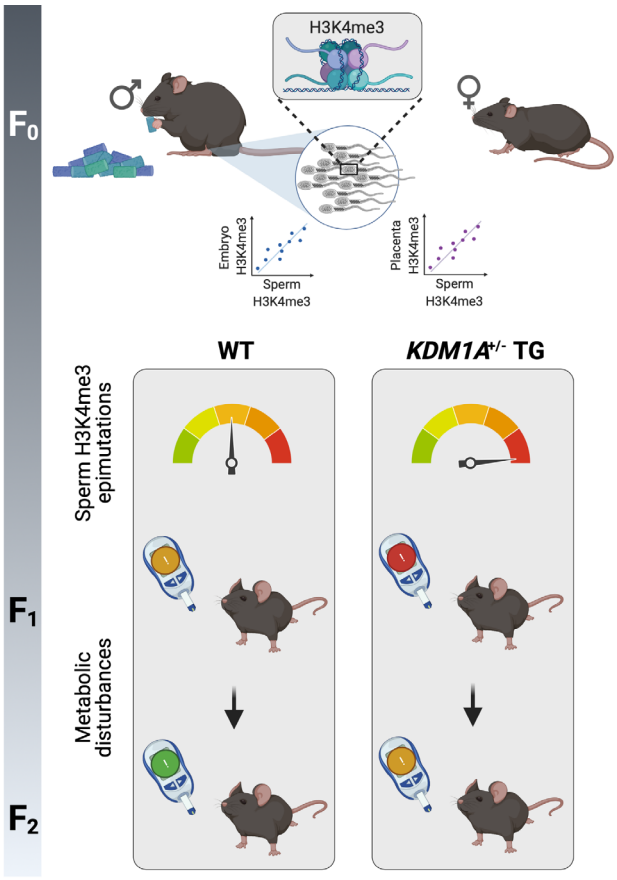

Figure 8: Graphical summary

- Sperm H3K4me3 serves as a metabolic sensor of HFD-induced obesity.
- Obesity-altered sperm H3K4me3 corresponds to embryonic transcription and chromatin profiles.
- HFD- and KDM1A-induced cumulative sperm epimutations enhanced F_1 metabolic dysfunction.
- Sperm epimutations may influence placenta function inducing F_1 metabolic phenotypes.

Figure obtained from [1] Copyright (2022) with permission from Elsevier.

11.7 Acknowledgements

We thank the team at the McGill University Small Animal Research Unit, Génome Québec Innovation Centre for performing the sequencing, and Dr. Deborah Sloboda (McMaster University) for advice on metabolic phenotyping methods. This research was funded by the Canadian Institute of Health Research (CIHR) grants to SK (358654 and 350129).

11.8 Author contributions

CRediT author statement

Anne-Sophie Pépin: Methodology, Data curation, Software, Investigation, Formal analysis, Visualization, Writing – Original draft preparation

Christine Lafleur: Resources, Investigation

Romain Lambrot: Resources

Vanessa Dumeaux: Software, Resources, Writing – Review & Editing

Sarah Kimmins: Supervision, Conceptualization, Funding acquisition, Writing – Original draft preparation

11.9 Declaration of interest

The authors declare no competing interest.

11.10 Supporting Information

The Supporting Information includes the following Figures and Tables:

Figure S1: **Paternal obesity increases body weight and fat accruement across generations**

Figure S2: **Paternal obesity alters metabolic profiles across generations in a sex-specific manner**

Figure S3: **Liver RNA-sequencing data quality assessment and normalization**

Figure S4: **Sperm ChIP-sequencing data quality assessment and normalization**

Figure S5: **Obesity-sensitive H3K4me3 regions are predominantly located in CpG islands, promoters, exons, and intergenic regions**

Figure S6: **Obesity alters sperm H3K4me3 at genes expressed in the 4-cell and morula embryos,**
trophectoderm and placenta

Figure S7: **Obesity-induced changes in H3K4me3 enrichment in sperm show minor overlap with**
genes altered in adult offspring liver

Table S1: Diets' energy density and macronutrients composition

Table S2: Number of animals used per group per sex per generation for metabolic characterization

Table S3: Litter size generated by F0 and F1 sires

Table S4: Sex ratios of litters generated by F0 and F1 sires

Table S8: Sperm H3K4me3 ChIP-Sequencing read numbers and alignment rates

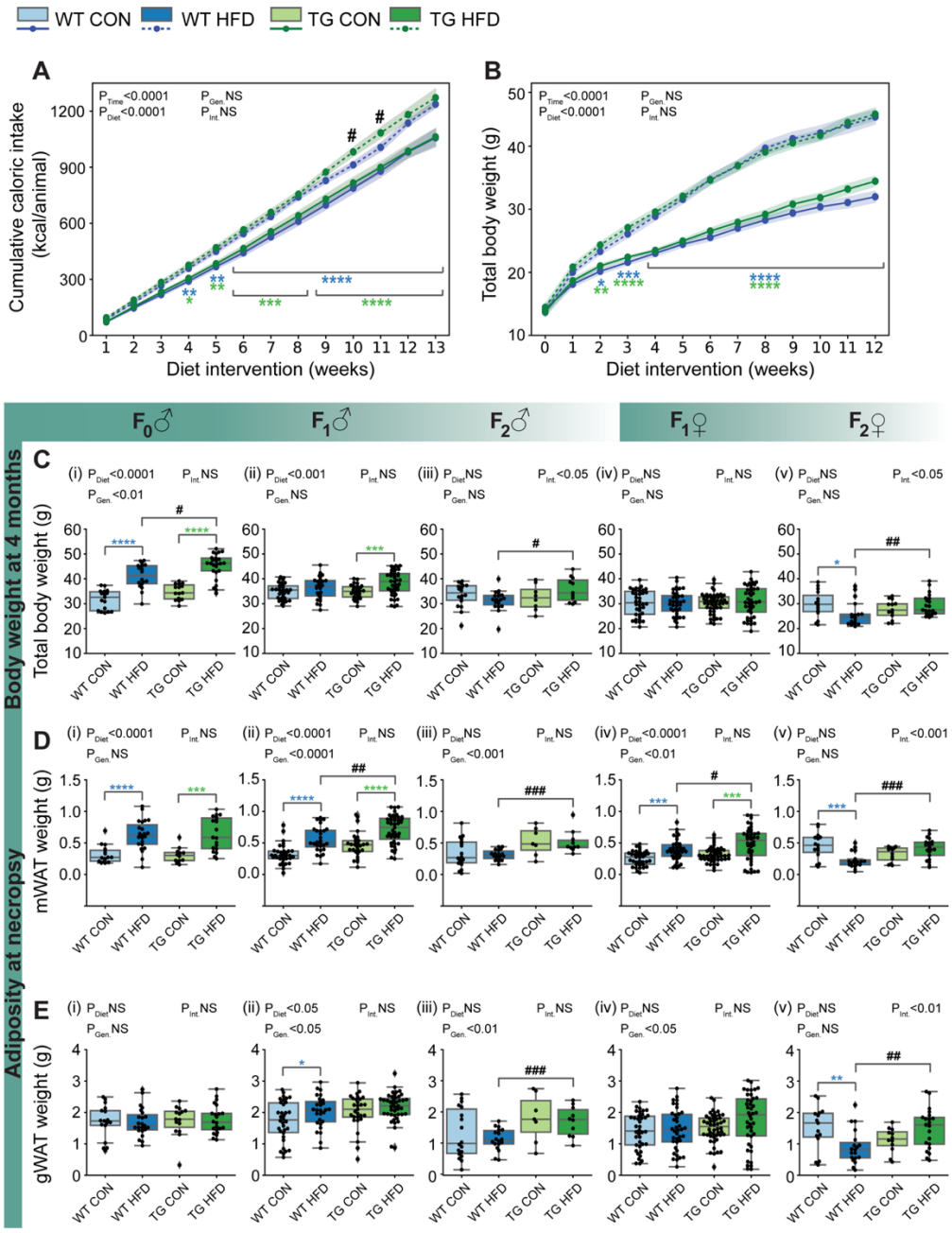

Figure S1: Paternal obesity increases body weight and fat accruement across generations

Cumulative energy intake during the dietary treatment. The amount of food consumed weekly per cage was measured and the cumulative caloric intake per mouse was calculated based on the calorie content specific to each diet. B) Growth trajectories of F_0 sires before and during the 12-week diet intervention. C) Total body weight at 4 months of age in F_0 males (i), F_1 males (ii), F_2 males (iii), F_1 females (iv) and F_2 females (v). D) Mesenteric white adipose tissue (mWAT) weight at necropsy in F_0 males (i), F_1 males (ii), F_2 males (iii), F_1 females (iv) and F_2 females (v). E) Gonadal white adipose tissue (gWAT) weight at necropsy in F_0 males (i), F_1 males (ii), F_2 males (iii), F_1 females (iv) and F_2 females (v). Results are shown as mean ± SEM.

Significance for main effects of diet, genotype, time, and for diet-genotype interactions are shown above each graph. NS, not significant (P>0.05). Significance for pairwise comparisons are shown as the following: *P<0.05, **P<0.01, ***P<0.001, ****P<0.0001 (in blue; WT CON vs WT HFD, in green; TG CON vs TG HFD) and #P<0.05, ##P<0.01, ###P<0.001 (WT HFD vs TG HFD). Obtained from [1] (Copyright 2022) with permission from Elsevier.

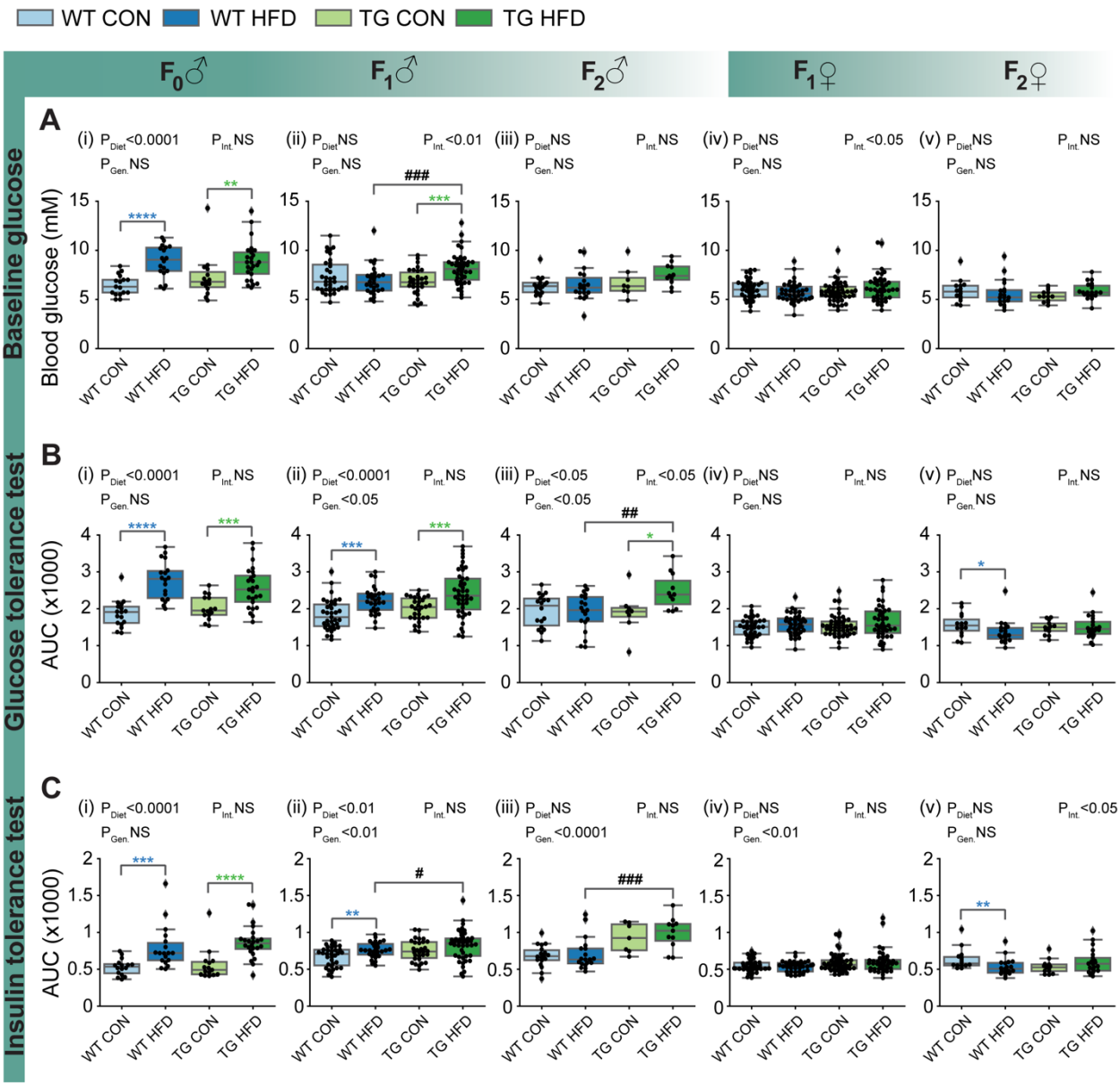

Figure S2: Paternal obesity alters metabolic profiles across generations in a sex-specific manner

A) Baseline blood glucose levels after overnight fasting (15 ± 1 hour) at 4 months of age in F_0 males (i), F_1 males (ii), F_2 males (iii), F_1 females (iv) and F_2 males (v). B) Glucose tolerance test area under the curve

(AUC) for F_0 males (i), F_1 males (ii), F_2 males (iii), F_1 females (iv) and F_2 females (v). C) Insulin tolerance test AUC for F_0 males (i), F_1 males (ii), F_2 males (iii), F_1 females (iv) and F_2 females (v). The AUC was calculated using the trapezoidal rule from individual animal glucose tolerance test curves (in Fig. 1D) and insulin tolerance test curves (in Fig. 1E). Results are shown as mean ± SEM. Significance for main effects of diet, genotype, and for diet-genotype interactions are shown above each graph. NS, not significant (P>0.05). Significance for pairwise comparisons are shown as the following: *P<0.05, **P<0.01, ***P<0.001, ****P<0.0001 (in blue; WT CON vs WT HFD, in green; TG CON vs TG HFD) and #P<0.05, ##P<0.01 (WT HFD vs TG HFD). Obtained from [1] (Copyright 2022) with permission from Elsevier.

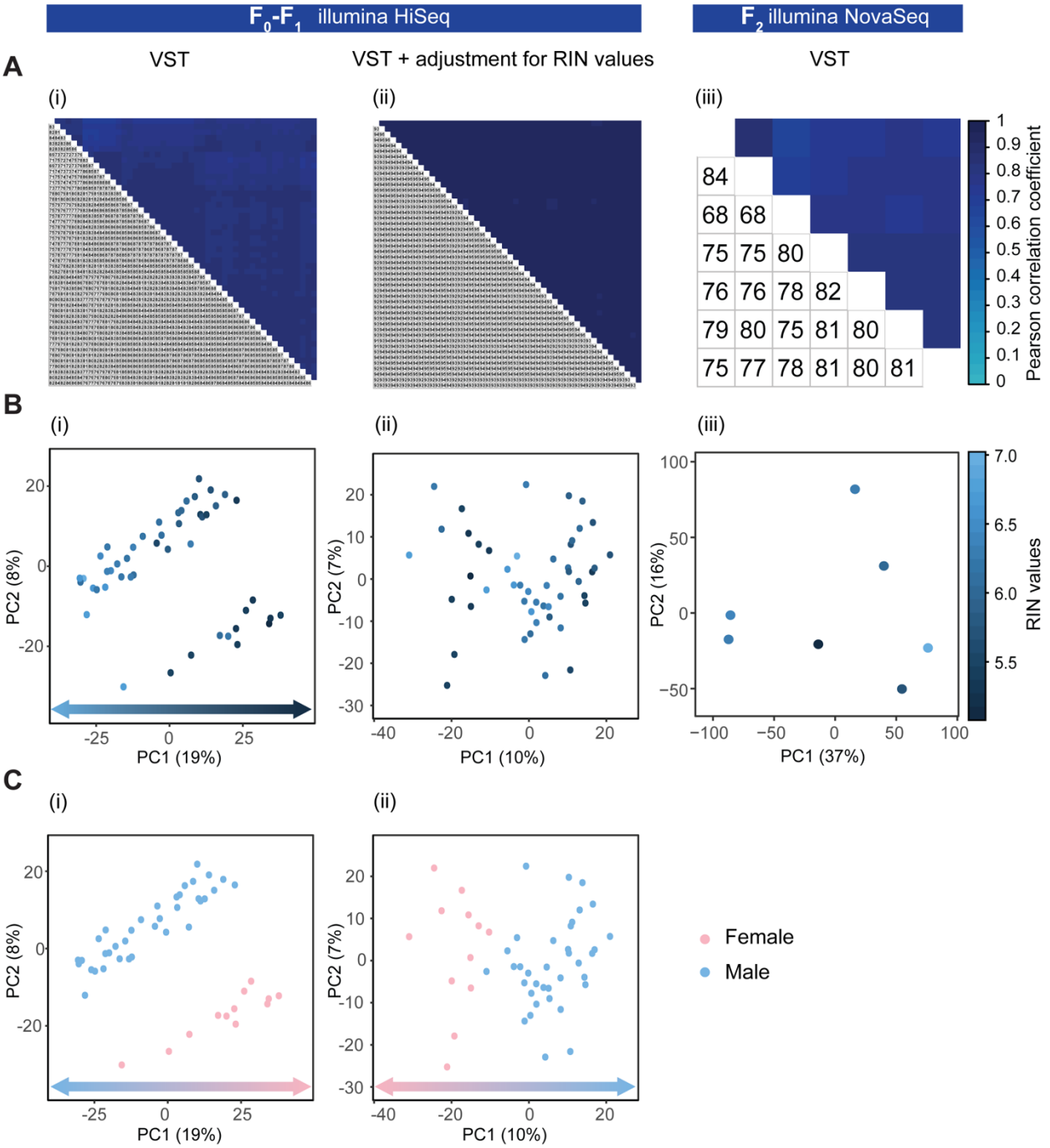

Figure S3: Liver RNA-sequencing data quality assessment and normalization

A) Pearson correlation heatmaps on transcripts with variance stabilizing transformation (VST), before (i) and after (ii) correcting for RIN values in F_0 and F_1 samples run on an illumina HiSeq platform, and in F_2 samples run on an illumine NovaSeq platform (iii). Color gradients indicate the Pearson correlation coefficients for each pairwise comparison of samples. B) Principal component analysis on transcripts with variance stabilizing transformation (VST), with samples labeled by RIN value before (i) and after (ii) correcting for RINs in F_0 and F_1 samples (illumina HiSeq) and in F_2 samples (illumina NovaSeq) (iii). C)

Principal component analysis on transcripts with variance stabilizing transformation (VST), with samples labeled by sex before (i) and after (ii) correcting for RINs in F_0 and F_1 samples (illumina HiSeq). Obtained from [1] (Copyright 2022) with permission from Elsevier.

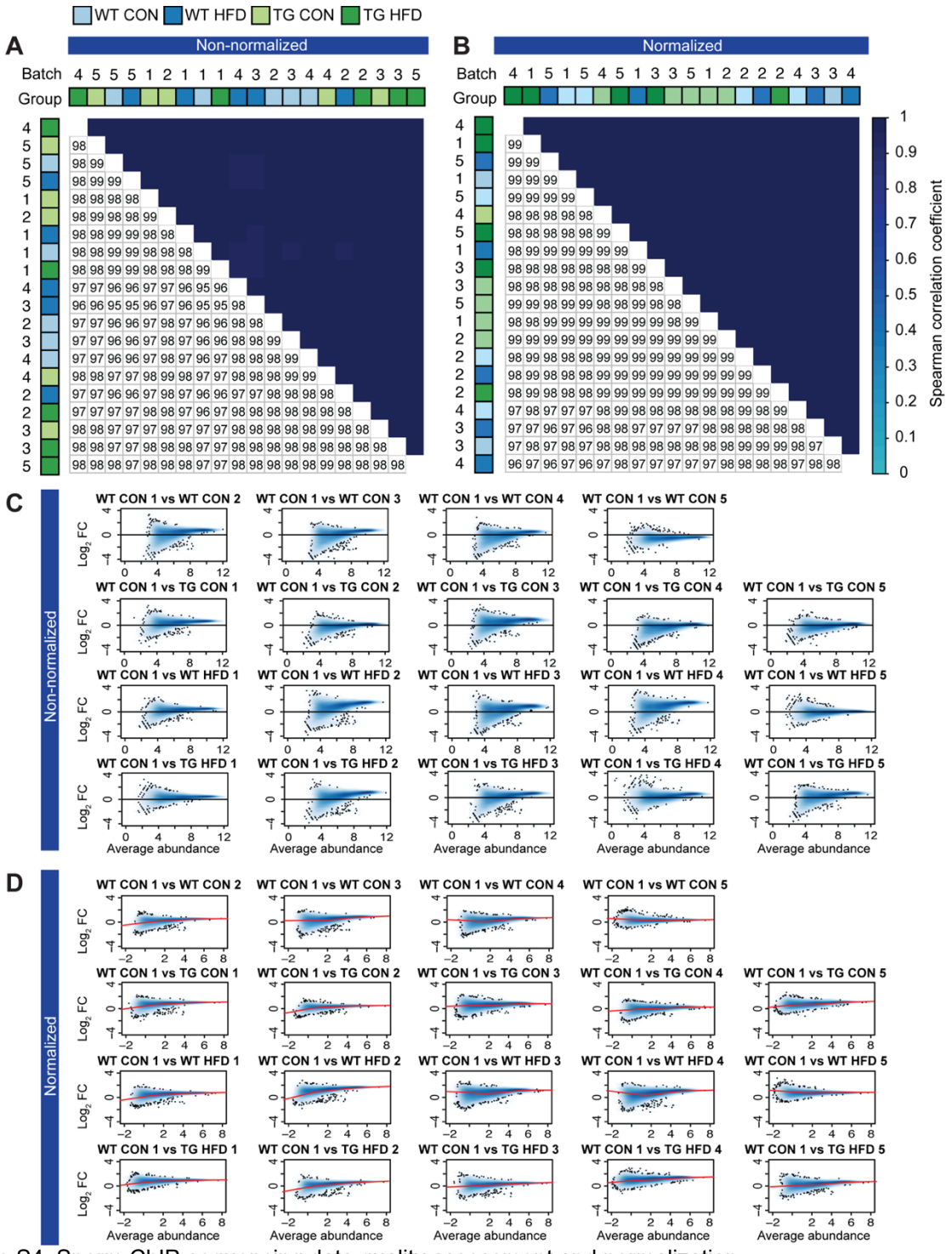

Figure S4: Sperm ChIP-sequencing data quality assessment and normalization

A-B) Spearman correlation heatmaps for genomic regions enriched with H3K4me3, before (A) and after (B) TMM normalization and batch correction. Colored boxes indicate sample groups (light blue=WT CON, dark blue=WT HFD, light green=TG CON, dark green=TG HFD) and numbers (from 1 to 5) indicate the sample batch. Color gradients indicate the Spearman correlation coefficients for each pairwise comparison of

samples. C-D) MA-plots of pairwise comparisons between WT CON (rep 1) and all other samples, before (C) and after (D) TMM normalization and batch correction. Obtained from [1] (Copyright 2022) with permission from Elsevier.

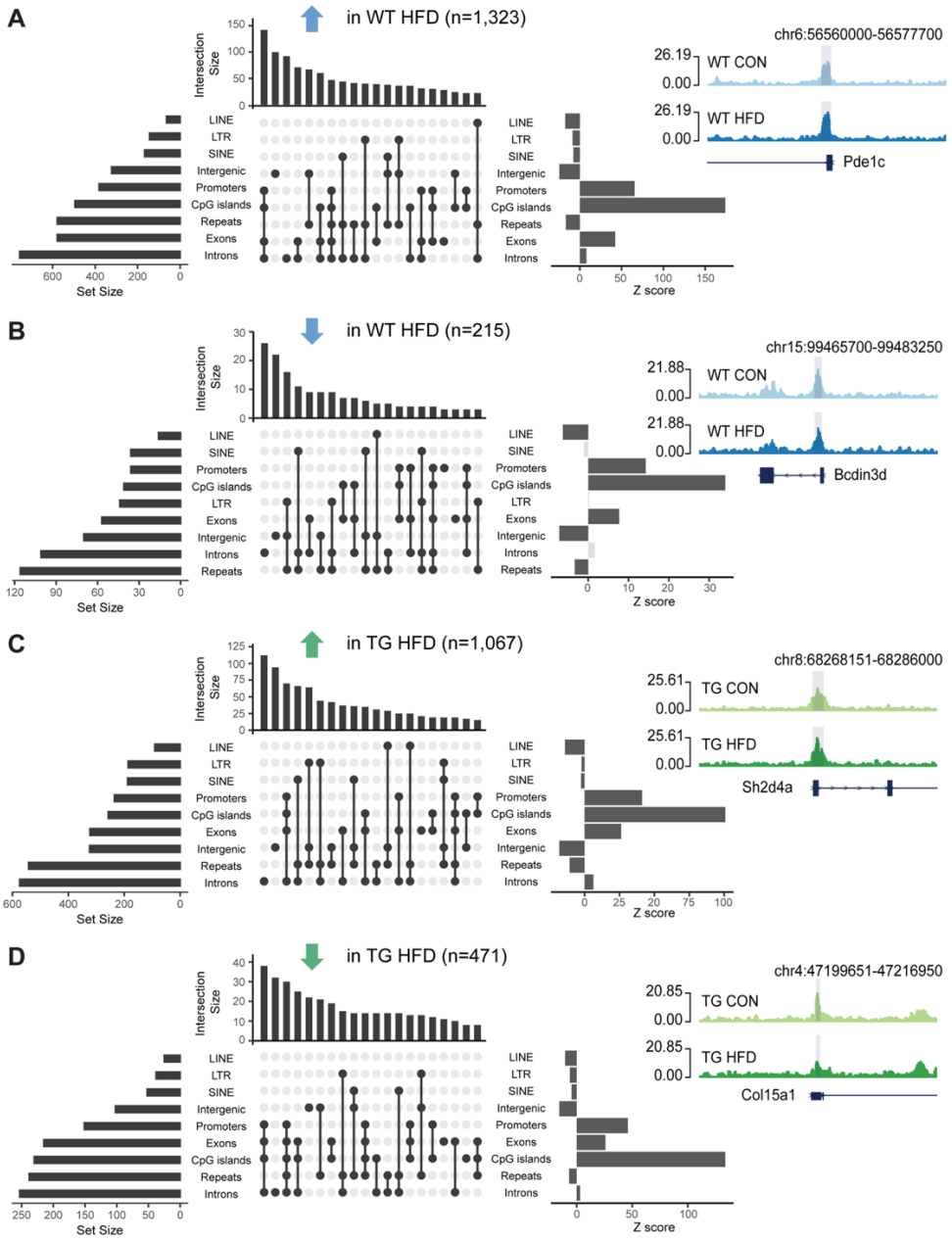

Figure S5: Obesity-sensitive H3K4me3 regions are predominantly located in CpG islands, promoters, exons, and intergenic regions

A-D) Upset plots show genome annotation identifying the functional regions with obesity-induced differential enrichment of H3K4me3 in sperm according to directionality change, with increased enrichment in WT HFD (A), decreased enrichment in TG HFD (B), increased enrichment in TG HFD (C) and decreased enrichment in TG HFD (D). Horizontal bars on the left represent the number of regions belonging to each genomic annotation (set size). Vertical bars represent the number of regions belonging to intersecting annotations (intersection size). Intersection sets are represented by connecting nodes. Horizontal bars on the right represent the enrichment (z-score) for each respective annotation compared to what would be expected by

chance if regions of similar sizes were randomly located across the genome ($p<0.05$, 1,000 permutations). Dark grey bars represent significant enrichment whereas light grey bars are not significant. Genome browser snapshots show genes with deH3K4me3 in sperm (WT CON light blue, WT HFD dark blue, TG CON light green and TG HFD dark green). Obtained from [1] (Copyright 2022) with permission from Elsevier.

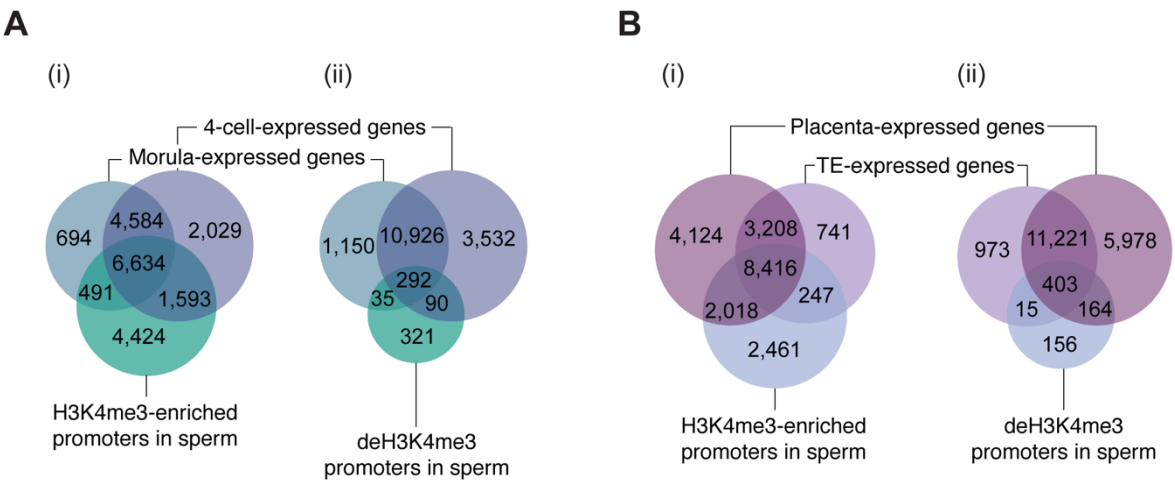

Figure S6: Obesity alters sperm H3K4me3 at genes expressed in the 4-cell and morula embryos, trophectoderm and placenta

A) Venn diagrams showing the overlap between genes expressed in the 4-cell embryo and genes expressed in the morula embryo, with genes with H3K4me3-enriched promoters in sperm (i) or with genes with diet-induced deH3K4me3 at promoters in sperm (ii). B) Venn diagrams showing the overlap between genes expressed in the trophectoderm and genes expressed in the placenta, with genes with H3K4me3-enriched promoters in sperm (i) or with genes with diet-induced deH3K4me3 at promoters in sperm (ii). Obtained from [1] (Copyright 2022) with permission from Elsevier.

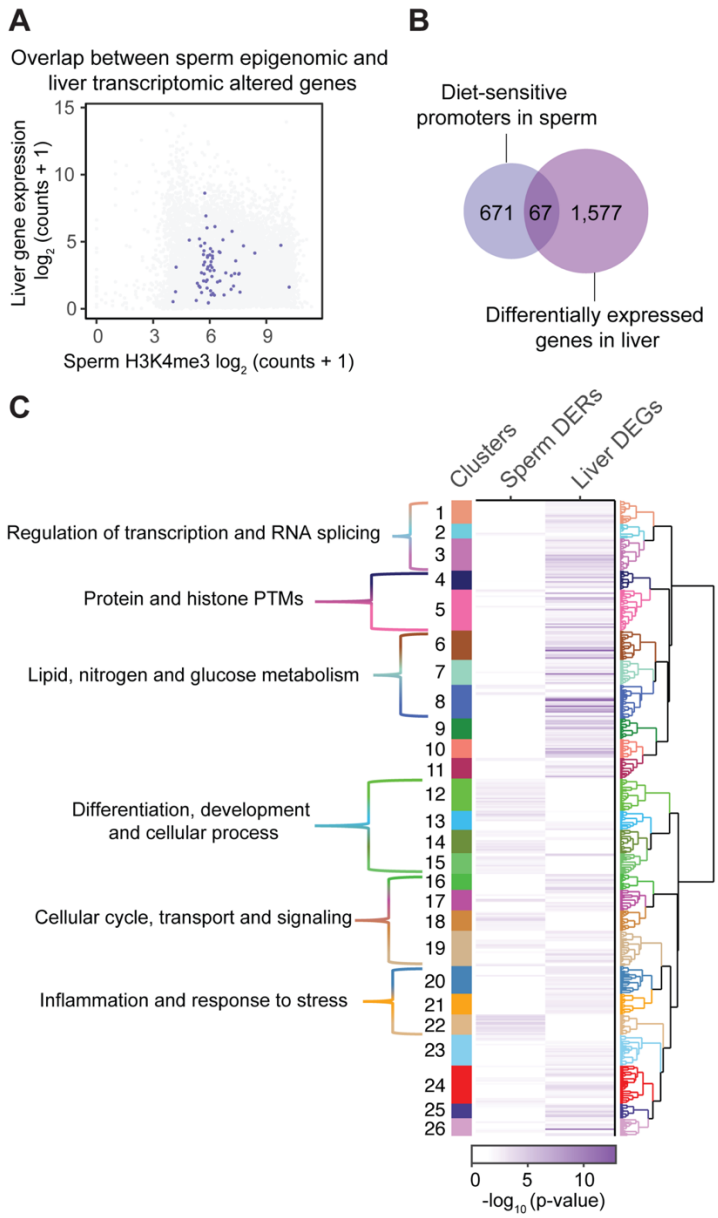

Figure S7: Obesity-induced changes in H3K4me3 enrichment in sperm show minor overlap with genes altered in adult offspring liver

A) Scatterplot showing liver RNA expression values (y axis; log2 counts +1) and sperm H3K4me3 enrichment values (x axis; log2 counts + 1) for genes with paternal-diet induced differential expression in livers of F_1 males overlapping with deH3K4me3 at promoters in sperm. B) Venn diagram showing the overlap of genes enriched with diet-induced deH3K4me3 at promoters in sperm and genes with paternal-diet induced differential expression in livers of F_1 males. C) Heatmap of significant GO terms, comparing enriched biological functions in diet-induced sperm differentially enriched regions at promoters and liver differentially expressed genes in F_1 males WT and TG HFD. Rows represent enriched GO terms which are ordered by hierarchical clustering based on Wang's semantic similarity distance and ward.D2 aggregation

criterion. Each column represents a comparison of interest for which enriched GO terms were annotated based on the list of significant genes. The color gradient depicts the GO term enrichment significance (-log10 p-value). An interactive version of this heatmap can be found in Supplemental file 5 and the complete list of significantly enriched GO terms can be found in Table S22. Obtained from [1] (Copyright 2022) with permission from Elsevier.

Table S1: Diets' energy density and macronutrients composition

	Control diet (CON; D12450J, Research Diets Inc.)	**High-fat diet** (HFD; D12492, Research Diets Inc.)	**Regular chow diet** (2020X, Teklad Diets)
Energy density (kcal/g)	3.85	5.24	3.1
Calories from Protein (%)	20	20	24
Calories from Fat (%)	10	60	16
Calories from Carbohydrate (%)	70	20	60

Table S2: Number of animals used per group per sex per generation for metabolic characterization

	F0 males	**F1 males**	**F2 males**	**F1 females**	**F2 females**
WT CON	17	35	18	38	15
WT HFD	18	28	19	39	19
TG CON	15	30	8	49	13
TG HFD	25	43	11	42	21

Table S3: Litter size generated by F_0 and F_1 sires

Group	**WT CON**	**TG CON**	**WT HFD**	**TG HFD**	**Significance**
F0 litter size Mean ± SEM (N=)	6.833 ± 0.458 (12)	7.9 ± 0.767 (10)	6.333 ± 0.607 (12)	6.2 ± 0.48 (15)	N S
F1 litter size Mean ± SEM (N=)	7 ± 0.5 (8)	4.6 ± 1.288 (5)	5.667 ± 0.689 (12)	4.875 ± 0.666 (8)	N S

Table S4: Sex ratios of litters generated by F_0 and F_1 sires

Group	WT CON	TG CON	WT HFD	TG HFD	Significance
F0 sex ratio Mean ± SEM(N=)	0.509 ± 0.068 (12)	0.343 ± 0.069 (10)	0.534 ± 0.071 (12)	0.579 ± 0.055 (15)	NS
F1 sex ratio Mean ± SEM (N=)	0.476 ± 0.072 (8)	0.548 ± 0.141 (5)	0.598 ± 0.073 (12)	0.425 ± 0.095 (8)	NS

Table S8. Sperm H3K4me3 ChIP-Sequencing read numbers and alignment rates

Batch	Diet	Genotype	Reads #	Alignment rate (%)
1	CON	WT	25,237,875	91.24
2	CON	WT	36,679,172	98.04
3	CON	WT	44,156,311	97.58
4	CON	WT	38,188,136	97.57
5	CON	WT	32,891,823	97.25
1	HFD	WT	30,356,006	94.03
2	HFD	WT	36,934,484	97.11
3	HFD	WT	31,718,194	97.38
4	HFD	WT	27,841,763	97.9
5	HFD	WT	30,902,900	96.91
1	CON	TG	29,310,441	96.88
2	CON	TG	38,274,515	96.88
3	CON	TG	27,291,467	97.27
4	CON	TG	39,918,514	97.81
5	CON	TG	30,925,671	97.68
1	HFD	TG	23,856,350	94.75
2	HFD	TG	39,534,589	97.93
3	HFD	TG	38,469,968	97.73
4	HFD	TG	28,052,094	98.14
5	HFD	TG	35,028,161	98.13
		Average	33,278,421.7	96.9105

Supplementary data can be accessed via the following link:

https://doi.org/10.1016/j. molmet.2022.101463

Exploring the placental origins of paternally-induced adult-onset metabolic diseases

In Chapter 2, our study revealed that a paternal diet-induced obesity can have intergenerational impacts on metabolic functions, with more severe and transgenerational effects when combined with a previously altered sperm epigenome. Furthermore, we have identified epigenetic regions in sperm with altered histone H3K4me3 upon diet-induced obesity. Interestingly, these detected diet-sensitive regions were found to be enriched for genes involved in placenta formation and development. Our analyses revealed sperm H3K4me3 profiles reflected those of trophectoderm and placental tissues. Additionally, sperm H3K4me3 enrichment corresponded with gene expression in these tissues. Through the next chapter, we direct our focus towards exploring the connection between the sperm chromatin and placental development.

Growing evidence suggests that paternal exposures can alter the placental epigenome and transcriptome. However, studies have been limited to targeted approaches to link changes in the placenta methylome or transcriptome associated with paternal factors [489,541,696]. A recent study demonstrated that paternal high-fat diet preconception can lead to deregulated hypoxia and impaired vascularization in the placenta [510]. Nonetheless, no study has assessed the connection between paternal obesity, the sperm epigenome and its impact on placenta development, at the genome-wide level.

In the next chapter, we were interested in exploring the potential involvement of placental gene expression in the developmental origins of paternally-induced phenotypes. Similarly to our initial study, we used a paternal diet-induced obesity model. We aimed to (1) determine whether diet-induced changes in the sperm chromatin would be reproducible across two different studies, (2) explore the potential molecular determinants of epigenetic hotspots in sperm at identified diet-sensitive regions, (3) reveal molecular connections between the sperm epigenome and placental transcriptomic networks, and (4) assess functional consequences of paternal obesity on placental cellular composition.

Chapter 3: Paternal obesity alters the sperm epigenome and is associated with changes in the placental transcriptome and cellular composition

Pépin, A.-S., Jazwiec, P.A., Dumeaux, V., Sloboda, D.M., Kimmins, S., 2022. Paternal obesity alters the sperm epigenome and is associated with changes in the placental transcriptome and cellular composition. BioRxiv: 2022.08.30.503982, Doi: https://doi.org/10.1101/2022.08.30.503982.

13.1 Abstract

Paternal obesity has been implicated in adult-onset metabolic disease in offspring. However, the molecular mechanisms driving these paternal effects and the developmental processes involved remain poorly understood. One underexplored possibility is the role of paternally driven gene expression in placenta function. To address this, we investigated paternal high-fat diet-induced obesity in relation to sperm epigenetic signatures, the placenta transcriptome and cellular composition. C57BL6/J males were fed either a control or high-fat diet for 10 weeks beginning at 6 weeks of age. Males were timed-mated with control-fed C57BL6/J females to generate pregnancies, followed by collection of sperm, and placentas at embryonic day (E)14.5. Chromatin immunoprecipitation targeting histone H3 lysine 4 tri-methylation (H3K4me3) followed by sequencing (ChIP-seq) was performed on sperm to define obesity-associated changes in enrichment. Paternal obesity corresponded with altered sperm H3K4me3 enrichment at imprinted genes, and at promoters of genes involved in metabolism and development. Notably, sperm altered H3K4me3 was localized at placental enhancers and genes implicated in placental development and function. Bulk RNA-sequencing on placentas detected paternal obesity-induced sex-specific changes in gene expression associated with hypoxic processes such as angiogenesis, nutrient transport and imprinted genes. Paternal obesity was also linked to placenta development; specifically, a deconvolution analysis revealed altered trophoblast cell lineage specification. These findings implicate paternal obesity-effects on placenta development and function as one mechanism underlying offspring metabolic disease.

13.2 Introduction

The placenta is an extraembryonic organ that regulates fetal growth and development, and contributes to long-term adult health [586]. Placental defects can result in obstetrical complications such as pre-eclampsia, stillbirth, preterm birth and fetal growth restriction [697]. Intrauterine growth restriction (IUGR) in turn, is associated with a heightened risk for adult-onset cardiometabolic diseases, coronary heart disease and stroke, supporting a placental role in long-term health of offspring [698–705]. Despite the many adverse pregnancy outcomes involving placental defects, the molecular and cellular factors that impact placental development are poorly understood [577,706]. Until recently, most studies on the origins of placental pathology have focused on maternal factors. For example, placental insufficiency occurs in 10 to 15% of pregnancies, and underlying causes include advanced maternal age [707–709], hypertension [710], obesity [711–715], cigarette smoking [716], drug and alcohol use, and medications [717]. However, emerging studies, indicate that the paternal preconception environment including diet and obesity also play a critical role in placental development and offspring health [489,491,510,541].

The placenta is a complex tissue arising from the differentiation of distinct cell subtypes important for its functions. In the mouse, the cells that give rise to the placenta, the trophectoderm cell lineage, first appear in the pre-implantation blastocyst at embryonic day 3.5 (E3.5). Blastocyst implantation commences at E4.5, triggering a cascade of paracrine, endocrine and immune-related events that participate in endometrial decidualization. Cells of the trophectoderm overlying the embryonic inner cell mass serve as a source of multipotent trophoblast stem cells (TSCs) that diversify as a result of spatially and epigenetically regulated transcriptional cascades, giving rise to specialized trophoblast-subtypes. The first placental fate segregation is between the extraembryonic ectoderm (EXE) and ectoplacental cone (EPC). Cells of the EPC in direct contact with the decidua give rise to the cells with invasive and endocrine capacity, including trophoblast giants (TGCs), glycocen trophoblast (GlyT), and spongiotrophoblast (SpT). Cells of the chorion will produce two layers of fused, multinucleate syncytiotrophoblast (SynT-I and SynT-II) and sinusoidal TGCs. From E8.5, the embryonic allantois becomes fused with the chorion, permitting invagination of mesoderm-derived angiogenic progenitors that form the basis of the placental vascular bed (Hemberger,

Hanna, & Dean, 2020). Together, these cells form a transportive interface, the placental labyrinth zone, which is functionally critical for sustaining fetal growth throughout gestation (Rossant & Cross, 2001; Simmons & Cross, 2005). Interhemal transfer between maternal and fetal circulation commences at E10.5, and by E12.5 all terminally differentiated cell types of the mature placenta are present.

Genetic studies of placental development using mouse mutants have identified key genes for development, differentiation, maintenance and function [577,718]. For example, homeobox transcription factors are required for trophoblast lineage development (e.g. *Cdx2, Eomes*) [719–723], and maintenance of SPT requires *Ascl2* and *Egfr* [724–728].

Genomic imprinting refers to monoallelic gene expression that is dependent on whether the gene was inherited maternally or paternally [729]. The expression of imprinted genes is regulated by DNA methylation, acting in concert with chromatin modifications, such as histone H3 lysine 4 tri-methylation (H3K4me3) and histone H3 lysine 9 di-methylation (H3K9me2) [730–732]. There exists 228 imprinted genes in humans and 260 in mice; many are strongly expressed in the placenta [427–429,592]. Disruption of placental imprinting is associated with aberrant fetal growth, preeclampsia and IUGR [733–735]. Notably, genetic manipulation studies have determined that the paternal genome is essential for extraembryonic and trophoblast development, and paternally expressed genes dominate placenta gene expression [587–592]

The connection between paternal gene expression and placenta development has led to a growing interest in the role of paternal factors in placental development and function and offspring health [592]. In mice, we demonstrated that paternal folate deficiency was associated with an altered sperm epigenome, differential gene expression in the placenta, and abnormal fetal development [541]. In other mouse models, advanced paternal age and toxicant exposure have been linked to altered placental imprinting and reduced placental weight [595,596]. In human studies, recurrent pregnancy loss is associated with increased seminal reactive oxygen species (ROS) and sperm DNA damage [593]. Male partner metabolic syndrome and being overweight have been associated with an increased risk for pre-eclampsia and negative pregnancy outcomes [594,736]. Animal models suggest that pregnancy complications that have been associated with paternal metabolic complications may be a consequence of placental dysfunction. Indeed, in mice, paternal

obesity was linked to alterations in placental DNA methylation, aberrant allocation of cell lineage to trophectoderm (TE), hypoxia, abnormal vasculature, increased expression of inflammatory factors and impaired nutrient transporters [489,491,510]. These findings support the hypothesis that paternal factors impact placental development and can have negative effects on pregnancy outcomes. To explore the relationship between paternal obesity, the sperm epigenome and offspring health we previously profiled H3K4me3, a gene-activating epigenetic mark, in mouse sperm from sires fed a high-fat diet (HFD) [1]. There was an association between HFD-induced obesity, altered sperm H3K4me3, and metabolic dysfunction in offspring. However, there remains a gap in our mechanistic understanding of the connection between the sperm epigenome and offspring metabolism. Interestingly, a significant portion of genes with altered H3K4me3 in sperm after HFD were related to placental formation and function.

In the current study, we test the hypothesis that obesity-associated changes in sperm H3K4me3 drives aberrant gene expression during placental formation leading to placental dysfunction, and abnormal offspring metabolic phenotypes. To test this hypothesis, sperm was collected from obese sires and placentas from obese-sired pregnancies. Obesity-altered H3K4me3 in sperm occurred at placenta-specific enhancers and the placental transcriptome was altered in a sex-specific manner. Changes in gene expression included genes critical for placental functions that support fetal and organ system development. A deconvolution analysis revealed changes in the placental lineage specification comparable with pathological changes observed in placental defects that are associated with adult-onset cardiometabolic diseases [626,737–739]. Comparative analysis between placental transcriptomic profiles from our paternal HFD-induced obesity model with that of a hypoxia-induced fetal growth restriction model, revealed common placental defects across the two models [626] consistent with our previous work that sire-obesity induces placental hypoxia [510]. This study revealed that paternal obesity was linked with transcriptomic and cellular defects in the placenta and may drive developmental origins of cardiometabolic disease in offspring. Confirmation of such paternal effects in humans are needed.

13.3 Methods

13.3.1 Resource availability

13.3.1.1 Lead contact

Further information and requests for resources and reagents should be directed to and will be fulfilled by the Lead Contacts, D. Sloboda (sloboda@mcmaster.ca) and S. Kimmins (sarah.kimmins@mcgill.ca).

13.3.1.2 Materials availability

This study did not generate new unique reagents.

13.3.1.3 Data and code availability

The sperm H3K4me3 ChIP-Seq and placenta RNA-Seq data generated in this study are deposited at GEO under the SuperSeries GSE207326.

13.3.2 Experimental model and subject details

13.3.2.1 Animals husbandry and dietary treatment

Animal experiments were conducted at the McMaster University Central Animal Facility, approved by the Animal Research Ethics Board, and in accordance with the Canadian Council on Animal Care guidelines. Six-week-old C57BL/6J male mice were randomly allocated to either the control (n=8; CON; standard chow diet, Harlan 8640, Teklad 22/5 Rodent Diet; 17% kcal fat, 54% kcal carbohydrates, 29% kcal protein, 3 kcal/g) or high-fat diet (n=16; HFD; Research Diets Inc., D12492; 20% kcal protein, 20% kcal carbohydrates, 60% kcal fat, 5.21 kcal/g) group, for 10-12 weeks. All animals had free access to water and food *ad libitum*, housed in the same room which was maintained at 25°C on a controlled 12-hour/12-hour light/dark cycle. After the diet intervention, male mice were housed with one or two virgin C57BL/6J females overnight. To confirm mating, females were examined the following morning, and the presence of a copulatory plug was referred to as embryonic day 0.5 (E0.5). Females confirmed as pregnant were individually housed throughout gestation and fed a standard chow diet (Harlan 8640, Teklad 22/5 Rodent Diet). Pregnant females (n=4 CON; n=5 HFD) were sacrificed at E14.5 by cervical dislocation to collect placenta samples for RNA-seq. One male and one female placenta samples per dam were collected. Placenta were cut in half, with one half snap frozen in

liquid nitrogen and kept at -80°C until RNA extraction. CON- and HFD-fed male mice were sacrificed at 4-5 months of age via cervical dislocation, and sperm was collected.

13.3.3 Methods details

13.3.3.1 Sperm isolation

Sperm was collected at necropsy from paired caudal epididymides as previously described [1,614,615]. Caudal epididymides were cut in 5 mL of Donners medium (25 mM $NaHCO_3$, 20 mg ml^{-1} BSA, 1 mM sodium pyruvate, 0.53% vol/vol sodium DL-lactate in Donners stock), and spermatozoa were allowed to swim out by agitating the solution for 1 hour at 37°C. Sperm cells were collected by passing the solution through a 40-µm strainer (Fisher Scientific, #22363547) followed by three washes with phosphate-buffered saline (PBS). The sperm pellet was cryopreserved at -80°C in freezing medium (Irvine Scientific, cat. #90128) until used for the chromatin immunoprecipitation.

13.3.3.2 Chromatin Immunoprecipitation, library preparation, and sequencing

Chromatin immunoprecipitation experiment was performed as previously described [1,614,615]. In brief, samples were thawed on ice and washed with phosphate-buffered saline. Spermatozoa were counted under a microscope using a hemocytometer and 12 million cells were used per experiment. Sperm from 2-7 male mice were pooled per sample (Table S1). We used 1 M dithiothreitol (DTT, Bio Shop, cat #3483-12-3) to decondense the chromatin and N-ethylmaleimide (NEM) was used to quench the reaction. Cell lysis was performed with a lysis buffer (0.3M sucrose, 60mM KCl, 15mM Tris-HCl pH 7.5, 0.5mM DTT, 5mM McGl2, 0.1mM EGTA, 1% deoxycholate and 0.5% NP40). DNA digestion was performed in aliquots containing 2 million spermatozoa (6 aliquots per sample), with micrococcal nuclease (MNase,15 units per tube; Roche, #10107921001) in an MNase buffer (0.3 M sucrose, 85 mM Tris-HCl pH 7.5, 3mM $MgCl_2$ and 2 mM $CaCl_2$) for 5 minutes at 37°C. The reaction was stopped with 5 mM EDTA. Supernatants of the 6 aliquots were pooled back together for each sample after a 10 minutes centrifugation at maximum speed. A 1X solution of protease inhibitor (complete Tablets EASYpack, Roche, #04693116001) was added to each tube. Magnetic beads (DynaBeads, Protein A, Thermo Fisher Scientific, #10002D) used in subsequent steps were pre-blocked in

0.5% Bovine Serum Albumin (BSA, Sigma Aldrich, #BP1600-100) solution for 4 hours at 4°C. Pre-clearing of the chromatin was done with the pre-blocked beads for 1 hour at 4°C. Magnetic beads were allowed to bind with 5 µg of antibody (Histone H3 Lysine 4 trimethylation; H3K4me3; Cell Signaling Technology, cat. #9751) by incubating for 8 hours at 4°C. The pre-cleared chromatin was pulled down with the beads-antibody suspension overnight at 4°C. Beads-chromatin complexes were subjected to 3 rounds of washes; one wash with a low-salt buffer (50 mM Tris-HCl pH 7.5, 10 mM EDTA, 75 mM NaCl) and two washes with a high-salt buffer (50 mM Tris-HCl pH 7.5, 10 mM EDTA, 125 mM NaCl). Elution of the chromatin was done in two steps with 250 µL (2 x 125 µL) of elution buffer (0.1 M HaHCO3, 0.2% SDS, 5 mM DTT) by shaking the solution at 400 rpm for 10 minutes at 65°C, vortexing vigorously, and transferring the eluate in a clean tube. The eluate was subjected to an RNase A (5 µL, Sigma Aldrich, #10109169001) treatment shaking at 400 rpm for 1 hour at 37°C, followed by an overnight Proteinase K (5 µL , Sigma Aldrich, #P2308) treatment
at 55°C. The *ChIP DNA Clean and Concentrator* (Zymo Research, #D5201) kit was used following the manufacturer's protocol to purify the eluted DNA with 25 µL of the provided elution buffer. Libraries were prepared and sequenced at the McGill University and *Génome Québec* Innovative Centre, with single-end 100 base-pair reads on the illumina HiSeq 2500 sequencing platform (n=3 pooled samples per diet group, Table S1).

13.3.3.3 RNA extraction, library preparation and sequencing

Extraction of RNA from placentas was performed using the RNeasy Mini Kit (Qiagen, cat. #74104) following the manufacturer's protocol. In brief, 10-20 mg of frozen placenta were cut on dry ice. Samples were lysed in a denaturing buffer and homogenized with homogenizer pestles. Lysates were centrifuged, supernatants transferred into a clean tube, and 70% ethanol was added to lysates. An additional DNase digestion step was performed to avoid DNA contamination. Spin columns were washed twice, and total RNA was eluted with 30 µL of RNase-free water. Libraries were prepared and sequenced at the McGill Genome Centre with paired-end 100 base-pair reads on the illumina NovaSeq 6000 sequencing platform (n=4 per sex per diet group).

13.3.3.4 Pre-processing

13.3.3.4.1 Sperm ChIP-Sequencing data

Pre-processing of the data was performed as previously described [1]. Sequencing reads were trimmed using the *Trimmomatic* package (version 0.36) on single-end mode filtering out adapters and low-quality reads (parameters: ILLUMINACLIP:2:30:15 LEADING:30 TRAILING:30) [620]. Reads were aligned to the mouse genome assembly (*Mus Musculus*, mm10) with *Bowtie2* (version 2.3.4) [621]. *SAMtools* (version 1.9) was used to filter out unmapped reads and *Perlcode* to remove reads with more than 3 mismatches [618]. BAM coverage files (BigWig) files were created with *deeptools2* (version 3.2.1) (parameters: -of bigwig -bs 25 -p 20 --normalizeUsing RPKM -e 160 --ignoreForNormalization chrX) [622].

13.3.3.4.2 Placenta RNA-Sequencing data

Sequencing data was pre-processed as previously described [1]. Sequencing reads were trimmed with *Trim Galore* (version 0.5.0) in paired-end mode to remove adapters and low-quality reads (parameters: --paired --retain_unpaired --phred33 --length 70 -q 5 --stringency 1 -e 0.1) [616]. Reads were aligned to the mouse reference primary assembly (GRCm38) with *hisat2* (version 2.1.0, parameters -p 8 --dta) [740]. The generated SAM files were converted into BAM format and sorted by genomic position with *SAMtools* (version 1.9) [618]. *Stringtie* (version 2.1.2) was used to build transcripts and calculate their abundances (parameters: -p 8 -e -B -A) [619].

13.3.3.4.3 Publicly available datasets

Raw files for bulk RNA-sequencing in control and hypoxic placentas (n=7 and 8, respectively) were downloaded from the National Centre for Biotechnology Information (NCBI) with the Sequencing Read Archive (SRA) Toolkit (NCBI SRA: SRP137723) [666]. Files were pre-processed as described above for RNA-sequencing on single-end mode. Processed files with raw counts for single-cell RNA-sequencing data from E14.5 mouse placenta were downloaded from NCBI (GEO: GSE108097) and metadata matrix and cluster annotations were downloaded from https://figshare.com/s/865e694ad06d5857db4b [738].

13.3.4 Quantification and statistical analysis

13.3.4.1 Visualization, statistical, and bioinformatic analyses

Bioinformatic data analyses were conducted using R (version 4.0.2) [632] and Python (version 3.7.4) [741]. Figures were generated using the R package ggplot2 (version 3.3.3) [640] and the Python package *seaborn* (version 0.9.0) [628]. Statistical analysis were conducted using R version 4.0.2 [632]. For all statistical tests, a p-value less than 0.05 was considered significant. To assess significance of overlap between different sets of genes, a Fisher's exact test was performed using the *fisher.test* function from the *stats* package (version 4.0.2), and the numbers that were used to assess statistical significance were those found in the common universe (background) of both lists being compared. To assess differences in cell type proportions across experimental groups, a beta regression was performed using *betareg* function from the *betareg* package (version 3.1-4) [742].

13.3.4.2 Sperm ChIP-Sequencing data

ChIP-sequencing data was processed and analyzed as previously described [1]. Using *csaw* (version 1.22.1), sequencing reads were counted into 150 base-pair windows along the genome, and those with a fold-change enrichment of 4 over the number of reads in 2,000 base-pair bins were considered as genomic regions enriched with H3K4me3 in sperm [643]. Enriched windows less than 100 base-pair apart were merged allowing a maximum width of 5,000 base-pair (n=35,186 merged enriched regions in total). Reads were counted in those defined regions, and those with a mean count below 10 across samples were filtered out (conferring a total of n=35,184 regions). Read counts within enriched regions were normalized with TMM and corrected for batch effects arising from experimental day, using the *sva* package (version 3.36.0) [644,645]. Spearman correlation heatmaps were generated using *corrplot* (version 0.88) and mean-average (MA) plots with *graphics* packages [638].

To detect the obesity-sensitive regions, Principal Component Analysis (PCA) was performed. We selected the top 5% regions contributing the separation of samples according to diet group along Principal Component 1 (PC1), conferring a total of 1,760 regions associated with dietary treatment. Those regions were split according to

directionality change based on positive and negative log_2 fold-change values (increased versus decreased enrichment in high-fat diet group, respectively) from the median normalized counts of each group. The selected obesity-sensitive regions were visualized with *Pheatmap* (version 1.0.12) [639]. Profile plots were generated using *deeptools* [622]. The distance from the nearest transcription start site (TSS) from each selected region was calculated and visualized with *chipenrich* (version 2.12.0) [647]. The genes for which their promoters overlapped the detected obesity-sensitive regions were used in the Gene Ontology (GO) analysis using *topGO* (version 2.40.0) with Biological Process ontology category and Fisher's exact test (*weight01Fisher* algorithm) to test enrichment significance [648]. A *weight01Fisher* p-value below 0.05 was considered significant. Genome browser snapshots of examples of detected obesity-sensitive regions were generated using *trackplot* [652]. Annotations for tissue-specific enhancers were downloaded from ENCODE [625] (GEO: GSE29184) and genome coordinates were converted from the mm9 to the mm10 mouse assembly using the *liftOver* function from the *rtracklayer* package (version 1.48.0) [743]. To determine the corresponding genes that could be regulated by tissue-specific enhancers, we scanned the landscape surrounding putative enhancer genomic coordinates, and selected the nearest gene located less than 200 kb away, given that enhancers interact with promoters located within the same domain [625,744]. To retrieve the gene annotations, we used the function *annotateTranscripts* with the annotation database *TxDb.Mmusculus.UCSC.mm10.knownGene* (version 3.10.0) and the annotation package *org.Mm.eg.db* (version 3.11.4) from the *bumphunter* package (version 1.30.0) [745,746]. From the same package, the function *matchGenes* was used to annotate the putative tissue-specific enhancer genomic coordinates with the closest genes. Annotations for transposable elements and repeats were obtained from *annotatr* (version 1.14.0) [649] and RepeatMasker (https://www.repeatmasker.org/). Upset plots were generated using the UpSetR package (version 1.4.0) [650]. The motif analysis was performed using HOMER (version 4.10.4) [747], with the binomial statistical test and standard parameters. *ViSEAGO* (version 1.2.0) [642] was used for visualization, semantic similarity and enrichment analysis of gene ontology (Fig. S1 I). Gene symbols and annotations were obtained from the *org.Mm.eg.db* database for the *Mus Musculus* species. The Biological Process ontology category was used, and statistical significance

was assessed with a Fisher's exact test with the classic algorithm. A p-value less than 0.01 was considered significant. Enriched terms are clustered by hierarchical clustering based on Wang's semantic similarity distance and the *ward.D2* aggregation criterion.

13.3.4.3 Placenta RNA-Sequencing data

Placenta bulk RNA-sequencing data from this study and from [666] was processed and analyzed using the same approach, as previously described [1]. In brief, transcripts with low read counts were filtered out (mean count<10), for a total of 47,268 and 49,999 transcripts detected in male and female placentas, respectively, and 32,392 transcripts in placentas from [666]. Differential analysis was conducted with *DESeq2* (version 1.28.1) [748]. For the data generated in this study, we included the batch information (RNA extraction day) and dietary group in the design formula and performed a stratified analysis by running male and female samples separately (Fig. S3 B-C). For the data generated in [666], only male samples were analyzed given there was not a sufficient number of female samples, and we included the experimental group in the formula. Independent hypothesis weighting (IHW, version 1.16) [634] was used for multiple testing correction and prioritization of hypothesis testing. We performed a gene-level analysis at single-transcript resolution using the Lancaster method (*aggregation* package, version 1.0.1) [749]. This method aggregates p-values from individual transcript to detect differentially expressed genes based on changes at the transcript level. A p-value less than 0.05 was considered significant.

For visualization, variance stabilized transcript counts were used without blind dispersion estimation [750]. Spearman correlation heatmaps were plotted with *corrplot* (version 0.88) [638] with samples clustered by hierarchical clustering. Transcripts coding for detected differentially expressed genes were visualized with *pheatmap* (version 1.0.12) [639], with samples clustered with hierarchical clustering and transcripts by k-means clustering (n kmeans=2). Gene ontology analysis was performed as described above for the sperm ChIP-seq data. For the genomic imprinting analysis, the list of known mouse imprinted genes was retrieved from [429].

13.3.4.4 Deconvolution analysis

We used single-cell RNA-sequencing datasets from mouse E14.5 placenta from to deconvolute our bulk RNA-sequencing data [738]. The following Python packages were used: *seaborn* (version 0.9.0) [628], *numpy* (version 1.17.2) [629], *pandas* (version 0.25.2) [630], *pickle* (version 4.0) [751], *scanpy* (version 1.8.2) [752], *scipy* (version 1.7.3) [753], and *autogenes* (version 1.0.4) [737]. The *pyplot* module was loaded from the *matplotlib* library (version 3.4.2) [631]. The deconvolution analysis was performed following the AutoGeneS package's available code (version 1.0.4) [737]. In brief, single-cell counts were log normalized and the 4,000 most highly variable genes were selected. A principal component analysis was performed (Fig. S4 A) and the cell types previously annotated in [738] were visualized (Fig. S4 B). The means of each centroids for each cell type cluster was used for optimization and feature selection. AutoGeneS uses a multi-objective optimization approach to select marker genes. In this process, a search algorithm explores a set of optimal solutions (commonly called Pareto-optimal solutions) and evaluates the objective functions (in this case, correlation and distance between the cell-type specific clusters; Fig. S4 C-D). This optimization technique allows to select the 400 marker genes (Fig. S4 E). Lastly, the Nu-support vector machine (Nu-SVR) regression model [754] was used to estimate the cell-type proportions for the bulk RNA-seq data from this study and from [666]. The estimated cell-type proportions were visualized as box plots for each cell type. The cell-types with percent abundance values of zero across all samples were excluded. Statistical significance across experimental groups was assessed with beta regression on the cell-types that had a median relative abundance of at least 1.5%.

13.3.4.5 Placenta RNA-Sequencing differential analysis with cell-type proportion adjustment

To adjust for cell-type proportions in the differential analysis, while reducing the number of covariates in the model, and to account for dependence between the cell-type proportions, a principal component analysis was performed with the deconvolved cell type proportions using the *prcomp* function from R's base statistics. The top 3 or 4 principal components were selected to capture most of the sample variance (Fig. S6 A and D, Fig. S7 E). The differential analysis described above was repeated, with the selected principal

components added as covariates in the design formula to form the cell-type adjusted model.

13.4 Results

13.4.1 High-fat diet-induced obesity alters the sperm epigenome at regions implicated in metabolism, cellular stress and placentation

Figure 1 describes the previously phenotypically characterized paternal HFD-induced obesity mouse model used in this study [510]. Of note, it differs from our previous model [1] by mouse sub-strain (C57BL/6J vs C57BL/6NCrl), research setting, timing of diet exposure (at 6 vs 3 weeks of age), and the control diet (chow vs low-fat diet). This difference in experimental design allows to test the robustness of our previous results linking HFD with alteration of sperm H3K4me3. This study also newly examines functional genomic regions in relation to the placenta cell composition and transcriptomic profile including imprinted genes, placenta enhancers and transcription factor binding motifs.

Figure 1

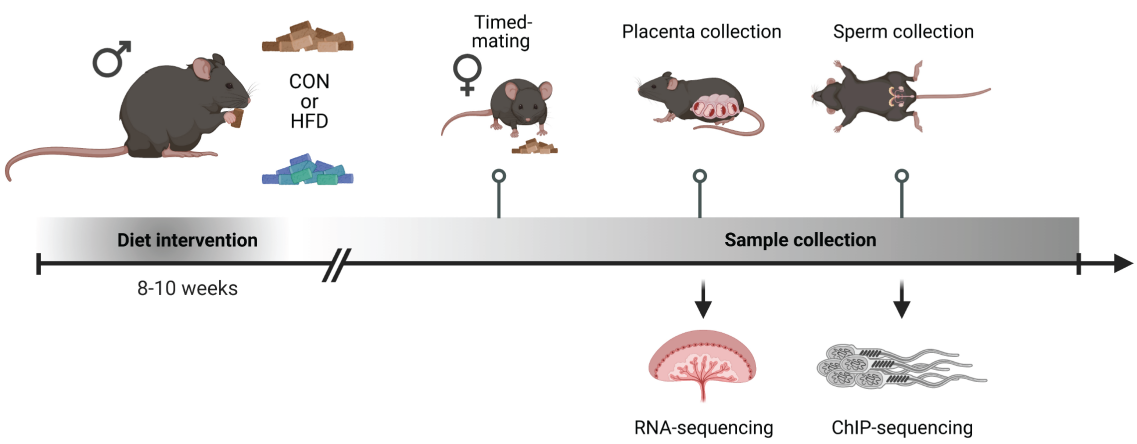

Figure 1: Experimental design showing the timeline and methods used to study the consequences of an obesity-induced altered sperm epigenome on the placenta.

A) Six-week-old C57BL/6J sires were fed either a control or high-fat diet (CON or HFD, respectively) for 8-10 weeks. Males were then time-mated with CON-fed C57BL/6J females to generate pregnancies. Pregnant females were sacrificed at embryonic day (E)14.5 and placentas were collected to perform RNA-sequencing (RNA-seq, n=4 per sex per dietary group). Sires were sacrificed at 5 months of age and sperm from cauda epididymides was collected for chromatin immunoprecipitation sequencing (ChIP-seq, n=3 per dietary group) targeting histone H3 lysine 4 tri-methylation (H3K4me3). Created with BioRender.com.

Sperm from CON- and HFD-fed sires was profiled using ChIP-seq targeting H3K4me3 (n=3 per dietary group, Table S1). A total of 35,184 regions in sperm were enriched for H3K4me3 (Fig. S1 A; Methods), of which 28,279 were also detected in our previous study [1]. H3K4me3 profiles were highly concordant across samples which demonstrate the robustness of our profiling approach (Fig. S1 B). Principal component analysis on counts at sperm H3K4me3-enriched regions revealed separation of samples along Principal Component 1 (PC1) according to dietary treatment, after trimmed Mean of M-values (TMM) normalization and batch adjustment (Fig. S1 C). The top 5% regions (n=1,760) contributing to PC1 were considered the most sensitive to HFD-induced obesity and were selected for downstream analysis (Fig. S1 C, Fig. 2). Despite differences in experimental design and animal models, we found a significant overlap in regions showing differential H3K4me3 (deH3K4me3) from both studies (128 overlapping regions, Fisher's exact test P=2.2e-16, Fig. S1 D). Additionally, there were similarities in terms of enriched processes between both lists of deH3K4me3 regions overlapping promoters - in particular metabolic and neurodevelopmental pathways (Fig S1 E, Table S2, Supp file 1). Consistent with our previous study, the majority of obesity-associated regions showed an increase in enrichment for H3K4me3 (n=1,257 versus n=503, 71.4%, Fig. 2 A-B). Regions losing H3K4me3 showed moderate H3K4me3-enrichment in CON sperm, with predominantly low CpG density, whereas regions gaining H3K4me3 showed low-to-moderate enrichment with mainly high CpG density (Fig. 2 C). Regions not impacted by diet showed high H3K4me3 enrichment in CON sperm, with low and high CpG density (Fig. 2 C). Consistent with our previous study, regions losing H3K4me3 were predominantly located >5 kilobase (kb) from the transcription start site (TSS), likely in intergenic spaces (Fig. 2 D i). Regions gaining H3K4me3 in HFD sperm were located near the TSS (within 1 kb), likely at promoter regions (Fig. 2 D ii). Obesity-associated

deH3K4me3 regions overlapping promoters were found at genes involved in metabolic processes, cellular stress responses, vasculature development, and placentation (Fig. 2 E i-ii, Tables S3-4). Examples of genes showing deH3K4me3 in sperm include, *Cbx7* (Chromobox protein homolog 7; a component of the polycomb repressive complex 1, involved in transcriptional regulation of genes including the *Hox* gene family), *Prdx6* (Peroxiredoxin 6; an antioxidant enzyme involved in cell redox regulation by reducing molecules such as hydrogen peroxide and fatty acid hyperoxides), and *Slc19a1* (Solute carrier family 19 member 1 or folate transporter 1; a folate organic phosphate antiporter involved in the regulation of intracellular folate concentrations) (Fig 2F). We identified deH3K4me3 in HFD-sperm at *Igf2* (Fig. 2 F ii – Insulin-like growth factor 2), a paternally-expressed imprinted gene with an essential role in promoting cellular growth and proliferation in the placenta. Importantly *Igf2* function has been related to metabolic disease and obesity (Kadakia & Josefson, 2016; Livingstone & Borai, 2014; reviewed in St-Pierre et al., 2012). Other imprinted genes with deH3K4me3 included the homeodomain-containing transcription factor *Otx2* (involved in brain and sense organs development), and the voltage-gated potassium channel *Kcnq1* gene (required for cardiac action potential).

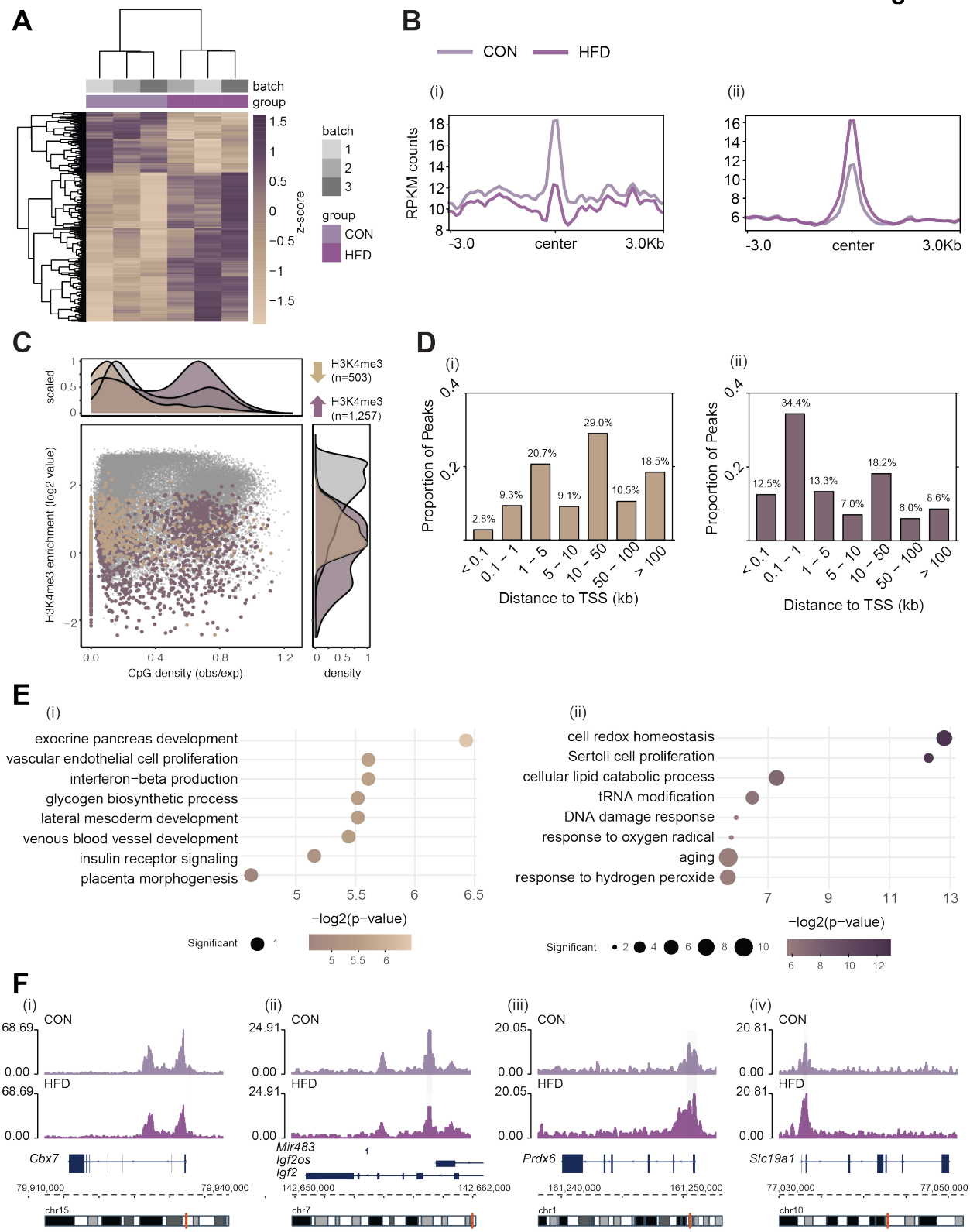

Figure 2: H3K4me3 signal profile at obesity-sensitive regions in sperm.

A) Heatmap of log2 normalized counts for obesity-sensitive regions in sperm (n=1,760). Columns (samples) and rows (genomic regions) are arranged by hierarchical clustering with complete-linkage clustering based on Euclidean distance. Samples are labeled by batch (grey shades) and by dietary group.
B) Profile plots showing RPKM H3K4me3 counts +/- 3 kilobase around the center of genomic regions with decreased (i) and increased (ii) H3K4me3 enrichment in HFD-sperm compared to CON-sperm.
C) Scatter plot showing H3K4me3 enrichment (log2 counts) versus CpG density (observed/expected) for all H3K4me3-enriched regions in sperm (n=35,184, in grey), regions with HFD-induced decreased H3K4me3 enrichment (n=503, in beige), and regions with increased H3K4me3 enrichment (n=1,257, in purple). The upper and right panels represent the data points density for CpG density and H3K4me3 enrichment, respectively.
D) Bar plots showing the proportion of peaks for each category of distance from the transcription start site (TSS) of the nearest gene in kilobase (kb), for obesity-sensitive regions with decreased (i) and increased (ii) H3K4me3 enrichment in HFD-sperm.
E) Gene ontology (GO) analysis for promoters at obesity-sensitive regions with decreased (i) and increased (ii) H3K4me3 enrichment in HFD-sperm. The bubble plot highlights 8 significantly enriched GO terms, with their -log2(p-value) depicted on the y-axis and with the color gradient. The size of the bubbles represents the number of significant genes annotated to a specific GO term. Tables S3-4 include the full lists of significant GO terms.
F) Genome browser snapshots showing genes with altered sperm H3K4me3 at promoter regions (CON pale purple, HFD dark purple).

13.4.2 Differentially enriched H3K4me3 in HFD sperm occurred at enhancers involved in placenta development, and at transcription factor binding sites

We previously showed that changes in sperm H3K4me3 associate with altered embryonic gene expression [477]. To gain functional insight into how deH3K4me3 in sperm may impact embryonic gene expression, we assessed the association between deH3K4me3 and tissue-specific and embryonic enhancers. Notably, deH3K4me3 localized at enhancers implicated in gene regulation of the testes, placenta, and embryonic stem cells (Fig. S2 A-B) [625]. Interestingly, when searching for closest genes potentially regulated by placenta-specific enhancers, 3 were paternally-expressed imprinted genes [429]. These included the transmembrane protein *Tmem174*, the zinc finger protein *Plagl1* (a suppressor of cell growth), and the growth factor *Pdgfb* (a member of the protein family of platelet-derived and vascular endothelial growth factors; plays essential roles in embryonic development, cellular proliferation and migration).

Since H3K4me3 often localizes to promoters and can serve in the recruitment of transcription factors (TFs) [758,759], we asked whether deH3K4me3 were significantly enriched in known TF binding site locations across the genome. Changes in H3K4me3 at

these specific locations in sperm could impact embryonic gene expression – for example TFs, such as *Foxa1,* maintain an open chromatin state from the sperm to the embryo on the paternal chromatin [471,760]. To explore this possibility, we searched for known TF binding motifs enriched in deH3K4me3 regions in sperm (Methods). The regions that gained H3K4me3 were significantly enriched for 202 TF binding motifs (P<0.05, binomial statistical test, q-value<0.05; Fig. 3 A and Supp file 2) [747] whereas regions that had reduced H3K4me3 were not significantly enriched for TF binding motifs (q-value>0.05). Of the top 10 motifs enriched at regions with increased H3K4me3 signal in HFD-sperm, these genomic sequences were predicted to be bound by TFs belonging to the ETS, THAP, and ZF motif families (P<1e-10, q-value<0.0001; Fig. 3A). Interestingly, changes in sperm DNA methylation upon HFD feeding has been previously reported, and ETS motifs have been found to be DNA-methylation sensitive, including in spermatogonial stem cells [761–764]. Strikingly, *Sp1*, a pregnancy-specific TF associated with recurrent miscarriage, was found to be among the top TF-associated motif hits (P=1e-16, q-value<0.0001) in regions gaining H3K4me3 in sperm from obese sires [765]. Furthermore, another TF of interest enriched at regions gaining H3K4me3 in HFD sperm is the Activating Transcription Factor 7 (*Atf7*; p-value=1e-3, q-value=0.0044, Supplemental File 3). Of note, this TF has been associated with oxidative stress-induced epigenetic changes in male germ cells in a mouse model of low-protein diet [540].

Figure 3

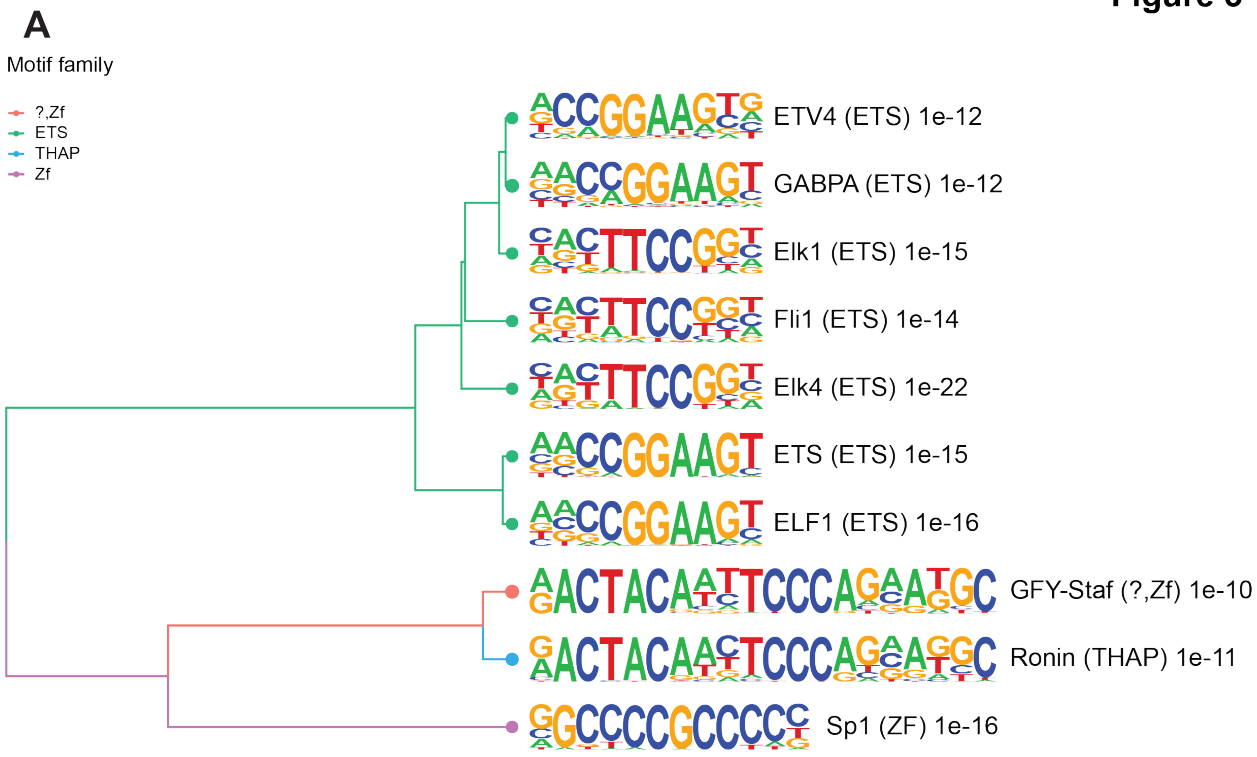

Figure 3: Enriched motifs at obesity-sensitive regions in sperm.
A) Top 10 significantly enriched known motifs at obesity-sensitive regions with increased H3K4me3 enrichment in HFD-sperm. Motifs are clustered based on sequence similarity with hierarchical clustering. Branches of the dendrogram tree are color-coded by motif family. The name of the motif is indicated on the right, with the motif family in parenthesis, and the associated p-value for enrichment significance (binomial statistical test). The full list of enriched motifs can be found in Supplemental files 2.

Taken together we have shown there is consistency in the impacts of HFD on sperm H3K4me3 and in this model we extended our findings with a deeper functional analysis. Namely we identified novel functional genomic regions including enhancers, imprinted genes and transcription factor binding sites with altered H3K4me3 that are likely connected to paternal transmission of metabolic disease in offspring.

13.4.3 Placental gene expression is altered by paternal high-fat diet-induced obesity in a sex-specific manner

As deH3K4me3 in sperm was located at genes involved in placental formation (Fig. 2 E and Pepin et al., 2022), we assessed whether paternal obesity was associated with

changes in gene expression of the placenta. We isolated RNA from E14.5 placentas derived from CON- or HFD-fed sires and performed RNA-sequencing (RNA-seq), yielding high quality data (Spearman correlation coefficient >0.89; Fig. S3 A-C). In response to paternal obesity, we detected 2,035 and 2,365 differentially expressed genes (DEGs) in female and male placentas, respectively (Fig. 4 A-B). These dysregulated genes were significantly enriched in pathways related to placental function, such as cholesterol, vitamin and protein transport, transcriptional and mRNA splicing processes, angiogenesis, and organ growth (Fig. 4 C-D, Tables S5-6). Perhaps reflecting the brain-placenta axis [580,766], other significantly enriched processes were implicated in brain and neuron development [580]. Given that correct imprinted gene expression is critical for development, particularly of the placenta, it is noteworthy that in HFD-sired placentas 23 and 28 imprinted genes were differentially expressed in female and male placentas, respectively (Fig. 4 E-F).

Figure 4

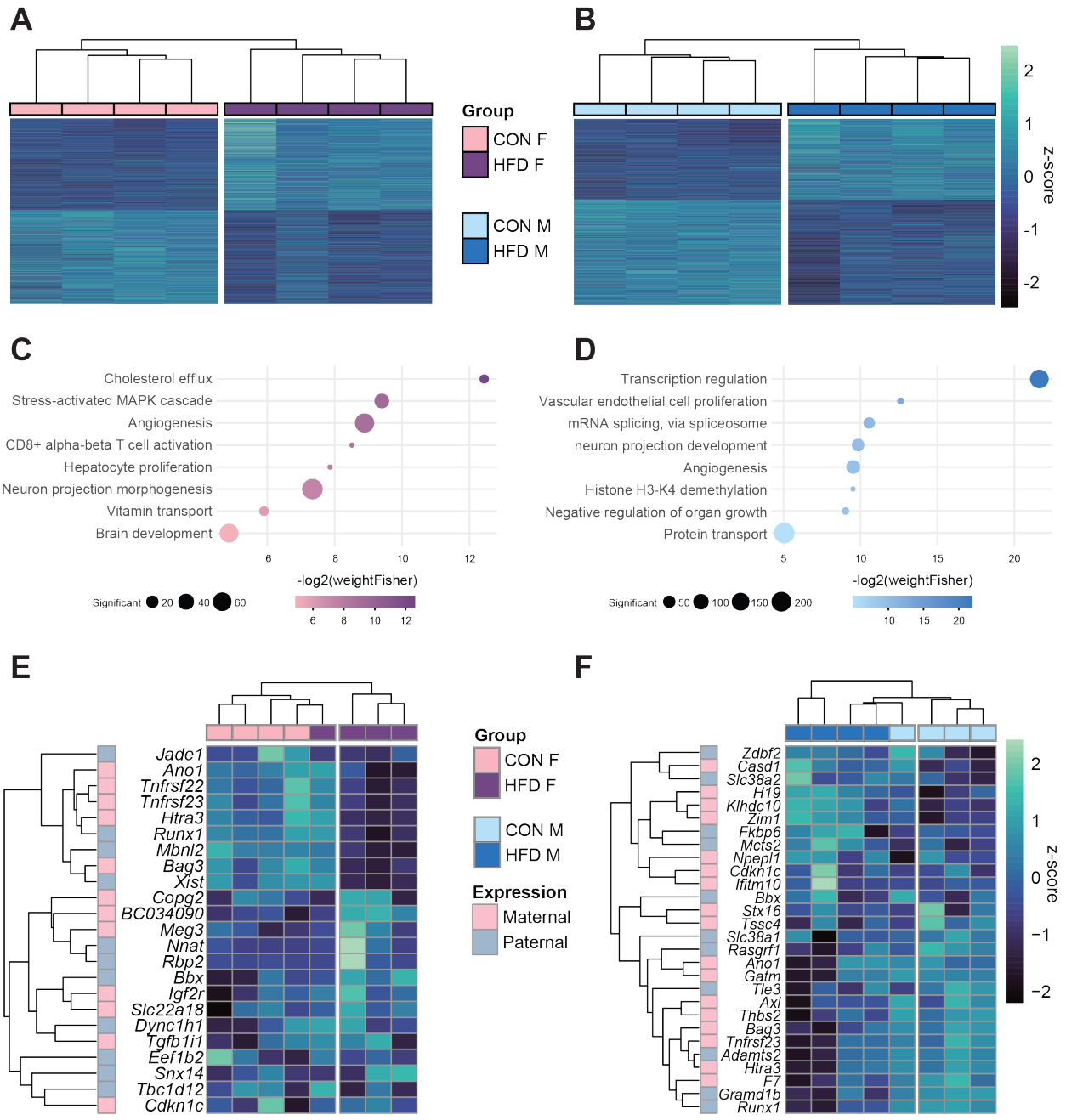

Figure 4: Paternal obesity alters the F_1 placental transcriptome in a sex-specific manner.
A-B) Heatmaps of normalized counts scaled by row (z-score) for transcripts that code for the detected differentially expressed genes (Lancaster p<0.05) in female (A, n=2,035 genes) and male (B, n=2,365 genes) placentas. Rows are orders by k-means clustering and columns are arranged by hierarchical clustering with complete-linkage based on Euclidean distances.
C-D) Gene ontology (GO) analysis for differentially expressed genes in female (C) and male (D) placentas. The bubble plot highlights 8 significantly enriched GO terms, with their -log2(p-value) depicted on the y-axis and with the color gradient. The size of the bubbles represents the number of significant genes annotated to a specific enriched GO term. Tables S5-6 include the full lists of significant GO terms.

E-F) Heatmaps of normalized counts scaled by row (z-score) for detected differentially expressed imprinted genes (Lancaster p<0.05) in female (E, n=23 genes) and male (F, n=28 genes) placentas. Genes are labeled based on their allelic expression (paternally expressed genes in pale grey, maternally expressed genes in pale pink). Rows are orders by k-means clustering and columns are arranged by hierarchical clustering with complete-linkage based on Euclidean distances.

Of note, although a significant number of DEGs overlapped between female and male placentas (n=359, Fisher's exact test P=1.5e-19; Fig. S3 D i), 82% of female DEGs and 85% of male DEGs were uniquely de-regulated, indicating sex-specific placental responses to paternal obesity. The findings are concordant with previous studies which observed sex-specific effects of paternal factors on offspring metabolism [489,510,535,767]. This suggests some sexually dimorphic responses may originate *in utero* due to differences in placental development and function. To assess the link between sperm H3K4me3 and the placental transcriptome, we overlapped deH3K4me3 at promoters (n=508) with DEGs in the placenta, and identified 45 and 48 DEGs in female and male placentas, respectively (Fig. S3 D ii-iii). Next, we assessed deH3K4me3 in sperm at putative placenta-specific enhancers in relation to placenta DEGs. We identified 139 putative enhancers with increased H3K4me3 and 46 with reduced H3K4me3 in HFD-sperm (Fig. S2 A-B). We then focused the analysis on the predicted genes (200 kb range) regulated by these putative enhancers [625,744], and defined 18 genes that were DEG in female and 19 in male placentas (Fig. S3 D iv-v). Taken together these findings show there was minor overlap between genome regulatory regions bearing deH3K4me3 and placenta DEGs. This may reflect the terminally differentiated state and heterogenous nature of the placenta at E14.5. Greater correspondence between sperm deH3K4me3 may have been observed if we had analyzed gene expression earlier in development when H3K4me3 in sperm may have a greater influence on gene expression in the first embryonic lineage of the placenta, the TE from PND 3.5. Indeed, we previously found by *in silico* analysis that there was a significant overlap between sperm and TE H3K4me3, and TE gene expression [1]. It is also worth considering that placenta profiles in this study are from bulk homogenates of whole placenta which represent a heterogeneous mixture of cell types. Bulk tissue RNA-seq measures average gene expression across these

molecularly diverse cell types in distinct cellular states and the identification of DEGs can therefore be confounded by cell composition.

13.4.4 Deconvolution analysis of bulk RNA-seq reveals paternal obesity alters placental cellular composition

To assess whether there were changes in placental cellular composition associated with paternal obesity, we performed a deconvolution analysis on our bulk RNA-seq data (Fig. S4) [737] using a single-cell RNA-sequencing dataset that matched the samples' developmental stage (E14.5) and mouse strain (C57BL/6J) [738]. Of the 28 different cell types identified [738] (Table S7; Fig. S4 A), we detected 15 cell types in our deconvolved placenta bulk RNA-seq data (Fig. 5 A and Fig. S5 A). The bulk placenta profiles were enriched for 3 trophoblast, 1 stroma and 1 endothelial cell subtypes (Figure 5A). Two of the three trophoblast cell types belonged to the spongiotrophoblast (SPT) lineage including the invasive SPT cells and SPT cells molecularly defined by highly-expressing 11-ß hydroxysteroid dehydrogenase type 2 *(Hsd11b2*). Paternal obesity was associated with changes in both SPT cell populations (Fig. 5A); we detected a significant decrease in invasive SPT cell relative abundance in female placentas (P=0.02; Fig. 5 A) and an increase in high-*Hsd11b2* SPT cells in both male and female placentas (P=0.01 and P=0.06, respectively; Fig. 5 A). These changes in SPT cellular composition indicated by this analysis upon paternal HFD-induced obesity could contribute to adult-onset metabolic dysfunction in offspring sired by obese males as observed in previous studies [1,510].

Figure 5

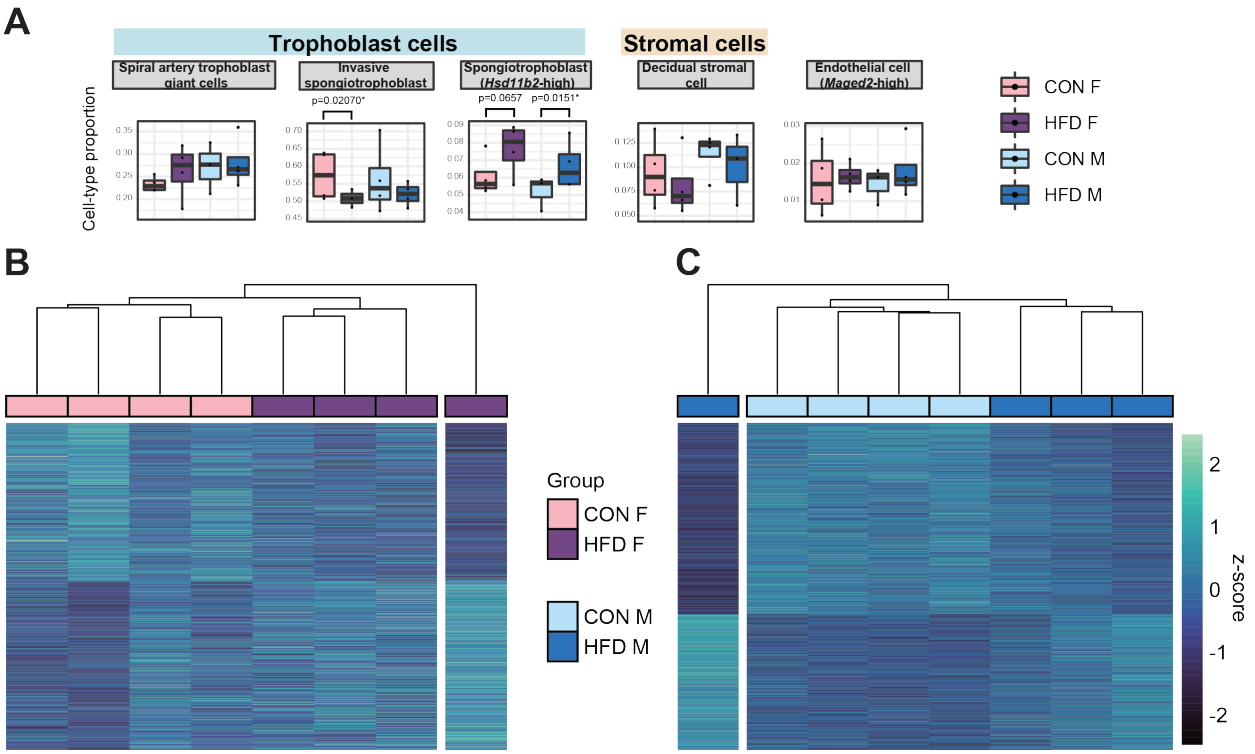

Figure 5: Paternal obesity-induced changes in placental cellular composition and differential expression. A) Boxplots showing sample-specific proportions for the top 5 cell types with highest proportions detected in the bulk RNA-seq data deconvolution analysis across experimental groups. Beta regression was used to assess differences in cell-type proportions associated with paternal obesity for each placental sex. P<0.05 was considered significant.

B-C) Heatmaps of normalized counts scaled by row (z-score) for transcripts that code for the detected differentially expressed genes (Lancaster p<0.05) in female (B, n=423 genes) and male (C, n=1,487 genes) placentas, after adjusting for cell-type proportions. Rows are orders by k-means clustering and columns are arranged by hierarchical clustering with complete-linkage based on Euclidean distances.

To further identify gene expression changes associated with paternal obesity we performed similar differential gene expression analysis for male and female placentas but adjusted for estimated cell-type proportions (Fig. S6 A-F). We first encoded cell-type composition using the top 4 and 3 principal components identified by PCA (Fig. S6 A, B, D and E). As expected, cell types contributing the most to the sample variances for both male and female placentas included the most abundant cell types – namely invasive SPT and spiral artery TGCs, and decidual stromal cells, and endodermal cells (Fig. S6 C and F). After adjustment for placental cellular composition, we detected de-regulated genes in female (n=423 DEGS) and male placentas (n=1,487 DEGs, Fig. 5 B-C, Fig. S6 G-H),

respectively. There were similarities between the bulk RNA-Seq and deconvoluted analysis in that there was overlap of DEGs detected before and after adjusting for cell-type proportions (Fig. S6 G-H). This differential gene expression analysis accounting for cellular composition provides insight into how paternal obesity may impact placental development and function.

13.4.5 Hypoxic and paternal obese-sired placentas show common transcriptomic deregulation and cell-type composition changes

Placentas derived from obese sires, like hypoxic placentas, exhibit changes in gene expression and altered angiogenesis, vasculature, and development [489,491,510,696,736,768]. Hypoxia is a tightly regulated process during placental development which is essential for proper vascular formation. To determine whether paternal obese-sired placentas resemble transcriptomic and pathological phenotypes of hypoxic placentas, we compared our HFD placenta RNA-seq data to a hypoxia-induced IUGR mouse model RNA-seq data set [626]. We conducted differential gene expression analysis of the RNA-seq data from the IUGR mouse model using the same parameters as the obese-sired placenta analysis. Because this dataset did not include a sufficient number of female placenta samples, we focused the analysis on male samples only (n=5 control, n=5 hypoxic placentas). This differential analysis identified 1,935 DEGs in hypoxic placentas (Fig. S7 A-C). Likewise, we applied our deconvolution analysis described above to this bulk RNA-seq data from hypoxic placentas and detected the same principal cell types as those detected in our samples; a total of 17 different cell types were detected (Fig. 6A, Fig. S7D). Remarkably, the proportion values for each individual cell types were highly comparable across the placenta from the HFD sire model and the hypoxia mouse models (Fig. 6B). Similar to placentas derived from obese sires, hypoxic placentas showed a significant decrease in invasive SPT cell abundance (p=0.003, Fig. 6 A). Hypoxic placentas also showed a significant increase in progenitor trophoblast (*Gjb3*-high), primitive endoderm (PE) lineage (*Gkn2*-high), erythroblast (*Hbb-y*-high), and endodermal (*Afp*-high) cells, compared to control (p=0.000004, p=0.01, p=0.000003, p=0.005, respectively; Fig. 6A).

Overall, the trends for directionality of changes in specific cellular abundances were consistent across the two mouse models (Fig. 6B).

Figure 6

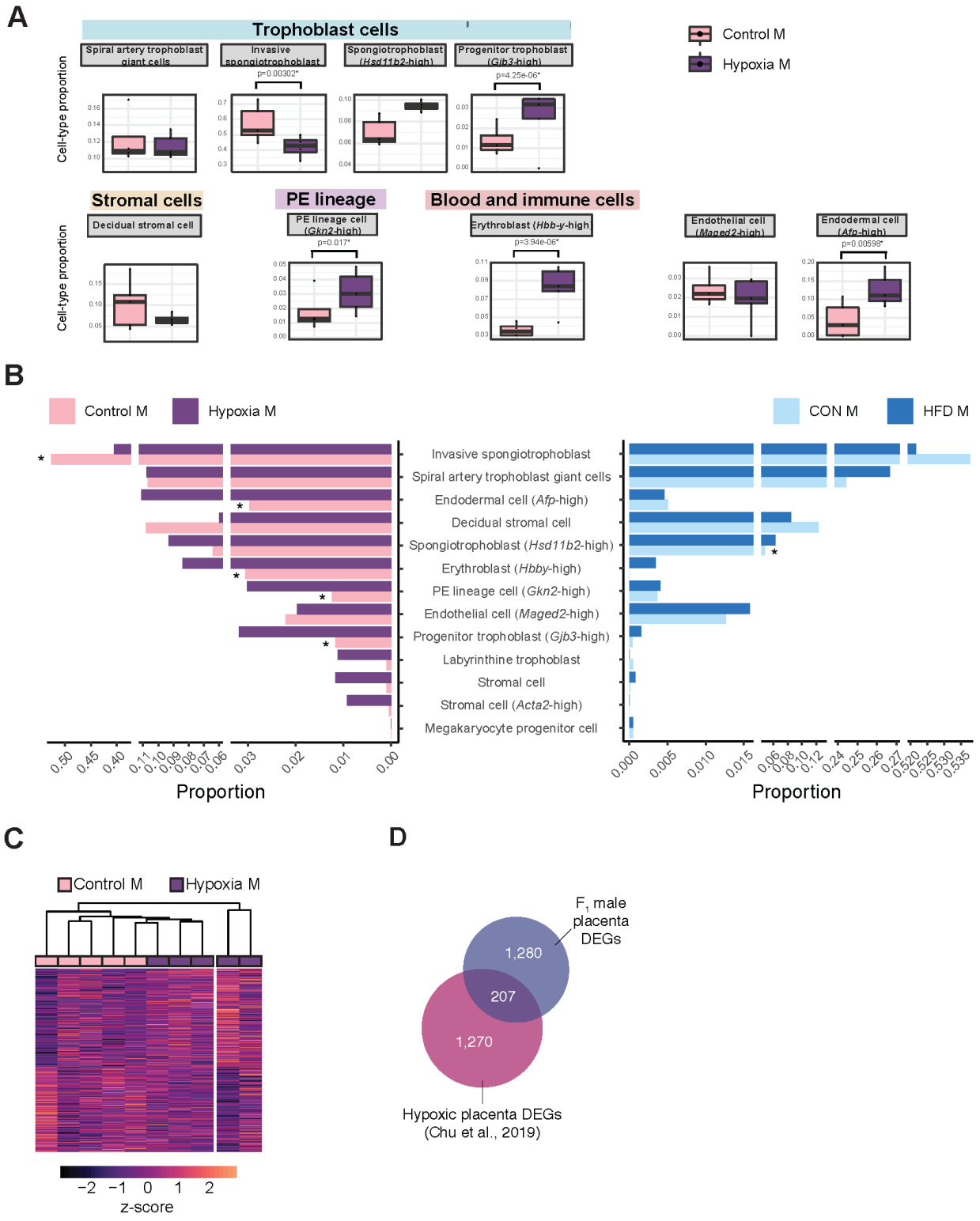

Figure 6: Hypoxia-induced growth restriction is associated with changes in placental cellular composition and differential expression.
A) Boxplots showing sample-specific proportions for the top 10 cell types with highest proportions detected in the bulk RNA-sequencing data deconvolution analysis across experimental groups. Beta regression was used to assess differences in cell-type proportions associated with hypoxia-induced intrauterine growth restriction. P<0.05 was considered significant.
B) Pyramid plot showing the median values of cell-type proportions commonly detected in both datasets assessed. The asterix (*) denote significance (P<0.05) between control versus hypoxia groups or CON M versus HFD groups, as calculated by beta regression.
C) Heatmap of normalized counts scaled by row (z-score) for transcripts that code for the detected differentially expressed genes (Lancaster p<0.05, n=1,477 genes) in hypoxic placentas, after adjusting for cell-type proportions. Rows are orders by k-means clustering and columns are arranged by hierarchical clustering with complete-linkage based on Euclidean distances.
D) Venn diagrams showing overlap between hypoxia-induced de-regulated genes in an intrauterine growth restriction model (Chu et al., 2019), with paternal obesity-induced de-regulated genes (this study) in male placentas.

Next, we sought to similarly investigate how much the observed changes in cellular composition within hypoxic tissues might contribute to the differential gene expression observed between conditions. Principal component analysis on placental cellular proportion values revealed a separation of samples between the control and hypoxic placentas (Fig. S7 E). Similar to the analysis of HFD-placentas, we used the top principal components (n=4 explaining 98.8% of the sample cell proportion variance) to adjust the differential expression analysis for cellular composition (Fig. S7 F). Similarly to placentas derived from HFD-fed sires, the cell types contributing the most to sample variance included the invasive SPT cells, endodermal cells (*Afp*-high), decidual stromal cells, and (Fig. S7 G). Additionally, erythroblast cells (*Hbb-y*-high) and spiral artery TGCs also strongly contributed to sample variance (Fig. S7 G). Accounting for cell-type proportions allowed for the detection of 1,477 DEGs associated with hypoxia and growth restriction (Fig. 6C), of which 356 overlapped with those initially detected before cellular composition adjustment (24%; Fig. S7 H). These data suggest that like paternal obesity-induced placental de-regulated genes, differential gene expression in hypoxic placentas is partly driven by changes in cellular composition.

Importantly, after adjusting for cell-type proportions, 207 of the paternal-obesity-induced dysregulated genes in male placentas were also found to be differentially expressed in hypoxic placentas (Fisher's exact test P=5.1e-16; Fig. 6 D). A key gene, supporting this similarity in the molecular pathology of hypoxic placenta and obese sired

placenta was the dysregulation of the imprinted gene *Igf2*. Collectively, our comparative analyses of placental transcriptomic data from both models indicate that paternal obesity, like gestational hypoxia, induces pathological and molecular consequences that are hallmarks of placental defects, and may elicit serious pregnancy complications like preeclampsia.

13.5 Discussion

Paternal health and environmental exposures impact the establishment of the sperm epigenome and are associated with altered development of the placenta, embryo, and offspring health. However, the molecular and cellular mechanisms underlying paternal obesity effects on offspring are still unclear. Our findings build on prior knowledge to show that paternal obesity alters sperm chromatin, specifically H3K4me3, in connection with widespread changes in the placental transcriptome. We provide a significant advance towards understanding the cellular and molecular drivers at the level of the sperm epigenome and placenta transcriptome that could underlie paternally-induced placental pathogenesis, growth impeded embryo development and adult-onset metabolic phenotypes.

We further observed that paternal HFD-induced obesity alters the placental transcriptome in a sex-specific manner. There is strong evidence demonstrating sex disparity in metabolic phenotypes and cardiometabolic disease risks (reviewed in Tramunt et al., 2020). These sex-specific effects are thought to be driven by sex chromosomes, hormonal factors, the gut microbiome, as well as differential fetal programming across sex in response to pre-conception and *in utero* exposures (reviewed in Sandovici, Fernandez-Twinn, Hufnagel, Constância, & Ozanne, 2022). Here, our findings suggest some of the post-natal metabolic disturbances observed in paternally-induced offspring sexually dimorphic phenotypes are established in the placenta. Interestingly, some of the de-regulated genes included imprinting genes. These genes are epigenetically controlled and inherited in a parent-of-origin manner, and the placenta is a key organ for imprinted gene function [771]. According to the conflict hypothesis, maternally imprinted genes (paternally expressed) support fetal growth, whereas paternally imprinted genes (maternally expressed) restrict fetal growth [772–774]. Some of

the dysregulated imprinted genes we identified have been implicated in placental defects and pregnancy complications. For example, deletion of the gene *Htra3* (identified here as a DEG in female placentas) in mice has been implicated in IUGR owing to the disorganization of placental labyrinthine capillaries and thereby affecting offspring growth trajectories postnatally [775]. The maternally expressed gene *Copg2* (identified here as a DEG in female placentas) has been associated with pregnancies with small for gestational age infants [776]. Loss of the paternally expressed gene *Snx14* in mice (identified here as a DEG in female placentas) causes severe placental pathology involving aberrant SynT differentiation, leading to mid-gestation embryonic lethality [777]. The paternally expressed gene *Zdbf2* (DEG in male placentas) has been implicated in reduced fetal growth in mice, associated with altered appetite signals in the hypothalamic circuit [778]. Placental deficiency of the paternally expressed gene *Slc38a2* (identified here as a DEG in male placentas) leads to fetal growth restriction in mice [779]. Lastly, mice deficient for the paternally expressed transcriptional co-repressor *Tle3* (identified here as a DEG in male placentas) show abnormal placental development including TGC differentiation failure, resulting in fetal death [780]. Importantly, disrupting the expression of a single imprinted gene can result in placental defect and consequently compromise fetal health or survival. It is therefore likely that the differential expression of imprinted genes detected in female and male placentas as a result of paternal obesity could at least partly explain metabolic phenotypes observed in this mouse model [1,510].

We identified changes in sperm H3K4me3 associated with paternal obesity, some of which were enriched for transcription factor binding sites. This could in turn alter TF functions. This phenomenon has been described in a mouse model of paternal low-protein diet, where oxidative stress-induced phosphorylation of the *Atf7* TF was suggested to impede its DNA-binding affinity in germ cells, leading to a decrease in H3K9me2 at target regions [540]. As in the low-protein diet model, oxidative stress is a hallmark of obesity and increased levels of reactive oxygen species have been observed in testes of diet-induced obesity mouse models and linked to impaired embryonic development [488,490,781]. These findings provide avenues for further investigation such as whether epigenetic changes on paternal alleles may impact TF binding during early embryogenesis.

The identification of alterations of cell type proportion must be considered within the limitations of a deconvolution analysis. This analysis only provides estimates of cell-type relative within a heterogeneous tissue. This allowed us to adjust for the effect of differences in cell-type composition, but exact cell-type composition and their specific gene expression changes need to be validated by single-cell approaches such as single-cell RNA-seq or spatial transcriptomics. Furthermore, even though we used a reference dataset which included cells representative of placental tissues, the detection capacity of this approach is limited for low-abundant cell types, such as blood cells, immune cells, and inflammatory cells, which would be highly informative of placental pathological states. For example, aberrant abundance of decidual inflammatory cells, such as natural killer (NK) cells, have been linked to the pathogenesis of preeclampsia [782–786]. Incidentally, it was previously shown that paternal diet-induced obesity is associated with placental inflammation [510,535]. Interestingly, many GO terms related to inflammatory processes were enriched in the obesity-induced deH3K4me3 in sperm (Fig. 2E, Table S3-4, and Pepin et al., 2022), suggesting sperm deH3K4me3 might be partly influencing placental inflammation. However due to the low representation of immune cells in the data set this could not be assessed.

13.5.1 Speculation and perspectives

Many of the DEGs in the paternal obese-sired placentas were involved in the regulation of the heart and brain. This is in line with paternal obesity associated to the developmental origins of neurological, cardiovascular, and metabolic disease in offspring [1,488,515,521,577,606,787–792,489–491,504–506,510,513]. The brain-placenta and heart-placenta axes refer to their developmental linkage to the trophoblast which produces various hormones, neurotransmitters, and growth factors that are central to brain and heart development [580,793]. This is further illustrated in studies where placental pathology is linked to cardiovascular and heart abnormalities [789–791]. For example, in a study of the relationship between placental pathology and neurodevelopment of infants, possible hypoxic conditions were a significant predictor of lower Mullen Scales of Early Learning [792]. A connecting factor between the neural and cardiovascular phenotypes is the neural crest

cells which make a critical contribution to the developing heart and brain [577,766]. Notably, neural crest cells are of ectodermal origin which arises from the TE [794], which is in turn governed by paternally-driven gene expression. It is worth considering the routes by which TE dysfunction may be implicated in the paternal origins of metabolic and cardiovascular disease. First, altered placenta gene expression beginning in the TE could influence the specification of neural crest cells which are a developmental adjacent cell lineage in the early embryo. TE signaling to neural crest cells could alter their downstream function. Second, altered trophoblast endocrine function will influence cardiac and neurodevelopment [766].

In line with these possible routes to developmental origins of obesity and metabolic disease, paternal obesity was associated with altered trophoblast lineage specification. During placentation, invasive SPT have the ability to migrate and invade the maternal-fetal interface and replace maternal vascular endothelial cells, a critical step for maternal arterial remodeling to facilitate low resistance high volume blood flow to the fetus [795]. Consequently, improper trophoblastic invasion has been linked to various obstetrical complications, including premature birth, fetal growth restriction, pre-eclampsia and placenta creta [796–798]. Paternal obesity also induced changes in trophoblast expressing the glucocorticoid metabolizing enzyme *Hsd11b2*. In the placenta, *Hsd11b2* is responsible for the conversion of cortisol into its inactive form, cortisone, which limits fetal exposure to maternal glucocorticoid levels. Interestingly, de-regulation of *Hsd11b2* has been observed in rodent fetal growth restriction models [626,739,799]. These aberrant cellular composition profiles suggest that paternal factors, such as diet, can induce functional changes in the placenta that mirror placental defects associated with adult-onset cardiometabolic phenotypes.

Next, it will be important to assess earlier developmental time points to determine when and how these effects originate. Indeed, studies have shown that paternal diet-induced obesity alters preimplantation development, such as cellular allocation to TE versus ICM lineages [491]. Investigating multiple and earlier time points would help reveal the dynamic trajectory of paternally-induced deregulated transcriptomic and epigenetic signatures which might be at the origin of adult-onset disease. Translating these findings to humans would be beneficial to better understand the paternal preconception

contribution to placental health. This is of particular relevance, given that although most obstetrical complications are thought to be rooted in the placenta, in many cases placental defects are only detected in late gestation and the etiology of these defects are oftentimes idiopathic [586,766]. There are no established guidelines or clinical procedures that predict pregnancy complications and placental defects associated with paternal factors. The connections we report here between paternal effects and the placental transcriptome open new avenues for the development of epigenome-based sperm diagnostics that could be used to predict pregnancy pathologies and the developmental origins of adult disease.

13.6 Acknowledgements

We thank the team from Genome Quebec for the sequencing of the ChIP-seq experiment, and the team from the Applied Genomics Innovation Core of the McGill Genome Centre for the sequencing of the RNA-seq experiment.

13.7 Author Contributions

PAJ developed the murine model and provided the tissue samples. ASP performed the experiments, developed methodology, curated data, performed the formal analysis, visualization, and writing of the original draft. SK provided supervision, conceptualization, funding acquisition, and writing of the manuscript. VD advised and provided oversight of the data and statistical analysis. DMS provided supervision, conceptualization, and funding acquisition. PAJ, DMS and VD reviewed and edited the manuscript. SK is a Canada Research Chair in Epigenomics, Reproduction and Development and funding for this study is provided by the Canadian Institutes of Health Research grants to SK (DOHaD Team grant 358654 and Operating 350129) and grant (CIHR Team grant 146333; Operating 175293) to DMS. ASP is supported by scholarships from the McGill University Faculty of Medicine and Health Sciences, the Desjardins Foundation, and the McGill Centre for Research in Reproduction and Development.

13.8 Declaration of interest

The authors declare no competing interest.

13.9 Supporting information

The Supporting Information includes the following Figures and Tables:

Figure S1: Sperm H3K4me3 ChIP-sequencing data quality and normalization.

Figure S2: Obesity-sensitive regions in sperm are found at tissue-specific enhancers important for development.

Figure S3: Placenta RNA-sequencing data quality assessment.

Figure S4: Cell-type specific marker genes selection using reference mouse E14.5 placenta single-cell RNA-sequencing dataset.

Figure S5: Estimated cell type proportions across experimental groups for male and female E14.5 bulk placenta tissues derived from CON- and HFD-fed sires.

Figure S6: Principal component analysis (PCA) of estimated cell-type proportions

Figure S7: Quality assessment, processing, differential analysis, and deconvolution of RNA-sequencing data from mouse placenta in a hypoxia-induced intrauterine growth restriction mouse model.

Supplemental tables and files can be accessed at the following link: https://www.biorxiv.org/content/10.1101/2022.08.30.503982v1.supplementary-material

Table S1: ChIP-sequencing sample information

Table S2: Significant gene ontology terms enriched in HFD-sperm deH3K4me3 regions at promoters detected in our previous study and this study, related to Fig S1 E

Table S3: Significant gene ontology terms enriched in HFD-sperm at regions showing a decrease in H3K4me3 at promoters, related to Fig 2 E i

Table S4: Significant gene ontology terms enriched in HFD-sperm at regions showing an increase in H3K4me3 at promoters, related to Fig 2 E ii

Table S5: Significant gene ontology terms enriched in differentially expressed genes in female placentas derived from HFD-sires, related to Fig 4 C

Table S6: Significant gene ontology terms enriched in differentially expressed genes in male placentas derived from HFD-sires, related to Fig 4 D

Table S7: Reference single-cell RNA-sequencing data information – number of cells per cell type, related to Fig S4

Supplemental file 1: Interactive heatmap for significant gene ontology terms enriched in HFD-sperm deH3K4me3 regions at promoters detected in our previous study and this study, related to Fig. S1 I

Supplemental file 2: Motif analysis, showing significantly enriched known motifs in regions gaining H3K4me3 in HFD-sperm, related to Fig 3 A

Figure S1

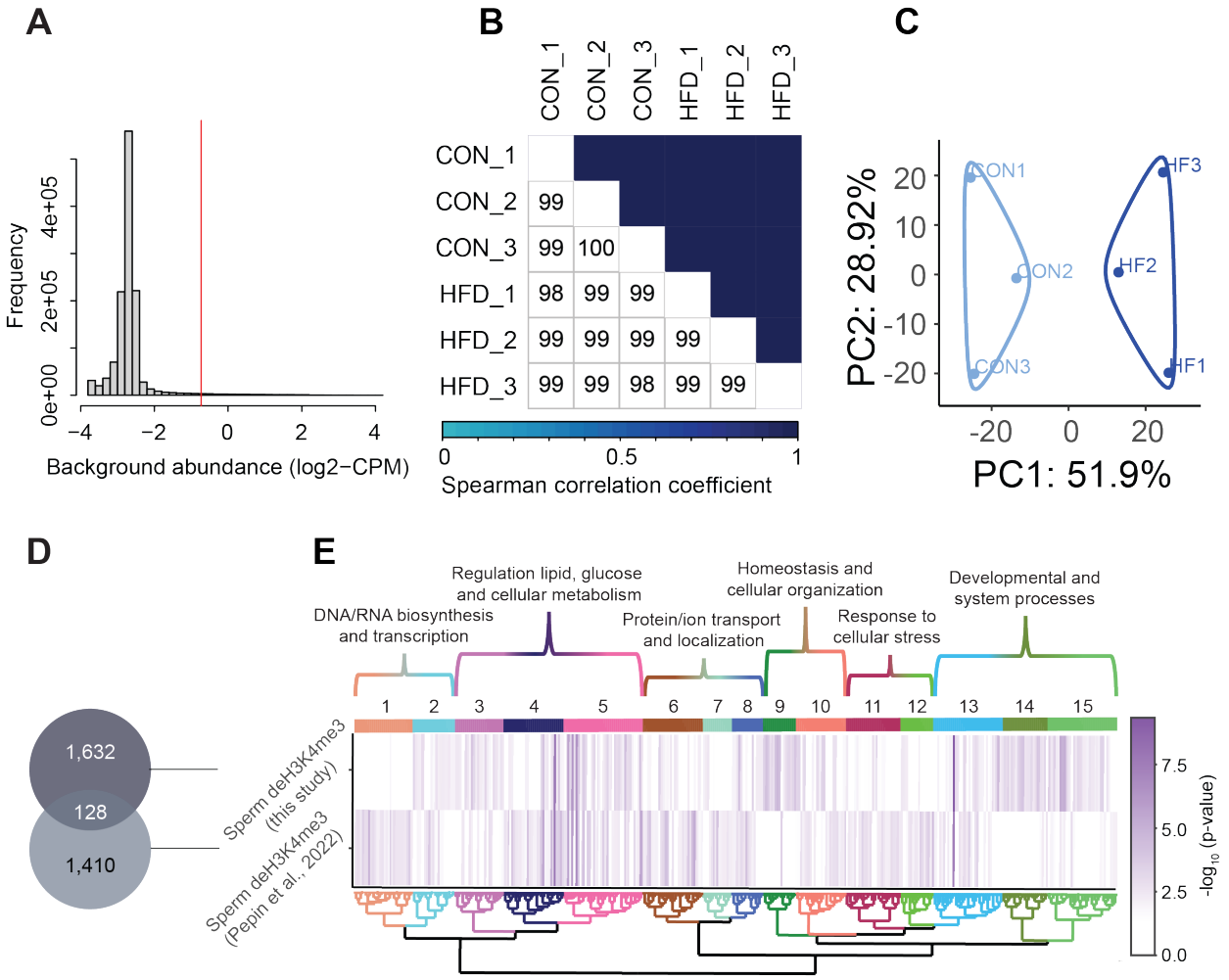

Figure S 1: Sperm H3K4me3 ChIP-sequencing data quality and normalization.

A) Histogram showing frequency distributions of read abundances of genome-wide 150 bp windows. The vertical red line indicates the cut-off where windows with low read counts were filtered out (abundance below log2(4) fold over 2,000 bp bins). The remaining windows (considered enriched for H3K4me3) which were less than 100 bp apart were merged allowing a maximum width of 5,000 bp (n=35,184 merged regions enriched for H3K4me3 in sperm).

B) Spearman correlation heatmap on counts at sperm H3K4me3-enriched genomic regions after TMM normalization and batch adjustment. Color gradients represent correlation coefficients for each pairwise comparison.

C) Principal component analysis (PCA) plot for counts in H3K4me3-enriched regions in sperm after normalization. The top 5% regions contributing to Principal Component 1 (PC1) were selected as those associated with sample separation according to dietary treatment (E).

D) Venn diagram showing the overlap of detected obesity-sensitive regions from this study (dark grey) and our previous study (Pepin et al., 2022; pale grey). Significance was tested with a Fisher exact test and the p-value is shown under the graph.

E) Heatmap showing significant gene ontology (GO) terms clustered based on functional similarity, comparing enriched biological functions in obesity-sensitive regions located at promoters detected in this

study (top row) and in our previous study (Pepin et al., 2022, bottom row). Columns represent enriched GO terms ordered by hierarchical clustering based on Wang's semantic similarity distance and *ward.D2* aggregation criterion. The color intensity represents the GO term enrichment significance (-log10 p-value). Interactive versions of these figures can be found in Supplemental file 1 and the complete lists of significantly enriched GO terms can be found in Table S2.

Figure S2

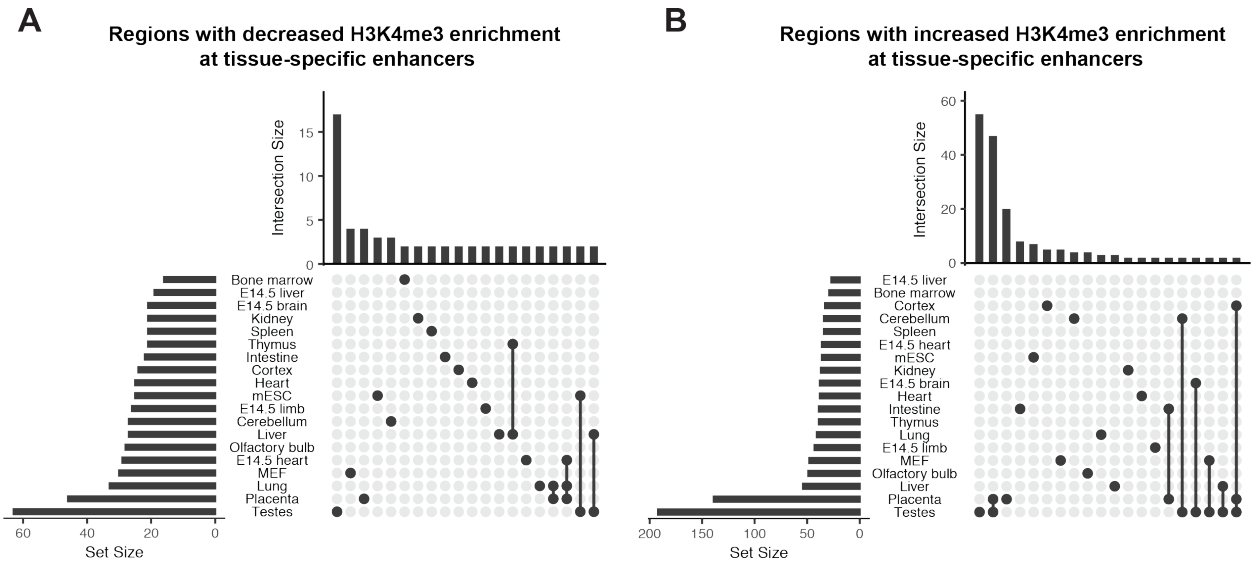

Figure S 2: Obesity-sensitive regions in sperm are found at tissue-specific enhancers important for development.

A-B) Upset plots showing annotations for tissue-specific enhancers overlapping with deH3K4me3 regions with decreased enrichment in HFD sperm (A) and increased enrichment in HFD sperm (B).

Horizontal bars on the left sides of each panel represent the number of regions overlapping with each genomic annotation (set size). Vertical bars on the top of each panel represent the number of regions belonging to intersecting annotations (intersection size). Intersection sets are represented by connecting nodes.

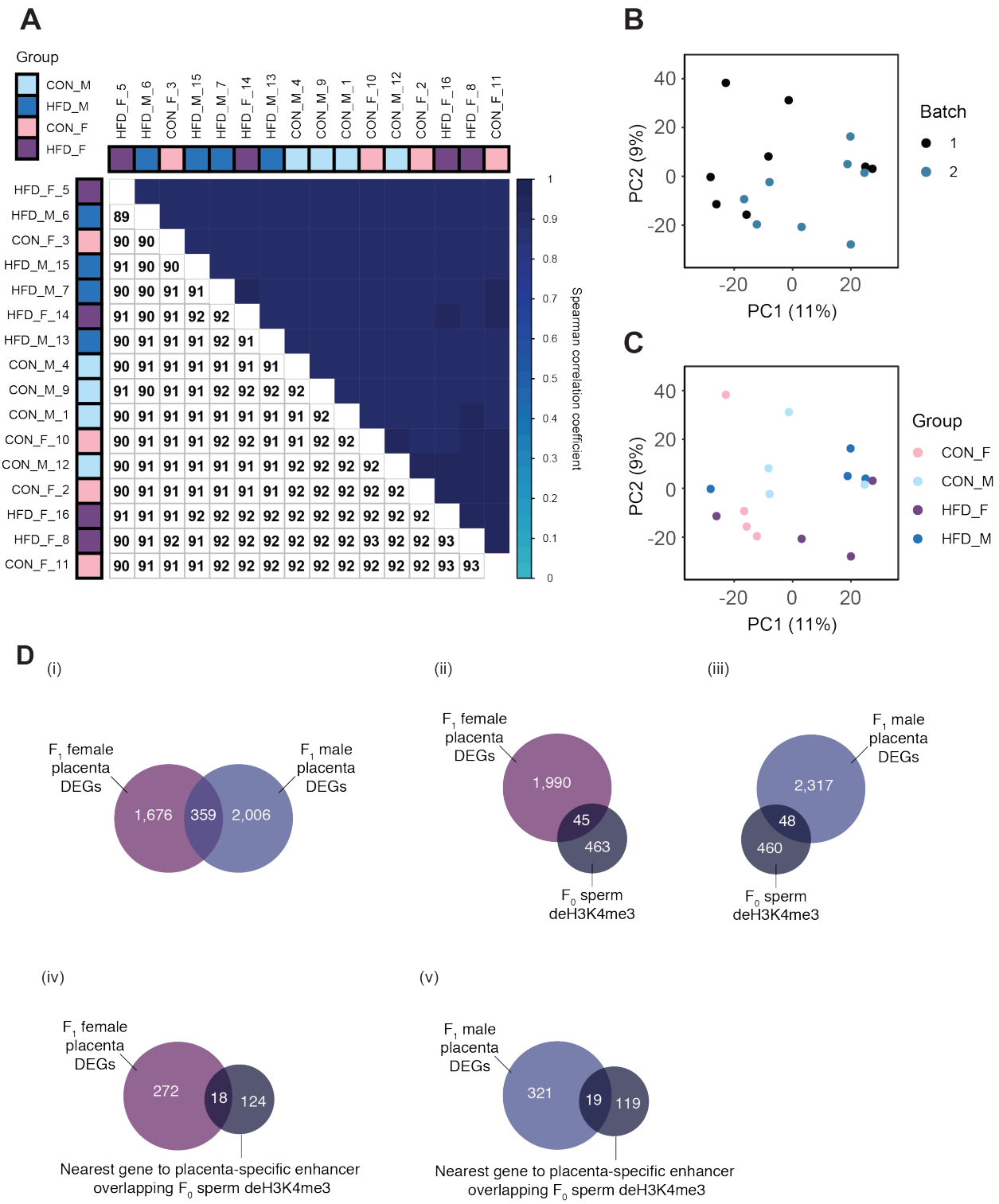

Figure S 3: Placenta RNA-sequencing data quality assessment.

A) Spearman correlation heatmap on variance stabilized transcripts. The color gradient represents the Spearman correlation coefficient for each sample pairwise comparison.

B-C) Principal Component Analysis (PCA) on variance stabilized transcripts with samples labeled by batch (B) and experimental group (C).
D) Venn diagrams showing the overlap of paternal obesity-induced de-regulated genes between female and male placentas (i), with sperm obesity-sensitive regions at promoters (ii and iii), and with the nearest gene to placental-specific enhancer overlapping sperm deH3K4me3 (iv and v).

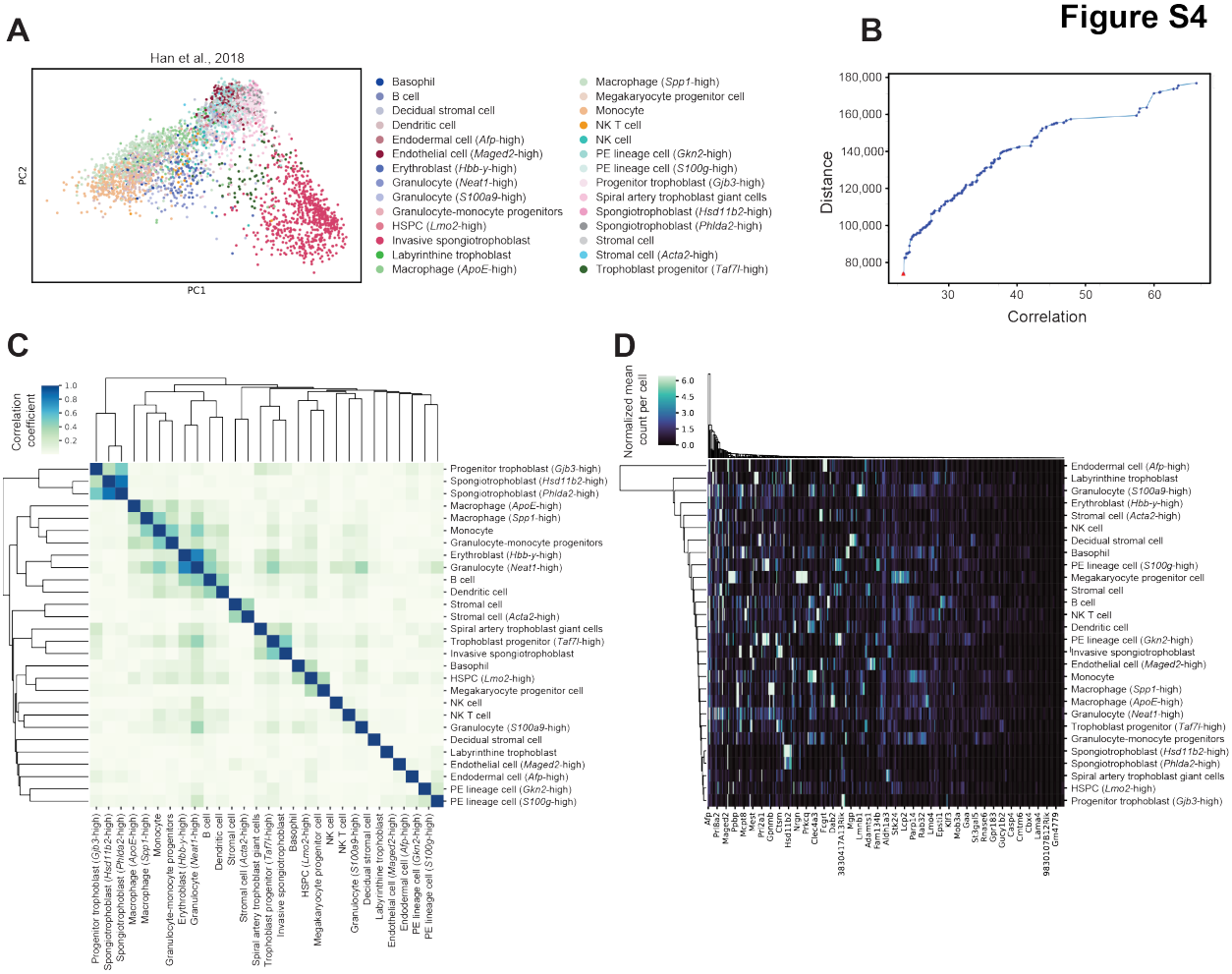

Figure S 4: Cell-type specific marker genes selection using reference mouse E14.5 placenta single-cell RNA-sequencing dataset.

A) Principal Component Analysis (PCA) plot of 4,346 single cells from mouse E14.5 placenta, with the 28 different cell types previously identified within the placenta (Han et al., 2018). The number of cells annotated to each cell type can be found in Table S7.

B) The 4,000 most highly variable genes were used for feature selection using a multi-objective optimization approach with the AutoGeneS package (Aliee & Theis, 2021). The plot shows distance and correlation values for each Pareto-optimal solution. The red triangle indicates the Pareto-optimal solution used to select the 400 marker genes which maximizes distance and minimizes correlation values across cell types.

C) Heatmap showing Pearson correlation between each cell-type based on expression values of the selected marker genes. The color gradient represents the Pearson correlation coefficients. Cell types are arranged by hierarchical clustering.

D) Expression signatures of marker genes distinguishing the different cell types detected. The heatmap shows the mean normalized counts per cell type (rows) for the 400 marker genes (columns) as identified by AutoGeneS (Aliee & Theis, 2021). Rows and columns are arranged by hierarchical clustering.

Figure S5

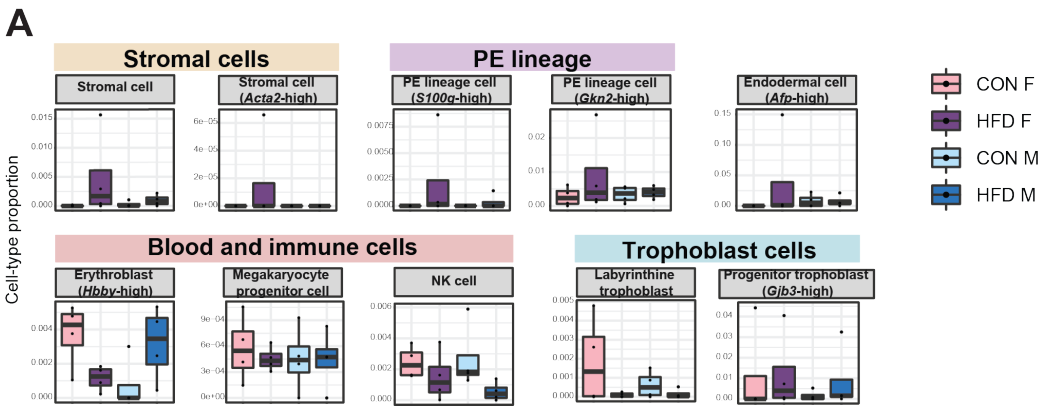

Figure S 5: Estimated cell type proportions across experimental groups for male and female E14.5 bulk placenta tissues derived from CON- and HFD-fed sires.

A) Boxplots showing sample-specific proportions for the remaining cell types detected in the bulk RNA-seq data deconvolution analysis across experimental groups. Beta regression was used to assess differences in cell-type proportions associated with paternal obesity for each placental sex. $P<0.05$ was considered significant.

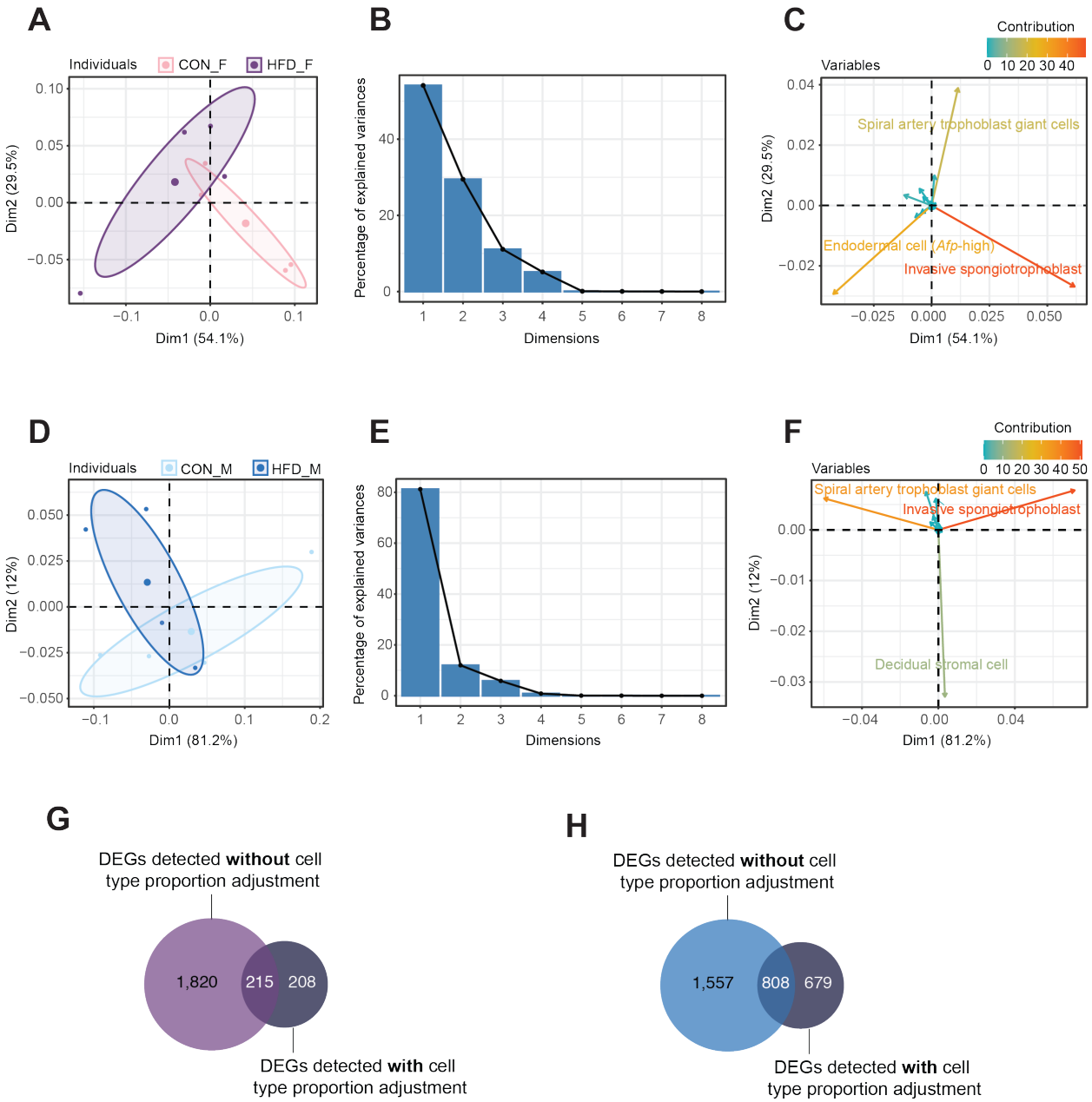

Figure S 6: Principal component analysis (PCA) of estimated cell-type proportions

A-F) Principal component results for female (A-C) and male (D-F) placentas.

A and D) Principal component analysis plot of cell-proportions. Confidence ellipses are drawn around mean points for each experimental group.

B and E) Scree plots showing percentage of variances explained by each principal component (dimension).

C and F) Variables factor map showing the top cell types contributing to sample variances. The color gradients on vectors represent the contribution values for each variable (cell type).

G-H) Venn diagrams showing the overlap between the differentially expressed genes in female (G) and male (H) placentas, before and after adjusting for cell-type proportions.

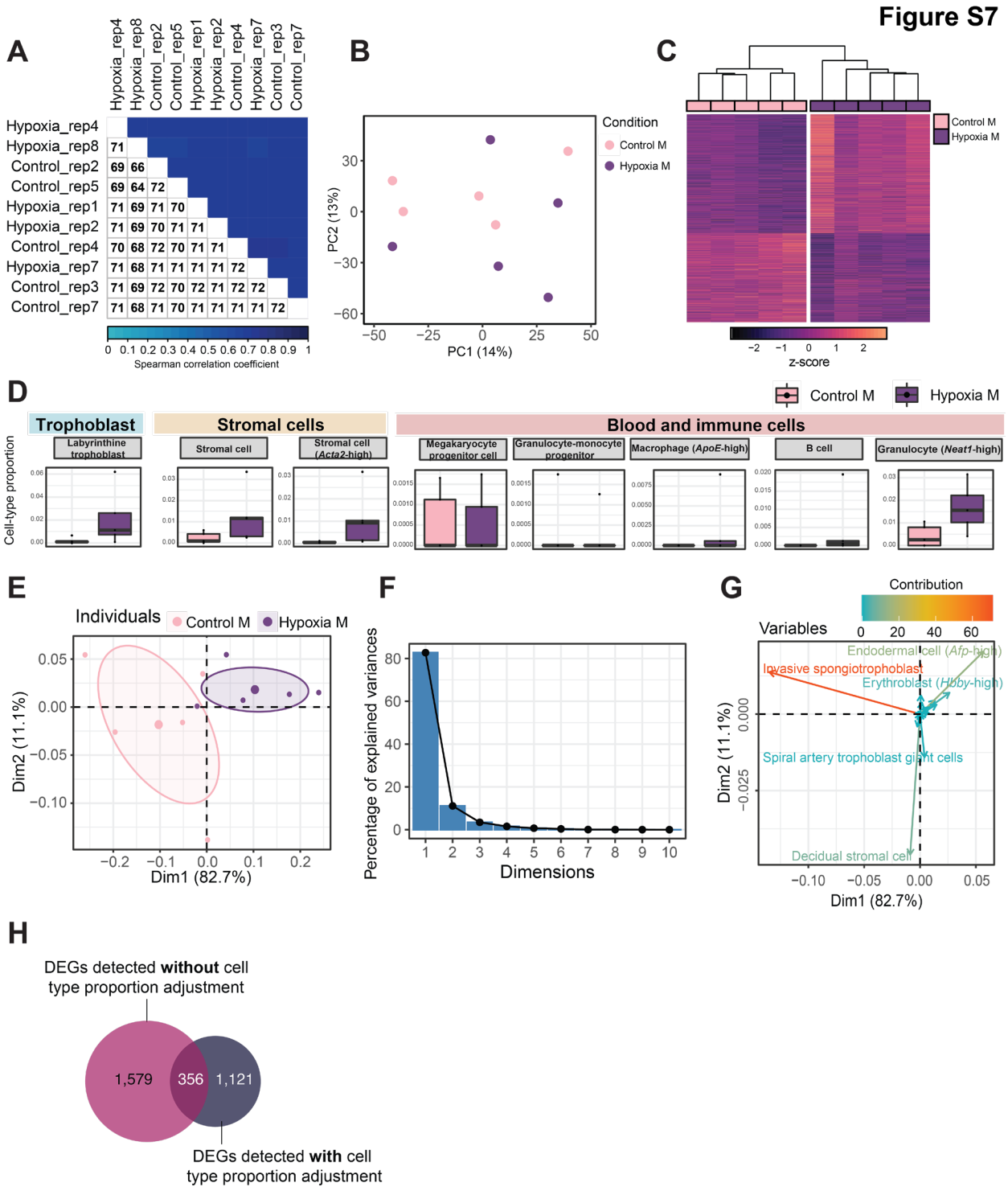

Figure S 7: Quality assessment, processing, differential analysis, and deconvolution of RNA-sequencing data from mouse placenta in a hypoxia-induced intrauterine growth restriction mouse model.

A) Spearman correlation heatmap on variance stabilized transcripts. The color gradient represents the Spearman correlation coefficient for each sample pairwise comparison.

B) Principal Component Analysis (PCA) on variance stabilized transcripts with samples labeled by experimental group.
C) Heatmap of normalized counts scaled by row (z-score) for transcripts that code for the detected differentially expressed genes (Lancaster $p<0.05$, n=1,935 genes) placentas. Rows are orders by k-means clustering and columns are arranged by hierarchical clustering with complete-linkage based on Euclidean distances.
D) Boxplots showing sample-specific proportions for cell types detected in the bulk RNA-sequencing data deconvolution analysis across experimental groups.
E-G) Principal component analysis of estimated cell-type proportions.
E) Principal component analysis plot of cell-type proportions. Confidence ellipses are drawn around mean points for each experimental group.
F) Scree plot showing percentage of variances explained by each principal component (dimension).
G) Variables factor map showing the top cell types contributing to sample variances. The color gradients on vectors represent the contribution values for each variable (cell type).
H) Venn diagram showing the overlap between the differentially expressed genes detected in hypoxic placentas, before and after adjusting for cell-type proportions.

Summary of the thesis and contributions to original knowledge

The present work included in this thesis aimed to explore the consequences of paternal diet-induced obesity on the sperm chromatin, placenta functions and offspring metabolic health. The contributions to original knowledge I provide through this work are as follows:

In my first manuscript (Chapter 2), by combining two mouse models, namely a paternal diet-induced obesity model, and a genetic model of epigenetic inheritance, I assessed the effects on the sperm epigenome, and offspring metabolic health.

(1) I demonstrated that multiple paternal sperm epimutation-inducing factors can result in more severe and transgenerational metabolic phenotypes in offspring, that are associated with transcriptomic changes in the liver across generations.

(2) Using refined protocols that allow to scale-down the input sample while maintaining good signal to perform native immunoprecipitation sequencing to profile the sperm chromatin, I identified histone H3K4me3 as a metabolic sensor of paternal obesity.

(3) This was the first study generating genome-wide sperm chromatin profiling data for H3K4me3 profiles associated with diet-induced obesity. Sperm histone H3K4me3 signatures in response to obesity revealed changes in enrichment at genes involved in metabolism that correspond to offspring phenotypes.

(4) Using publicly available epigenetic profiling and transcriptomic data from oocytes, pre-implantation embryos, trophectoderm and placenta tissues, I provided evidence that sperm epigenetic profiles greatly resemble those of embryos, trophectoderm and placenta, whereas oocyte profiles did not. My analyses suggest a potential transmission of epigenetic information to impact embryonic and placental development.

(5) By comparing sperm H3K4me3 profiles from obese KDM1A transgenic sires with lean wildtype males, I showed that combining the diet-induced obesity model with the germline-specific KDM1A overexpression resulted in a cumulation of changes in the sperm epigenome. These effects reflected the more severe and transgenerationally lasting phenotypes in offspring.

In my second manuscript (Chapter 3), using a similar paternal diet-induced obesity model, I assessed the implication of paternal obesity on placental functions.

(1) I profiled sperm H3K4me3 and identified obesity-sensitive regions that showed some consistency across our two independent studies, despite differences in experimental design, technical approaches, and animal models.

(2) The motif enrichment analysis provides avenues for future studies to delineate the molecular mechanisms underlying metabolically-driven changes in the sperm epigenome (further discussed in the general discussion of this thesis in the next chapter).

(3) I generated transcriptome-wide gene expression data from placentas derived from obese sires. Building on a recent study showing that paternal obesity induced placental hypoxia and altered vasculature, I demonstrated that the placenta transcriptome is altered in association with paternal diet, at imprinted genes and genes critical for placenta functions. Importantly, some of the sperm obesity-associated regions at promoters and enhancers overlapped with placental differentially expressed genes.

(4) Using novel bioinformatics analysis methods and publicly available single-cell RNA-sequencing data from mouse placenta, I was able to infer cell-type proportions and detect cellular composition changes associated with paternal obesity, which corresponded with features that are characteristic of placental defects associated with intrauterine growth restriction.

(5) I established that paternally-induced placental aberrant transcriptomic and estimated cellular composition profiles correspond with those of a hypoxia-induced intrauterine growth restriction model.

Collectively, I have made significant advances studying paternal effects on the sperm chromatin, the impact on offspring metabolic health, and the implications on placental functions. Furthermore, I have generated valuable datasets that have been deposited online, and these publicly available data will be useful for researchers in the field of epigenetics, reproduction, development, and metabolism. My work highlights the urgent need to better understand the paternal contribution on placenta health, pregnancy outcomes, and on the determinants of the metabolic health of future generations.

Chapter 4: General Discussion

15.1 Potential molecular mechanisms underlying diet-induced epigenetic changes in sperm

Growing evidence suggests that the sperm epigenome is dynamic, responds to the paternal environment, and is a sensor of metabolic health. As described in previous chapters of this thesis, a number of human studies have drawn associations between various environmental exposures with epigenetic signatures in sperm, such as exposures to flame retardants or DDT, chemotherapy drugs, smoking, supplementation of folate or antioxidants, and alcohol consumption, as well as certain health conditions such as elevated BMI or exercise [470,520,800–806]. Additionally, numerous paternal factors, such as obesity, birth weight, high-fat and low-protein diets, undernutrition, diabetes, hyperglycaemia, age, smoking, and chemical exposures, can influence offspring cardiometabolic health (reviewed in [518]). Linking alterations in sperm epigenetic signatures with paternal factors, and understanding the underlying mechanisms inducing these epimutations could provide avenues to develop strategies to reverse the paternal transmission of complex diseases and estimate transmission risks.

15.1.1 Interplay between metabolic pathways and the epigenome

Both studies in this thesis have presented evidence that diet-induced obesity is associated with enrichment changes of histone H3K4me3 in sperm. A question that remains is how mechanistically these epigenetics changes occur as a result of diets and obesity. There is a dynamic interplay between metabolic pathways as well as processes involved in gene regulation, via chromatin remodeling, which has been previously largely unappreciated. More generally, the metabolic regulation of the epigenome involves a number of processes that alter the abundance and tissue distribution of chromatin-modifying metabolites. Metabolites taken up by cells can also be further metabolized by metabolic enzymes resulting in substrates or co-factors that serve in chromatin-remodeling processes. The impact of intracellular metabolites abundance changes on the rate of chromatin modification changes also depends on the kinetic and thermodynamic properties of the enzymes and proteins involved. Consequently, the resulting epigenetic changes observed depend on the metabolic pathways altered in the context of obesity.

Obesity is a complex, multifactorial health conditions that involves a plethora of functional and molecular changes at the tissue level and at the cellular level. In order to speculate on the metabolic factors potentially mediating epigenetic alterations in sperm in our model, the molecular events that are characteristic of an obesity phenotype must be taken into considerations. These include – but are not restricted to – metabolic changes related to the one-carbon metabolism cycle and oxidative stress, the hormonal changes, and the molecular changes occurring in semen. Indeed, only a handful of molecular pathways will be discussed in this thesis, but it is important to keep in mind that more factors are likely involved and contributing to the epigenetic changes observed in sperm associated with obesity and high-fat diets, highlighting the complexity of the phenomena.

15.1.1.1 Changes in the one-carbon cycle in obesity and impact on methylation reactions

One of the most well-studied epigenetic modifications is the methylation of DNA and histone proteins. The methyl group that is either added to DNA, or to lysine or arginine residues of histones, is derived from the one-carbon metabolism pathway. One-carbon (1C) metabolism is comprised of a series of interconnected metabolic pathways (folate cycle, methionine remethylation, and transsulfuration pathways; see Figure 1) that facilitate the transfer of 1C moieties to support various physiological processes, such as DNA biosynthesis, amino acid homeostasis, the production of phospholipids, epigenetic maintenance, and redox balance. Methionine metabolism mainly takes place in the liver [807]. Upon dietary uptake, methionine is converted into s-adenosylmethionine (SAM) – the universal methyl-donor metabolite – which serves as a substrate for the methylation of DNA, RNA, histones and other proteins, as well as the synthesis of phosphatidylcholine, creatine, methylarginines, and more [808,809]. Through methylation reactions utilizing SAM, this metabolite gets converted into s-adenosylhomocysteine (SAH) and subsequently to homocysteine [810]. Homocysteine can then either be remethylated as methionine, or be utilized in the transsulfuration cycle to produce glutathione, an antioxidant enzyme involved in limiting oxidative stress and damage [811].

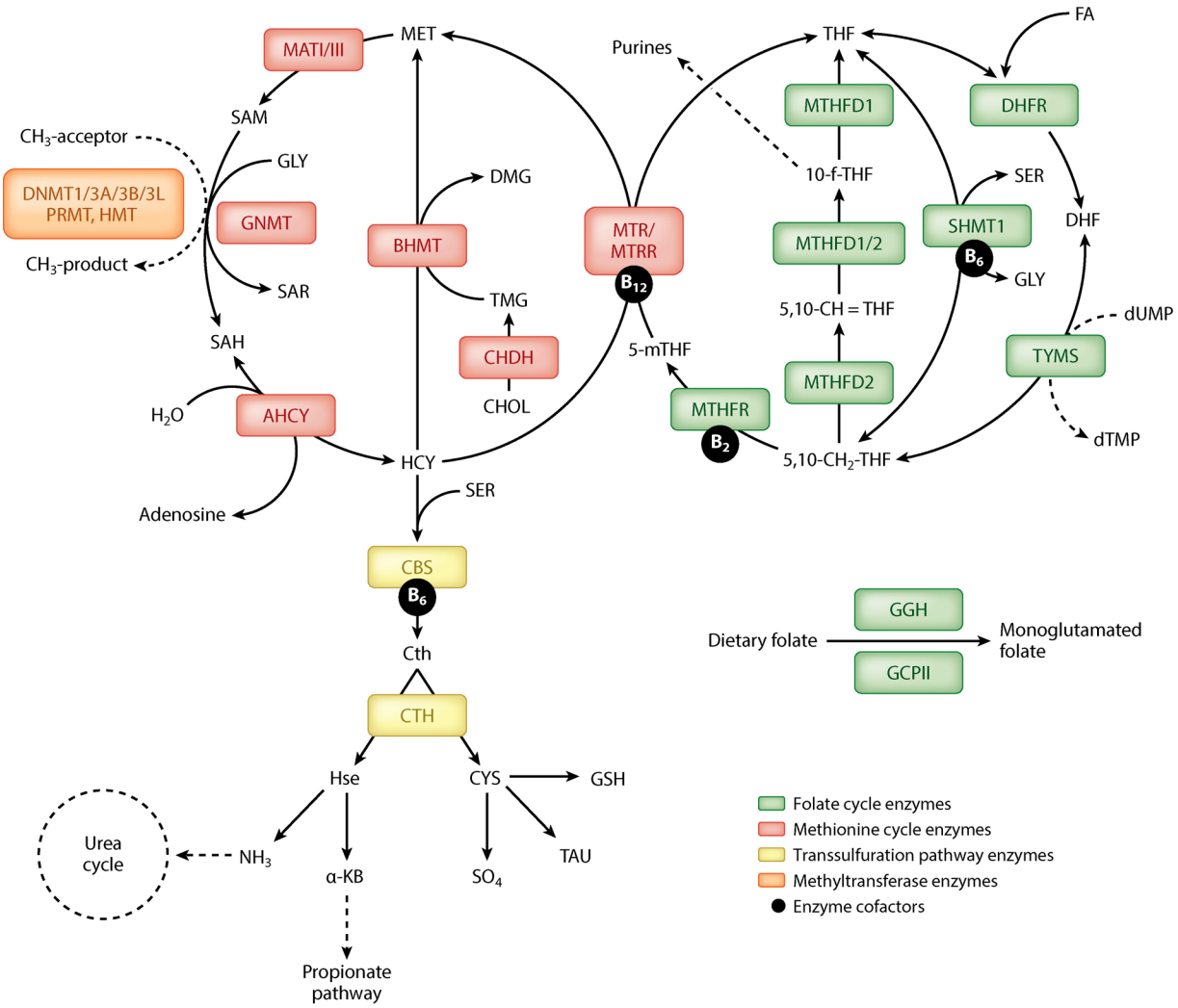

Clare CE, et al. 2019.
Annu. Rev. Anim. Biosci. 7:263–87

Figure 1: Schematic representation of the interconnected pathways of the one-carbon metabolism cycle.

The folate cycle, methionine cycle, and transsulfuration pathways. Abbreviations: 5-mTHF, 5-methyltetrahydrofolate; 10-f-THF, 10-formyl-tetrahydrofolate; α-KB, α-ketobutyrate; AHCY; S-adenosyl-L-homocysteine hydrolase; BHMT, betaine-homocysteine S-methyltransferase; CBS, cystathionine β-synthase; CHDH, choline dehydrogenase; CHOL, choline; CTH, cystathionine γ-lyase; Cth, cystathionine; CYS, cysteine; DHF, dihydrofolate; DHFR, dihydrofolate reductase; DMG, dimethylglycine; DNMT1/3A/3B/3L DNA methyltransferases; dTMP, thymidine monophosphate; dUMP, deoxyuridine monophosphate; FA, folic acid; GLY, glycine; GCPII, glutamate carboxypeptidase; GGH, γ-glutamyl hydrolase; GNMT, glycine N-methyltransferase; GSH, glutathione; HCY, homocysteine; HMT, histone methyltransferase; Hse, homoserine; MATI/III, methionine adenosyltransferase; MET, methionine; MTHFD1/2, methylenetetrahydrofolate dehydrogenase; MTHFR, 5,10-methylenetetrahydrofolate reductase; MTR, methionine synthase; MTRR, methionine synthase reductase NH3, ammonia; PRMT, protein arginine methyltransferase; SAH, S-adenosylhomocysteine;

SAM, S-adenosylmethionine; SAR, sarcosine; SER, serine; SHMT, serine hydroxymethyltransferase; SO4, sulphate; THF, tetrahydrofolate; TYMS, thymidylate synthase. Figure obtained from [812] (Copyright 2013) with permission from Annual Reviews, Inc.

Disruptions in the one-carbon metabolism, such as via changes in the intake of methionine or folate, the modulation of the activity of enzymes involved in these pathways, or single nucleotide polymorphisms in genes involved in this cycle, have been shown to impact metabolites and cofactors abundance [813,814]. These metabolites level changes can result in epigenetic changes at the level of methylation of DNA, RNA, and histones, and thereby correlate to corresponding changes in gene expression [815–823]. As described in previous chapters of this thesis, obesity has been previously linked to altered sperm DNA methylation profiles, levels of methylated small RNA species, and enrichment of histone methylation in sperm of diet-induced obesity mouse models and of obese men [1,514,520]. These epigenetic alterations detected in sperm could arise from changes in the 1C metabolism as a result of changes in abundances in factors involved in these pathways.

There are several lines of evidence supporting the idea that 1C metabolism is disrupted in obesity via changes in metabolite abundances. In humans, several studies have drawn correlations between blood levels of various 1C metabolism metabolites with obesity and associated comorbidities. For example, severe NAFLD was associated with reduced serum folate concentrations, and BMI was inversely correlated with serum folate [824]. Hyperhomocysteinemia has been linked to the incidence of cryptogenic stroke, and correlated with obesity in adult patients [825]. Hyperinsulinemic obese subjects show higher fasting levels of homocysteine and triglyceride levels, with homocysteine levels correlating with insulin levels [673]. In obese children and teenagers, similar associations have been drawn with elevated plasma homocysteine correlating with obesity status, serum leptin and serum apolipoprotein B [826].

In rodents, high-fat diet feeding increases plasma homocysteine, but decreases homocysteine levels in the liver [827]. These lower hepatic homocysteine levels were partly attributed to (1) a down-regulation of the enzyme *S*-adenosylhomocysteine hydrolase, which is responsible to convert *S*-adenosylhomocysteine (SAH) into homocysteine, and

(2) a decrease in the SAM:SAH ratio – which can serve as an index for transmethylation potential. These findings suggested the obesity-associated elevated plasma homocysteine levels could be as a result of enhanced hepatic efflux of homocysteine as well as altered sulfur amino acid metabolism. In a similar DIO model feeding mice a high-fat high-cholesterol diet – associated with weight gain, hepatic steatosis and fibrosis – in-depth metabolomics, enzymatic, and molecular analyses revealed changes in various protein levels, enzymatic activity, and metabolite levels, of factors involved in 1C metabolism [663]. In the methionine cycle, changes included hepatic methionine depletion, increased SAM:methionine ratio, elevated SAH and homocysteine levels, and decrease SAH hydrolase levels. In the transsulfuration pathway, decreased serine levels, increased cystathionine and cysteine, and decreased glutathione levels were detected. Lastly, in the transmethylation pathway, there was an increase in PC:PE ratio, indicative of elevated PEMT activity. These metabolomic changes suggest obesity-associated methionine deficiency and homocysteine elevation could be attributed to impaired homocysteine remethylation and changes in methyltransferase activity. Finally, further supporting the link between the 1C metabolism cycle and lipid metabolism, is the finding that folate deficiency is associated with hepatic fat accumulation via PC synthesis impairment [828,829]. Indeed, folate deficiency reduces choline and PC levels in the liver, via (1) reduced choline synthesis by PEMT, (2) increased choline use as a source of methyl groups, and (3) decreased activity of PEMT [830,831]. The limited PC production causes accumulation of triglycerides in the liver resulting from reduced VLDL secretion [832,833].

Another important connection between 1C metabolism and lipid metabolism is via the action of an important methyltransferase enzyme. SAM is a cofactor for the action of the enzyme phosphatidylethanolamine N-methyltransferase (PEMT), which converts phosphatidylethanolamine (PE) into phosphatidylcholine (PC) [834–836]. PC is the most abundant phospholipid found in mammalian cell membranes and bile, as well as an important constituent of lipoproteins, which facilitate lipids transport [837]. PC can be synthesized through the cytidine diphosphate(CDP)-choline pathway via dietary choline intake, or within the liver through the conversion of phosphatidylethanolamine into PC by the enzyme phosphatidylethanolamine N-methyltransferase (PEMT) [835]. It follows that the biosynthetic demand on PEMT to produce PC is higher when the fatty acid influx

increases such as upon a high-fat diet intake or with elevated adiposity in obesity. Consequently, a greater pool of SAM is mobilized to package lipids via the production of lipoprotein constituents. These changes can impact the epigenome given that methylation reactions rely on methyl groups availability from SAM [838]. Collectively, these findings support the idea that the 1C pathway is disrupted at multiple levels during obesity, both in humans and in DIO models similar to the ones presented in the studies included in this thesis. Although we did not measure changes in levels or activity of components of this metabolism cycle, we can hypothesize that these effects also occurred in our DIO models. The disruptions in the 1C cycle could at least partly explain the changes in sperm H3K4me3 observed in our studies, as well as aberrant sperm DNA methylation on that of others upon high-fat feeding. Manipulating components of this cycle in parallel with high-fat feeding could help determine whether these substrate availability changes serve a causal role in the detected epimutations. For example, supplementation of some of the depleted substrates and cofactors could be administered to mice fed a high-fat diet (such as SAM or methionine), or transgenic mice that show elevated activity of some enzymes that have reduced activity upon HFD (such as S-adenosyl-L-homocysteine hydrolase) could be used in combination with high-fat feeding, to determine whether HFD-induced sperm epimutations would be blunted upon these 1C component manipulations.

Taken together, findings from the literature suggest there is a connection between obesity, lipid metabolism, and the epigenome, and one logical route by which obesity could influence the epigenome is through the 1C metabolism. These interconnected metabolic cycles show clear disruptions upon high-fat feeding in rodents and obesity in humans, with changes in levels of a number of substrates and cofactors, proteins and enzymes involved in these pathways.

15.1.1.2 Obesity-related oxidative stress and impact on the epigenome

The central principle of oxidative stress is the imbalance between oxidants and antioxidants, with oxidants favouring oxidative damage. As described in the first chapter of this thesis (Introduction), obesity is characterized by a systemic oxidative stress state, with elevated production of reactive oxygen species (ROS) and reduced activity of antioxidant enzymes [287]. Male germ cells are not proofed from oxidative stress, as evidence by increased ROS and DNA damage in obese individuals and animals, and with

infertile and subfertile patients exhibiting sperm ROS damage [294,484,844–846,490,506,781,839–843]. Additionally, global oxidative damage has been observed in sperm of mice fed a HFD [847]. Of note, sperm cells are transcriptionally inactive and lack endogenous repair defence systems, making developing germ cells *increasingly* vulnerable to insults such as oxidative stress and damage as they advance through spermatogenesis [848]. The male reproductive system is equipped with antioxidative systems to minimize oxidative damage, such as through the expression of antioxidant enzymes in Sertoli cells, the presence of antioxidant enzymes and molecules in semen such as vitamin C, E, and Zinc, and protamines deposited during spermiogenesis protecting the paternal genome from damage [848].Nevertheless, if there is an imbalance in ROS such as during obesity, this could potentially result in oxidative damage in germ cells. Importantly, oxidative DNA damage as a result of ROS can result in the formation of 8-oxoguanine (8-oxo-G), which represents the most common form of oxidative damage [849–852]. 8-oxo-G has been associated with oxidative stress-related conditions including diabetes [853,854]. Importantly, oxidative stress is also known to modulate the epigenome, including potentially that of sperm. If such 8-oxo-G accumulates throughout spermatogenesis as a result of obesity-induced ROS, and impact the epigenome, this can have implications for paternal obesity-associated epigenetic inheritance.

The epigenetic roles of oxidative stress related to 8-oxo-G can involve multiple mechanisms that can induce transcriptional changes. First, 8-oxo-G at promoter regions can induce the recruitment of repair proteins that interact with regulatory proteins to control transcription [855]. For example, this modification at the promoters of VEGF, TNF-α, BCL2 and SIRT1 is associated with increased transcription of these genes [856–859]. Interestingly, the oxidative-stress induced VEGF increased expression was found to be associated with increased binding of the SP1 transcription factor (TF), a motif that was enriched in our diet-sensitive regions [597,860]. Similarly, hypoxia-induced genes were shown to recruit the OGG1 and APE1 repair proteins, promoting the binding of HIF1α and induce transcription – another motif that was enriched at obesity-associated regions [597,859]. Second, 8-oxo-G is also thought to exert crosstalk with histone modifications. This oxidative damage mark can arise as a result of histone demethylation reactions that induces the binding of the repair enzyme OGG1 and subsequently induce transcription.

This was observed in breast cancer cells, whereby increased estrogen levels induced estrogen receptor binding to its target genes, and promoted the removal of H3K9me2 methylation via LSD1 action. This enzymatic reaction resulted in local H_2O_2-induced 8-oxo-G accumulation, repair proteins and TFs recruitment, resulting in transcriptional activation [857]. Similar effects involving LSD1 action to demethylate H3K4me2 were observed with the induction of H_2O_2-induced guanine oxidation and transcriptional activation of androgen-induced target genes in prostate cancer cells [861,862]. Although speculative, given the increased estrogen levels and decreased testosterone levels observed in obese individuals, and with the overexpression of LSD1 (KDM1A) in our genetic model of epigenetic inheritance, it is possible that these mechanisms occurred in high-fat fed KDM1A transgenic, resulting in an accumulation of epimutations that could explain the more severe phenotypes in offspring [1]. Third and lastly, 8-oxo-G can also impact DNA methylation. Indeed, 8-oxo-G inhibits the methylation of cytosines by reducing the binding affinity for DNA methyltransferase enzymes [863–865]. Additionally, 8-oxo-G impacts the binding of methyl-CpG binding proteins (MBPs) such as MeCP2, interfering with their transcriptional repression activity [866]. Furthermore, oxidative stress can also induce DNA demethylation. This occurs via the recruitment of repair enzymes at 8-oxo-G bases that next induces the recruitment of TET1 enzymes to induce DNA demethylation [867].

It remains to be tested whether germ cells accumulate 8-oxoG as a result of obesity-induced oxidative stress, and whether these oxidative DNA damages can be linked to epigenetic changes in male germ cells. Such phenomenon could be tested using the Click-Code-Seq method, a technique that allows the mapping of oxidative DNA damage in the form of 8-oxoG, genome-wide and at nucleotide-resolution [868]. While oxidative damage is more likely to persist at heterochromatin in somatic cells, where small ROS molecules can accumulate but regions that cannot be reached by large repair enzymes, this may not hold true for 8-oxo-G profiles in sperm [869,870]. There are at least three possibilities for genomic locations that could be more prone to oxidative damage in sperm and that vary based on the timing of exposure during spermatogenesis. (1) 8-oxo-G could accumulate at heterochromatin during earlier stages of spermatogenesis with similar genomic features as somatic cells. (2) Oxidative damage could potentially impact

protamine deposition during spermiogenesis thereby making regions normally bearing protamines at heightened risk for oxidative attack after this spermatogenesis step. (3) Oxidative damage could occur at regions free of protamines in mature sperm, given that these proteins protect the sperm chromatin against ROS-associated damage. All three options are possible given that ROS exposure occurs throughout spermatogenesis during obesity, a state of chronic and systemic oxidative stress. Using antibody-based methods targeting oxidized guanine (8OHdG), previous studies have found heightened vulnerability to oxidative DNA damage in sperm at regions with lower chromatin compaction and attached to the nuclear matrix [871,872]. Overall, mapping of oxidative damage in sperm coupled with the mapping of epigenetic marks could provide further insights on the contribution to oxidative damage to obesity-induced sperm epimutations.

15.1.2 What makes specific epigenetic regions sensitive to diet-induced obesity?

The comparative analysis on the diet-sensitive regions detected in sperm in two different high-fat diet mouse models from both manuscripts included in this thesis (Chapters 2 and 3) revealed some minor overlap across studies. Although modest, this significant overlap suggests that specific genomic regions could be more prone to epigenetic changes as a result of diet-induced obesity, rather than occurring randomly in the genome. This heightened sensitivity could be explained by various factors that are involved in the establishment of these epimutations, thereby the underlying mechanisms that induce the epigenetic changes. Although speculative, these possibilities will be explored in this section, through the motif enrichment analysis of obesity-associated epimutations presented in the second manuscript (Chapter 3).

The sensitivity of epigenetic regions impacted by diet could reflect sequence-specificity of DNA-binding proteins that are impacted upon obesity or high-fat feeding. One class of DNA-binding protein that could be involved in promoting such sequence specificity to diet-sensitive regions are transcription factors (TFs). These proteins have the ability to recognize and bind to specific DNA motif sequences, usually located at regulatory regions, and to regulate transcription [873]. TFs are composed of a DNA-binding domain (which recognizes specific motifs), a trans-activating domain (which complexes with effector proteins that either have activator or repressor functions), and an optional

signal-sensing of ligand-binding domain (which regulates TFs activity) [874]. Importantly, TFs exert their transcriptional regulatory roles via their activation domain, which interacts with other TFs, coactivators, and chromatin remodelers, to regulate RNA polymerase II activity and location [875]. What determines TF sensitivity to chromatin is not fully understood, but conceivably involves motif sequences recognized by TFs, epigenetic modifications and chromatin structure permitting physical access of TFs to DNA, and context-dependent mechanisms [876,877]. Thus, motif enrichment of diet-sensitive epigenetic regions could possibly be conferred by TFs, whose expression or binding affinity is altered upon obesity. One example of such mechanism was described in a recent article involving an ATF7-dependent mechanism underlying low-protein diet (LPD)-induced epigenetic changes in male germ cells [540]. The mechanism involved suggests that LPD-associated oxidative stress induces ATF7 phosphorylation, thereby reducing its binding affinity to the chromatin. Consequently, ATF7-target genes show decreased H3K9me2 levels and increased expression of tRNA fragments. Interestingly, ATF7 was among the hits in the motif analysis – showing some enrichment of ATF7's target motif in HFD-sensitive regions – suggesting a potential role for ATF7 in our model. Supporting this possibility is the knowledge that obesity is associated with systemic oxidative stress. However, the implication of the described model in our HFD model is strictly speculative and remains to be confirmed.

Although speculative, digging into the top hits of our motif analysis (enriched motifs at regions gaining H3K4me3 in sperm of high-fat fed sires) can provide insights into potential mechanisms underlying obesity-induced epigenetic changes in sperm, and the sensitivity of specific epigenetic regions to obesity-induced altered metabolism. Alternatively, these enriched motifs can be informative on the downstream effects the sperm-transmitted epimutations could have during embryogenesis, whereby the epimutations could impact TF binding and transcriptional regulation. Here are some insights on what is known in the literature as to a potential link between the regulation or targets of selected TF hits from our analyses (ETV4, GABPA, Fli1, Ronin, and Sp1), and how these molecular targets could come into play in the obesity-induced sperm epimutations and their impact on development. It is important to keep in mind that these

links are purely speculative and are only meant to illustrate potential mechanisms involved in our model.

ETV4 (ETS motif family) is a transcription factor whose role has been most described in the context of cancer of various tissues (prostate, pancreas, breast, liver, intestine, and more) [878–882]. Interestingly, ETV4 has been found to cooperate with estrogen receptor (ER) and control estrogen signalling by impacting chromatin accessibility and gene expression [883,884]. Given that increased adipose tissue is associated with elevated estrogen levels, there is a possible connexion for obesity-induced elevated estrogen to impact ETV4 activity and contribute to epigenetic changes to its target genes [883,885,886]. Importantly, ETV4 has been shown to interact with MED25, a subunit of the Mediator complex [887]. This complex is a transcriptional coactivator comprised of ~30 subunits that facilitate promoter-enhancer communication by interacting with TFs, RNA polymerase II, elongation factors, and chromatin modifiers [888]. MED25 binds to response elements and recruits chromatin modifier enzymes to induce a permissive chromatin state [889]. Additionally, the ETV4-MED25 complex occupies enhancers and regulate transcription at target genes [887]. These findings may illustrate a potential mechanism in male germ cells, by which obesity-associated increase in estrogen could facilitate ETV4 action and recruitment to the chromatin with MED25 and chromatin-modifier enzymes that promote a permissive state. It remains to be tested whether these interactions take place in male germ cells and could underlying the detected obesity-induced changes in H3K4me3.

The TF GABPA (ETS motif family) has been shown to be sensitive to ROS, and ROS-induced TNF-alpha can mediate the dissociation of GABP complex in liver [890]. Depletion of GAPBA has been shown to induce the deposition of acetylation of histones at target genes [891]. Given that the TF GABPA is expressed in testes and its activity is disrupted upon ROS, and given that testicular ROS levels are elevated in obese men, it is possible that GAPBA functions may be altered during spermatogenesis as a result of obesity-associated ROS and thereby alter histone modification patterns [892]. Of note, while GABPA has been shown to be expressed in testes, its role in this tissue is still unknown [893].

The motifs of the TFs Fli1 (ETS motif family) and Ronin (THAP motif family) were both enriched at obesity-associated regions gaining H3K4me3 in sperm. Both of these TFs have been shown to play roles in embryonic development. Fli1 acts as a transcriptional

regulator for hemangioblast specification (hematopoietic and endothelial cell precursor) and governs vascular morphogenesis during embryogenesis [894,895]. Ronin is a TF that targets genes involved in protein biosynthesis and energy production in mouse embryonic stem cells, and binds to a hyper-conserved enhancer element [896]. This TF is critical for cardiogenesis during midgestation [897]. The activity of Ronin coincides with Hcf-1 recruitment (which acts as a cofactor) and presence of H3K4me3 at target genes [896]. Recently, H3K4me3 has been shown to have the potential of causally instruct transcriptional activation [898]. Therefore, it follows that sperm-transmitted H3K4me3 epimutations could potentially impact transcription during early embryonic development, and lead to premature expression of genes targeted by Fli1 or Ronin which bear aberrant H3K4me3 profile in sperm. It remains to be determined whether Fli1 and Ronin are expressed in early embryogenesis, and whether these aberrant H3K4me3 patterns would induce the recruitment of the TFs and thereby result in aberrant gene expression.

The last TF that will be highlighted from the enriched motifs in HFD-altered H3K4me3 sperm regions is Sp1. Sp1 binding to DNA can be induced by oxidative stress, and restricted by DNA hypermethylation [860,874,899,900]. This TF regulates chromatin looping and recruits chromatin remodelers such as the histone acetylase p300 to its target genes [901–903]. It is therefore possible that obesity-related oxidative stress and changed in DNA methylation could impact Sp1 binding during spermatogenesis, resulting in changes in chromatin looping and histone modification marking upon recruitment of chromatin remodelers. Interestingly, genomic regions that are marked by H3K4me3 in sperm and persist in the pre-implantation embryo are enriched for Sp1 motifs at genes involved in RNA splicing [904]. Sperm-transmitted epimutations could potentially impact RNA splicing during early development.

These speculative ideas provide avenues of research to determine the molecular mechanisms that induce epigenetic changes associated with obesity and the factors that render the genomic regions more prone to obesity-associated epimutations. Furthermore, these mechanisms could also be extrapolated to predict the cascade of events that occur post-fertilization, and how sperm epimutations can result in altered embryonic development and thereby result in paternally-induced phenotypes. Indeed, these target sequences represent the location of sperm-transmitted epimutations, and binding sites

for specific TFs. If the sperm epimutations are transmitted to the embryo and escape post-fertilization programming, aberrant epigenetic profiles may impact the binding of TFs at these target regions. Incidentally, these targets could impact the development and differentiation of tissues and in part underlie paternally-induced metabolic maladaptation.

A caveat of the motif analysis presented is, although we can identify enriched motifs in a set of regions of interest, it does not necessarily mean that the corresponding transcription factors actually bind at these regions in this specific cell type and specific context. In order to validate the speculated mechanisms described above, the following set of follow-up experiments could be performed. First, candidate TFs should be selected, such as the five proteins highlighted above (ETV4, GABPA, Fli1, Ronin and Sp1). Next, sperm and embryos derived from control- and HFD-fed sires should be collected, and a chromatin immunoprecipitation followed by sequencing should be performed in these two tissues, targeting the TFs stated above. Next, a differential enrichment analysis should be performed with these generated datasets to determine whether the targeted TFs differentially bind in sperm or embryos at the previously detected target regions bearing altered sperm H3K4me3. Further studies should also assess how the activity of these candidate TFs is altered upon obesity (for example, as a result of oxidative stress), whether these changes in TF activity also impact chromatin remodelers' recruitment, and whether these effects can have a causal role in obesity-induced sperm epimutation. As well, it should be investigated whether the sperm-transmitted epimutations impact TFs binding during early development and result in altered gene regulation and expression.

15.1.3 Other considerations: Are there other factors that could contribute to the non-genetic transmission of paternally-induced phenotypes?

While this has not been investigated in this thesis, it is important to acknowledge that factors present in the seminal fluid from semen – other than the sperm epigenome – have been shown to contribute to fertility and offspring health. Indeed, ablation of seminal glands resulted in reduced fertility and fecundity, impaired preimplantation embryo development, hypertrophic placentas, offspring with altered postnatal growth trajectories, increased central adipose depots, and impaired metabolism, with more severe phenotypes in male offspring [905]. These seminal fluid-induced effects are thought to occur

by impacting sperm survival and functional competence, as well as through indirect effects, by affecting the female reproductive tract [905–908]. Both human data and animal models have shown that obesity impacts seminal composition, which can in turn impact sperm integrity [905,909–914]. The molecular composition of seminal fluid has not been assessed in our studies, though the findings highlighted above suggest it is possible that high-fat fed males from our cohorts would have exhibited alterations in seminal content.

Although the contribution of seminal fluid molecular factors in the transmission of paternally-induced phenotypes cannot be ruled out, these factors are unlikely to be the main or sole carriers of paternal information, and instead may be dispensable to induce offspring metabolic phenotypes. Indeed, offspring derived from in vitro fertilization (IVF) from gametes with either one or both high-fat fed parents, showed elevated body weight and metabolic disturbances [515]. Further studies would be warranted to dissect the exact contributions of the sperm epigenome versus seminal fluid factors, on the non-genetic transmission of paternal environmentally-induced offspring phenotypes, particularly in the context of obesity. Given the potential for the cumulative impacts on the sperm epigenome and offspring health upon multiple stress factors [1,477], it is conceivable to expect potential cumulative detrimental effects of the sperm epigenome and seminal fluid compositions on metabolic impairments in the progeny (conceived via natural mating).

15.2 Consistency and discrepancies of findings from this thesis versus the literature

15.2.1 Sperm epimutations transmission of somatic tissues in offspring

The first manuscript of this thesis included a comparative analysis of the obesity-induced changes in the H3K4me3 with the paternally-induced differentially expressed genes in offspring livers. The findings suggested that there was minimal overlap between sperm-altered H3K4me3 promoters and genes showing hepatic differential expression in offspring, with also distinct transcriptomic programs enriched in each deregulated gene sets across tissues. Various animal studies have provided contradictory findings as to whether there is a direct transmission of sperm epimutations to offspring metabolic tissues. For example, several studies have linked sperm epigenetic patterns with offspring altered gene expression in various somatic tissues such as the liver, gonadal white adipose tissue, skeletal muscle, and pancreatic islets [505,521,607]. Nevertheless, these studies usually lack genome-wide information or demonstrate only modest changes in the epigenetic changes on somatic tissues, and highlighting only a few genomic targets assessed. In contrast, several studies on various mouse models of parental exposures of undernutrition, folate deficiency, or cigarette smoking, inducing offspring phenotypes, have identified sperm differentially methylated regions (DMRs) that did not correspond to offspring somatic tissue DMRs [541,556,562,915]. Given the numerous cellular events that separate the sperm from fully matured somatic tissues, such as cellular division, differentiation, migration, maturation and more, it might be unlikely that a sperm-mediated epimutations can directly impact adult somatic tissues. Instead, it may be more likely that sperm-inherited epigenetic changes upon obesity are (at least partly) retained in the embryo, and induce a cascade of molecular events that subsequently result in altered somatic tissue functions, expression, and epigenetic patterns.

15.2.2 Discrepancies in sexually dimorphic responses to paternal obesity: Challenges in making comparisons on metabolic characterization across studies

A number of studies in the fields of obesity, metabolism, DOHaD, and POHaD research, have also observed variations in the severity or presence of metabolic phenotypes when comparing male and female offspring sired by males fed a special diet. In some studies,

females are more vulnerable, whereas in other papers males are more susceptible. An important reason for the discrepancies in findings is due to the fact that data in the literature are fragmented and therefore not always directly comparable because results are obtained under different conditions, using different endpoints and using different animal models of obesity. The lack of harmonization in rodent metabolic phenotyping makes it difficult to make any clear conclusions regarding the exact sexually dimorphic effects of paternally-induced obesity, therefore cautions should be made when comparing findings from one study to another. Indeed, a plethora of parameters differ across studies.

First, the species (mouse versus rat), and the strain and substrain varies across studies, and (sub)strain-specific single nucleotide polymorphism can influence metabolism [916–919]. For example, BALB/c mouse strain is known to be resistant to HFD-induced obesity, and the J and N substrains of the C57BL/6 show variable susceptibility [916,920]. Of note, the J-versus-N metabolic differences are thought to arise – at least partly – from lower energy expenditure in C57BL/6J mice, with more marked differences in female mice [916]. This is of importance as some studies report increased metabolic sensitivity in females, whereas others state this susceptibility in males – potentially due to differences in substrains used. Second, the timing and length of the dietary exposure can vary – with chronic versus acute interventions showing variable metabolic consequences, and age being a significant factor impacting metabolism [921]. Third, the diets used greatly differ across studies: the type of control diets (chow versus low-fat diets) and obesity-inducing diets used (high-fat, high-fructose high-sucrose, Western diets, etc.), and the diet compositions and characteristics (the percentage energy coming from macronutrients, and the source of fat, etc.). Every diet can induce different degrees of severity of phenotypes measured [922]. Fourth, the endpoints measured also greatly vary across studies, as well as the methods used for measurements. For example, adiposity and body composition can be measured by weighting relevant tissues, or with different scans (dual X-ray absorptiometry – DEXA, micro computed tomography – microCT, etc.); metabolic functions can be assessed with a wide range of tests such as oral or intraperitoneal glucose tolerance test (o/ipGTT); the area under or above the curve (AUC or AAC, respectively) can be calculated and compared; and a number of different metabolites can be measured in the blood. When it comes to these different endpoints,

the timing of the test (during the day), the length of fasting before testing, and the concentration of the solution administered for a test can vary.

Overall, the exponential number of possible combinations in terms of animal model, experimental design, endpoint measured, and methods used, highlight the difficulties in faithfully comparing findings from one study to another, and can at least partly explain the potential discrepancies observed across different studies addressing similar research questions.

In order to improve the ability to compare findings across studies that involve rodent metabolic characterization, standard operating procedures should be reinforced in such studies in order to improve reproducibility [923]. During the review process for publication, reviewers and editors should make mandatory the inclusion of information related to study design and animal models used to allow proper comparisons and reproducibility of findings. This is of particular relevance, as unfortunately, many articles omit to mention the strain and/or substrain of mice being used, or the sex of the animals assessed are not specified, for example, making it impossible to accurately compare results. In terms of study design, although more costly and time-consuming, it would be worth characterizing metabolically all animals within a litter, instead of only few randomly selected animals. Indeed, there can be high variability in terms of metabolic phenotypes within a litter, and this variability is not captured or well represented when only select animals are assessed. This would allow to better predict the penetrance of phenotypes and estimate risks for offspring phenotypes. Lastly, it would be beneficial to establish strain- substrain-, sex- and age-specific scale and cutoffs for various metabolic measurements (for example: BMI, fasting glucose levels, etc.) to establish clear diagnostic criteria for metabolic conditions in rodents. Overall, these harmonized data could be deposited in publicly available repositories, similarly to the following (https://www.mousephenotype.org/about-impc/), but open for researchers to provide their raw data.

15.2.3 Mechanisms underlying sexually dimorphic responses associated with paternal obesity

Some of the sexually-dimorphic characteristics of obesity and its associated co-morbidities can translate to what is observed in humans [924]. Worldwide, obesity is more prevalent among women [925]. However, women are less likely to develop type 2 diabetes in comparison to men [926]. Gonadal hormones are thought to play a central role in the sexual dimorphism observed with respect to obesity phenotypes, risks, and associated co-morbidities, by acting on different tissues and throughout a life-course. One such gonadal hormone-targeted tissue are fat deposits. As described in the first section of this thesis, visceral fat has the most impact on metabolic health in comparison with lower body fat which consists of subcutaneous depot [927]. Incidentally, women – and female rodents – accumulate more subcutaneous and less visceral adipose depots than men or male rodents [928,929]. Supporting a contributing role of female gonadal hormones on adipose tissue biology is the finding that surgical ablation of ovaries – preventing the endogenous production of estradiol and progesterone – results in increased susceptibility to diet-induced metabolic disturbances in female rodents [612,930–932].

Next, a non-gonadal hormone mechanism underlying sexually dimorphic susceptibility to obesity and metabolic syndrome involves a neuro-immune pathway [612]. A study showed that diet-induced obesity resulted in increased neuro-inflammation in males which resulted in microglia activation, peripheral macrophage infiltration in the hypothalamus. This male-specific inflammation was also associated with impaired hypothalamic function, decreased synaptic proteins and reduced numbers of GnRH neuron spines. Although the factor that causes this male-specific neuro-inflammation was not identified, females showed increased levels of the anti-inflammatory cytokine IL-10.

Other brain differences are thought to underly sexually dimorphic susceptibility to obesity. Estradiol establishes neural sex differences in development, and has a strong influence on energy balance in adulthood. This hormone exerts its action via the transcription factor estrogen receptor-alpha (ER**α**), which orchestrates sex-biased gene expression program in the brain [933]. Estrogen also plays a role in driving physical activity by acting through melanocortin-4 receptor (MC4R) signalling [934]. Importantly, this

pathway is known to be central in the regulation of food intake and has been linked to monogenic forms of obesity [47].

Lastly, another example of mechanisms that can explain sex differences in metabolic phenotypes and sensitivity to diet-induced obesity involved the microbiome. Gut microbiome depletion was found to abolish differences in glucose homeostasis between male and female mice. Additionally, microbiota transfer from a male donor induced insulin resistance in female recipients. Castration of males inducing androgen depletion resulted in changes in microbiome content to resemble more that of females, improved glucose tolerance. These effects were counteracted upon dihydrotestosterone treatment. These androgen-dependent effects were shown to be modulated via changes in circulating glutamine and glutamate levels to induce glucose homeostasis sex differences [935].

15.2.4 Intergenerational and transgenerational effects of paternal diet-induced obesity

In the second chapter of this thesis, our manuscript described transgenerational transmission of obesity phenotypes only in descendants of sires that were exposed to two epimutation-inducing stressors: a diet-induced obesity, and a germline-specific overexpression of a histone modifier enzyme. In contrast, descendants of wildtype males fed a high-fat diet did not exhibit transgenerational metabolic disturbances. Because descendants (F_1) of high-fat fed KDM1A transgenics showed more severe phenotypes compared to offspring of obese wildtype sires, it is possible that the severity of the phenotypes influences the probability of the next generation to exhibit detectable phenotypes. This was exemplified by the finding that the combination of high-fat feeding and KDM1A germline overexpression resulted in increased sperm epimutations at the level of H3K4me3 [1]. In other words, more severe phenotypes (in the F_1 generation) as a result of paternal overnutrition, may be sufficient to induce similar sperm epimutations as those detected in F_0, and result in the transmission of similar metabolic disturbances in the next generation (F_2).

It remains to be determined how mechanistically these effects can persist and be transmitted transgenerationally. In this study, we did not profile the sperm chromatin of the F_1 generation, and therefore cannot conclude that this mark was still altered in the

sperm of these animals, nor that H3K4me3 specifically is associated with the transgenerational transmission of metabolic disturbances in the F_2 generation. This epigenetic mark remains a potential candidate given its previous association with the transgenerational transmission of developmental abnormalities [476,543]. Furthermore, we did not phenotypically characterize animals beyond the F_2 generation. It is likely that if phenotypic effects were detected beyond the F_2 generation, the metabolic phenotypes would be diluted across generations. Indeed, although not tested statistically, a gradual reduction in the severity of phenotypes across generations could already be observed in some of the metabolic parameters tested as well as the number of differentially expressed genes in the livers in our study from F_0 to F_2 animals [1]. These effects could arise from a gradual shift in epigenetic patterns in sperm across generations, as the generational distance increases from the F_0 generation. Such generational dilution of epimutations has been observed in previous studies of transgenerational effects, including in a rodent model of vinclozolin toxicant exposure, as well as in two transgenerational epigenetic inheritance models of heat-induced stress in *C. elegans* [936–938].

Absence of evidence is not evidence of absence: It is worth noting that although we did not observe transgenerational effects in descendants of wildtype males fed a high-fat diet, it is possible that offspring of the F_2 generation may still show increased susceptibility to metabolic disturbances. In other words, these animals may be more prone to develop obesity and metabolic syndrome, upon a “second hit” such as a high-fat diet challenge. This is concordant with obesogens such as endocrine-disrupting chemicals that do not induce obesity on their own, but enhance obesity development risk [117].

Currently, to my knowledge, the only reports of transgenerational inheritance of obesity through the male germline in rodents either involves a dietary challenge in the F_2 generation [607], a genetic model of epigenetic inheritance (the A^{vy} Agouti mouse) combined with a Western diet challenge in the descendants [606], the use of pharmacological agents to induce insulitis and thereby prediabetes in sires [521], or paternal high-fat feeding with only very subtle effects in F_2 offspring [506]. These findings suggest there is still a lack of clear evidence to support transgenerational transmission of paternal obesity in rodents that do not rely on dietary challenge or that are not initiated by genetic mutations. As suggested, it appears that F_2 offspring may not show obvious metabolic disturbances, but

instead be at heightened risk to develop such conditions upon a dietary challenge or other obesity-inducing exposures.

15.3 Limitations of experimental approaches and model used, and translatability to human conditions

15.3.1 Diet-induced obesity model

The diet-induced obesity mouse model has been established about six decades ago and has been widely used to model obesity, type 2 diabetes, and metabolic syndrome [503]. While the use of this model has allowed to unravel the etiology and molecular mechanisms involved in these conditions, this model involves some limitations, and cautions must be taken when drawing conclusions with findings derived from such rodent model to extrapolate to human conditions.

15.3.1.1 The diets and animal model

Both studies included in this thesis involved the use of a high-fat diet (HFD) to induce obesity (60% kcal fat, D12492, Research Diets Inc. was used in both studies). This standardized laboratory animal diet ensures experimental reproducibility and has been widely used worldwide and characterized in-depth over the years. In rodents, this HFD consistently induces obesity, hyperglycemia, insulin resistance, liver steatosis, hypertriglyceridemia, adipocyte hypertrophy, hypertension, impaired intestinal barrier integrity, with some variability in phenotypes as a result of different strains/substrains used and length of dietary intervention [939]. While these formulated diets can replicate some of the metabolic disturbances and obesity-associated pathology observed in humans, it does not fully recapitulate the dietary patterns such as Western diets consumed by humans [940]. Indeed, according to the National Health and Nutrition Examination Study (NHANES), a typical Western diet consists of 49% kcal from carbohydrates, 35% kcal from fat, and 16% kcal from protein [941]. This is substantially different from the macronutrient compositions of the formulated HFD for rodents, which is composed of 20%, 60%, and 20%, energy from carbohydrates, fat, and protein, respectively. Additionally, given these HFDs are formulated to maintain animal health, the micronutrient content also differs from that of a Western diet. Although a HFD in rodents can largely recapitulate human obesity phenotypes and associated comorbidities, the model may not fully emulate the progression of the condition, such as the transition of NAFLD to NASH [942]. Other diets have been developed to better recapitulate humans

eating patterns, such as the “cafeteria diet” whereby mice are free to select from various palatable foods. Nevertheless, these diets are poorly defined in terms of micronutrient composition and therefore show reduced replicability [943,944]. To study NAFLD and NASH conditions and their progression, choline- and methionine-deficiency diets have been used, which impact hepatic lipid metabolism resulting in liver damage. Although these diets model some of the characteristics of NAFLD and NASH, they do not recapitulate metabolic disturbances observed in humans affected with these conditions [945]. Lastly, given obesity is a multifactorial condition in humans, involving many underlying intertwined causes and interacting factors, the simplistic nature of these rodent DIO models cannot emulate the complexity of human obesity. Overall, it is generally accepted that no diets can perfectly model human conditions including the complexity of obesity causes, characteristics and progression [939,940,946]. Nevertheless, they can be useful to study mechanisms underlying these conditions, such as epigenetic inheritance mechanisms in the presented studies.

In the manuscripts included in this thesis, two different diets were used as control. In the first study, we used a low-fat diet (10%kcal fat; D12450, Research Diets Inc.), whereas in the second article we used a regular chow diet (17% kcal fat; Harlan 8640 Teklad 22/5 Rodent Diet). The low-fat diet (used in the first study) matched its corresponding high-fat diet for sucrose amount, nutrients and vitamin content, allowing to strictly assess the impact of obesity resulting from increased fat content. In contrast, the regular chow diet (used in the second study) does not allow to control for these specific dietary components. Nevertheless, whether the HFD treatment is compared to either control diets, in both cases the HFD induces obesity, paternal obesity is associated with reproducible and comparable effects in offspring, and there are overlaps between the detected sperm epimutations [1,510,597]. While there can be pros and cons in using either the low-fat or the chow diet as control, using different parameters in the experimental design across studies allowed us to determine whether these experimental discrepancies – among other differences in technical approaches across both studies – could produce comparable results in terms of the detected sperm epimutations. Indeed, we did observe some overlap on the diet-sensitive regions detected, with comparable genomic characteristics of obesity-associated regions across studies, as well as similar functional

pathways enriched. While this remains to be directly tested, it is conceivable to expect that using the same control diet in both studies would have resulted in a greater overlap of obesity-associated regions in sperm across studies.

While the animal models used in the present studies cannot fully recapitulate human metabolic disorders and obesity phenotypes, they allow to control for numerous factors such as environmental exposures, diets, genetic background. Thus, allowing to make conclusions strictly from paternal diet-induced obesity, the impact on the sperm epigenome, and on offspring health. Such studies and experimental design are not suitable for human subjects. In the future, it would be interesting to clearly dissect the differential effects of various paternal diets that induce obesity and how they variably impact the sperm epigenome and offspring health.

15.3.1.2 Impact of maternal preconception exposures to obese sires during mating

Although great care was given to minimize preconception maternal interactions with sires used for breeding, maternal exposure to these males was inevitable given natural mating as breeding method, and therefore this should be kept in mind as a limitation. In order to completely prevent maternal preconception exposures to obese sires, assisted reproductive technologies (ART) such as in vitro fertilization (IVF) would have been required, where gametes would be collected separately. We opted not to perform IVF given that ART can impact the epigenome and embryonic development [566]. As such, we did not want to confound any factors with these epimutation-inducing procedures. Nevertheless, effects on maternal exposure to paternal diet, their microbiome, and other potential factors, are likely minimal. Indeed, as mentioned in a previous section, females require more time in order to gain excess weight on a HFD, and to elicit metabolic disturbances [612]. Additionally, it was reported that natural mating of chow-fed females with high-fat fed males did not alter maternal adaptation to pregnancy, maternal glucose metabolism, compared to females that were mated with (nonobese) sires fed a regular diet [510].

15.3.2 Obesity phenotype characterization and hepatic molecular profiling

The second chapter of this thesis involved the metabolic characterization and hepatic transcriptomic profiling of animals across generations to delineate the metabolic health

consequences of paternal diet-induced obesity in combination with an epigenetic model of inheritance with the germline-specific KDM1A overexpression. For the metabolic characterization, there are several pros and cons on the different tests chosen, and more tests could have been performed in order to provide a more in-depth characterization as well as to allow to differentiate the intricacies of the effects of paternally-induced metabolic phenotypes in offspring.

For the glucose tolerance test (GTT), we performed an intraperitoneal injection of glucose. We followed the International Mouse Phenotyping Consortium, which exclusively uses the ipGTT for glucose metabolism assessment [923]. There are debates as to whether an intraperitoneal (ip) versus oral (o) glucose administration are preferable to assess glucose tolerance. Indeed, the glucose administration through an ipGTT results in gastrointestinal bypassing, thereby lacking the ability to detect the effects of incretins [947]. On the other hand, while the oGTT may be more physiologically relevant, this method is thought to be technically more challenging, more stressful for the animal – which introduces variability in the outcome – and can result in incomplete glucose retention, as well as injuries to the animal [948].

For the assessment of adiposity, we weighed two key fat deposits, namely the gonadal white adipose tissues and the mesenteric white adipose tissue. While this approach was inexpensive, rapid, and sufficient to detect changes across experimental groups, a whole-body scan would have revealed more valuable information to better characterize the animals. Indeed, dual-energy X-ray absorptiometry (DEXA), nuclear magnetic resonance spectroscopy (NMR), as well as micro computerized tomography (microCT) can be used in rodent models to simultaneously measure lean and fat mass [949].

The characterization of liver functions in the first study presented in this thesis (Chapter 2) allowed to confirm whether animals exhibited transcriptomic changes across generations and whether these changes could relate back to obesity-induced alterations in the sperm epigenome. Although information, alternative methods could have been used which would have provided higher-content information. First, regarding the hepatic transcriptomic experiment, a single-cell RNA-sequencing or single-cell spatial RNA-sequencing experiment could have been performed. Indeed, bulk RNA-sequencing

consist of samples with heterogeneous mixtures of cell types and therefore represent averaged expression levels, in contrast to single-cell omics methods which provide expression levels from individual cells [737]. Additionally, bulk RNA-sequencing is confounded by the differences in cell-type proportions. The liver is of particular interest for single-cell profiling, given the highly heterogenous nature of hepatocyte transcriptomic profiles. This heterogeneity arises from the unique architecture of the liver, consisting of lobular zonation. Additionally, single-cell profiling would be important in this experimental setting, given that we have detected differentially expressed genes in offspring of obese sires, which were enriched for genes related to inflammatory pathways, particularly in male offspring [1]. These deregulated pathways may reflect the infiltration of inflammatory cells, a hallmark of the progressive form of non-alcoholic fatty liver disease (NAFLD) – namely, non-alcoholic steatohepatitis (NASH) [950]. Currently, single-cell (and spatial) transcriptomic maps have been established in whole liver from mice and humans, and have revealed coordinate-specific division of labour of hepatocytes, with approximately half of genes that are significantly zonated [265,951–953].

Next, in order to further assess the pathology of the livers, a histological scoring system could have been applied to our liver samples [950]. These protocols have been previously established and showed high reproducibility across different rodent models and across all stages of NAFLD. This preclinical scoring system consists of analyzing histological slides with defined criteria that assess the extent of steatosis, hepatocellular hypertrophy, inflammation, and fibrosis in the samples. These analyses could have revealed whether the animals showed signs of various stages of NAFLD or NASH. More interestingly, it would have been interesting to assess whether female offspring show any signs of NAFLD, given that they did not exhibit obvious metabolic disturbances, but showed different hepatic gene expression. The histological scoring could have allowed to determine whether female livers show early signs of steatosis.

15.3.3 Sperm epigenome and profiling

Spermatozoa are challenging cells to profile histone marks and other DNA-binding proteins, owed to their highly compacted chromatin via disulfide bonds formed with sperm-specific proteins – protamines [430]. The past decade has been marked with the

development and advancement of technologies to profile sperm chromatin, with the adaptation of classic methodologies such as chromatin immunoprecipitation followed by sequencing (ChIP-seq) to be compatible with the uniqueness of the sperm chromatin features and structure [614,615]. While the ChIP-seq approach used in this thesis was the best available method for sperm chromatin profiling at the time the experiments were performed, this technique has some caveats that should not go unrecognized. First, ChIP-seq is limited by the inherent challenges that antibody-based methods possess. Antibodies can sometimes result in non-specific binding as well cross-reactivity with other epitopes [954]. To circumvent the potential non-specific binding, we focus our analyses on genomic regions showing enrichment for the histone mark of interest. We have found reproducible profiles across studies using this protocol and antibody, with good sample-to-sample correlation [1,221,476,477,597,615]. Additionally, while the H3K4me3-specific antibody used may elicit some cross-reactivity with other H3K4 methylation states, data from previous studies from the lab suggest the antibody can at least discriminate between H3K4me2 and H3K4me3, given that KDM1A-induced enrichment changes at these two marks showed opposite directionality change [476].

In the years that have followed the execution of the ChIP-seq experiments presented in the manuscripts of this thesis, new methodologies have been developed which have some advantages over classical ChIP-seq methods. Namely, Cleavage Under Targets and Tagmentation (CUT&Tag) and Cleavage Under Targets and Release Using Nuclease (CUT&RUN) [955,956]. Both of these methods share the same underlying principle, where antibody-targeted controlled enzymatic cleavage induces the release of targeted DNA-protein complexes. This strategy provides exceptionally high signal-to-noise ratio given that the unbound chromatin is not fragmented nor subjected to immunoprecipitation. While these techniques seem like attractive alternatives to currently available ChIP-seq methods for sperm chromatin profiling, they still pose some challenges. For example, this method has been validated for various histone marks, but not widely for less abundant DNA-binding proteins such as transcription factors. This is because CUT&Tag works most efficiently when the epitope of interest is abundant, which would be a challenge to target histone modifications in sperm given the vast majority are replaced by protamines. It was also proposed in a new preprint that this method may

slightly be biased towards open chromatin regions, resulting in potential misinterpretation of the detected signal distributions and changes upon conditions (such as obesity) with this technique [957]. Additionally, these methods have yet to be adapted or made widely available to be used in sperm cells, with – to my knowledge – only one publication thus far that leveraged the CUT&Tag method to map a histone mark in sperm [958]. If these challenges can be surpassed, establishing a sperm-adapted protocol from these recently introduced methods would be beneficial to generate sperm histone maps with improved signal-to-noise ratio. In the long run, these methods could even bring sperm chromatin mapping to the single-cell level with inclusion of multi-omics profiling, given that CUT&Tag has recently been adapted for these purposes (single-cell multi CUT&Tag) in somatic cells [959,960].

15.3.4 Paternally-induced placenta gene expression changes and cellular composition

The second manuscript (Chapter 3) involved in assessing the transcriptional impact of paternal diet-induced obesity on mid-gestation placentas. Our differential gene expression analysis revealed deregulated genes in placentas as a result of paternal obesity. Using a deconvolution analysis, we detected changes in cell-type proportions, which resembled those detected in hypoxic placentas associated with intrauterine growth restriction. While this work provides advancements in our knowledge on the paternal transmission to placental defects, as well as valuable datasets for such research, there are limitations and knowledge gaps that remain from these analyses.

There were differentially expressed genes in placentas that were detected in association with paternal obesity. However, these data do not provide information on whether the differentially expressed genes detected are as a result of changes in cellular functions, or aberrant cellular composition within this tissue. While the deconvolution analysis suggests there are some changes in cell-type proportions, the former possibility cannot be ruled out, and one outcome does not prevent the other. Future studies should repeat these experiments using single-cell RNA-sequencing approaches in order to detect cell-type-specific differential expression, which would provide deeper information on the pathophysiological changes occurring in placentas as a result of paternal preconception obesity. Additionally, these experiments would permit the validation of the

cellular proportion changes estimated via the deconvolution approach. Furthermore, this would also allow to detect changes in cell-types that are found in smaller proportions within the tissue, such as inflammatory cells, which currently cannot be reliably estimated with a deconvolution analysis. Such single-cell and single-nuclei approaches have already been adapted for placenta tissues [961–966], and improved protocols have recently been published for the dissociation of single cells [967].

Importantly, only one developmental stage was assessed in this study (E14.5). The mouse model used has been previously characterized showing altered placenta phenotypes associated with paternal obesity at E14.5 and E18.5 fetal developmental stages [510]. While we can safely state that it is established that the placenta defects previously observed manifest in mid-to-late gestation, these effects likely originate early in development. This possibility is exemplified by studies revealing changes in cellular allocation to the trophectoderm versus inner-cell mass of the blastocyst as a result of paternal obesity [489,491]. Consequently, it would be worth performing multiple RNA-sequencing experiments – preferably at the single-cell level – assessing multiple time points earlier in development. These experiments would provide a map of the developmental trajectories of aberrant gene expression, and would permit to track these differentially expressed genes as early as the pre-implantation embryo and throughout development. Additionally, one could (1) identify the deregulated genes that persist across developmental stages, cellular division and differentiation, and most importantly (2) determine the cell-type-specific deregulation of gene expression (using single-cell methodologies) to better understand the molecular mechanisms underlying paternally-induced placenta defects.

Regarding the translatability of the data related to our placenta work, cautions should be made regarding the extrapolation of the findings to human health. While many studies using rodent models have been useful in studying the placenta, its development and pathophysiology, there exist some differences between mice and human placentas in terms of anatomical structures, cellular composition, trophoblast subtypes, and molecular content. [576,966,968].

First, at the anatomical level, there are several structures that differ between mouse and human placentas. In mice, the labyrinth comprises three layers of trophoblasts

between the maternal and fetal blood, whereas in humans, the chorionic villi contain two layers in earlier stages of gestation, and then one layer later in gestation [576]. Additionally, in mice, the trophoblast cells that anchor the placenta to the uterine wall (which are composed of parietal giant cells and glycogen trophoblasts) show less invasiveness than that of humans, which correspond to the extravillous trophoblasts [969–972]. At the cellular level, both species show equivalency in terms of cell-types present in the placenta, with some cells' formation that arise from differing mechanisms [973]. For example, hyperdiploid trophoblast cells form at the placental implantation site for both species, but the hyperdiploidy of the cells occur in divergent mechanisms. In mice, trophoblast giant cells result from DNA synthesis that takes place without nuclear division (i.e. endoreduplication), whereas in humans, extravillous trophoblasts arise from mechanisms that are still poorly understood [974]. Third, at the transcriptional program level, mouse and human placentas slightly differ. For example, the transcription factors ESRRB and SOX2 seem to have a more prominent role in mouse trophoblast development than in humans, as they show low expression levels in this latter species, and humans lack the receptor isoform (FGFR2C) which drives expression of *Esrrb* and *Sox2* in mice [975–977]. Another marked difference is the absence of EOMES in human trophectoderm and placenta, an essential transcription factor for mouse trophoblast self-renewal [978–980].

Nevertheless, placentation and associated abnormalities are challenging to study, and the mouse has served as a valuable model to study these processes, given the core features of placentation are still similar across species. Indeed, both species have a hemochorial placenta that also share similar molecular regulation [570]. That is, the anatomical arrangement of the placenta where the maternal blood comes in direct contact with the fetal-derived trophoblast-lined villi. Additionally, these two species share approximately 80% of regulatory conserved genes that serve for placentation, as well as some key markers and signalling pathways [576,968]. The inter-species differences related to placentation highlight the importance to validate placental mouse processes to the human system.

15.4 Remaining gaps in knowledge and future directions

15.4.1 Are paternal effects on the sperm epigenome and on future generations health reversible?

Findings shown in this thesis as well as in the literature support that paternal environmental factors such as obesity can induce sperm epimutations and are associated with phenotypes in offspring. An important question that remains in the fields of paternal epigenetic inheritance and paternal preconception health in the context of obesity, is whether these effects are reversible at the level of the sperm epigenome, and whether offspring metabolic phenotypes can be prevented. There are several lines of evidence in the literature that support these possibilities.

15.4.1.1 Reversibility of offspring phenotypes

In the context of obesity, paternal exercise has been suggested to protect from the detrimental metabolic impacts of paternal diet-induced obesity on offspring. Indeed, a paternal diet-induced obesity (DIO) intervention, combined with chronic voluntary exercise, gave rise to males that sired offspring with reduced sensitivity to a HFD challenge [507]. Supporting these findings, paternal DIO followed by exercise, restores offspring metabolic functions, reduces adiposity, increases muscle mass, restores pancreatic islet morphology and miRNA profiles [516]. In contrast, another study showed conflicting results, where paternal long-term exercise alone resulted in offspring increased susceptibility to metabolic disturbances upon a HFD challenge [508]. These discrepancies may be due to the fact that this latter mentioned study performed an exercise intervention alone, rather than combined with a DIO intervention, as well as the small sample size used in some of these studies, for endpoints that are known to show relatively high variability. Nevertheless, the conflicting results highlight the need to further replicate these findings and provide conclusive evidence to determine whether paternal exercise can provide protection for metabolic disturbances in offspring *via* the sperm epigenome. Additionally, while some of these studies have brought advances in our knowledge that paternal preconception exercise following a diet-induced obesity intervention can prevent or reduce the detrimental impacts related to obesity in offspring, some of these reports have only investigated the effects in male offspring. Consequently, further investigation

will be required to determine whether the impacts differ in male and female offspring, and if so, how these sexually dimorphic effects take place.

Other preconception interventions following paternal HFD intervention in rodents that have shown to be beneficial to prevent offspring metabolic disturbances involved other weight loss-inducing procedures, such as exercise, exercise combined with diet reversal, or diet reversal alone [507,509,516,981–983]. Micronutrient supplementation including methyl donor or taurine supplement has also been shown to improve offspring phenotypes. These intervention studies suggest that the paternal transmission of obesity-associated phenotypes can be prevented by weight-loss strategies or by modulating metabolic pathways via micronutrients supplement [984].

15.4.1.2 Reversibility of sperm epimutations

Supporting the concept that an exercise intervention can restore sperm epigenetic signatures, paternal exercise not only reverses paternal effects of HFD on offspring metabolic phenotypes, but also improves sperm parameters and reverses changes in sperm RNA content [509]. Other intervention options that involve weight loss are likely strategies that would be successful in reversing the detrimental impacts of DIO on the sperm epigenome and offspring health. For example, a Roux-en-Y gastric bypass surgery (GBP) is one such intervention that is known to induce weight loss, improve insulin resistance and type 2 diabetes, in severely obese individuals. Paired analysis of individuals before, one week after, and one year after a GPB procedure, showed a reversal of sperm DNA methylation patterns [520]. Of note, this intervention is used as a last resort for weight loss and metabolic health improvement, with some risks associated to the procedure, and therefore is not a widely accessible or ideal solution. Nevertheless, these findings provide further evidence for the proof-of-concept that obesity-associated sperm epigenetic changes can be reversed upon weight loss. It remains to be tested whether these findings hold true for obesity-induced alterations in sperm histone methylation.

15.4.1.3 Other possible paternal preconception interventions to consider

Another question that remains, is whether other preconception interventions in future fathers – aside from exercise – can have protective effects on offspring metabolic health and sperm epimutations. While it is currently not possible to provide specific

interventions given the molecular mechanisms underlying obesity-induced epigenetic changes are not fully understood, there are several target strategies that could be worth exploring. From a general point-of-view, and keeping in mind some of the molecular and metabolic changes occurring in obesity and metabolic syndrome, targeting oxidative stress to reduce ROS burden (such as with antioxidants and vitamins), and the one-carbon metabolism (with micronutrient supplementation as described in previous studies) to modulate aberrant substrate availability and enzyme activity, would be pathways worth investigating in this context.

Collectively, there is cumulative evidence that support the concept that various interventions following paternal obesity can improve paternal phenotypes, sperm parameters and epigenetic signatures, as well as to protect offspring from the increased susceptibility of metabolic disorders. Future work should address these gaps in knowledge by generating a DIO model combined with a chronic exercise model – or other interventions that have weight loss, anti-inflammatory or anti-oxidative effects – in order to assess whether sperm epigenetic signatures, particularly sperm H3K4me3, can also reverse back to a lean-associated signature, improve offspring metabolic phenotypes, and susceptibility to a HFD challenge. Because studies have shown that paternal obesity can also impact sperm DNA methylation and non-coding RNA content, it would be interesting to simultaneously assess whether obesity-associated DNA methylation and RNA content signatures can be negated upon these interventions. Of note, it would be of particular relevance to determine the minimum length of the paternal intervention to reverse the sperm epigenome and prevent metabolic impairments.

15.4.2 Which obesity-sensitive epigenetic regions in sperm are required/sufficient to induce phenotypes in the next generation(s)?

It has become clear that various environmental exposures to the father can lead to epigenetic changes in the sperm. Furthermore, altering the sperm epigenome in the germline has been linked to abnormal phenotypes in offspring. Mechanistic studies will

be warranted in order to determine whether there are specific genomic regions in sperm altered by obesity that are required to induce metabolic disturbances in the next generation(s). To achieve this goal, several experiments should be performed in order to drill down the required phenotype-inducing sperm epigenetic regions and determine their causal relationship with offspring metabolic phenotypes.

First, in order to generate a list of potential regions that are changed upon diet-induced obesity, the DIO model should be replicated multiple times to identify the most consistent effects on the sperm epigenome. As opposed to what was performed across the two studies presented in this thesis, it would be important that the experimental design, technical approaches and animal model remain consistent across the different trials. This will allow to reveal the essential – and consistent – epigenetic regions that are induced by obesity, and associated with phenotype transmission in this **specific** model.

Next, once a list of obesity-sensitive regions that consistently change across trials is generated, mechanistic studies would have to be conducted in order to determine the regions that are essential to induce metabolic disturbances in offspring. One possible approach to achieve this goal would be to take advantage of epigenome editing methods such as the CRISPR-Cas9 system. The fusion of the nuclease-deactivated Cas9 to either a transcriptional activator or repressor, or an epigenetic modifying enzyme, permits the targeted manipulation of epigenetic marks and consequently gene expression [568]. Using this approach, the goal would be to generate mouse models with targeted epigenetic editing within the developing male germline. Guide RNAs would be designed to target the list of consistently changed epigenetic regions upon high-fat feeding. To induce increases in H3K4me3, the histone methytransferases could be fused to the dCas9 protein to induce epigenetic changes, such as MLL1-4, SETD1A/B, PRDM9, and SMYD3, [985]. To induce decreases in H3K4me3, the histone demethylase enzymes JARID1A-D or NO66, could be used [985]. Multiple models targeting different combinations of the selected target genomic regions would be generated, and offspring derived from sires bearing these sperm-borne epimutations would be characterized and compared. This model would allow to confirm (or refute) the proof of concept that obesity-associated sperm histone methylation can result in offspring metabolic disturbances.

15.4.2.1 Considerations, limitations, and challenges

The proposed experiments are not trivial, and would require a significant time, financial resources, and importantly there are still significant gaps in knowledge in order to execute such ambitious projects. First, CRISPR-based methods are known to have some degrees of off-target effects (i.e. targets other than those specific to the guide RNAs used), which would beg the question whether the phenotypes (if observed) result from the targeted epimutations, or some of the resulting off-target epimutations. Additionally, many chromatin-modifying enzymes do not target only one epigenetic mark, therefore the fact that other marks may be altered at the targeted sites should not be ignored.

Adding some complexity in this approach, is the fact that it is likely that many combinations of many sperm-borne epimutations can result in metabolic disturbances in offspring, meaning that it might not be possible to determine one single minimum list of epimutations to induce such effects. This possibility is in accordance with the multifactorial characteristic of obesity and metabolic syndrome, the variability in the manifestation of these conditions, as well as the polygenic nature of genetic forms of obesity.

Importantly, it would be important to ensure that the epigenome-editing system does not cause mosaicism across cells. Indeed, given that one sperm cell results in one embryo/individual, if the epigenetic-editing is not uniform across cells within the same sire, this approach will not be valid in order to determine the required epimutations to induce offspring phenotypes. To reduce mosaicism, the transgene should be expressed over multiple stages of spermatogenesis to ensure that the epimutations are established.

Another important point to keep in mind is that several studies have shown diet-induced changes in sperm at the level of DNA methylation and RNA content. This suggests that it is likely that many epigenetic marks, or many non-genetic layers of information contribute to the paternal transmission of metabolic phenotypes, which would not be accounted for in this transgenic model. Additionally, with the proposed experiments, it is therefore possible that the CRISPR-induced histone mark epimutations may result in epimutations at other marks as well as changes in sperm RNA content as a result of altering histone methylation, which would all contribute to the (potentially) resulting offspring phenotypes.

As well, it is also important to be reminded that we detected both increased and decreased enrichment for H3K4me3 at diet-sensitive regions. This poses a technical challenge, and it therefore may not be possible to simultaneously target these regions and induce bi-directional changes at different targets given that two different enzymes would have to be targeted at each different sets of regions. It would be more feasible to select only one chromatin remodeling enzyme for this model. Additionally, because many different histone modifier enzymes exist and either deposit or remove H3K4me3, it is possible that several are impacted by the HFD in our model. One strategy to select one enzyme of interest to test this approach would be to perform ChIP-sequencing for these various histone modifiers in sperm derived from control-fed sires to determine which of these enzymes binds to the detected diet-sensitive regions. Furthermore, a pre-existing better understanding on the molecular mechanisms that underly the diet-induced epigenetic changes in sperm would help determine the enzymes of choice to use.

Another outstanding question is: what are the essential genomic regions bearing obesity-induced epimutations in sperm that induce offspring metabolic disturbances? In the long term, determining these key epigenetic regions would have significant value for clinical purposes in order to be able to predict offspring metabolic outcomes with sperm samples that are epigenetically profiled at target regions. Before then, the clinical translation of these findings would have to be determined.

15.4.3 Bringing -omics technologies to the single-cell resolution for sperm epigenetic landscape profiling

A major progression for the field of paternal epigenetic inheritance will be the technological advancement that will permit epigenomic profiling of a single sperm. While bulk-sequencing methods provide valuable information on epigenetic and transcriptomic signatures reflecting mean enrichment or expression profiles, they lack information on cell-specific profiles, and mask individual cell heterogeneity. This is of particular relevance for sperm epigenetic profiling, given that one single sperm will give rise to one embryo/individual. The most recent advancement in -omics technologies now permit the assessment of transcriptomic, epigenomic and chromatin structure profiles at the single-cell and single-nucleus resolution, with options to profile multiple epigenetic marks (DNA

methylation, histone modifications, DNA-binding proteins, transcription factors, RNA content, and chromatin accessibility) in the same cell. The technical feasibility of such techniques in single-sperm has been validated using ejaculate from two individuals to profile DNA methylation [986,987]. However, these single-cell -omics methods have not been thus far made widely accessible or adapted for the unique molecular and structural characteristics of spermatozoa cells and chromatin, in order to compare profiles upon various paternal exposures and health conditions. Although this will be technically challenging, future studies should seek to develop such methods.

Recent work in a preprint from the research group of Romain Barrès in Copenhagen, showed that they have been able to perform single-sperm DNA methylome profiling in human samples [988]. The validity, quality, and reproducibility of these data are still to be confirmed, as the datasets are not yet publicly available, and the study has not yet gone through or completed peer review. Additionally, the work was done with ejaculates coming from 8 different individuals (4 lean and 4 obese; for a total of 87 motile spermatozoa), therefore it will be important to replicate the findings with increasing number of cells and from larger sample sizes. At this stage, the mapping rate is low and requires high sequencing depth – covering only 1-5% of CpG sites – making the cost efficiency of this technique quite low. Future work will need to either make use of computational and statistical approaches to predict methylation status at neighbouring CpG sites, use bisulfite free methylation methods, and/or refine protocols, in order to increase the mapping rate and reduce the associated costs [989,990]. Nonetheless, this work provides significant advancement towards bringing such techniques at the single-sperm level and will likely encourage the community to improve this method, and to adapt other epigenetic profiling techniques in single-sperm.

Using an adapted post-bisulfite adaptor tagging (PBAT)-based whole-genome single-cell bisulfite sequencing method, the authors found that obesity was associated with DNA methylation patterns defects [988]. The findings suggest that a subpopulation of spermatozoa cells may bear these epimutations, which could potentially result in varying intergenerational effects. This possibility is in accordance with the variability observed in metabolic phenotypes in our model and that of other DIO models. It is important to keep in mind that, in comparison with humans, mice bear multiparous pregnancies, which can

differentially impact the developmental growth of the fetuses [991]. Therefore, some of the intra-litter variability may result from differential energy and resource allocation *in utero*, in pregnancies with multiple conceptuses.

Because of the limited coverage in this experiment, it is still unclear whether within the subpopulation of affected cells, some cells carry most or all of the differentially methylated regions. Therefore, it remains to be confirmed whether single sperm carry epigenetic defects at multiple loci, and if so, whether these defects occur at distinct regions independently, resulting in similar offspring phenotypes. Given the multifactorial nature of obesity and metabolic syndrome phenotypes, as well as the polygenic characteristic of these conditions, this hypothetical mode of variable epigenetic pattern transmission is plausible. Further supporting this possibility, is the discordance between the magnitude of obesity-associated DNAme changes and the high rates of metabolically-affected offspring observed paternal DIO studies. Indeed, studies have identified minimal (5-15%) obesity-associated changes in DNAme (meaning that 1-3 sperm cells out of 20 would bear DNAme changes), whereas the penetrance of the transmission of metabolic phenotypes was high [600]. This implies a mosaicism pattern of DNA methylation, where different regions bearing aberrant DNAme could independently result in similar metabolic phenotypes in offspring. Alternatively, this may be due to the fact that other epigenetic marks aside from DNAme are altered in the model and contributing to offspring phenotypes. Of note, the differentially methylated regions detected in this study did not overlap with those detected from a bulk experiment from the same research group [520]. This is likely due to the differences in genomic regions covered across studies, different subjects assessed, small sample size, as well as the different methods used (bulk reduced representative bisulfite sequencing, versus PBAT single-cell bisulfite sequencing). Nevertheless, this further highlights the need for refining protocols to ensure reproducibility that will permit conclusive findings.

Whether obesity-induced H3K4 methylation changes in sperm across the genome are carried by a subpopulation of spermatozoa cells, and whether these changes occur in a mosaic-like manner is still unknown and remains to be determined. Interestingly, the variance in terms of severity and manifestation of offspring metabolic phenotypes support the potential variability in sperm-borne epimutations. Such inter-individual phenotypic

variability has also been observed in genetic models of epigenetic inheritance, with sperm epimutations associated with a wide-range of developmental abnormalities, and variable phenotypes with varying degrees of severity in offspring [543,556].

As mentioned, such single-sperm techniques targeting histone modifications have not been developed yet, and given the low mapping rate of the sperm scBS profiling data described above, there is a long way to go until we can reliably profile the epigenetic marks in sperm and draw any conclusions regarding obesity- and environmentally-induced chromatin changes at a single-sperm resolution. As eluded in the preliminary findings from the sperm scBS profiling data from lean and obese men, it is possible that histone H3K4me3 profiles exhibit mosaicism within a single ejaculate with different epigenetic pattern variations are integrated to result in the same offspring phenotypes [988]. The regions with obesity-associated H3K4me3 profile changes detected in our studies with bulk ChIP-seq protocols are likely occurring in a relatively greater fraction of sperm cells, whereas the epimutations affecting a smaller subpopulation of cells go undetected in our analyses.

Although at the moment, we cannot make any other conclusions regarding the epigenetic profiles of individual sperm cells at the level of obesity-induced H3K4me3 epimutations, phenotypes of offspring derived from our genetic model of epigenetic inheritance, as well as from our paternal folate deficiency model, suggest mosaicism of individual spermatozoa cells. Indeed, male germline-specific overexpression of KDM1A, and paternal preconception folate deficiency feeding, were both associated with sperm epigenetic changes at the level of H3K4me3, and a wide range of different developmental abnormalities, at varying degrees of severity [476,477,543].

In the clinic, individual sperm profiling could be used to predict pregnancy outcomes and offspring postnatal health, and eventually develop intervention strategies that are tailored to specific epigenetic signatures. If a list of specific epigenetic regions is identified and correlated with various outcomes such as different pregnancy complications or offspring phenotypes, single-sperm epigenetic profiling could be eventually used to measure the percentage of sperm that bear a specific epimutation, and thereby predict or estimate the risk for specific pregnancy or offspring health outcomes.

15.4.3.1 Single-cell epigenetic tracking of paternally-induced epimutations to the embryo

With the incentive of taking a step further into exploring paternal epigenetic inheritance mechanisms using single-cell technologies, future avenues of research would be to track down epigenomic and transcriptomic profiles during pre-implantation and post-implantation embryonic development. Such experiments would have multiple goals: first, to confirm that obesity-induced sperm epimutations are transmitted to the embryo and retained during early development, and second, to assess the potential lineage-specific retention of such epimutations and how they influence gene expression throughout development. Addressing these questions could help delineate the molecular routes underlying paternally-induced maladaptive fetal programming, track the developmental trajectory of epigenetic and transcriptomic deregulation as a result of paternal obesity, and determine which and how different tissues are affected downstream.

To address these questions, a similar paternal diet-induced obesity model as previously described could be generated using breeding partners where the sire and the dam have different genetic backgrounds, such as the C57BL/6 and CAST/EiJ mice. Following breeding, the collected embryos across pre-implantation stages would be subjected to single-cell CUT&Tag followed by sequencing, targeting histone H3K4me3 and RNA simultaneously in the same cell [959,960]. Because the genomes of the sire and dam differ at over 20 million single nucleotide polymorphisms (SNPs), bioinformatics tools can be used to separate sequencing reads in a parent-of-origin manner [992]. Single-cells from embryos can also be separated according to their lineage cell fate using specific expression markers, as well as according to their sex using expression levels of Y-chromosome-linked genes [993]. This experiment would allow to assess whether the sperm-transmitted epigenetic changes persist in embryos and whether they can be linked to transcriptional changes – as a result of paternal obesity – in an allele-, lineage- and sex-specific patterns. It is important to point out that, although this breeding scheme can provide valuable information, this approach involves an important caveat. Indeed, the mapping analyses being restricted to the genomic locations that contains SNPs limits the number of regions that can be assessed. In other words, if some or many of the sperm epimutations occur outside these SNP-containing genomic regions, these genes will not

be included in the analysis. Nevertheless, our initial analysis in the first manuscript (Chapter 2) showed that there are indeed some obesity-sensitive regions containing C57BL/6-CAST/EiJ SNPs, suggesting this approach would be suitable to confirm paternal-specific transmission of epimutations at least at these regions which would be sufficient to prove this concept.

Another avenue of research with such epigenetic and transcriptomic tracking over embryonic development would be to assess the extent by which epimutations persist or are diluted throughout cellular division and differentiation, and across developmental stages. Addressing this question would allow to determine which cellular lineages are being affected, thereby which tissues show altered programming, impaired functions, and at the origin of late-onset phenotypes. While the metabolic phenotypes observed in our paternal DIO model manifest in adulthood, and some defects have been detected at mid- and late-gestation in our models – such as altered hepatic and placental gene expression as well as placental abnormalities – these impairments likely arise early in development, but also persist across developmental stages, and act as a domino or butterfly effect, leading to altered organ system development [1,510,597]. By generating single-cell gene expression and chromatin profile maps throughout development, this would allow to connect the sperm-induced deregulation in specific cell lineages to organ phenotypes, and potentially delineate the cross-talk between different organs to influence fetal maladaptive metabolic programming. Indeed, as alluded in Chapter 3 of this thesis, placental misexpressed genes were enriched for various organ system development, which would support the idea that the placenta can impact the development of other tissues. Consequently, the observed paternally-induced phenotypes may in part arise from placenta action on organs such as the brain and the heart [766]. As discussed in the first chapter, the brain is an important site of regulation for satiety and hunger signals [16]. Target tissues (along with their precursors) to assess would be those whose development is influenced by the placenta, such as the heart and brain, as well as metabolic tissues such as the liver, pancreatic islets, adipose depots, and skeletal muscles.

Lastly, it would be interesting to further explore the connections between obesity-induced oxidative stress and altered epigenetic profiles. Male mice fed a HFD exhibit increased oxidative DNA damage lesions in sperm as measured by 8-hydroxyguanosine

(8OHdG), and these lesions have been shown to persist in the paternal pronucleus [847]. However, the method that was used could only provide global measures of oxidative DNA damage. Additionally, it is unknown when these lesions occur during spermatogenesis, whether these lesions persist further in development, and how they may impact embryonic gene expression. To address these knowledge gaps, it would be interesting to adapt the Click-Code-Seq method to single-cell resolution with simultaneous transcriptomic profiling, and apply this approach to germ cells throughout spermatogenesis as well as to the stages across pre-implantation embryo development. As a reminder, this method was described in a previous subsection, which profiles 8-oxoguanine (8-oxoG) genome-wide at single-nucleotide resolution. This would allow to (1) track obesity-induced oxidative damage throughout spermatogenesis, determine when these legions occur, whether some stages are more prone for oxidative damage and whether these lesions accumulate throughout spermatogenesis, (2) determine whether the obesity-induced 8-oxoG lesions in sperm are transmitted to the embryo, and (3) whether these lesions persist across developmental stages and impact gene expression.

Overall, these experiments would allow to show that (1) obesity-sensitive and oxidative DNA lesions are transmitted to the embryo, (2) these sperm-borne epimutations can directly impact embryonic gene expression, and lineage specification, (3) paternally-induced gene expression changes can result in a cascade of impairments that involves changes in developmental trajectories, metabolism, and inter-tissues cross-talk, and finally (4) the paternal-obesity-associated developmental changes are associated with adult-onset increased susceptibility to obesity and metabolic syndrome.

Concluding remarks and summary

The main goal of the present thesis was to further our understanding on the paternal contribution to metabolic health of future generations and on the molecular mechanisms underlying the non-genetic transmission of paternally-induced phenotypes. Using rodent models, we assessed whether paternal exposure to multiple factors can cumulatively impact the sperm epigenome and increase the risk to obesity and associated comorbidities in the subsequent generations. We also assessed the potential of obesity-induced sperm epimutations to impact embryonic gene expression and placental functions.

The findings presented provide evidence that sperm-borne histone methylation can act as a metabolic sensor of obesity, with increasing aberrant sperm epigenetic profiles upon multiple exposures, namely the diet-induced obesity and the germline-specific KDM1A overexpression. These cumulative effects were associated with more severe phenotypes in offspring with metabolic disturbances transmitted transgenerationally. These cumulatively damaging factors add further significance and concern for the increasing rise in obesity rates worldwide. They are reflective of the many interacting factors that can contribute to obesity development and highlight the previously underappreciated role of paternal exposures. The presented data also suggest obesity-sensitive epigenetic regions in sperm, at the level of histone methylation, can potentially alter embryonic and trophoblast gene expression and thereby impact the developmental trajectory of the offspring. These findings hint towards a potential role of placental functions in the developmental programming of paternally-induced maladaptive responses in the next generation.

In light of the limitations and knowledge gaps highlighted in the general discussion of this thesis, more studies are warranted to determine the exact paternal contribution to offspring metabolic health. Furthermore, a better understanding on the molecular mechanisms that involve the crosstalk between obesity-induced altered metabolism and epigenetic changes could reveal molecular targets and pathways for the development of preventative strategies to reduce the risk of transmission across generations. In the long term, identifying the molecular determinants of obesity-sensitive epigenetic regions in

sperm has the potential to predict pregnancy outcomes and offspring metabolic health, as well as to determine whether these effects are reversible.

As an example, the field of paternal epigenetic inheritance would benefit from significant advances in methodological approaches which take advantage of novel single-cell technologies to assess the mosaicism of sperm epimutations. Leveraging single-cell methods would also allow the tracking of sperm-transmitted epimutations in embryos and resulting transcriptomic changes across developmental stages and cell lineages. These studies would shed light on the early origins of paternally-induced pregnancy complications, placenta defects, and potentially adult-onset complex diseases.

Overall, these thesis chapters and knowledge gaps highlight the benefit to study the paternal contribution to pregnancy outcomes, placental integrity, with implications for maternal health as well as future generations health. These important future studies will help better define the determinants of health and develop strategies to improve paternal preconception health advising.

References

1. Pepin A-S, Lafleur C, Lambrot R, Dumeaux V, Kimmins S. Sperm histone H3 lysine 4 tri-methylation serves as a metabolic sensor of paternal obesity and is associated with the inheritance of metabolic dysfunction. *Mol Metab*. 2022;59:101463. doi:https://doi.org/10.1016/j.molmet.2022.101463
2. Abarca-Gómez L, Abdeen ZA, Hamid ZA, et al. Worldwide trends in body-mass index, underweight, overweight, and obesity from 1975 to 2016: a pooled analysis of 2416 population-based measurement studies in 128·9 million children, adolescents, and adults. *Lancet*. 2017;390(10113):2627-2642. doi:10.1016/S0140-6736(17)32129-3
3. The GBD 2015 Obesity Collaborators. Health Effects of Overweight and Obesity in 195 Countries over 25 Years. *N Engl J Med*. 2017;377(1):13-27. doi:10.1056/nejmoa1614362
4. Bodirsky BL, Dietrich JP, Martinelli E, et al. The ongoing nutrition transition thwarts long-term targets for food security, public health and environmental protection. *Sci Rep*. 2020;10(1):19778. doi:10.1038/s41598-020-75213-3
5. The GBD 2015 Obesity Collaborators. Health Effects of Overweight and Obesity in 195 Countries over 25 Years. *N Engl J Med*. 2017;377(1):13-27. doi:10.1056/NEJMoa1614362
6. Must A, Spadano J, Coakley EH, Field AE, Colditz G, Dietz WH. The Disease Burden Associated With Overweight and Obesity. *JAMA*. 1999;282(16):1523-1529. doi:10.1001/jama.282.16.1523
7. Koroukian SM, Dong W, Berger NA. Changes in Age Distribution of Obesity-Associated Cancers. *JAMA Netw Open*. 2019;2(8):e199261-e199261. doi:10.1001/jamanetworkopen.2019.9261
8. Bray GA. Medical Consequences of Obesity. *J Clin Endocrinol Metab*. 2004;89(6):2583-2589. doi:10.1210/jc.2004-0535
9. Fontaine KR, Barofsky I. Obesity and health-related quality of life. *Obes Rev an Off J Int Assoc Study Obes*. 2001;2(3):173-182. doi:10.1046/j.1467-789x.2001.00032.x
10. Barron E, Bakhai C, Kar P, et al. Associations of type 1 and type 2 diabetes with COVID-19-related mortality in England: a whole-population study. *Lancet Diabetes Endocrinol*. 2020;8(10):813-822. doi:https://doi.org/10.1016/S2213-8587(20)30272-2
11. Korakas E, Ikonomidis I, Kousathana F, et al. Obesity and COVID-19: immune and metabolic derangement as a possible link to adverse clinical outcomes. *Am J Physiol Metab*. 2020;319(1):E105-E109. doi:10.1152/ajpendo.00198.2020
12. Dobner J, Kaser S. Body mass index and the risk of infection - from underweight to obesity. *Clin Microbiol Infect*. 2018;24(1):24-28. doi:https://doi.org/10.1016/j.cmi.2017.02.013
13. Dai H, Alsalhe TA, Chalghaf N, Riccò M, Bragazzi NL, Wu J. The global burden of disease attributable to high body mass index in 195 countries and territories, 1990–2017: An analysis of the Global Burden of Disease Study. *PLOS Med*. 2020;17(7):e1003198. https://doi.org/10.1371/journal.pmed.1003198.
14. WHO. Global Health Estimates: Life expectancy and leading causes of death and

disability. https://www.who.int/data/gho/data/themes/mortality-and-global-health-estimates/global-health-estimates-leading-causes-of-dalys. Published 2020.
15. Bhattacharya J, Bundorf MK. The incidence of the healthcare costs of obesity. *J Health Econ*. 2009;28(3):649-658. doi:https://doi.org/10.1016/j.jhealeco.2009.02.009
16. Lustig RH, Collier D, Kassotis C, et al. Obesity I: Overview and molecular and biochemical mechanisms. *Biochem Pharmacol*. 2022;199:115012. doi:https://doi.org/10.1016/j.bcp.2022.115012
17. Rossi MA, Stuber GD. Overlapping Brain Circuits for Homeostatic and Hedonic Feeding. *Cell Metab*. 2018;27(1):42-56. doi:10.1016/j.cmet.2017.09.021
18. Lutter M, Nestler EJ. Homeostatic and hedonic signals interact in the regulation of food intake. *J Nutr*. 2009;139(3):629-632. doi:10.3945/jn.108.097618
19. Morton GJ, Meek TH, Schwartz MW. Neurobiology of food intake in health and disease. *Nat Rev Neurosci*. 2014;15(6):367-378. doi:10.1038/nrn3745
20. Kessler RM, Hutson PH, Herman BK, Potenza MN. The neurobiological basis of binge-eating disorder. *Neurosci Biobehav Rev*. 2016;63:223-238. doi:10.1016/j.neubiorev.2016.01.013
21. Baik J-H. Dopamine signaling in reward-related behaviors. *Front Neural Circuits*. 2013;7:152. doi:10.3389/fncir.2013.00152
22. Baik J-H. Dopaminergic Control of the Feeding Circuit. *Endocrinol Metab (Seoul, Korea)*. 2021;36(2):229-239. doi:10.3803/EnM.2021.979
23. Wiss DA, Criscitelli K, Gold M, Avena N. Preclinical evidence for the addiction potential of highly palatable foods: Current developments related to maternal influence. *Appetite*. 2017;115:19-27. doi:10.1016/j.appet.2016.12.019
24. Valassi E, Scacchi M, Cavagnini F. Neuroendocrine control of food intake. *Nutr Metab Cardiovasc Dis*. 2008;18(2):158-168. doi:https://doi.org/10.1016/j.numecd.2007.06.004
25. Sohn J-W. Network of hypothalamic neurons that control appetite. *BMB Rep*. 2015;48(4):229-233. doi:10.5483/bmbrep.2015.48.4.272
26. Matafome P, Seiça R. The Role of Brain in Energy Balance. *Adv Neurobiol*. 2017;19:33-48. doi:10.1007/978-3-319-63260-5_2
27. Heisler LK, Lam DD. An appetite for life: brain regulation of hunger and satiety. *Curr Opin Pharmacol*. 2017;37:100-106. doi:10.1016/j.coph.2017.09.002
28. Koliaki C, Liatis S, Dalamaga M, Kokkinos A. The Implication of Gut Hormones in the Regulation of Energy Homeostasis and Their Role in the Pathophysiology of Obesity. *Curr Obes Rep*. 2020;9(3):255-271. doi:10.1007/s13679-020-00396-9
29. Nelson LR, Bulun SE. Estrogen production and action. *J Am Acad Dermatol*. 2001;45(3 Suppl):S116-24. doi:10.1067/mjd.2001.117432
30. Kleinridders A, Ferris HA, Cai W, Kahn CR. Insulin action in brain regulates systemic metabolism and brain function. *Diabetes*. 2014;63(7):2232-2243. doi:10.2337/db14-0568
31. Stincic TL, Rønnekleiv OK, Kelly MJ. Diverse actions of estradiol on anorexigenic and orexigenic hypothalamic arcuate neurons. *Horm Behav*. 2018;104:146-155. doi:10.1016/j.yhbeh.2018.04.001
32. Zanchi D, Depoorter A, Egloff L, et al. The impact of gut hormones on the neural circuit of appetite and satiety: A systematic review. *Neurosci Biobehav Rev*.

2017;80:457-475. doi:10.1016/j.neubiorev.2017.06.013
33. Makris MC, Alexandrou A, Papatsoutsos EG, et al. Ghrelin and Obesity: Identifying Gaps and Dispelling Myths. A Reappraisal. *In Vivo*. 2017;31(6):1047-1050. doi:10.21873/invivo.11168
34. Muñoz C, Garcia-Vargas G, Pérez Morales R. Monogenic, Polygenic and Multifactorial Obesity in Children: Genetic and Environmental Factors. *Austin J Nutr Metab*. 2017;4:1052.
35. Loos RJF, Yeo GSH. The genetics of obesity: from discovery to biology. *Nat Rev Genet*. 2022;23(2):120-133. doi:10.1038/s41576-021-00414-z
36. INGALLS AM, DICKIE MM, SNELL GD. Obese, a new mutation in the house mouse. *J Hered*. 1950;41(12):317-318. doi:10.1093/oxfordjournals.jhered.a106073
37. P. HK, M. DM, L. CD. Diabetes, a New Mutation in the Mouse. *Science (80-)*. 1966;153(3740):1127-1128. doi:10.1126/science.153.3740.1127
38. Chen H, Charlat O, Tartaglia LA, et al. Evidence that the diabetes gene encodes the leptin receptor: identification of a mutation in the leptin receptor gene in db/db mice. *Cell*. 1996;84(3):491-495. doi:10.1016/s0092-8674(00)81294-5
39. Zhang Y, Proenca R, Maffei M, Barone M, Leopold L, Friedman JM. Positional cloning of the mouse obese gene and its human homologue. *Nature*. 1994;372(6505):425-432. doi:10.1038/372425a0
40. Bultman SJ, Michaud EJ, Woychik RP. Molecular characterization of the mouse agouti locus. *Cell*. 1992;71(7):1195-1204. doi:10.1016/s0092-8674(05)80067-4
41. Miller MW, Duhl DM, Vrieling H, et al. Cloning of the mouse agouti gene predicts a secreted protein ubiquitously expressed in mice carrying the lethal yellow mutation. *Genes Dev*. 1993;7(3):454-467. doi:10.1101/gad.7.3.454
42. Lu D, Willard D, Patel IR, et al. Agouti protein is an antagonist of the melanocyte-stimulating-hormone receptor. *Nature*. 1994;371(6500):799-802. doi:10.1038/371799a0
43. Fan W, Boston BA, Kesterson RA, Hruby VJ, Cone RD. Role of melanocortinergic neurons in feeding and the agouti obesity syndrome. *Nature*. 1997;385(6612):165-168. doi:10.1038/385165a0
44. Clément K, Vaisse C, Lahlou N, et al. A mutation in the human leptin receptor gene causes obesity and pituitary dysfunction. *Nature*. 1998;392(6674):398-401. doi:10.1038/32911
45. Jackson RS, Creemers JW, Ohagi S, et al. Obesity and impaired prohormone processing associated with mutations in the human prohormone convertase 1 gene. *Nat Genet*. 1997;16(3):303-306. doi:10.1038/ng0797-303
46. Huszar D, Lynch CA, Fairchild-Huntress V, et al. Targeted disruption of the melanocortin-4 receptor results in obesity in mice. *Cell*. 1997;88(1):131-141. doi:10.1016/s0092-8674(00)81865-6
47. Yeo GS, Farooqi IS, Aminian S, Halsall DJ, Stanhope RG, O'Rahilly S. A frameshift mutation in MC4R associated with dominantly inherited human obesity. *Nat Genet*. 1998;20(2):111-112. doi:10.1038/2404
48. Krude H, Biebermann H, Luck W, Horn R, Brabant G, Grüters A. Severe early-onset obesity, adrenal insufficiency and red hair pigmentation caused by POMC mutations in humans. *Nat Genet*. 1998;19(2):155-157. doi:10.1038/509

49. Yaswen L, Diehl N, Brennan MB, Hochgeschwender U. Obesity in the mouse model of pro-opiomelanocortin deficiency responds to peripheral melanocortin. *Nat Med*. 1999;5(9):1066-1070. doi:10.1038/12506
50. Challis BG, Coll AP, Yeo GSH, et al. Mice lacking pro-opiomelanocortin are sensitive to high-fat feeding but respond normally to the acute anorectic effects of peptide-YY(3-36). *Proc Natl Acad Sci U S A*. 2004;101(13):4695-4700. doi:10.1073/pnas.0306931101
51. van der Klaauw AA, Croizier S, Mendes de Oliveira E, et al. Human Semaphorin 3 Variants Link Melanocortin Circuit Development and Energy Balance. *Cell*. 2019;176(4):729-742.e18. doi:10.1016/j.cell.2018.12.009
52. Kurokawa N, Young EH, Oka Y, et al. The ADRB3 Trp64Arg variant and BMI: a meta-analysis of 44 833 individuals. *Int J Obes (Lond)*. 2008;32(8):1240-1249. doi:10.1038/ijo.2008.90
53. Shugart YY, Chen L, Day INM, et al. Two British women studies replicated the association between the Val66Met polymorphism in the brain-derived neurotrophic factor (BDNF) and BMI. *Eur J Hum Genet*. 2009;17(8):1050-1055. doi:10.1038/ejhg.2008.272
54. Benzinou M, Chèvre J-C, Ward KJ, et al. Endocannabinoid receptor 1 gene variations increase risk for obesity and modulate body mass index in European populations. *Hum Mol Genet*. 2008;17(13):1916-1921. doi:10.1093/hmg/ddn089
55. Wang D, Ma J, Zhang S, et al. Association of the MC4R V103I polymorphism with obesity: a Chinese case-control study and meta-analysis in 55,195 individuals. *Obesity (Silver Spring)*. 2010;18(3):573-579. doi:10.1038/oby.2009.268
56. Nead KT, Li A, Wehner MR, et al. Contribution of common non-synonymous variants in PCSK1 to body mass index variation and risk of obesity: a systematic review and meta-analysis with evidence from up to 331 175 individuals. *Hum Mol Genet*. 2015;24(12):3582-3594. doi:10.1093/hmg/ddv097
57. Tönjes A, Scholz M, Loeffler M, Stumvoll M. Association of Pro12Ala polymorphism in peroxisome proliferator-activated receptor gamma with Pre-diabetic phenotypes: meta-analysis of 57 studies on nondiabetic individuals. *Diabetes Care*. 2006;29(11):2489-2497. doi:10.2337/dc06-0513
58. Rankinen T, Zuberi A, Chagnon YC, et al. The human obesity gene map: the 2005 update. *Obesity (Silver Spring)*. 2006;14(4):529-644. doi:10.1038/oby.2006.71
59. Buniello A, MacArthur JAL, Cerezo M, et al. The NHGRI-EBI GWAS Catalog of published genome-wide association studies, targeted arrays and summary statistics 2019. *Nucleic Acids Res*. 2019;47(D1):D1005-D1012. doi:10.1093/nar/gky1120
60. Kilpeläinen TO, Zillikens MC, Stančákova A, et al. Genetic variation near IRS1 associates with reduced adiposity and an impaired metabolic profile. *Nat Genet*. 2011;43(8):753-760. doi:10.1038/ng.866
61. Lu Y, Day FR, Gustafsson S, et al. New loci for body fat percentage reveal link between adiposity and cardiometabolic disease risk. *Nat Commun*. 2016;7:10495. doi:10.1038/ncomms10495
62. Zillikens MC, Demissie S, Hsu Y-H, et al. Large meta-analysis of genome-wide association studies identifies five loci for lean body mass. *Nat Commun*.

2017;8(1):80. doi:10.1038/s41467-017-00031-7
63. Chu AY, Deng X, Fisher VA, et al. Multiethnic genome-wide meta-analysis of ectopic fat depots identifies loci associated with adipocyte development and differentiation. *Nat Genet*. 2017;49(1):125-130. doi:10.1038/ng.3738
64. Kilpeläinen TO, Carli JFM, Skowronski AA, et al. Genome-wide meta-analysis uncovers novel loci influencing circulating leptin levels. *Nat Commun*. 2016;7:10494. doi:10.1038/ncomms10494
65. Sun Q, Cornelis MC, Kraft P, et al. Genome-wide association study identifies polymorphisms in LEPR as determinants of plasma soluble leptin receptor levels. *Hum Mol Genet*. 2010;19(9):1846-1855. doi:10.1093/hmg/ddq056
66. Grarup N, Sandholt CH, Hansen T, Pedersen O. Genetic susceptibility to type 2 diabetes and obesity: From genome-wide association studies to rare variants and beyond. *Diabetologia*. 2014;57(8):1528-1541. doi:10.1007/s00125-014-3270-4
67. Winkler TW, Justice AE, Graff M, et al. The Influence of Age and Sex on Genetic Associations with Adult Body Size and Shape: A Large-Scale Genome-Wide Interaction Study. *PLoS Genet*. 2015;11(10):e1005378. doi:10.1371/journal.pgen.1005378
68. Graff M, Scott RA, Justice AE, et al. Genome-wide physical activity interactions in adiposity - A meta-analysis of 200,452 adults. *PLoS Genet*. 2017;13(4):e1006528. doi:10.1371/journal.pgen.1006528
69. Smith CE, Follis JL, Dashti HS, et al. Genome-Wide Interactions with Dairy Intake for Body Mass Index in Adults of European Descent. *Mol Nutr Food Res*. 2018;62(3). doi:10.1002/mnfr.201700347
70. Justice AE, Winkler TW, Feitosa MF, et al. Genome-wide meta-analysis of 241,258 adults accounting for smoking behaviour identifies novel loci for obesity traits. *Nat Commun*. 2017;8:14977. doi:10.1038/ncomms14977
71. Akiyama M, Okada Y, Kanai M, et al. Genome-wide association study identifies 112 new loci for body mass index in the Japanese population. *Nat Genet*. 2017;49(10):1458-1467. doi:10.1038/ng.3951
72. Ng MCY, Graff M, Lu Y, et al. Discovery and fine-mapping of adiposity loci using high density imputation of genome-wide association studies in individuals of African ancestry: African Ancestry Anthropometry Genetics Consortium. *PLoS Genet*. 2017;13(4):e1006719. doi:10.1371/journal.pgen.1006719
73. Gurdasani D, Carstensen T, Fatumo S, et al. Uganda Genome Resource Enables Insights into Population History and Genomic Discovery in Africa. *Cell*. 2019;179(4):984-1002.e36. doi:10.1016/j.cell.2019.10.004
74. Wojcik GL, Graff M, Nishimura KK, et al. Genetic analyses of diverse populations improves discovery for complex traits. *Nature*. 2019;570(7762):514-518. doi:10.1038/s41586-019-1310-4
75. Sergey N, Sergey K, Arang R, et al. The complete sequence of a human genome. *Science (80-)*. 2022;376(6588):44-53. doi:10.1126/science.abj6987
76. Voight BF, Scott LJ, Steinthorsdottir V, et al. Twelve type 2 diabetes susceptibility loci identified through large-scale association analysis. *Nat Genet*. 2010;42(7):579-589. doi:10.1038/ng.609
77. Maes HH, Neale MC, Eaves LJ. Genetic and environmental factors in relative body weight and human adiposity. *Behav Genet*. 1997;27(4):325-351.

doi:10.1023/a:1025635913927
78. Elks CE, den Hoed M, Zhao JH, et al. Variability in the heritability of body mass index: a systematic review and meta-regression. *Front Endocrinol (Lausanne)*. 2012;3:29. doi:10.3389/fendo.2012.00029
79. Willemsen G, Ward KJ, Bell CG, et al. The Concordance and Heritability of Type 2 Diabetes in 34,166 Twin Pairs From International Twin Registers: The Discordant Twin (DISCOTWIN) Consortium. *Twin Res Hum Genet*. 2015;18(6):762-771. doi:DOI: 10.1017/thg.2015.83
80. Lange SJ, Kompaniyets L, Freedman DS, et al. Longitudinal Trends in Body Mass Index Before and During the COVID-19 Pandemic Among Persons Aged 2 – 19 Years — United States , 2018 – 2020. *MMWR Morb Mortal Wkly Rep*. 2021;70(37):2018-2020.
81. Jenssen BP, Kelly MK, Powell M, Bouchelle Z, Mayne SL, Fiks AG. COVID-19 and Changes in Child Obesity. *Pediatrics*. 2021;147(5):e2021050123. doi:10.1542/peds.2021-050123
82. Swinburn BA, Sacks G, Hall KD, et al. The global obesity pandemic: shaped by global drivers and local environments. *Lancet (London, England)*. 2011;378(9793):804-814. doi:10.1016/S0140-6736(11)60813-1
83. Popkin BM, Adair LS, Ng SW. Global nutrition transition and the pandemic of obesity in developing countries. *Nutr Rev*. 2012;70(1):3-21. doi:10.1111/j.1753-4887.2011.00456.x
84. Igel U, Romppel M, Baar J, Brähler E, Grande G. Association between parental socio-economic status and childhood weight status and the role of urbanicity. *Public Health*. 2016;139:209-211. doi:https://doi.org/10.1016/j.puhe.2016.06.013
85. Hruby A, Hu FB. The Epidemiology of Obesity: A Big Picture. *Pharmacoeconomics*. 2015;33(7):673-689. doi:10.1007/s40273-014-0243-x
86. Malik VS, Willet WC, Hu FB. Nearly a decade on — trends, risk factors and policy implications in global obesity. *Nat Rev Endocrinol*. 2020;16(11):615-616. doi:10.1038/s41574-020-00411-y
87. Kearney J. Food consumption trends and drivers. *Philos Trans R Soc Lond B Biol Sci*. 2010;365(1554):2793-2807. doi:10.1098/rstb.2010.0149
88. Bixby H, Bentham J, Zhou B, et al. Rising rural body-mass index is the main driver of the global obesity epidemic in adults. *Nature*. 2019;569(7755):260-264. doi:10.1038/s41586-019-1171-x
89. Popkin BM. Urbanization, Lifestyle Changes and the Nutrition Transition. *World Dev*. 1999;27(11):1905-1916. doi:https://doi.org/10.1016/S0305-750X(99)00094-7
90. Pirgon Ö, Aslan N. The Role of Urbanization in Childhood Obesity. *J Clin Res Pediatr Endocrinol*. 2015;7(3):163-167. doi:10.4274/jcrpe.1984
91. Li VL, He Y, Contrepois K, et al. An exercise-inducible metabolite that suppresses feeding and obesity. *Nature*. 2022;606(7915):785-790. doi:10.1038/s41586-022-04828-5
92. Park YK, Yetley EA. Intakes and food sources of fructose in the United States. *Am J Clin Nutr*. 1993;58(5 Suppl):737S-747S. doi:10.1093/ajcn/58.5.737S
93. Popkin BM, Nielsen SJ. The sweetening of the world's diet. *Obes Res*. 2003;11(11):1325-1332. doi:10.1038/oby.2003.179
94. Marriott BP, Cole N, Lee E. National estimates of dietary fructose intake

increased from 1977 to 2004 in the United States. *J Nutr*. 2009;139(6):1228S-1235S. doi:10.3945/jn.108.098277
95. Gross LS, Li L, Ford ES, Liu S. Increased consumption of refined carbohydrates and the epidemic of type 2 diabetes in the United States: an ecologic assessment. *Am J Clin Nutr*. 2004;79(5):774-779. doi:10.1093/ajcn/79.5.774
96. Cutler DM, Glaeser EL, Shapiro JM. Why Have Americans Become More Obese? *J Econ Perspect*. 2003;17(3):93-118. doi:10.1257/089533003769204371
97. Löffler A, Luck T, Then FS, et al. Effects of psychological eating behaviour domains on the association between socio-economic status and BMI. *Public Health Nutr*. 2017;20(15):2706-2712. doi:10.1017/S1368980017001653
98. Blüher M. Obesity: global epidemiology and pathogenesis. *Nat Rev Endocrinol*. 2019;15(5):288-298. doi:10.1038/s41574-019-0176-8
99. Chan RSM, Woo J. Prevention of overweight and obesity: how effective is the current public health approach. *Int J Environ Res Public Health*. 2010;7(3):765-783. doi:10.3390/ijerph7030765
100. Aller EEJG, Abete I, Astrup A, Martinez JA, van Baak MA. Starches, sugars and obesity. *Nutrients*. 2011;3(3):341-369. doi:10.3390/nu3030341
101. Sacks FM, Bray GA, Carey VJ, et al. Comparison of weight-loss diets with different compositions of fat, protein, and carbohydrates. *N Engl J Med*. 2009;360(9):859-873. doi:10.1056/NEJMoa0804748
102. Abete I, Astrup A, Martínez JA, Thorsdottir I, Zulet MA. Obesity and the metabolic syndrome: role of different dietary macronutrient distribution patterns and specific nutritional components on weight loss and maintenance. *Nutr Rev*. 2010;68(4):214-231. doi:10.1111/j.1753-4887.2010.00280.x
103. Monro JA, Shaw M. Glycemic impact, glycemic glucose equivalents, glycemic index, and glycemic load: definitions, distinctions, and implications. *Am J Clin Nutr*. 2008;87(1):237S-243S. doi:10.1093/ajcn/87.1.237S
104. Mock K, Lateef S, Benedito VA, Tou JC. High-fructose corn syrup-55 consumption alters hepatic lipid metabolism and promotes triglyceride accumulation. *J Nutr Biochem*. 2017;39:32-39. doi:https://doi.org/10.1016/j.jnutbio.2016.09.010
105. Bellisle F, Drewnowski A, Anderson GH, Westerterp-Plantenga M, Martin CK. Sweetness, Satiation, and Satiety. *J Nutr*. 2012;142(6):1149S-1154S. doi:10.3945/jn.111.149583
106. Green SM, Wales JK, Lawton CL, Blundell JE. Comparison of high-fat and high-carbohydrate foods in a meal or snack on short-term fat and energy intakes in obese women. *Br J Nutr*. 2000;84(4):521-530.
107. Clifton P. High protein diets and weight control. *Nutr Metab Cardiovasc Dis*. 2009;19(6):379-382. doi:10.1016/j.numecd.2009.02.011
108. Havel PJ. Dietary fructose: implications for dysregulation of energy homeostasis and lipid/carbohydrate metabolism. *Nutr Rev*. 2005;63(5):133-157. doi:10.1301/nr.2005.may.133-157
109. Basciano H, Federico L, Adeli K. Fructose, insulin resistance, and metabolic dyslipidemia. *Nutr Metab (Lond)*. 2005;2(1):5. doi:10.1186/1743-7075-2-5
110. Koo H-Y, Wallig MA, Chung BH, Nara TY, Cho BHS, Nakamura MT. Dietary fructose induces a wide range of genes with distinct shift in carbohydrate and lipid

metabolism in fed and fasted rat liver. *Biochim Biophys Acta*. 2008;1782(5):341-348. doi:10.1016/j.bbadis.2008.02.007
111. Mayes PA. Intermediary metabolism of fructose. *Am J Clin Nutr*. 1993;58(5 Suppl):754S-765S. doi:10.1093/ajcn/58.5.754S
112. Anderson JW, Baird P, Davis Jr RH, et al. Health benefits of dietary fiber. *Nutr Rev*. 2009;67(4):188-205. doi:10.1111/j.1753-4887.2009.00189.x
113. Heindel JJ, Blumberg B. Environmental Obesogens: Mechanisms and Controversies. *Annu Rev Pharmacol Toxicol*. 2019;59(1):89-106. doi:10.1146/annurev-pharmtox-010818-021304
114. Heindel JJ, Howard S, Agay-Shay K, et al. Obesity II: Establishing causal links between chemical exposures and obesity. *Biochem Pharmacol*. 2022;199:115015. doi:https://doi.org/10.1016/j.bcp.2022.115015
115. La Merrill MA, Vandenberg LN, Smith MT, et al. Consensus on the key characteristics of endocrine-disrupting chemicals as a basis for hazard identification. *Nat Rev Endocrinol*. 2020;16(1):45-57. doi:10.1038/s41574-019-0273-8
116. Grün F, Blumberg B. Environmental obesogens: organotins and endocrine disruption via nuclear receptor signaling. *Endocrinology*. 2006;147(6 Suppl):S50-5. doi:10.1210/en.2005-1129
117. Heindel JJ, Blumberg B, Cave M, et al. Metabolism disrupting chemicals and metabolic disorders. *Reprod Toxicol*. 2017;68:3-33. doi:10.1016/j.reprotox.2016.10.001
118. Janesick A, Blumberg B. Endocrine disrupting chemicals and the developmental programming of adipogenesis and obesity. *Birth Defects Res C Embryo Today*. 2011;93(1):34-50. doi:10.1002/bdrc.20197
119. Janesick AS, Blumberg B. Obesogens: an emerging threat to public health. *Am J Obstet Gynecol*. 2016;214(5):559-565. doi:10.1016/j.ajog.2016.01.182
120. Durack J, Lynch S V. The gut microbiome: Relationships with disease and opportunities for therapy. *J Exp Med*. 2018;216(1):20-40. doi:10.1084/jem.20180448
121. Martino C, Dilmore AH, Burcham ZM, Metcalf JL, Jeste D, Knight R. Microbiota succession throughout life from the cradle to the grave. *Nat Rev Microbiol*. 2022. doi:10.1038/s41579-022-00768-z
122. Turnbaugh PJ, Ley RE, Mahowald MA, Magrini V, Mardis ER, Gordon JI. An obesity-associated gut microbiome with increased capacity for energy harvest. *Nature*. 2006;444(7122):1027-1031. doi:10.1038/nature05414
123. Ridaura VK, Faith JJ, Rey FE, et al. Gut microbiota from twins discordant for obesity modulate metabolism in mice. *Science*. 2013;341(6150):1241214. doi:10.1126/science.1241214
124. Bäckhed F, Ding H, Wang T, et al. The gut microbiota as an environmental factor that regulates fat storage. *Proc Natl Acad Sci U S A*. 2004;101(44):15718-15723. doi:10.1073/pnas.0407076101
125. Wan Y, Wang F, Yuan J, et al. Effects of dietary fat on gut microbiota and faecal metabolites, and their relationship with cardiometabolic risk factors: a 6-month randomised controlled-feeding trial. *Gut*. 2019;68(8):1417 LP - 1429. doi:10.1136/gutjnl-2018-317609

126. Gohir W, Kennedy KM, Wallace JG, et al. High-fat diet intake modulates maternal intestinal adaptations to pregnancy and results in placental hypoxia, as well as altered fetal gut barrier proteins and immune markers. *J Physiol*. 2019;597(12):3029-3051. doi:10.1113/JP277353
127. Taylor SR, Ramsamooj S, Liang RJ, et al. Dietary fructose improves intestinal cell survival and nutrient absorption. *Nature*. 2021;597(7875):263-267. doi:10.1038/s41586-021-03827-2
128. Wang X, Zhu L, Li X, Wang X, Hao R, Li J. Effects of high fructose corn syrup on intestinal microbiota structure and obesity in mice. *npj Sci Food*. 2022;6(1):17. doi:10.1038/s41538-022-00133-7
129. Li J-M, Yu R, Zhang L-P, et al. Dietary fructose-induced gut dysbiosis promotes mouse hippocampal neuroinflammation: a benefit of short-chain fatty acids. *Microbiome*. 2019;7(1):98. doi:10.1186/s40168-019-0713-7
130. Qin J, Li Y, Cai Z, et al. A metagenome-wide association study of gut microbiota in type 2 diabetes. *Nature*. 2012;490(7418):55-60. doi:10.1038/nature11450
131. Karlsson FH, Tremaroli V, Nookaew I, et al. Gut metagenome in European women with normal, impaired and diabetic glucose control. *Nature*. 2013;498(7452):99-103. doi:10.1038/nature12198
132. Larsen N, Vogensen FK, van den Berg FWJ, et al. Gut Microbiota in Human Adults with Type 2 Diabetes Differs from Non-Diabetic Adults. *PLoS One*. 2010;5(2):e9085. https://doi.org/10.1371/journal.pone.0009085.
133. Scheithauer TPM, Rampanelli E, Nieuwdorp M, et al. Gut Microbiota as a Trigger for Metabolic Inflammation in Obesity and Type 2 Diabetes. *Front Immunol*. 2020;11. https://www.frontiersin.org/article/10.3389/fimmu.2020.571731.
134. Cani PD, Van Hul M. Gut microbiota and obesity: causally linked? *Expert Rev Gastroenterol Hepatol*. 2020;14(6):401-403. doi:10.1080/17474124.2020.1758064
135. Jacob CM, Hanson M. Implications of the Developmental Origins of Health and Disease concept for policy-making. *Curr Opin Endocr Metab Res*. 2020;13:20-27. doi:https://doi.org/10.1016/j.coemr.2020.08.001
136. Hoffman DJ, Reynolds RM, Hardy DB. Developmental origins of health and disease: current knowledge and potential mechanisms. *Nutr Rev*. 2017;75(12):951-970. doi:10.1093/nutrit/nux053
137. Barker DJP, Osmond C. INFANT MORTALITY, CHILDHOOD NUTRITION, AND ISCHAEMIC HEART DISEASE IN ENGLAND AND WALES. *Lancet*. 1986;327(8489):1077-1081. doi:10.1016/S0140-6736(86)91340-1
138. Hales CN, Barker DJ, Clark PM, et al. Fetal and infant growth and impaired glucose tolerance at age 64. *BMJ*. 1991;303(6809):1019-1022. doi:10.1136/bmj.303.6809.1019
139. Osmond C, Barker DJ, Winter PD, Fall CH, Simmonds SJ. Early growth and death from cardiovascular disease in women. *BMJ*. 1993;307(6918):1519-1524. doi:10.1136/bmj.307.6918.1519
140. Fall CH, Vijayakumar M, Barker DJ, Osmond C, Duggleby S. Weight in infancy and prevalence of coronary heart disease in adult life. *BMJ*. 1995;310(6971):17-19. doi:10.1136/bmj.310.6971.17
141. Yang Z, Zhao W, Zhang X, et al. Impact of famine during pregnancy and infancy on health in adulthood. *Obes Rev an Off J Int Assoc Study Obes*. 2008;9 Suppl

1:95-99. doi:10.1111/j.1467-789X.2007.00447.x
142. Musa MG, Kagura J, Pisa PT, Norris SA. Relationship between early growth and CVD risk factors in adolescents. *J Dev Orig Health Dis*. 2016;7(2):132-143. doi:10.1017/S2040174415007953
143. Perng W, Hajj H, Belfort MB, et al. Birth Size, Early Life Weight Gain, and Midchildhood Cardiometabolic Health. *J Pediatr*. 2016;173:122-130.e1. doi:10.1016/j.jpeds.2016.02.053
144. Kannisto V, Christensen K, Vaupel JW. No increased mortality in later life for cohorts born during famine. *Am J Epidemiol*. 1997;145(11):987-994. doi:10.1093/oxfordjournals.aje.a009067
145. Victora CG, Barros FC, Lima RC, et al. The Pelotas birth cohort study, Rio Grande do Sul, Brazil, 1982-2001. *Cad Saude Publica*. 2003;19(5):1241-1256. doi:10.1590/s0102-311x2003000500003
146. Ravelli AC, van der Meulen JH, Michels RP, et al. Glucose tolerance in adults after prenatal exposure to famine. *Lancet (London, England)*. 1998;351(9097):173-177. doi:10.1016/s0140-6736(97)07244-9
147. Stein AD, Zybert PA, van der Pal-de Bruin K, Lumey LH. Exposure to famine during gestation, size at birth, and blood pressure at age 59 y: evidence from the Dutch Famine. *Eur J Epidemiol*. 2006;21(10):759-765. doi:10.1007/s10654-006-9065-2
148. Wang J, Li Y, Han X, et al. Exposure to the Chinese Famine in Childhood Increases Type 2 Diabetes Risk in Adults. *J Nutr*. 2016;146(11):2289-2295. doi:10.3945/jn.116.234575
149. Huang C, Li Z, Wang M, Martorell R. Early life exposure to the 1959-1961 Chinese famine has long-term health consequences. *J Nutr*. 2010;140(10):1874-1878. doi:10.3945/jn.110.121293
150. Finer S, Iqbal MS, Lowe R, et al. Is famine exposure during developmental life in rural Bangladesh associated with a metabolic and epigenetic signature in young adulthood? A historical cohort study. *BMJ Open*. 2016;6(11):e011768. doi:10.1136/bmjopen-2016-011768
151. Hanson HA, Smith KR. Early origins of longevity: prenatal exposures to food shortage among early Utah pioneers. *J Dev Orig Health Dis*. 2013;4(2):170-181. doi:10.1017/S2040174412000682
152. St Clair D, Xu M, Wang P, et al. Rates of adult schizophrenia following prenatal exposure to the Chinese famine of 1959-1961. *JAMA*. 2005;294(5):557-562. doi:10.1001/jama.294.5.557
153. Crookston BT, Dearden KA, Alder SC, et al. Impact of early and concurrent stunting on cognition. *Matern Child Nutr*. 2011;7(4):397-409. doi:10.1111/j.1740-8709.2010.00255.x
154. Walker SP, Chang SM, Powell CA, Grantham-McGregor SM. Effects of early childhood psychosocial stimulation and nutritional supplementation on cognition and education in growth-stunted Jamaican children: prospective cohort study. *Lancet (London, England)*. 2005;366(9499):1804-1807. doi:10.1016/S0140-6736(05)67574-5
155. Hoek HW, Brown AS, Susser E. The Dutch famine and schizophrenia spectrum disorders. *Soc Psychiatry Psychiatr Epidemiol*. 1998;33(8):373-379.

doi:10.1007/s001270050068
156. Crookston BT, Penny ME, Alder SC, et al. Children who recover from early stunting and children who are not stunted demonstrate similar levels of cognition. *J Nutr*. 2010;140(11):1996-2001. doi:10.3945/jn.109.118927
157. Crookston BT, Schott W, Cueto S, et al. Postinfancy growth, schooling, and cognitive achievement: Young Lives. *Am J Clin Nutr*. 2013;98(6):1555-1563. doi:10.3945/ajcn.113.067561
158. Walker SP, Chang SM, Wright A, Osmond C, Grantham-McGregor SM. Early childhood stunting is associated with lower developmental levels in the subsequent generation of children. *J Nutr*. 2015;145(4):823-828. doi:10.3945/jn.114.200261
159. Sokolovic N, Selvam S, Srinivasan K, Thankachan P, Kurpad A V, Thomas T. Catch-up growth does not associate with cognitive development in Indian school-age children. *Eur J Clin Nutr*. 2014;68(1):14-18. doi:10.1038/ejcn.2013.208
160. Mendez MA, Adair LS. Severity and timing of stunting in the first two years of life affect performance on cognitive tests in late childhood. *J Nutr*. 1999;129(8):1555-1562. doi:10.1093/jn/129.8.1555
161. Ravelli GP, Stein ZA, Susser MW. Obesity in young men after famine exposure in utero and early infancy. *N Engl J Med*. 1976;295(7):349-353. doi:10.1056/NEJM197608122950701
162. Stein AD, Lumey LH. The relationship between maternal and offspring birth weights after maternal prenatal famine exposure: the Dutch Famine Birth Cohort Study. *Hum Biol*. 2000;72(4):641-654.
163. Benyshek DC, Martin JF, Johnston CS. A reconsideration of the origins of the type 2 diabetes epidemic among Native Americans and the implications for intervention policy. *Med Anthropol*. 2001;20(1):25-64. doi:10.1080/01459740.2001.9966186
164. Eriksson J, Forsén T, Tuomilehto J, Osmond C, Barker D. Size at birth, childhood growth and obesity in adult life. *Int J Obes Relat Metab Disord J Int Assoc Study Obes*. 2001;25(5):735-740. doi:10.1038/sj.ijo.0801602
165. Newby PK, Dickman PW, Adami H-O, Wolk A. Early anthropometric measures and reproductive factors as predictors of body mass index and obesity among older women. *Int J Obes (Lond)*. 2005;29(9):1084-1092. doi:10.1038/sj.ijo.0802996
166. Eriksson JG, Forsen TJ, Osmond C, Barker DJP. Pathways of infant and childhood growth that lead to type 2 diabetes. *Diabetes Care*. 2003;26(11):3006-3010. doi:10.2337/diacare.26.11.3006
167. Eriksson JG, Osmond C, Kajantie E, Forsén TJ, Barker DJP. Patterns of growth among children who later develop type 2 diabetes or its risk factors. *Diabetologia*. 2006;49(12):2853-2858. doi:10.1007/s00125-006-0459-1
168. Huxley R, Owen CG, Whincup PH, Cook DG, Colman S, Collins R. Birth weight and subsequent cholesterol levels: exploration of the “fetal origins” hypothesis. *JAMA*. 2004;292(22):2755-2764. doi:10.1001/jama.292.22.2755
169. Huxley R, Neil A, Collins R. Unravelling the fetal origins hypothesis: is there really an inverse association between birthweight and subsequent blood pressure? *Lancet (London, England)*. 2002;360(9334):659-665. doi:10.1016/S0140-

6736(02)09834-3
170. Gluckman PD, Hanson MA. Living with the past: evolution, development, and patterns of disease. *Science*. 2004;305(5691):1733-1736. doi:10.1126/science.1095292
171. Newsome CA, Shiell AW, Fall CHD, Phillips DIW, Shier R, Law CM. Is birth weight related to later glucose and insulin metabolism?--A systematic review. *Diabet Med*. 2003;20(5):339-348. doi:10.1046/j.1464-5491.2003.00871.x
172. Inadera H. Developmental origins of obesity and type 2 diabetes: molecular aspects and role of chemicals. *Environ Health Prev Med*. 2013;18(3):185-197. doi:10.1007/s12199-013-0328-8
173. Barker DJ. The fetal and infant origins of adult disease. *BMJ*. 1990;301(6761):1111. doi:10.1136/bmj.301.6761.1111
174. Barker DJP. The origins of the developmental origins theory. *J Intern Med*. 2007;261(5):412-417. doi:https://doi.org/10.1111/j.1365-2796.2007.01809.x
175. Godfrey KM, Barker DJ. Fetal programming and adult health. *Public Health Nutr*. 2001;4(2B):611-624. doi:10.1079/phn2001145
176. Hales CN, Barker DJ. Type 2 (non-insulin-dependent) diabetes mellitus: the thrifty phenotype hypothesis. *Diabetologia*. 1992;35(7):595-601. doi:10.1007/BF00400248
177. Snoeck A, Remacle C, Reusens B, Hoet JJ. Effect of a low protein diet during pregnancy on the fetal rat endocrine pancreas. *Biol Neonate*. 1990;57(2):107-118. doi:10.1159/000243170
178. Alexander BT. Fetal programming of hypertension. *Am J Physiol Regul Integr Comp Physiol*. 2006;290(1):R1-R10. doi:10.1152/ajpregu.00417.2005
179. McMillen IC, Robinson JS. Developmental origins of the metabolic syndrome: prediction, plasticity, and programming. *Physiol Rev*. 2005;85(2):571-633. doi:10.1152/physrev.00053.2003
180. Langley-Evans SC. Critical differences between two low protein diet protocols in the programming of hypertension in the rat. *Int J Food Sci Nutr*. 2000;51(1):11-17. doi:10.1080/096374800100859
181. Maloney CA, Gosby AK, Phuyal JL, Denyer GS, Bryson JM, Caterson ID. Site-specific changes in the expression of fat-partitioning genes in weanling rats exposed to a low-protein diet in utero. *Obes Res*. 2003;11(3):461-468. doi:10.1038/oby.2003.63
182. Langley-Evans SC, Phillips GJ, Jackson AA. In utero exposure to maternal low protein diets induces hypertension in weanling rats, independently of maternal blood pressure changes. *Clin Nutr*. 1994;13(5):319-324. doi:10.1016/0261-5614(94)90056-6
183. Shiell AW, Campbell-Brown M, Haselden S, Robinson S, Godfrey KM, Barker DJ. High-meat, low-carbohydrate diet in pregnancy: relation to adult blood pressure in the offspring. *Hypertens (Dallas, Tex 1979)*. 2001;38(6):1282-1288. doi:10.1161/hy1101.095332
184. Garg M, Thamotharan M, Dai Y, et al. Early postnatal caloric restriction protects adult male intrauterine growth-restricted offspring from obesity. *Diabetes*. 2012;61(6):1391-1398. doi:10.2337/db11-1347
185. Dai Y, Thamotharan S, Garg M, Shin B-C, Devaskar SU. Superimposition of

postnatal calorie restriction protects the aging male intrauterine growth- restricted offspring from metabolic maladaptations. *Endocrinology*. 2012;153(9):4216-4226. doi:10.1210/en.2012-1206
186. Vickers MH, Breier BH, Cutfield WS, Hofman PL, Gluckman PD. Fetal origins of hyperphagia, obesity, and hypertension and postnatal amplification by hypercaloric nutrition. *Am J Physiol Endocrinol Metab*. 2000;279(1):E83-7. doi:10.1152/ajpendo.2000.279.1.E83
187. Levitt NS, Lindsay RS, Holmes MC, Seckl JR. Dexamethasone in the last week of pregnancy attenuates hippocampal glucocorticoid receptor gene expression and elevates blood pressure in the adult offspring in the rat. *Neuroendocrinology*. 1996;64(6):412-418. doi:10.1159/000127146
188. Benediktsson R, Lindsay RS, Noble J, Seckl JR, Edwards CR. Glucocorticoid exposure in utero: new model for adult hypertension. *Lancet (London, England)*. 1993;341(8841):339-341. doi:10.1016/0140-6736(93)90138-7
189. Nyirenda MJ, Lindsay RS, Kenyon CJ, Burchell A, Seckl JR. Glucocorticoid exposure in late gestation permanently programs rat hepatic phosphoenolpyruvate carboxykinase and glucocorticoid receptor expression and causes glucose intolerance in adult offspring. *J Clin Invest*. 1998;101(10):2174-2181. doi:10.1172/JCI1567
190. Barker DJ, Osmond C, Simmonds SJ, Wield GA. The relation of small head circumference and thinness at birth to death from cardiovascular disease in adult life. *BMJ*. 1993;306(6875):422-426. doi:10.1136/bmj.306.6875.422
191. Phillips DIW. Programming of the stress response: a fundamental mechanism underlying the long-term effects of the fetal environment? *J Intern Med*. 2007;261(5):453-460. doi:10.1111/j.1365-2796.2007.01801.x
192. Buhl ES, Neschen S, Yonemitsu S, et al. Increased hypothalamic-pituitary-adrenal axis activity and hepatic insulin resistance in low-birth-weight rats. *Am J Physiol Endocrinol Metab*. 2007;293(5):E1451-8. doi:10.1152/ajpendo.00356.2007
193. Gluckman PD, Hanson MA, Beedle AS. Early life events and their consequences for later disease: a life history and evolutionary perspective. *Am J Hum Biol Off J Hum Biol Counc*. 2007;19(1):1-19. doi:10.1002/ajhb.20590
194. Drong AW, Lindgren CM, McCarthy MI. The genetic and epigenetic basis of type 2 diabetes and obesity. *Clin Pharmacol Ther*. 2012;92(6):707-715. doi:10.1038/clpt.2012.149
195. Burdge GC, Lillycrop KA. Nutrition, epigenetics, and developmental plasticity: implications for understanding human disease. *Annu Rev Nutr*. 2010;30:315-339. doi:10.1146/annurev.nutr.012809.104751
196. Gluckman PD, Hanson MA, Cooper C, Thornburg KL. Effect of in utero and early-life conditions on adult health and disease. *N Engl J Med*. 2008;359(1):61-73. doi:10.1056/NEJMra0708473
197. Burdge GC, Slater-Jefferies J, Torrens C, Phillips ES, Hanson MA, Lillycrop KA. Dietary protein restriction of pregnant rats in the F0 generation induces altered methylation of hepatic gene promoters in the adult male offspring in the F1 and F2 generations. *Br J Nutr*. 2007;97(3):435-439. doi:10.1017/S0007114507352392
198. Drake AJ, Walker BR, Seckl JR. Intergenerational consequences of fetal

programming by in utero exposure to glucocorticoids in rats. *Am J Physiol Regul Integr Comp Physiol*. 2005;288(1):R34-8. doi:10.1152/ajpregu.00106.2004
199. Su Z, Denu JM. Reading the Combinatorial Histone Language. *ACS Chem Biol*. 2016;11(3):564-574. doi:10.1021/acschembio.5b00864
200. Hyun K, Jeon J, Park K, Kim J. Writing, erasing and reading histone lysine methylations. *Exp Mol Med*. 2017;49(4):e324-22. doi:10.1038/emm.2017.11
201. Moore LD, Le T, Fan G. DNA Methylation and Its Basic Function. *Neuropsychopharmacology*. 2013;38(1):23-38. doi:10.1038/npp.2012.112
202. Palazzo AF, Lee ES. Non-coding RNA: what is functional and what is junk? *Front Genet*. 2015;6. doi:10.3389/fgene.2015.00002
203. Soubry A. Epigenetics as a Driver of Developmental Origins of Health and Disease: Did We Forget the Fathers? *BioEssays*. 2018;40(1):1700113. doi:https://doi.org/10.1002/bies.201700113
204. Pembrey ME, Bygren LO, Kaati G, et al. Sex-specific, male-line transgenerational responses in humans. *Eur J Hum Genet*. 2006;14(2):159-166. doi:10.1038/sj.ejhg.5201538
205. Northstone K, Golding J, Davey Smith G, Miller LL, Pembrey M. Prepubertal start of father's smoking and increased body fat in his sons: further characterisation of paternal transgenerational responses. *Eur J Hum Genet*. 2014;22(12):1382-1386. doi:10.1038/ejhg.2014.31
206. Kobayashi H, Hiura H, John RM, et al. DNA methylation errors at imprinted loci after assisted conception originate in the parental sperm. *Eur J Hum Genet*. 2009;17(12):1582-1591. doi:10.1038/ejhg.2009.68
207. Hultman CM, Sandin S, Levine SZ, Lichtenstein P, Reichenberg A. Advancing paternal age and risk of autism: new evidence from a population-based study and a meta-analysis of epidemiological studies. *Mol Psychiatry*. 2011;16(12):1203-1212. doi:10.1038/mp.2010.121
208. Soubry A, Murphy SK, Wang F, et al. Newborns of obese parents have altered DNA methylation patterns at imprinted genes. *Int J Obes (Lond)*. 2015;39(4):650-657. doi:10.1038/ijo.2013.193
209. Soubry A, Schildkraut JM, Murtha A, et al. Paternal obesity is associated with IGF2 hypomethylation in newborns: results from a Newborn Epigenetics Study (NEST) cohort. *BMC Med*. 2013;11:29. doi:10.1186/1741-7015-11-29
210. Yehuda R, Daskalakis NP, Bierer LM, et al. Holocaust Exposure Induced Intergenerational Effects on FKBP5 Methylation. *Biol Psychiatry*. 2016;80(5):372-380. doi:10.1016/j.biopsych.2015.08.005
211. Wu H, Ashcraft L, Whitcomb BW, et al. Parental contributions to early embryo development: influences of urinary phthalate and phthalate alternatives among couples undergoing IVF treatment. *Hum Reprod*. 2017;32(1):65-75. doi:10.1093/humrep/dew301
212. Svanes C, Koplin J, Skulstad SM, et al. Father's environment before conception and asthma risk in his children: a multi-generation analysis of the Respiratory Health In Northern Europe study. *Int J Epidemiol*. 2017;46(1):235-245. doi:10.1093/ije/dyw151
213. Feinberg JI, Bakulski KM, Jaffe AE, et al. Paternal sperm DNA methylation associated with early signs of autism risk in an autism-enriched cohort. *Int J*

Epidemiol. 2015;44(4):1199-1210. doi:10.1093/ije/dyv028
214. Horsthemke B. A critical view on transgenerational epigenetic inheritance in humans. *Nat Commun*. 2018;9(1):1-4. doi:10.1038/s41467-018-05445-5
215. Houfflyn S, Matthys C, Soubry A. Male Obesity: Epigenetic Origin and Effects in Sperm and Offspring. *Curr Mol Biol reports*. 2017;3(4):288-296. doi:10.1007/s40610-017-0083-5
216. Ghanayem BI, Bai R, Kissling GE, Travlos G, Hoffler U. Diet-induced obesity in male mice is associated with reduced fertility and potentiation of acrylamide-induced reproductive toxicity. *Biol Reprod*. 2010;82(1):96-104. doi:10.1095/biolreprod.109.078915
217. Mohajer N, Joloya EM, Seo J, Shioda T, Blumberg B. Epigenetic Transgenerational Inheritance of the Effects of Obesogen Exposure. *Front Endocrinol (Lausanne)*. 2021;12. https://www.frontiersin.org/article/10.3389/fendo.2021.787580.
218. Hur SSJ, Cropley JE, Suter CM. Paternal epigenetic programming: Evolving metabolic disease risk. *J Mol Endocrinol*. 2017;58(3):R159-R168. doi:10.1530/JME-16-0236
219. Hammoud SS, Nix DA, Zhang H, Purwar J, Douglas T, Cairns BR. Distinctive Chromatin in Human Sperm Packages Genes for Embryo Development. 2009;460(7254):473-478.
220. Brykczynska U, Hisano M, Erkek S, et al. Repressive and active histone methylation mark distinct promoters in human and mouse spermatozoa. *Nat Struct Mol Biol*. 2010;17(6):679-687. doi:10.1038/nsmb.1821
221. Lambrot R, Chan D, Shao X, et al. Whole-genome sequencing of H3K4me3 and DNA methylation in human sperm reveals regions of overlap linked to fertility and development. *Cell Rep*. 2021;36(3):109418. doi:https://doi.org/10.1016/j.celrep.2021.109418
222. Teperek M, Simeone A, Gaggioli V, et al. Sperm is epigenetically programmed to regulate gene transcription in embryos. *Genome Res*. 2016;26(8):1034-1046. doi:10.1101/gr.201541.115
223. Erkek S, Hisano M, Liang CY, et al. Molecular determinants of nucleosome retention at CpG-rich sequences in mouse spermatozoa. *Nat Struct Mol Biol*. 2013;20(7):868-875. doi:10.1038/nsmb.2599
224. Chan JCN, Cheung JCK, Stehouwer CDA, et al. The central roles of obesity-associated dyslipidaemia, endothelial activation and cytokines in the Metabolic Syndrome—an analysis by structural equation modelling. *Int J Obes*. 2002;26(7):994-1008. doi:10.1038/sj.ijo.0802017
225. Stefan N. Causes, consequences, and treatment of metabolically unhealthy fat distribution. *Lancet Diabetes Endocrinol*. 2020;8(7):616-627. doi:https://doi.org/10.1016/S2213-8587(20)30110-8
226. Andolfi C, Fisichella PM. Epidemiology of Obesity and Associated Comorbidities. *J Laparoendosc Adv Surg Tech A*. 2018;28(8):919-924. doi:10.1089/lap.2018.0380
227. Huang PL. A comprehensive definition for metabolic syndrome. *Dis Model Mech*. 2009;2(5-6):231-237. doi:10.1242/dmm.001180
228. Landsberg L, Aronne LJ, Beilin LJ, et al. Obesity-Related Hypertension:

Pathogenesis, Cardiovascular Risk, and Treatment. *J Clin Hypertens*. 2013;15(1):14-33. doi:https://doi.org/10.1111/jch.12049
229. Mathieu P, Lemieux I, Després J-P. Obesity, Inflammation, and Cardiovascular Risk. *Clin Pharmacol \& Ther*. 2010;87(4):407-416. doi:https://doi.org/10.1038/clpt.2009.311
230. Smith U, Kahn BB. Adipose tissue regulates insulin sensitivity: role of adipogenesis, de novo lipogenesis and novel lipids. *J Intern Med*. 2016;280(5):465-475. doi:https://doi.org/10.1111/joim.12540
231. Arner P. Fat Tissue Growth and Development in Humans. In: *Nestlé Nutrition Institute Workshop Series*. Vol 89. ; 2018:37-45. doi:10.1159/000486491
232. Lynes MD, Tseng Y-H. Deciphering adipose tissue heterogeneity. *Ann N Y Acad Sci*. 2018;1411(1):5-20. doi:https://doi.org/10.1111/nyas.13398
233. Ussar S, Lee KY, Dankel SN, et al. ASC-1, PAT2, and P2RX5 are cell surface markers for white, beige, and brown adipocytes. *Sci Transl Med*. 2014;6(247):247ra103-247ra103. doi:10.1126/scitranslmed.3008490
234. Sidossis L, Kajimura S. Brown and beige fat in humans: thermogenic adipocytes that control energy and glucose homeostasis. *J Clin Invest*. 2015;125(2):478-486. doi:10.1172/JCI78362
235. Cypess AM, Chen Y-C, Sze C, et al. Cold but not sympathomimetics activates human brown adipose tissue in vivo. *Proc Natl Acad Sci U S A*. 2012;109(25):10001-10005. doi:10.1073/pnas.1207911109
236. Vishvanath L, Gupta RK. Contribution of adipogenesis to healthy adipose tissue expansion in obesity. *J Clin Invest*. 2019;129(10):4022-4031. doi:10.1172/JCI129191
237. Heinonen S, Jokinen R, Rissanen A, Pietiläinen KH. White adipose tissue mitochondrial metabolism in health and in obesity. *Obes Rev*. 2020;21(2):e12958. doi:https://doi.org/10.1111/obr.12958
238. Carpentier AC, Blondin DP, Virtanen KA, Richard D, Haman F, Turcotte ÉE. Brown Adipose Tissue Energy Metabolism in Humans. *Front Endocrinol (Lausanne)*. 2018;9. doi:10.3389/fendo.2018.00447
239. Cinti S. Pink Adipocytes. *Trends Endocrinol Metab*. 2018;29(9):651-666. doi:https://doi.org/10.1016/j.tem.2018.05.007
240. Bjørndal B, Burri L, Staalesen V, Skorve J, Berge RK. Different adipose depots: Their role in the development of metabolic syndrome and mitochondrial response to hypolipidemic agents. *J Obes*. 2011;2011. doi:10.1155/2011/490650
241. Ibrahim MM. Subcutaneous and visceral adipose tissue: structural and functional differences. *Obes Rev*. 2010;11(1):11-18. doi:https://doi.org/10.1111/j.1467-789X.2009.00623.x
242. Haarbo J, Marslew U, Gotfredsen A, Christiansen C. Postmenopausal hormone replacement therapy prevents central distribution of body fat after menopause. *Metab - Clin Exp*. 1991;40(12):1323-1326. doi:10.1016/0026-0495(91)90037-W
243. Gambacciani M, Ciaponi M, Cappagli B, et al. Body Weight, Body Fat Distribution, and Hormonal Replacement Therapy in Early Postmenopausal Women. *J Clin Endocrinol Metab*. 1997;82(2):414-417. doi:10.1210/jcem.82.2.3735
244. Grove KL, Fried SK, Greenberg AS, Xiao XQ, Clegg DJ. A microarray analysis of sexual dimorphism of adipose tissues in high-fat-diet-induced obese mice. *Int J*

Obes. 2010;34(6):989-1000. doi:10.1038/ijo.2010.12
245. Chusyd DE, Wang D, Huffman DM, Nagy TR. Relationships between Rodent White Adipose Fat Pads and Human White Adipose Fat Depots. *Front Nutr*. 2016;3:10. doi:10.3389/fnut.2016.00010
246. Bastien M, Poirier P, Brassard P, et al. Effect of PPARγ agonist on aerobic exercise capacity in relation to body fat distribution in men with type 2 diabetes mellitus and coronary artery disease: a 1-yr randomized study. *Am J Physiol Metab*. 2019;317(1):E65-E73. doi:10.1152/ajpendo.00505.2018
247. Samocha-Bonet D, Dixit VD, Kahn CR, et al. Metabolically healthy and unhealthy obese – the 2013 Stock Conference report. *Obes Rev*. 2014;15(9):697-708. doi:https://doi.org/10.1111/obr.12199
248. Porter SA, Massaro JM, Hoffmann U, Vasan RS, O'Donnel CJ, Fox CS. Abdominal Subcutaneous Adipose Tissue: A Protective Fat Depot? *Diabetes Care*. 2009;32(6):1068-1075. doi:10.2337/dc08-2280
249. Mohammed BS, Cohen S, Reeds D, Young VL, Klein S. Long-term Effects of Large-volume Liposuction on Metabolic Risk Factors for Coronary Heart Disease. *Obesity*. 2008;16(12):2648-2651. doi:https://doi.org/10.1038/oby.2008.418
250. Torre YS-D la, Wadeea R, Rosas V, Herbst KL. Lipedema: friend and foe. *Horm Mol Biol Clin Investig*. 2018;33(1). doi:10.1515/hmbci-2017-0076
251. Hajer GR, van Haeften TW, Visseren FLJ. Adipose tissue dysfunction in obesity, diabetes, and vascular diseases. *Eur Heart J*. 2008;29(24):2959-2971. doi:10.1093/eurheartj/ehn387
252. Wajchenberg BL. Subcutaneous and visceral adipose tissue: their relation to the metabolic syndrome. *Endocr Rev*. 2000;21(6):697-738. doi:10.1210/edrv.21.6.0415
253. Chowdhury B, Sjöström L, Alpsten M, Kostanty J, Kvist H, Löfgren R. A multicompartment body composition technique based on computerized tomography. *Int J Obes Relat Metab Disord J Int Assoc Study Obes*. 1994;18(4):219-234.
254. Rytka JM, Wueest S, Schoenle EJ, Konrad D. The portal theory supported by venous drainage-selective fat transplantation. *Diabetes*. 2011;60(1):56-63. doi:10.2337/db10-0697
255. Item F, Konrad D. Visceral fat and metabolic inflammation: the portal theory revisited. *Obes Rev an Off J Int Assoc Study Obes*. 2012;13 Suppl 2:30-39. doi:10.1111/j.1467-789X.2012.01035.x
256. Chiu JD, Ader M, Hucking K, et al. Why Visceral Fat is Bad: Mechanisms of the Metabolic Syndrome. *Obesity*. 2008;14(2S):16S-19S. doi:10.1038/oby.2006.277
257. Kabir M, Catalano KJ, Ananthnarayan S, et al. Molecular evidence supporting the portal theory: a causative link between visceral adiposity and hepatic insulin resistance. *Am J Physiol Metab*. 2005;288(2):E454-E461. doi:10.1152/ajpendo.00203.2004
258. Hoffstedt J, Arner P, Hellers G, Lönnqvist F. Variation in adrenergic regulation of lipolysis between omental and subcutaneous adipocytes from obese and non-obese men. *J Lipid Res*. 1997;38(4):795-804.
259. Gruzdeva O V, Borodkina AD, Akbasheva OE, et al. Influence of visceral obesity on the secretion of adipokines with epicardial adipocytes in patients with coronary

heart disease. *Ter Arkh*. 2018;90(10):71-78. doi:10.26442/terarkh2018901071-78
260. Britton KA, Fox CS. Ectopic Fat Depots and Cardiovascular Disease. *Circulation*. 2011;124(24):e837-e841. doi:10.1161/CIRCULATIONAHA.111.077602
261. Lee EH, Kim JY, Yang HR. Association between ectopic pancreatic and hepatic fat and metabolic risk factors in children with non-alcoholic fatty liver disease. *Pediatr Obes*. 2021;16(10):e12793. doi:https://doi.org/10.1111/ijpo.12793
262. Isserow JA, Siegelman ES, Mammone J. Focal fatty infiltration of the pancreas: MR characterization with chemical shift imaging. *AJR Am J Roentgenol*. 1999;173(5):1263-1265. doi:10.2214/ajr.173.5.10541101
263. Sase S, Monden M, Oka H, Dono K, Fukuta T, Shibata I. Hepatic blood flow measurements with arterial and portal blood flow mapping in the human liver by means of xenon CT. *J Comput Assist Tomogr*. 2002;26(2):243-249. doi:10.1097/00004728-200203000-00014
264. Birchmeier W. Orchestrating Wnt signalling for metabolic liver zonation. *Nat Cell Biol*. 2016;18(5):463-465. doi:10.1038/ncb3349
265. Halpern KB, Shenhav R, Matcovitch-Natan O, et al. Single-cell spatial reconstruction reveals global division of labour in the mammalian liver. *Nature*. 2017;542(7641):352-356. doi:10.1038/nature21065
266. Jungermann K, Sasse D. Heterogeneity of liver parenchymal cells. *Trends Biochem Sci*. 1978;3(3):198-202. doi:https://doi.org/10.1016/S0968-0004(78)91764-4
267. Jungermann K. Metabolic zonation of liver parenchyma: significance for the regulation of glycogen metabolism, gluconeogenesis, and glycolysis. *Diabetes Metab Rev*. 1987;3(1):269-293. doi:10.1002/dmr.5610030112
268. Jungermann K, Katz N. Functional specialization of different hepatocyte populations. *Physiol Rev*. 1989;69(3):708-764. doi:10.1152/physrev.1989.69.3.708
269. Jungermann K, Kietzmann T. Zonation of parenchymal and nonparenchymal metabolism in liver. *Annu Rev Nutr*. 1996;16:179-203. doi:10.1146/annurev.nu.16.070196.001143
270. Gebhardt R. Metabolic zonation of the liver: regulation and implications for liver function. *Pharmacol Ther*. 1992;53(3):275-354. doi:10.1016/0163-7258(92)90055-5
271. Katz NR. Metabolic heterogeneity of hepatocytes across the liver acinus. *J Nutr*. 1992;122(3 Suppl):843-849. doi:10.1093/jn/122.suppl_3.843
272. Traber PG, Chianale J, Gumucio JJ. Physiologic significance and regulation of hepatocellular heterogeneity. *Gastroenterology*. 1988;95(4):1130-1143. doi:10.1016/0016-5085(88)90194-1
273. Fabbrini E, Sullivan S, Klein S. Obesity and nonalcoholic fatty liver disease: biochemical, metabolic, and clinical implications. *Hepatology*. 2010;51(2):679-689. doi:10.1002/hep.23280
274. Tiniakos DG, Vos MB, Brunt EM. Nonalcoholic fatty liver disease: pathology and pathogenesis. *Annu Rev Pathol*. 2010;5:145-171. doi:10.1146/annurev-pathol-121808-102132
275. Williams CD, Stengel J, Asike MI, et al. Prevalence of nonalcoholic fatty liver disease and nonalcoholic steatohepatitis among a largely middle-aged population

utilizing ultrasound and liver biopsy: a prospective study. *Gastroenterology*. 2011;140(1):124-131. doi:10.1053/j.gastro.2010.09.038
276. Lazo M, Clark JM. The epidemiology of nonalcoholic fatty liver disease: a global perspective. *Semin Liver Dis*. 2008;28(4):339-350. doi:10.1055/s-0028-1091978
277. Younossi ZM. Review article: current management of non-alcoholic fatty liver disease and non-alcoholic steatohepatitis. *Aliment Pharmacol Ther*. 2008;28(1):2-12. doi:10.1111/j.1365-2036.2008.03710.x
278. Anstee QM, McPherson S, Day CP. How big a problem is non-alcoholic fatty liver disease? *BMJ*. 2011;343:d3897. doi:10.1136/bmj.d3897
279. Dharmalingam M, Yamasandhi PG. Nonalcoholic Fatty Liver Disease and Type 2 Diabetes Mellitus. *Indian J Endocrinol Metab*. 2018;22(3):421-428. doi:10.4103/ijem.IJEM_585_17
280. Rosen ED, Spiegelman BM. What we talk about when we talk about fat. *Cell*. 2014;156(1-2):20-44. doi:10.1016/j.cell.2013.12.012
281. Klöting N, Fasshauer M, Dietrich A, et al. Insulin-sensitive obesity. *Am J Physiol Endocrinol Metab*. 2010;299(3):E506-15. doi:10.1152/ajpendo.00586.2009
282. Chait A, den Hartigh LJ. Adipose Tissue Distribution, Inflammation and Its Metabolic Consequences, Including Diabetes and Cardiovascular Disease. *Front Cardiovasc Med*. 2020;7:22. doi:10.3389/fcvm.2020.00022
283. Virtue S, Vidal-Puig A. Adipose tissue expandability, lipotoxicity and the Metabolic Syndrome--an allostatic perspective. *Biochim Biophys Acta*. 2010;1801(3):338-349. doi:10.1016/j.bbalip.2009.12.006
284. Rahman MS, Hossain KS, Das S, et al. Role of Insulin in Health and Disease: An Update. *Int J Mol Sci*. 2021;22(12):6403. doi:10.3390/ijms22126403
285. Butler AE, Janson J, Bonner-Weir S, Ritzel R, Rizza RA, Butler PC. β-Cell Deficit and Increased β-Cell Apoptosis in Humans With Type 2 Diabetes. *Diabetes*. 2003;52(1):102-110. doi:10.2337/diabetes.52.1.102
286. Weir GC. Glucolipotoxicity, β-Cells, and Diabetes: The Emperor Has No Clothes. *Diabetes*. 2020;69(3):273-278. doi:10.2337/db19-0138
287. Marseglia L, Manti S, D'Angelo G, et al. Oxidative stress in obesity: a critical component in human diseases. *Int J Mol Sci*. 2014;16(1):378-400. doi:10.3390/ijms16010378
288. Amirkhizi F, Siassi F, Minaie S, Djalali M, Rahimi A, Chamari M. IS OBESITY ASSOCIATED WITH INCREASED PLASMA LIPID PEROXIDATION AND OXIDATIVE STRESS IN WOMEN. *ARYA Atheroscler*. 2007;2:189-192.
289. Khan NI, Naz L, Yasmeen G. Obesity: an independent risk factor for systemic oxidative stress. *Pak J Pharm Sci*. 2006;19(1):62-65.
290. Goossens GH. The role of adipose tissue dysfunction in the pathogenesis of obesity-related insulin resistance. *Physiol Behav*. 2008;94(2):206-218. doi:10.1016/j.physbeh.2007.10.010
291. Duvnjak M, Lerotić I, Barsić N, Tomasić V, Virović Jukić L, Velagić V. Pathogenesis and management issues for non-alcoholic fatty liver disease. *World J Gastroenterol*. 2007;13(34):4539-4550. doi:10.3748/wjg.v13.i34.4539
292. Tereshin E V. [A role of fatty acids in the development of oxidative stress in aging. A hypothesis]. *Adv Gerontol = Uspekhi Gerontol*. 2007;20(1):59-65.
293. Rzheshevsky A V. Fatal "triad": lipotoxicity, oxidative stress, and phenoptosis.

Biochemistry (Mosc). 2013;78(9):991-1000. doi:10.1134/S0006297913090046
294. Palmer NO, Bakos HW, Fullston T, Lane M. Impact of obesity on male fertility, sperm function and molecular composition. *Spermatogenesis*. 2012;2(4):253-263. doi:10.4161/spmg.21362
295. Nguyen RHN, Wilcox AJ, Skjærven R, Baird DD. Men ' s body mass index and infertility. *Hum Reprod*. 2007;22(9):2488-2493. doi:10.1093/humrep/dem139
296. Keltz J, Zapantis A, Jindal SK, Lieman HJ, Santoro N, Polotsky AJ. Overweight men: clinical pregnancy after ART is decreased in IVF but not in ICSI cycles. *J Assist Reprod Genet*. 2010;27(9-10):539-544. doi:10.1007/s10815-010-9439-y
297. Hinz S, Rais-Bahrami S, Kempkensteffen C, Weiske WH, Miller K MA. Effect of obesity on sex hormone levels, antisperm antibodies, and fertility after vasectomy reversal. *Urology*. 2010;76(4):851-866.
298. Bakos HW, Henshaw RC, Mitchell M, Lane M. Paternal body mass index is associated with decreased blastocyst development and reduced live birth rates following assisted reproductive technology. *Fertil Steril*. 2011;95(5):1700-1704. doi:10.1016/j.fertnstert.2010.11.044
299. Ramlau-Hansen CH, Thulstrup AM, Nohr EA, Bonde JP, Sørensen TIA, Olsen J. Subfecundity in overweight and obese couples. *Hum Reprod*. 2007;22(6):1634-1637. doi:10.1093/humrep/dem035
300. Palmer NO, Bakos HW, Owens JA, Setchell BP, Lane M. Diet and exercise in an obese mouse fed a high-fat diet improve metabolic health and reverse perturbed sperm function. *Am J Physiol Endocrinol Metab*. 2012;302(7):E768-80. doi:10.1152/ajpendo.00401.2011
301. Palmer NO, Fullston T, Mitchell M, Setchell BP, Lane M. SIRT6 in mouse spermatogenesis is modulated by diet-induced obesity. *Reprod Fertil Dev*. 2011;23(7):929-939. doi:10.1071/RD10326
302. Fernandez CDB, Bellentani FF, Fernandes GSA, et al. Diet-induced obesity in rats leads to a decrease in sperm motility. *Reprod Biol Endocrinol*. 2011;9:32. doi:10.1186/1477-7827-9-32
303. Bakos HW, Mitchell M, Setchell BP, Lane M. The effect of paternal diet-induced obesity on sperm function and fertilization in a mouse model. *Int J Androl*. 2011;34(5 Pt 1):402-410. doi:10.1111/j.1365-2605.2010.01092.x
304. Setchell BP, Breed WG. CHAPTER 17 - Anatomy, Vasculature, and Innervation of the Male Reproductive Tract. In: Neill JDBT-K and NP of R (Third E, ed. St Louis: Academic Press; 2006:771-825. doi:https://doi.org/10.1016/B978-012515400-0/50022-1
305. Larose H, Shami AN, Abbott H, Manske G, Lei L, Hammoud SS. Gametogenesis: A journey from inception to conception. *Curr Top Dev Biol*. 2019;132:257-310. doi:10.1016/bs.ctdb.2018.12.006
306. Ramaswamy S, Weinbauer GF. Endocrine control of spermatogenesis: Role of FSH and LH/ testosterone. *Spermatogenesis*. 2015;4(2):e996025-e996025. doi:10.1080/21565562.2014.996025
307. Heckert LL, Griswold MD. The expression of the follicle-stimulating hormone receptor in spermatogenesis. *Recent Prog Horm Res*. 2002;57:129-148. doi:10.1210/rp.57.1.129
308. Dierich A, Sairam MR, Monaco L, et al. Impairing follicle-stimulating hormone

(FSH) signaling in vivo: targeted disruption of the FSH receptor leads to aberrant gametogenesis and hormonal imbalance. *Proc Natl Acad Sci U S A*. 1998;95(23):13612-13617. doi:10.1073/pnas.95.23.13612
309. Haywood M, Spaliviero J, Jimemez M, King NJC, Handelsman DJ, Allan CM. Sertoli and germ cell development in hypogonadal (hpg) mice expressing transgenic follicle-stimulating hormone alone or in combination with testosterone. *Endocrinology*. 2003;144(2):509-517. doi:10.1210/en.2002-220710
310. O'Shaughnessy PJ, Monteiro A, Verhoeven G, De Gendt K, Abel MH. Effect of FSH on testicular morphology and spermatogenesis in gonadotrophin-deficient hypogonadal mice lacking androgen receptors. *Reproduction*. 2010;139(1):177-184. doi:10.1530/REP-09-0377
311. Meachem SJ, McLachlan RI, de Kretser DM, Robertson DM, Wreford NG. Neonatal exposure of rats to recombinant follicle stimulating hormone increases adult Sertoli and spermatogenic cell numbers. *Biol Reprod*. 1996;54(1):36-44. doi:10.1095/biolreprod54.1.36
312. Hess RA, Cooke PS, Bunick D, Kirby JD. Adult testicular enlargement induced by neonatal hypothyroidism is accompanied by increased Sertoli and germ cell numbers. *Endocrinology*. 1993;132(6):2607-2613. doi:10.1210/endo.132.6.8504761
313. Orth JM, Gunsalus GL, Lamperti AA. Evidence from Sertoli cell-depleted rats indicates that spermatid number in adults depends on numbers of Sertoli cells produced during perinatal development. *Endocrinology*. 1988;122(3):787-794. doi:10.1210/endo-122-3-787
314. Cortes D, Müller J, Skakkebaek NE. Proliferation of Sertoli cells during development of the human testis assessed by stereological methods. *Int J Androl*. 1987;10(4):589-596. doi:10.1111/j.1365-2605.1987.tb00358.x
315. Sharpe RM, McKinnell C, Kivlin C, Fisher JS. Proliferation and functional maturation of Sertoli cells, and their relevance to disorders of testis function in adulthood. *Reproduction*. 2003;125(6):769-784. doi:10.1530/rep.0.1250769
316. Smith BE, Braun RE. Germ cell migration across Sertoli cell tight junctions. *Science*. 2012;338(6108):798-802. doi:10.1126/science.1219969
317. Kopera IA, Bilinska B, Cheng CY, Mruk DD. Sertoli–germ cell junctions in the testis: a review of recent data. *Philos Trans R Soc B Biol Sci*. 2010;365(1546):1593-1605. doi:10.1098/rstb.2009.0251
318. Cheng CY, Mruk DD. The blood-testis barrier and its implications for male contraception. *Pharmacol Rev*. 2012;64(1):16-64. doi:10.1124/pr.110.002790
319. Pelletier R-M. The blood-testis barrier: the junctional permeability, the proteins and the lipids. *Prog Histochem Cytochem*. 2011;46(2):49-127. doi:https://doi.org/10.1016/j.proghi.2011.05.001
320. Chakraborty P, William Buaas F, Sharma M, et al. Androgen-dependent sertoli cell tight junction remodeling is mediated by multiple tight junction components. *Mol Endocrinol*. 2014;28(7):1055-1072. doi:10.1210/me.2013-1134
321. Kaur G, Thompson LA, Dufour JM. Sertoli cells--immunological sentinels of spermatogenesis. *Semin Cell Dev Biol*. 2014;30:36-44. doi:10.1016/j.semcdb.2014.02.011
322. Petersen C, Söder O. The Sertoli Cell – A Hormonal Target and 'Super' Nurse for

Germ Cells That Determines Testicular Size. *Horm Res Paediatr*. 2006;66(4):153-161. doi:10.1159/000094142
323. Byskov AG. Differentiation of mammalian embryonic gonad. *Physiol Rev*. 1986;66(1):71-117. doi:10.1152/physrev.1986.66.1.71
324. Siril Ariyaratne HB, Chamindrani Mendis-Handagama SML, Buchanan Hales D, Ian Mason J. Studies on the Onset of Leydig Precursor Cell Differentiation in the Prepubertal Rat Testis1. *Biol Reprod*. 2000;63(1):165-171. doi:10.1095/biolreprod63.1.165
325. Shima Y, Miyabayashi K, Haraguchi S, et al. Contribution of Leydig and Sertoli cells to testosterone production in mouse fetal testes. *Mol Endocrinol*. 2013;27(1):63-73. doi:10.1210/me.2012-1256
326. Haider SG. Cell biology of Leydig cells in the testis. *Int Rev Cytol*. 2004;233:181-241. doi:10.1016/S0074-7696(04)33005-6
327. Baker PJ, O'Shaughnessy PJ. Role of gonadotrophins in regulating numbers of Leydig and Sertoli cells during fetal and postnatal development in mice. *Reproduction*. 2001;122(2):227-234. doi:10.1530/rep.0.1220227
328. Walker WH. Testosterone signaling and the regulation of spermatogenesis. *Spermatogenesis*. 2011;1(2):116-120. doi:10.4161/spmg.1.2.16956
329. Potter SJ, DeFalco T. Role of the testis interstitial compartment in spermatogonial stem cell function. *Reproduction*. 2017;153(4):R151-R162. doi:10.1530/REP-16-0588
330. Maekawa M, Kamimura K, Nagano T. Peritubular myoid cells in the testis: their structure and function. *Arch Histol Cytol*. 1996;59(1):1-13. doi:10.1679/aohc.59.1
331. Welsh M, Moffat L, Belling K, et al. Androgen receptor signalling in peritubular myoid cells is essential for normal differentiation and function of adult Leydig cells. *Int J Androl*. 2012;35(1):25-40. doi:10.1111/j.1365-2605.2011.01150.x
332. Chen L-Y, Willis WD, Eddy EM. Targeting the Gdnf Gene in peritubular myoid cells disrupts undifferentiated spermatogonial cell development. *Proc Natl Acad Sci U S A*. 2016;113(7):1829-1834. doi:10.1073/pnas.1517994113
333. Ernst C, Odom DT, Kutter C. The emergence of piRNAs against transposon invasion to preserve mammalian genome integrity. *Nat Commun*. 2017;8(1):1411. doi:10.1038/s41467-017-01049-7
334. Saitou M, Barton SC, Surani MA. A molecular programme for the specification of germ cell fate in mice. *Nature*. 2002;418(6895):293-300. doi:10.1038/nature00927
335. Coucouvanis E, Martin GR. BMP signaling plays a role in visceral endoderm differentiation and cavitation in the early mouse embryo. *Development*. 1999;126(3):535-546. doi:10.1242/dev.126.3.535
336. Ying Y, Liu XM, Marble A, Lawson KA, Zhao GQ. Requirement of Bmp8b for the generation of primordial germ cells in the mouse. *Mol Endocrinol*. 2000;14(7):1053-1063. doi:10.1210/mend.14.7.0479
337. Ohinata Y, Ohta H, Shigeta M, Yamanaka K, Wakayama T, Saitou M. A signaling principle for the specification of the germ cell lineage in mice. *Cell*. 2009;137(3):571-584. doi:10.1016/j.cell.2009.03.014
338. McLaren A. Primordial germ cells in the mouse. *Dev Biol*. 2003;262(1):1-15. doi:10.1016/s0012-1606(03)00214-8
339. Loebel DAF, Watson CM, De Young RA, Tam PPL. Lineage choice and

differentiation in mouse embryos and embryonic stem cells. *Dev Biol*. 2003;264(1):1-14. doi:10.1016/s0012-1606(03)00390-7
340. Lawson KA, Dunn NR, Roelen BA, et al. Bmp4 is required for the generation of primordial germ cells in the mouse embryo. *Genes Dev*. 1999;13(4):424-436. doi:10.1101/gad.13.4.424
341. de Sousa Lopes SMC, Roelen BAJ, Monteiro RM, et al. BMP signaling mediated by ALK2 in the visceral endoderm is necessary for the generation of primordial germ cells in the mouse embryo. *Genes Dev*. 2004;18(15):1838-1849. doi:10.1101/gad.294004
342. Magnúsdóttir E, Dietmann S, Murakami K, et al. A tripartite transcription factor network regulates primordial germ cell specification in mice. *Nat Cell Biol*. 2013;15(8):905-915. doi:10.1038/ncb2798
343. Kurimoto K, Yamaji M, Seki Y, Saitou M. Specification of the germ cell lineage in mice: a process orchestrated by the PR-domain proteins, Blimp1 and Prdm14. *Cell Cycle*. 2008;7(22):3514-3518. doi:10.4161/cc.7.22.6979
344. Hayashi K, de Sousa Lopes SMC, Surani MA. Germ cell specification in mice. *Science*. 2007;316(5823):394-396. doi:10.1126/science.1137545
345. Saitou M, Yamaji M. Primordial germ cells in mice. *Cold Spring Harb Perspect Biol*. 2012;4(11). doi:10.1101/cshperspect.a008375
346. Richardson BE, Lehmann R. Mechanisms guiding primordial germ cell migration: strategies from different organisms. *Nat Rev Mol Cell Biol*. 2010;11(1):37-49. doi:10.1038/nrm2815
347. Yamaji M, Seki Y, Kurimoto K, et al. Critical function of Prdm14 for the establishment of the germ cell lineage in mice. *Nat Genet*. 2008;40(8):1016-1022. doi:10.1038/ng.186
348. Vincent SD, Dunn NR, Sciammas R, et al. The zinc finger transcriptional repressor Blimp1/Prdm1 is dispensable for early axis formation but is required for specification of primordial germ cells in the mouse. *Development*. 2005;132(6):1315-1325. doi:10.1242/dev.01711
349. Ancelin K, Lange UC, Hajkova P, et al. Blimp1 associates with Prmt5 and directs histone arginine methylation in mouse germ cells. *Nat Cell Biol*. 2006;8(6):623-630. doi:10.1038/ncb1413
350. Schöler HR, Hatzopoulos AK, Balling R, Suzuki N, Gruss P. A family of octamer-specific proteins present during mouse embryogenesis: evidence for germline-specific expression of an Oct factor. *EMBO J*. 1989;8(9):2543-2550. doi:10.1002/j.1460-2075.1989.tb08392.x
351. Schöler HR, Ruppert S, Suzuki N, Chowdhury K, Gruss P. New type of POU domain in germ line-specific protein Oct-4. *Nature*. 1990;344(6265):435-439. doi:10.1038/344435a0
352. Avilion AA, Nicolis SK, Pevny LH, Perez L, Vivian N, Lovell-Badge R. Multipotent cell lineages in early mouse development depend on SOX2 function. *Genes Dev*. 2003;17(1):126-140. doi:10.1101/gad.224503
353. Chambers I, Silva J, Colby D, et al. Nanog safeguards pluripotency and mediates germline development. *Nature*. 2007;450(7173):1230-1234. doi:10.1038/nature06403
354. Sato M, Kimura T, Kurokawa K, et al. Identification of PGC7, a new gene

expressed specifically in preimplantation embryos and germ cells. *Mech Dev*. 2002;113(1):91-94. doi:10.1016/s0925-4773(02)00002-3
355. Tam PP, Zhou SX. The allocation of epiblast cells to ectodermal and germ-line lineages is influenced by the position of the cells in the gastrulating mouse embryo. *Dev Biol*. 1996;178(1):124-132. doi:10.1006/dbio.1996.0203
356. CHIQUOINE AD. The identification, origin, and migration of the primordial germ cells in the mouse embryo. *Anat Rec*. 1954;118(2):135-146. doi:10.1002/ar.1091180202
357. Fox N, Damjanov I, Martinez-Hernandez A, Knowles BB, Solter D. Immunohistochemical localization of the early embryonic antigen (SSEA-1) in postimplantation mouse embryos and fetal and adult tissues. *Dev Biol*. 1981;83(2):391-398. doi:10.1016/0012-1606(81)90487-5
358. Ginsburg M, Snow MH, McLaren A. Primordial germ cells in the mouse embryo during gastrulation. *Development*. 1990;110(2):521-528. doi:10.1242/dev.110.2.521
359. Yamaguchi S, Kimura H, Tada M, Nakatsuji N, Tada T. Nanog expression in mouse germ cell development. *Gene Expr Patterns*. 2005;5(5):639-646. doi:10.1016/j.modgep.2005.03.001
360. Ohta H, Tohda A, Nishimune Y. Proliferation and differentiation of spermatogonial stem cells in the w/wv mutant mouse testis. *Biol Reprod*. 2003;69(6):1815-1821. doi:10.1095/biolreprod.103.019323
361. Runyan C, Schaible K, Molyneaux K, Wang Z, Levin L, Wylie C. Steel factor controls midline cell death of primordial germ cells and is essential for their normal proliferation and migration. *Development*. 2006;133(24):4861-4869. doi:10.1242/dev.02688
362. Gu Y, Runyan C, Shoemaker A, Surani A, Wylie C. Steel factor controls primordial germ cell survival and motility from the time of their specification in the allantois, and provides a continuous niche throughout their migration. *Development*. 2009;136(8):1295-1303. doi:10.1242/dev.030619
363. Raz E. Guidance of primordial germ cell migration. *Curr Opin Cell Biol*. 2004;16(2):169-173. doi:10.1016/j.ceb.2004.01.004
364. Ewen K, Baker M, Wilhelm D, Aitken RJ, Koopman P. Global survey of protein expression during gonadal sex determination in mice. *Mol Cell Proteomics*. 2009;8(12):2624-2641. doi:10.1074/mcp.M900108-MCP200
365. Lei L, Spradling AC. Mouse primordial germ cells produce cysts that partially fragment prior to meiosis. *Development*. 2013;140(10):2075-2081. doi:10.1242/dev.093864
366. DeFalco T, Capel B. Gonad morphogenesis in vertebrates: divergent means to a convergent end. *Annu Rev Cell Dev Biol*. 2009;25:457-482. doi:10.1146/annurev.cellbio.042308.13350
367. Brennan J, Capel B. One tissue, two fates: molecular genetic events that underlie testis versus ovary development. *Nat Rev Genet*. 2004;5(7):509-521. doi:10.1038/nrg1381
368. Gubbay J, Collignon J, Koopman P, et al. A gene mapping to the sex-determining region of the mouse Y chromosome is a member of a novel family of embryonically expressed genes. *Nature*. 1990;346(6281):245-250.

doi:10.1038/346245a0
369. Koopman P, Gubbay J, Vivian N, Goodfellow P, Lovell-Badge R. Male development of chromosomally female mice transgenic for Sry. *Nature*. 1991;351(6322):117-121. doi:10.1038/351117a0
370. Chaboissier M-C, Kobayashi A, Vidal VIP, et al. Functional analysis of Sox8 and Sox9 during sex determination in the mouse. *Development*. 2004;131(9):1891-1901. doi:10.1242/dev.01087
371. DeFalco T, Bhattacharya I, Williams A V, Sams DM, Capel B. Yolk-sac-derived macrophages regulate fetal testis vascularization and morphogenesis. *Proc Natl Acad Sci U S A*. 2014;111(23):E2384-93. doi:10.1073/pnas.1400057111
372. Western PS, Miles DC, van den Bergen JA, Burton M, Sinclair AH. Dynamic regulation of mitotic arrest in fetal male germ cells. *Stem Cells*. 2008;26(2):339-347. doi:10.1634/stemcells.2007-0622
373. Mamsen LS, Brøchner CB, Byskov AG, Møllgard K. The migration and loss of human primordial germ stem cells from the hind gut epithelium towards the gonadal ridge. *Int J Dev Biol*. 2012;56(10-12):771-778. doi:10.1387/ijdb.120202lm
374. Richards AJ, Enders GC, Resnick JL. Differentiation of murine premigratory primordial germ cells in culture. *Biol Reprod*. 1999;61(4):1146-1151. doi:10.1095/biolreprod61.4.1146
375. Enders GC, May JJ 2nd. Developmentally regulated expression of a mouse germ cell nuclear antigen examined from embryonic day 11 to adult in male and female mice. *Dev Biol*. 1994;163(2):331-340. doi:10.1006/dbio.1994.1152
376. Culty M. Gonocytes, the forgotten cells of the germ cell lineage. *Birth Defects Res C Embryo Today*. 2009;87(1):1-26. doi:10.1002/bdrc.20142
377. Kluin PM, Kramer MF, de Rooij DG. Spermatogenesis in the immature mouse proceeds faster than in the adult. *Int J Androl*. 1982;5(3):282-294. doi:10.1111/j.1365-2605.1982.tb00257.x
378. Yoshida S, Sukeno M, Nakagawa T, et al. The first round of mouse spermatogenesis is a distinctive program that lacks the self-renewing spermatogonia stage. *Development*. 2006;133(8):1495-1505. doi:10.1242/dev.02316
379. Mori C, Nakamura N, Dix DJ, et al. Morphological analysis of germ cell apoptosis during postnatal testis development in normal and Hsp 70-2 knockout mice. *Dev Dyn an Off Publ Am Assoc Anat*. 1997;208(1):125-136. doi:10.1002/(SICI)1097-0177(199701)208:1<125::AID-AJA12>3.0.CO;2-5
380. Eugene F. Oakberg. DURATION OF SPERMATOGENESIS IN THE MOUSE AND TIMING OF STAGES OF THE CYCLE OF THE SEMINIFEROUS EPITHELIUM. *Dev Dyn*. 1956;99(3):507-516. doi:10.1002/jmor.1051060102
381. Clermont Y. Kinetics of spermatogenesis in mammals: seminiferous epithelium cycle and spermatogonial renewal. *Physiol Rev*. 1972;52(1):198-236. doi:10.1152/physrev.1972.52.1.198
382. Misell LM, Holochwost D, Boban D, et al. A stable isotope-mass spectrometric method for measuring human spermatogenesis kinetics in vivo. *J Urol*. 2006;175(1):242-246; discussion 246. doi:10.1016/S0022-5347(05)00053-4
383. LEBLOND CP, CLERMONT Y. Definition of the stages of the cycle of the seminiferous epithelium in the rat. *Ann N Y Acad Sci*. 1952;55(4):548-573.

doi:10.1111/j.1749-6632.1952.tb26576.x
384. Oakberg EF. Spermatogonial stem-cell renewal in the mouse. *Anat Rec*. 1971;169(3):515-531. doi:10.1002/ar.1091690305
385. Valli H, Sukhwani M, Dovey SL, et al. Fluorescence- and magnetic-activated cell sorting strategies to isolate and enrich human spermatogonial stem cells. *Fertil Steril*. 2014;102(2):566-580.e7. doi:10.1016/j.fertnstert.2014.04.036
386. Phillips BT, Gassei K, Orwig KE. Spermatogonial stem cell regulation and spermatogenesis. *Philos Trans R Soc London Ser B, Biol Sci*. 2010;365(1546):1663-1678. doi:10.1098/rstb.2010.0026
387. Huckins C. The spermatogonial stem cell population in adult rats. I. Their morphology, proliferation and maturation. *Anat Rec*. 1971;169(3):533-557. doi:10.1002/ar.1091690306
388. Nagano M, Avarbock MR, Leonida EB, Brinster CJ, Brinster RL. Culture of mouse spermatogonial stem cells. *Tissue Cell*. 1998;30(4):389-397. doi:10.1016/s0040-8166(98)80053-0
389. Tegelenbosch RA, de Rooij DG. A quantitative study of spermatogonial multiplication and stem cell renewal in the C3H/101 F1 hybrid mouse. *Mutat Res*. 1993;290(2):193-200. doi:10.1016/0027-5107(93)90159-d
390. de Rooij DG. Spermatogonial stem cell renewal in the mouse. I. Normal situation. *Cell Tissue Kinet*. 1973;6(3):281-287. doi:10.1111/j.1365-2184.1973.tb01617.x
391. MORALES C, GRISWOLD MD. RETINOL-INDUCED STAGE SYNCHRONIZATION IN SEMINIFEROUS TUBULES OF THE RAT. *Endocrinology*. 1987;121(1):432-434. doi:10.1210/endo-121-1-432
392. Russell LD, Ettlin RA, Hikim APS, Clegg ED. Histological and Histopathological Evaluation of the Testis. *Int J Androl*. 1993;16(1):83. doi:https://doi.org/10.1111/j.1365-2605.1993.tb01156.x
393. Huckins C, Oakberg EF. Morphological and quantitative analysis of spermatogonia in mouse testes using whole mounted seminiferous tubules, I. The normal testes. *Anat Rec*. 1978;192(4):519-528. doi:10.1002/ar.1091920406
394. Anderson EL, Baltus AE, Roepers-Gajadien HL, et al. Stra8 and its inducer, retinoic acid, regulate meiotic initiation in both spermatogenesis and oogenesis in mice. *Proc Natl Acad Sci U S A*. 2008;105(39):14976-14980. doi:10.1073/pnas.0807297105
395. OAKBERG EF. A description of spermiogenesis in the mouse and its use in analysis of the cycle of the seminiferous epithelium and germ cell renewal. *Am J Anat*. 1956;99(3):391-413. doi:10.1002/aja.1000990303
396. Soh YQS, Mikedis MM, Kojima M, Godfrey AK, de Rooij DG, Page DC. Meioc maintains an extended meiotic prophase I in mice. *PLOS Genet*. 2017;13(4):e1006704. https://doi.org/10.1371/journal.pgen.1006704.
397. Sakai Y, Nakamoto T, Yamashina S. Dynamic changes in Sertoli cell processes invading spermatid cytoplasm during mouse spermiogenesis. *Anat Rec*. 1988;220(1):51-57. doi:https://doi.org/10.1002/ar.1092200107
398. Sakai Y, Yamashina S. Mechanism for the removal of residual cytoplasm from spermatids during mouse spermiogenesis. *Anat Rec*. 1989;223(1):43-48. doi:10.1002/ar.1092230107
399. Lehti MS, Sironen A. Formation and function of sperm tail structures in

association with sperm motility defects†. *Biol Reprod*. 2017;97(4):522-536. doi:10.1093/biolre/iox096
400. Cornwall GA. New insights into epididymal biology and function. *Hum Reprod Update*. 2009;15(2):213-227. doi:10.1093/humupd/dmn055
401. Green CD, Ma Q, Manske GL, et al. A Comprehensive Roadmap of Murine Spermatogenesis Defined by Single-Cell RNA-Seq. *Dev Cell*. 2018;46(5):651-667.e10. doi:10.1016/j.devcel.2018.07.025
402. Soumillon M, Necsulea A, Weier M, et al. Cellular source and mechanisms of high transcriptome complexity in the mammalian testis. *Cell Rep*. 2013;3(6):2179-2190. doi:10.1016/j.celrep.2013.05.031
403. Brawand D, Soumillon M, Necsulea A, et al. The evolution of gene expression levels in mammalian organs. *Nature*. 2011;478(7369):343-348. doi:10.1038/nature10532
404. Ramsköld D, Wang ET, Burge CB, Sandberg R. An Abundance of Ubiquitously Expressed Genes Revealed by Tissue Transcriptome Sequence Data. *PLOS Comput Biol*. 2009;5(12):e1000598. https://doi.org/10.1371/journal.pcbi.1000598.
405. Schultz N, Hamra FK, Garbers DL. A multitude of genes expressed solely in meiotic or postmeiotic spermatogenic cells offers a myriad of contraceptive targets. *Proc Natl Acad Sci U S A*. 2003;100(21):12201-12206. doi:10.1073/pnas.1635054100
406. Shima JE, McLean DJ, McCarrey JR, Griswold MD. The murine testicular transcriptome: characterizing gene expression in the testis during the progression of spermatogenesis. *Biol Reprod*. 2004;71(1):319-330. doi:10.1095/biolreprod.103.026880
407. Seisenberger S, Andrews S, Krueger F, et al. The dynamics of genome-wide DNA methylation reprogramming in mouse primordial germ cells. *Mol Cell*. 2012;48(6):849-862. doi:10.1016/j.molcel.2012.11.001
408. Seki Y, Yamaji M, Yabuta Y, et al. Cellular dynamics associated with the genome-wide epigenetic reprogramming in migrating primordial germ cells in mice. *Development*. 2007;134(14):2627-2638. doi:10.1242/dev.005611
409. Kagiwada S, Kurimoto K, Hirota T, Yamaji M, Saitou M. Replication-coupled passive DNA demethylation for the erasure of genome imprints in mice. *EMBO J*. 2013;32(3):340-353. doi:10.1038/emboj.2012.331
410. Shirane K, Kurimoto K, Yabuta Y, et al. Global Landscape and Regulatory Principles of DNA Methylation Reprogramming for Germ Cell Specification by Mouse Pluripotent Stem Cells. *Dev Cell*. 2016;39(1):87-103. doi:10.1016/j.devcel.2016.08.008
411. Hargan-Calvopina J, Taylor S, Cook H, et al. Stage-Specific Demethylation in Primordial Germ Cells Safeguards against Precocious Differentiation. *Dev Cell*. 2016;39(1):75-86. doi:10.1016/j.devcel.2016.07.019
412. Hackett JA, Sengupta R, Zylicz JJ, et al. Germline DNA demethylation dynamics and imprint erasure through 5-hydroxymethylcytosine. *Science*. 2013;339(6118):448-452. doi:10.1126/science.1229277
413. Vincent JJ, Huang Y, Chen P-Y, et al. Stage-specific roles for tet1 and tet2 in DNA demethylation in primordial germ cells. *Cell Stem Cell*. 2013;12(4):470-478. doi:10.1016/j.stem.2013.01.016

414. Ng J-H, Kumar V, Muratani M, et al. In vivo epigenomic profiling of germ cells reveals germ cell molecular signatures. *Dev Cell*. 2013;24(3):324-333. doi:10.1016/j.devcel.2012.12.011
415. Hajkova P, Jeffries SJ, Lee C, Miller N, Jackson SP, Surani MA. Genome-wide reprogramming in the mouse germ line entails the base excision repair pathway. *Science*. 2010;329(5987):78-82. doi:10.1126/science.1187945
416. Kobayashi H, Sakurai T, Miura F, et al. High-resolution DNA methylome analysis of primordial germ cells identifies gender-specific reprogramming in mice. *Genome Res*. 2013;23(4):616-627. doi:10.1101/gr.148023.112
417. Yamaguchi S, Shen L, Liu Y, Sendler D, Zhang Y. Role of Tet1 in erasure of genomic imprinting. *Nature*. 2013;504(7480):460-464. doi:10.1038/nature12805
418. Wolff EM, Byun H-M, Han HF, et al. Hypomethylation of a LINE-1 promoter activates an alternate transcript of the MET oncogene in bladders with cancer. *PLoS Genet*. 2010;6(4):e1000917-e1000917. doi:10.1371/journal.pgen.1000917
419. Seki Y, Hayashi K, Itoh K, Mizugaki M, Saitou M, Matsui Y. Extensive and orderly reprogramming of genome-wide chromatin modifications associated with specification and early development of germ cells in mice. *Dev Biol*. 2005;278(2):440-458. doi:10.1016/j.ydbio.2004.11.025
420. Hajkova P, Ancelin K, Waldmann T, et al. Chromatin dynamics during epigenetic reprogramming in the mouse germ line. *Nature*. 2008;452(7189):877-881. doi:10.1038/nature06714
421. Kaneda M, Okano M, Hata K, et al. Essential role for de novo DNA methyltransferase Dnmt3a in paternal and maternal imprinting. *Nature*. 2004;429(6994):900-903. doi:10.1038/nature02633
422. Bourc'his D, Xu GL, Lin CS, Bollman B, Bestor TH. Dnmt3L and the establishment of maternal genomic imprints. *Science*. 2001;294(5551):2536-2539. doi:10.1126/science.1065848
423. Bourc'his D, Bestor TH. Meiotic catastrophe and retrotransposon reactivation in male germ cells lacking Dnmt3L. *Nature*. 2004;431(7004):96-99. doi:10.1038/nature02886
424. Bestor TH, Bourc'his D. Transposon silencing and imprint establishment in mammalian germ cells. *Cold Spring Harb Symp Quant Biol*. 2004;69:381-387. doi:10.1101/sqb.2004.69.381
425. Kato Y, Kaneda M, Hata K, et al. Role of the Dnmt3 family in de novo methylation of imprinted and repetitive sequences during male germ cell development in the mouse. *Hum Mol Genet*. 2007;16(19):2272-2280. doi:10.1093/hmg/ddm179
426. Li J-Y, Lees-Murdock DJ, Xu G-L, Walsh CP. Timing of establishment of paternal methylation imprints in the mouse. *Genomics*. 2004;84(6):952-960. doi:10.1016/j.ygeno.2004.08.012
427. Coan PM, Burton GJ, Ferguson-Smith AC. Imprinted genes in the placenta--a review. *Placenta*. 2005;26 Suppl A:S10-20. doi:10.1016/j.placenta.2004.12.009
428. Morison IM, Ramsay JP, Spencer HG. A census of mammalian imprinting. *Trends Genet*. 2005;21(8):457-465. doi:10.1016/j.tig.2005.06.008
429. Tucci V, Isles AR, Kelsey G, et al. Genomic Imprinting and Physiological Processes in Mammals. *Cell*. 2019;176(5):952-965. doi:https://doi.org/10.1016/j.cell.2019.01.043

430. Sassone-Corsi P. Unique Chromatin Remodeling and Transcriptional Regulation in Spermatogenesis. 2002;296(June):2176-2177.
431. Kimmins S, Sassone-Corsi P. Chromatin remodelling and epigenetic features of germ cells. *Nature*. 2005;434(7033):583-589. doi:10.1038/nature03368
432. Hoghoughi N, Barral S, Vargas A, Rousseaux S, Khochbin S. Histone variants: essential actors in male genome programming. *J Biochem*. 2018;163(2):97-103. doi:10.1093/jb/mvx079
433. FELIX K. Protamines. *Adv Protein Chem*. 1960;15:1-56. doi:10.1016/s0065-3233(08)60307-1
434. Dixon GH, Smith M. Nucleic acids and protamine in salmon testes. *Prog Nucleic Acid Res Mol Biol*. 1968;8:9-34. doi:10.1016/s0079-6603(08)60541-3
435. Oliva R. Protamines and male infertility. *Hum Reprod Update*. 2006;12(4):417-435. doi:10.1093/humupd/dml009
436. Ando T, Yamasaki M, Suzuki K. Protamines. Isolation, characterization, structure and function. *Mol Biol Biochem Biophys*. 1973;12(0):1-114.
437. Govin J, Caron C, Lestrat C, Rousseaux S, Khochbin S. The role of histones in chromatin remodelling during mammalian spermiogenesis. *Eur J Biochem*. 2004;271(17):3459-3469. doi:10.1111/j.1432-1033.2004.04266.x
438. Bao J, Bedford MT. Epigenetic regulation of the histone-to-protamine transition during spermiogenesis. *Reproduction*. 2016;151(5):R55-R70. doi:10.1530/REP-15-0562
439. Goudarzi A, Zhang D, Huang H, et al. Dynamic Competing Histone H4 K5K8 Acetylation and Butyrylation Are Hallmarks of Highly Active Gene Promoters. *Mol Cell*. 2016;62(2):169-180. doi:10.1016/j.molcel.2016.03.014
440. Goudarzi A, Shiota H, Rousseaux S, Khochbin S. Genome-scale acetylation-dependent histone eviction during spermatogenesis. *J Mol Biol*. 2014;426(20):3342-3349. doi:10.1016/j.jmb.2014.02.023
441. Liu S, Yu H, Liu Y, et al. Chromodomain Protein CDYL Acts as a Crotonyl-CoA Hydratase to Regulate Histone Crotonylation and Spermatogenesis. *Mol Cell*. 2017;67(5):853-866.e5. doi:10.1016/j.molcel.2017.07.011
442. Franklin SG, Zweidler A. Non-allelic variants of histones 2a, 2b and 3 in mammals. *Nature*. 1977;266(5599):273-275. doi:10.1038/266273a0
443. Ueda J, Harada A, Urahama T, et al. Testis-Specific Histone Variant H3t Gene Is Essential for Entry into Spermatogenesis. *Cell Rep*. 2017;18(3):593-600. doi:10.1016/j.celrep.2016.12.065
444. Celeste A, Petersen S, Romanienko PJ, et al. Genomic instability in mice lacking histone H2AX. *Science*. 2002;296(5569):922-927. doi:10.1126/science.1069398
445. Greaves IK, Rangasamy D, Devoy M, Marshall Graves JA, Tremethick DJ. The X and Y chromosomes assemble into H2A.Z-containing [corrected] facultative heterochromatin [corrected] following meiosis. *Mol Cell Biol*. 2006;26(14):5394-5405. doi:10.1128/MCB.00519-06
446. van der Heijden GW, Derijck AAHA, Pósfai E, et al. Chromosome-wide nucleosome replacement and H3.3 incorporation during mammalian meiotic sex chromosome inactivation. *Nat Genet*. 2007;39(2):251-258. doi:10.1038/ng1949
447. Wu BJ, Dong FL, Ma XS, Wang XG, Lin F, Liu HL. Localization and expression of histone H2A variants during mouse oogenesis and preimplantation embryo

development. *Genet Mol Res*. 2014;13(3):5929-5939. doi:10.4238/2014.August.7.8
448. Li A, Maffey AH, Abbott WD, et al. Characterization of nucleosomes consisting of the human testis/sperm-specific histone H2B variant (hTSH2B). *Biochemistry*. 2005;44(7):2529-2535. doi:10.1021/bi048061n
449. Montellier E, Boussouar F, Rousseaux S, et al. Chromatin-to-nucleoprotamine transition is controlled by the histone H2B variant TH2B. *Genes Dev*. 2013;27(15):1680-1692. doi:10.1101/gad.220095.113
450. Govin J, Escoffier E, Rousseaux S, et al. Pericentric heterochromatin reprogramming by new histone variants during mouse spermiogenesis. *J Cell Biol*. 2007;176(3):283-294. doi:10.1083/jcb.200604141
451. Shires A, Carpenter MP, Chalkley R. New histones found in mature mammalian testes. *Proc Natl Acad Sci U S A*. 1975;72(7):2714-2718. doi:10.1073/pnas.72.7.2714
452. Urahama T, Horikoshi N, Osakabe A, Tachiwana H, Kurumizaka H. Structure of human nucleosome containing the testis-specific histone variant TSH2B. *Acta Crystallogr Sect F, Struct Biol Commun*. 2014;70(Pt 4):444-449. doi:10.1107/S2053230X14004695
453. Padavattan S, Thiruselvam V, Shinagawa T, et al. Structural analyses of the nucleosome complexes with human testis-specific histone variants, hTh2a and hTh2b. *Biophys Chem*. 2017;221:41-48. doi:10.1016/j.bpc.2016.11.013
454. Padavattan S, Shinagawa T, Hasegawa K, Kumasaka T, Ishii S, Kumarevel T. Structural and functional analyses of nucleosome complexes with mouse histone variants TH2a and TH2b, involved in reprogramming. *Biochem Biophys Res Commun*. 2015;464(3):929-935. doi:10.1016/j.bbrc.2015.07.070
455. Hada M, Masuda K, Yamaguchi K, Shirahige K, Okada Y. Identification of a variant-specific phosphorylation of TH2A during spermiogenesis. *Sci Rep*. 2017;7:46228. doi:10.1038/srep46228
456. Hada M, Kim J, Inoue E, et al. TH2A is phosphorylated at meiotic centromere by Haspin. *Chromosoma*. 2017;126(6):769-780. doi:10.1007/s00412-017-0638-5
457. Shinagawa T, Huynh LM, Takagi T, et al. Disruption of Th2a and Th2b genes causes defects in spermatogenesis. *Development*. 2015;142(7):1287-1292. doi:10.1242/dev.121830
458. Soboleva TA, Parker BJ, Nekrasov M, et al. A new link between transcriptional initiation and pre-mRNA splicing: The RNA binding histone variant H2A.B. *PLoS Genet*. 2017;13(2):e1006633. doi:10.1371/journal.pgen.1006633
459. Soboleva TA, Nekrasov M, Ryan DP, Tremethick DJ. Histone variants at the transcription start-site. *Trends Genet*. 2014;30(5):199-209. doi:10.1016/j.tig.2014.03.002
460. Soboleva TA, Nekrasov M, Pahwa A, Williams R, Huttley GA, Tremethick DJ. A unique H2A histone variant occupies the transcriptional start site of active genes. *Nat Struct Mol Biol*. 2011;19(1):25-30. doi:10.1038/nsmb.2161
461. Yuen BTK, Bush KM, Barrilleaux BL, Cotterman R, Knoepfler PS. Histone H3.3 regulates dynamic chromatin states during spermatogenesis. *Development*. 2014;141(18):3483-3494. doi:10.1242/dev.106450
462. Tang MCW, Jacobs SA, Mattiske DM, et al. Contribution of the two genes

encoding histone variant h3.3 to viability and fertility in mice. *PLoS Genet*. 2015;11(2):e1004964. doi:10.1371/journal.pgen.1004964
463. Talbert PB, Henikoff S. Histone variants on the move: substrates for chromatin dynamics. *Nat Rev Mol Cell Biol*. 2017;18(2):115-126. doi:10.1038/nrm.2016.148
464. Jin C, Felsenfeld G. Nucleosome stability mediated by histone variants H3.3 and H2A.Z. *Genes Dev*. 2007;21(12):1519-1529. doi:10.1101/gad.1547707
465. Jin C, Zang C, Wei G, et al. H3.3/H2A.Z double variant-containing nucleosomes mark “nucleosome-free regions” of active promoters and other regulatory regions. *Nat Genet*. 2009;41(8):941-945. doi:10.1038/ng.409
466. Meistrich ML, Mohapatra B, Shirley CR, Zhao M. Roles of transition nuclear proteins in spermiogenesis. *Chromosoma*. 2003;111(8):483-488. doi:10.1007/s00412-002-0227-z
467. Barral S, Morozumi Y, Tanaka H, et al. Histone Variant H2A.L.2 Guides Transition Protein-Dependent Protamine Assembly in Male Germ Cells. *Mol Cell*. 2017;66(1):89-101.e8. doi:10.1016/j.molcel.2017.02.025
468. Wyrobek AJ, Meistrich ML, Furrer R, Bruce WR. Physical characteristics of mouse sperm nuclei. *Biophys J*. 1976;16(7):811-825. doi:10.1016/S0006-3495(76)85730-X
469. Molaro A, Hodges E, Fang F, et al. Sperm Methylation Profiles Reveal Features of Epigenetic Inheritance and Evolution in Primates. *Cell*. 2011;146(6):1029-1041. doi:https://doi.org/10.1016/j.cell.2011.08.016
470. Chan D, Shao X, Dumargne MC, et al. Customized methylc-capture sequencing to evaluate variation in the human sperm DNA methylome representative of altered folate metabolism. *Environ Health Perspect*. 2019;127(8):87002. doi:10.1289/EHP4812
471. Jung YH, Sauria MEG, Lyu X, et al. Chromatin States in Mouse Sperm Correlate with Embryonic and Adult Regulatory Landscapes. *Cell Rep*. 2017;18(6):1366-1382. doi:10.1016/j.celrep.2017.01.034
472. Hammoud SS, Nix DA, Zhang H, Purwar J, Carrell DT, Cairns BR. Distinctive chromatin in human sperm packages genes for embryo development. *Nature*. 2009;460(7254):473-478. doi:10.1038/nature08162
473. Carone BR, Hung J-H, Hainer SJ, et al. High-resolution mapping of chromatin packaging in mouse embryonic stem cells and sperm. *Dev Cell*. 2014;30(1):11-22. doi:10.1016/j.devcel.2014.05.024
474. Samans B, Yang Y, Krebs S, et al. Uniformity of Nucleosome Preservation Pattern in Mammalian Sperm and Its Connection to Repetitive DNA Elements. *Dev Cell*. 2014;30(1):23-35. doi:https://doi.org/10.1016/j.devcel.2014.05.023
475. Royo H, Stadler MB, Peters AHFM. Alternative Computational Analysis Shows No Evidence for Nucleosome Enrichment at Repetitive Sequences in Mammalian Spermatozoa. *Dev Cell*. 2016;37(1):98-104. doi:https://doi.org/10.1016/j.devcel.2016.03.010
476. Lismer A, Siklenka K, Lafleur C, Dumeaux V, Kimmins S. Sperm histone H3 lysine 4 trimethylation is altered in a genetic mouse model of transgenerational epigenetic inheritance. *Nucleic Acids Res*. 2020;48(20):11380-11393. doi:10.1093/nar/gkaa712
477. Lismer A, Dumeaux V, Lafleur C, et al. Histone H3 lysine 4 trimethylation in sperm

is transmitted to the embryo and associated with diet-induced phenotypes in the offspring. *Dev Cell*. 2021;56(5):671-686.e6. doi:10.1016/j.devcel.2021.01.014
478. Lambrot R, Lafleur C, Siklenka K, Kimmins S. The Genomic Distribution of Histone H3K4me2 in Spermatogonia is Highly Conserved in Sperm. *Biol Reprod*. April 2019. doi:10.1093/biolre/ioz055
479. Arpanahi A, Brinkworth M, Iles D, et al. Endonuclease-sensitive regions of human spermatozoal chromatin are highly enriched in promoter and CTCF binding sequences. *Genome Res*. 2009;19(8):1338-1349. doi:10.1101/gr.094953.109
480. Wu S-F, Zhang H, Cairns BR. Genes for embryo development are packaged in blocks of multivalent chromatin in zebrafish sperm. *Genome Res*. 2011;21(4):578-589. doi:10.1101/gr.113167.110
481. Hammoud SS, Low DHP, Yi C, Carrell DT, Guccione E, Cairns BR. Chromatin and transcription transitions of mammalian adult germline stem cells and spermatogenesis. *Cell Stem Cell*. 2014;15(2):239-253. doi:10.1016/j.stem.2014.04.006
482. Agarwal A, Mulgund A, Hamada A, Chyatte MR. A unique view on male infertility around the globe. *Reprod Biol Endocrinol*. 2015;13:37. doi:10.1186/s12958-015-0032-1
483. Belloc S, Cohen-Bacrie M, Amar E, et al. High body mass index has a deleterious effect on semen parameters except morphology: Results from a large cohort study. *Fertil Steril*. 2014;102(5):1268-1273. doi:10.1016/j.fertnstert.2014.07.1212
484. Campbell JM, Lane M, Owens JA, Bakos HW. Paternal obesity negatively affects male fertility and assisted reproduction outcomes: A systematic review and meta-analysis. *Reprod Biomed Online*. 2015;31(5):593-604. doi:10.1016/j.rbmo.2015.07.012
485. Craig JR, Jenkins TG, Carrell DT, Hotaling JM. Obesity, male infertility, and the sperm epigenome. *Fertil Steril*. 2017;107(4):848-859. doi:10.1016/j.fertnstert.2017.02.115
486. Guo D, Wu W, Tang Q, et al. The impact of BMI on sperm parameters and the metabolite changes of seminal plasma concomitantly. *Oncotarget*. 2017;8(30):48619-48634. doi:10.18632/oncotarget.14950
487. Kasturi SS, Tannir J, Brannigan RE. The metabolic syndrome and male infertility. *J Androl*. 2008;29(3):251-259. doi:10.2164/jandrol.107.003731
488. Fullston T, Palmer NO, Owens JA, Mitchell M, Bakos HW, Lane M. Diet-induced paternal obesity in the absence of diabetes diminishes the reproductive health of two subsequent generations of mice. *Hum Reprod*. 2012;27(5):1391-1400. doi:10.1093/humrep/des030
489. Binder NK, Beard SA, Kaitu'U-Lino TJ, Tong S, Hannan NJ, Gardner DK. Paternal obesity in a rodent model affects placental gene expression in a sex-specific manner. *Reproduction*. 2015;149(5):435-444. doi:10.1530/REP-14-0676
490. Mitchell M, Bakos HW, Lane M. Paternal diet-induced obesity impairs embryo development and implantation in the mouse. *Fertil Steril*. 2011;95(4):1349-1353. doi:10.1016/j.fertnstert.2010.09.038
491. Binder NK, Hannan NJ, Gardner DK. Paternal Diet-Induced Obesity Retards Early Mouse Embryo Development, Mitochondrial Activity and Pregnancy Health. *PLoS One*. 2012;7(12). doi:10.1371/journal.pone.0052304

492. Pembrey M, Saffery R, Bygren LO lo. Human transgenerational responses to early-life experience: potential impact on development, health and biomedical research. *J Med Genet*. 2014;51(9):563-572. doi:10.1136/jmedgenet-2014-102577
493. Miska EA, Ferguson-smith AC. Transgenerational inheritance: Models and mechanisms of non – DNA sequence – based inheritance. 2016;354(6308):778-782.
494. Vågerö D, Pinger PR, Aronsson V, van den Berg GJ. Paternal grandfather's access to food predicts all-cause and cancer mortality in grandsons. *Nat Commun*. 2018;9(1):1-7. doi:10.1038/s41467-018-07617-9
495. Vågerö D, Cederström A, van den Berg GJ. Food abundance in men before puberty predicts a range of cancers in grandsons. *Nat Commun*. 2022;13(1):7507. doi:10.1038/s41467-022-35217-1
496. Danielzik S, Langnäse K, Mast M, Spethmann C, Müller MJ. Impact of parental BMI on the manifestation of overweight 5-7 year old children. *Eur J Nutr*. 2002;41(3):132-138. doi:10.1007/s00394-002-0367-1
497. Figueroa-Colon R, Arani RB, Goran MI, Weinsier RL. Paternal body fat is a longitudinal predictor of changes in body fat in premenarcheal girls. *Am J Clin Nutr*. 2000;71(3):829-834. doi:10.1093/ajcn/71.3.829
498. Li L, Law C, Conte R Lo, Power C. Intergenerational influences on childhood body mass index: the effect of parental body mass index trajectories. *Am J Clin Nutr*. 2009;89(5):551-557. doi:10.3945/ajcn.2008.26759.INTRODUCTION
499. Wang C, Liao JK. A Mouse Model of Diet-Induced Obesity and Insulin Resistance. 2012;821(5):1-11. doi:10.1007/978-1-61779-430-8
500. Surwit RS, Kuhn CM, Cochrane C, McCubbin JA, Feinglos MN. Diet-Induced Type II Diabetes in C57BL/6J Mice. *Diabetes*. 1988;37(9):1163-1167. doi:10.2337/diab.37.9.1163
501. Kraegen EW, James DE, Storlien LH, Burleigh KM, Chisholm DJ. In vivo insulin resistance in individual peripheral tissues of the high fat fed rat: assessment by euglycaemic clamp plus deoxyglucose administration. *Diabetologia*. 1986;29(3):192-198. doi:10.1007/BF02427092
502. Storlien LH, James DE, Burleigh KM, Chisholm DJ, Kraegen EW. Fat feeding causes widespread in vivo insulin resistance, decreased energy expenditure, and obesity in rats. *Am J Physiol*. 1986;251(5 Pt 1):E576-83. doi:10.1152/ajpendo.1986.251.5.E576
503. SCHMIDT-NIELSEN K, HAINES HB, HACKEL DB. DIABETES MELLITUS IN THE SAND RAT INDUCED BY STANDARD LABORATORY DIETS. *Science*. 1964;143(3607):689-690. doi:10.1126/science.143.3607.689
504. Ng S-F, Lin RCY, Laybutt DR, Barres R, Owens JA, Morris MJ. Chronic high-fat diet in fathers programs β-cell dysfunction in female rat offspring. *Nature*. 2010;467(7318):963-966. doi:10.1038/nature09491
505. Terashima M, Barbour S, Ren J, Yu W, Han Y, Muegge K. Effect of high fat diet on paternal sperm histone distribution and male offspring liver gene expression. *Epigenetics*. 2015;10(9):861-871. doi:10.1080/15592294.2015.1075691
506. Fullston T, Teague EMCO, Palmer NO, et al. Paternal obesity initiates metabolic disturbances in two generations of mice with incomplete penetrance to the F2

generation and alters the transcriptional profile of testis and sperm microRNA content. *FASEB J*. 2013;27(10):4226-4243. doi:10.1096/fj.12-224048
507. Krout D, Roemmich JN, Bundy A, Garcia RA, Yan L, Claycombe-Larson KJ. Paternal exercise protects mouse offspring from high-fat-diet-induced type 2 diabetes risk by increasing skeletal muscle insulin signaling. *J Nutr Biochem*. 2018;57:35-44. doi:10.1016/j.jnutbio.2018.03.013
508. Murashov AK, Pak ES, Koury M, et al. Paternal long-term exercise programs offspring for low energy expenditure and increased risk for obesity in mice. *FASEB J*. 2016;30(2):775-784. doi:10.1096/fj.15-274274
509. Stanford KI, Rasmussen M, Baer LA, et al. Paternal Exercise Improves Glucose Metabolism in Adult Offspring. *Diabetes*. 2018;67(December):db180667. doi:10.2337/db18-0667
510. Jazwiec PA, Patterson VS, Ribeiro TA, et al. Paternal obesity induces placental hypoxia and sex-specific impairments in placental vascularization and offspring metabolism†. *Biol Reprod*. April 2022:ioac066. doi:10.1093/biolre/ioac066
511. de Castro Barbosa T, Alm PS, Krook A, Barrès R, Zierath JR. Paternal high-fat diet transgenerationally impacts hepatic immunometabolism. *FASEB J*. 2019;33(5):6269-6280. doi:10.1096/fj.201801879RR
512. Morita S, Horii T, Kimura M, et al. Paternal allele influences high fat diet-induced obesity. *PLoS One*. 2014;9(1):1-9. doi:10.1371/journal.pone.0085477
513. Grandjean V, Fourré S, De Abreu DAF, Derieppe MA, Remy JJ, Rassoulzadegan M. RNA-mediated paternal heredity of diet-induced obesity and metabolic disorders. *Sci Rep*. 2015;5(June):1-9. doi:10.1038/srep18193
514. Zhang Y, Zhang X, Shi J, et al. Dnmt2 mediates intergenerational transmission of paternally acquired metabolic disorders through sperm small non-coding RNAs. *Nat Cell Biol*. 2018;20(5):535-540. doi:10.1038/s41556-018-0087-2
515. Huypens P, Sass S, Wu M, et al. Epigenetic germline inheritance of diet-induced obesity and insulin resistance. *Nat Genet*. 2016;48(5):497-499. doi:10.1038/ng.3527
516. McPherson NO, Lane M, Sandeman L, Owens JA, Fullston T. An exercise-only intervention in obese fathers restores glucose and insulin regulation in conjunction with the rescue of pancreatic islet cell morphology and microRNA expression in male offspring. *Nutrients*. 2017;9(2). doi:10.3390/nu9020122
517. Chen Q, Yan M, Cao Z, et al. Sperm tsRNAs contribute to intergenerational inheritance of an acquired metabolic disorder. *Science (80-)*. 2016;351(6271):397-400. doi:10.1126/science.aad7977
518. Eberle C, Kirchner MF, Herden R, Stichling S. Paternal metabolic and cardiovascular programming of their offspring: A systematic scoping review. *PLoS One*. 2020;15(12):e0244826. doi:10.1371/journal.pone.0244826
519. Jin B, Li Y, Robertson KD. DNA methylation: superior or subordinate in the epigenetic hierarchy? *Genes Cancer*. 2011;2(6):607-617. doi:10.1177/1947601910393957
520. Donkin I, Versteyhe S, Ingerslev LR, et al. Obesity and bariatric surgery drive epigenetic variation of spermatozoa in humans. *Cell Metab*. 2016;23(2):369-378. doi:10.1016/j.cmet.2015.11.004
521. Wei Y, Yang C-R, Wei Y-P, et al. Paternally induced transgenerational inheritance

of susceptibility to diabetes in mammals. *Proc Natl Acad Sci*. 2014;111(5):1873-1878. doi:10.1073/pnas.1321195111
522. Youngson N, Lecomte V, Maloney C, et al. Obesity-induced sperm DNA methylation changes at satellite repeats are reprogrammed in rat offspring. *Asian J Androl*. 2016;18(6):930-936. doi:10.4103/1008-682X.163190
523. Carninci P, Sandelin A, Lenhard B, et al. Genome-wide analysis of mammalian promoter architecture and evolution. *Nat Genet*. 2006;38(6):626-635. doi:10.1038/ng1789
524. Birney E, Stamatoyannopoulos JA, Dutta A, et al. Identification and analysis of functional elements in 1% of the human genome by the ENCODE pilot project. *Nature*. 2007;447(7146):799-816. doi:10.1038/nature05874
525. Djebali S, Davis CA, Merkel A, et al. Landscape of transcription in human cells. *Nature*. 2012;489(7414):101-108. doi:10.1038/nature11233
526. Mattick JS, Taft RJ, Faulkner GJ. A global view of genomic information – moving beyond the gene and the master regulator. *Trends Genet*. 2010;26(1):21-28. doi:10.1016/j.tig.2009.11.002
527. Dunham I, Kundaje A, Aldred SF, et al. An integrated encyclopedia of DNA elements in the human genome. *Nature*. 2012;489(7414):57-74. doi:10.1038/nature11247
528. Ecker JR, Bickmore WA, Barroso I, Pritchard JK, Gilad Y, Segal E. ENCODE explained. *Nature*. 2012;489(7414):52-54. doi:10.1038/489052a
529. Statello L, Guo C-J, Chen L-L, Huarte M. Gene regulation by long non-coding RNAs and its biological functions. *Nat Rev Mol Cell Biol*. 2021;22(2):96-118. doi:10.1038/s41580-020-00315-9
530. Ren X, Chen X, Wang Z, Wang D. Is transcription in sperm stationary or dynamic? *J Reprod Dev*. 2017;63(5):439-443. doi:10.1262/jrd.2016-093
531. Siomi MC, Sato K, Pezic D, Aravin AA. PIWI-interacting small RNAs: the vanguard of genome defence. *Nat Rev Mol Cell Biol*. 2011;12(4):246-258. doi:10.1038/nrm3089
532. Esposito T, Magliocca S, Formicola D, Gianfrancesco F. piR_015520 Belongs to Piwi-Associated RNAs Regulates Expression of the Human Melatonin Receptor 1A Gene. *PLoS One*. 2011;6(7):e22727. https://doi.org/10.1371/journal.pone.0022727.
533. Brennecke J, Malone CD, Aravin AA, Sachidanandam R, Stark A, Hannon GJ. An Epigenetic Role for Maternally Inherited piRNAs in Transposon Silencing. *Science (80-)*. 2008;322(5906):1387-1392. doi:10.1126/science.1165171
534. Ashe A, Sapetschnig A, Weick E-M, et al. piRNAs Can Trigger a Multigenerational Epigenetic Memory in the Germline of C. elegans. *Cell*. 2012;150(1):88-99. doi:https://doi.org/10.1016/j.cell.2012.06.018
535. Claycombe-Larson KG, Bundy AN, Roemmich JN. Paternal high-fat diet and exercise regulate sperm miRNA and histone methylation to modify placental inflammation, nutrient transporter mRNA expression and fetal weight in a sex-dependent manner. *J Nutr Biochem*. 2020;81:108373. doi:10.1016/j.jnutbio.2020.108373
536. Kiani J, Grandjean V, Liebers R, et al. RNA–Mediated Epigenetic Heredity Requires the Cytosine Methyltransferase Dnmt2. *PLOS Genet*.

2013;9(5):e1003498. https://doi.org/10.1371/journal.pgen.1003498.
537. Zhang X, Cozen AE, Liu Y, Chen Q, Lowe TM. Small RNA Modifications: Integral to Function and Disease. *Trends Mol Med*. 2016;22(12):1025-1034. doi:10.1016/j.molmed.2016.10.009
538. Chen Q, Yan W, Duan E. Epigenetic inheritance of acquired traits through sperm RNAs and sperm RNA modifications. *Nat Rev Genet*. 2016;17(12):733-743. doi:10.1038/nrg.2016.106
539. Terashima M, Barbour S, Ren J, et al. Effect of high fat diet on paternal sperm histone distribution and male offspring liver gene expression. *Epigenetics*. 2015;2294(September 2017):861-871. doi:10.1080/15592294.2015.1075691
540. Yoshida K, Maekawa T, Ly NH, et al. ATF7-Dependent Epigenetic Changes Are Required for the Intergenerational Effect of a Paternal Low-Protein Diet. *Mol Cell*. 2020;78(3):445-458.e6. doi:10.1016/j.molcel.2020.02.028
541. Lambrot R, Xu C, Saint-Phar S, et al. Low paternal dietary folate alters the mouse sperm epigenome and is associated with negative pregnancy outcomes. *Nat Commun*. 2013;4. doi:10.1038/ncomms3889
542. Lesch BJ, Silber SJ, McCarrey JR, Page DC. Parallel evolution of male germline epigenetic poising and somatic development in animals. *Nat Genet*. 2016;48(8):888-894. doi:10.1038/ng.3591
543. Siklenka K, Erkek S, Godmann M, et al. Disruption of histone methylation in developing sperm impairs offspring health transgenerationally. *Science (80-)*. 2015;350(6261). doi:10.1126/science.aab2006
544. Aoshima K, Inoue E, Sawa H, Okada Y. Paternal H3K4 methylation is required for minor zygotic gene activation and early mouse embryonic development. *EMBO Rep*. 2015;16(7):803-812. doi:10.15252/embr.201439700
545. Kishigami S, Wakayama S, Nguyen VT, Wakayama T. Similar time restriction for intracytoplasmic sperm injection and round spermatid injection into activated oocytes for efficient offspring production. *Biol Reprod*. 2004;70(6):1863-1869. doi:10.1095/biolreprod.103.025171
546. Kimura Y, Yanagimachi R. Mouse oocytes injected with testicular spermatozoa or round spermatids can develop into normal offspring. *Development*. 1995;121(8):2397-2405. doi:10.1242/dev.121.8.2397
547. Zhang B, Zheng H, Huang B, et al. Allelic reprogramming of the histone modification H3K4me3 in early mammalian development. *Nature*. 2016;537(7621):553-557. doi:10.1038/nature19361
548. Ishiuchi T, Abe S, Inoue K, et al. Reprogramming of the histone H3.3 landscape in the early mouse embryo. *Nat Struct Mol Biol*. 2021;28(1):38-49. doi:10.1038/s41594-020-00521-1
549. Santenard A, Ziegler-Birling C, Koch M, Tora L, Bannister AJ, Torres-Padilla M-E. Heterochromatin formation in the mouse embryo requires critical residues of the histone variant H3.3. *Nat Cell Biol*. 2010;12(9):853-862. doi:10.1038/ncb2089
550. Skinner MK. What is an epigenetic transgenerational phenotype? F3 or F2. *Reprod Toxicol*. 2008;25(1):2-6. doi:10.1016/j.reprotox.2007.09.001
551. Martienssen EH and RA. Transgenerational Epigenetic Inheritance: myths and mechanisms. *Cell*. 2014;157(1):95-109. doi:10.1016/j.cell.2014.02.045.Transgenerational

552. Zeng L, Fagotto F, Zhang T, et al. The Mouse Fused Locus Encodes Axin, an Inhibitor of the Wnt Signaling Pathway That Regulates Embryonic Axis Formation. *Cell*. 1997;90(1):181-192. doi:10.1016/S0092-8674(00)80324-4
553. Duhl DMJ, Vrieling H, Miller KA, Wolff GL, Barsh GS. Neomorphic agouti mutations in obese yellow mice. *Nat Genet*. 1994;8(1):59-65. doi:10.1038/ng0994-59
554. Rakyan VK, Chong S, Champ ME, et al. Transgenerational inheritance of epigenetic states at the murine AxinFu allele occurs after maternal and paternal transmission. *Proc Natl Acad Sci U S A*. 2003;100(5):2538-2543. doi:10.1073/pnas.0436776100
555. Padmanabhan N, Jia D, Geary-joo C, et al. Mutation in Folate Metabolism Causes Epigenetic Instability and Transgenerational Effects on Development. *Cell*. 2013;155(1):81-93. doi:10.1016/j.cell.2013.09.002
556. Blake GET, Zhao X, Yung H wa, et al. Defective folate metabolism causes germline epigenetic instability and distinguishes Hira as a phenotype inheritance biomarker. *Nat Commun*. 2021;12(1):3714. doi:10.1038/s41467-021-24036-5
557. Gapp K, Jawaid A, Sarkies P, et al. Implication of sperm RNAs in transgenerational inheritance of the effects of early trauma in mice. *Nat Neurosci*. 2014;17(5):667-669. doi:10.1038/nn.3695
558. Zhou C, Gao L, Flaws JA. Exposure to an Environmentally Relevant Phthalate Mixture Causes Transgenerational Effects on Female Reproduction in Mice. *Endocrinology*. 2017;158(6):1739-1754. doi:10.1210/en.2017-00100
559. Chen J, Wu S, Wen S, et al. The Mechanism of Environmental Endocrine Disruptors (DEHP) Induces Epigenetic Transgenerational Inheritance of Cryptorchidism. *PLoS One*. 2015;10(6):e0126403. doi:10.1371/journal.pone.0126403
560. Manikkam M, Guerrero-Bosagna C, Tracey R, Haque MM, Skinner MK. Transgenerational actions of environmental compounds on reproductive disease and identification of epigenetic biomarkers of ancestral exposures. *PLoS One*. 2012;7(2):e31901. doi:10.1371/journal.pone.0031901
561. Shea JM, Serra RW, Carone BR, et al. Genetic and Epigenetic Variation, but Not Diet, Shape the Sperm Methylome. *Dev Cell*. 2015;35(6):750-758. doi:10.1016/j.devcel.2015.11.024
562. Radford EJ, Ito M, Shi H, et al. In utero undernourishment perturbs the adult sperm methylome and intergenerational metabolism. *Science (80-)*. 2014;345(6198):1255903. doi:10.1126/science.1255903
563. Sharma U, Conine CC, Shea JM, et al. Biogenesis and function of tRNA fragments during sperm maturation and fertilization in mammals. 2016;351(6271):391-396. doi:10.1126/science.aad6780.Biogenesis
564. Carone BR, Fauquier L, Habib N, et al. Paternally induced transgenerational environmental reprogramming of metabolic gene expression in mammals. *Cell*. 2010;143(7):1084-1096. doi:10.1016/j.cell.2010.12.008
565. Whidden L, Martel J, Rahimi S, Chaillet JR, Chan D, Trasler JM. Compromised oocyte quality and assisted reproduction contribute to sex-specific effects on offspring outcomes and epigenetic patterning. *Hum Mol Genet*. 2016;25(21):4649-

4660. doi:10.1093/hmg/ddw293
566. Mani S, Ghosh J, Coutifaris C, Sapienza C, Mainigi M. Epigenetic changes and assisted reproductive technologies. *Epigenetics*. 2020;15(1-2):12-25. doi:10.1080/15592294.2019.1646572
567. Chen Q, Shi J, Peng H, et al. Sperm tsRNAs contribute to intergenerational inheritance of an acquired metabolic disorder. 2016;(February).
568. Gemberling MP, Siklenka K, Rodriguez E, et al. Transgenic mice for in vivo epigenome editing with CRISPR-based systems. *Nat Methods*. 2021;18(8):965-974. doi:10.1038/s41592-021-01207-2
569. Yao C, Zhang W, Shuai L. The first cell fate decision in pre-implantation mouse embryos. *Cell Regen (London, England)*. 2019;8(2):51-57. doi:10.1016/j.cr.2019.10.001
570. Adamson SL, Lu Y, Whiteley KJ, et al. Interactions between trophoblast cells and the maternal and fetal circulation in the mouse placenta. *Dev Biol*. 2002;250(2):358-373. doi:10.1016/s0012-1606(02)90773-6
571. Maltepe E, Fisher SJ. Placenta: the forgotten organ. *Annu Rev Cell Dev Biol*. 2015;31:523-552. doi:10.1146/annurev-cellbio-100814-125620
572. Shibata S, Kobayashi EH, Kobayashi N, Oike A, Okae H, Arima T. Unique features and emerging in vitro models of human placental development. *Reprod Med Biol*. 2020;19(4):301-313. doi:10.1002/rmb2.12347
573. Simmons DG, Fortier AL, Cross JC. Diverse subtypes and developmental origins of trophoblast giant cells in the mouse placenta. *Dev Biol*. 2007;304(2):567-578. doi:10.1016/j.ydbio.2007.01.009
574. Woods L, Perez-Garcia V, Hemberger M. Regulation of Placental Development and Its Impact on Fetal Growth-New Insights From Mouse Models. *Front Endocrinol (Lausanne)*. 2018;9:570. doi:10.3389/fendo.2018.00570
575. Simmons DG, Natale DRC, Begay V, Hughes M, Leutz A, Cross JC. Early patterning of the chorion leads to the trilaminar trophoblast cell structure in the placental labyrinth. *Development*. 2008;135(12):2083-2091. doi:10.1242/dev.020099
576. Soncin F, Natale D, Parast MM. Signaling pathways in mouse and human trophoblast differentiation: a comparative review. *Cell Mol Life Sci*. 2015;72(7):1291-1302. doi:10.1007/s00018-014-1794-x
577. Perez-Garcia V, Fineberg E, Wilson R, et al. Placentation defects are highly prevalent in embryonic lethal mouse mutants. *Nature*. 2018;555(7697):463-468. doi:10.1038/nature26002
578. Bonnin A, Goeden N, Chen K, et al. A transient placental source of serotonin for the fetal forebrain. *Nature*. 2011;472(7343):347-350. doi:10.1038/nature09972
579. Ho L, van Dijk M, Chye STJ, et al. ELABELA deficiency promotes preeclampsia and cardiovascular malformations in mice. *Science*. 2017;357(6352):707-713. doi:10.1126/science.aam6607
580. Rosenfeld CS. The placenta-brain-axis. *J Neurosci Res*. 2021;99(1):271-283. doi:10.1002/jnr.24603
581. Mericq V, Ong KK, Bazaes R, et al. Longitudinal changes in insulin sensitivity and secretion from birth to age three years in small- and appropriate-for-gestational-age children. *Diabetologia*. 2005;48(12):2609-2614. doi:10.1007/s00125-005-

0036-z
582. Ibáñez L, Ong K, Dunger DB, de Zegher F. Early development of adiposity and insulin resistance after catch-up weight gain in small-for-gestational-age children. *J Clin Endocrinol Metab*. 2006;91(6):2153-2158. doi:10.1210/jc.2005-2778
583. Greenwood PL, Bell AW. Consequences of intra-uterine growth retardation for postnatal growth, metabolism and pathophysiology. *Reprod (Cambridge, England) Suppl*. 2003;61:195-206.
584. De Blasio MJ, Gatford KL, Robinson JS, Owens JA. Placental restriction of fetal growth reduces size at birth and alters postnatal growth, feeding activity, and adiposity in the young lamb. *Am J Physiol Regul Integr Comp Physiol*. 2007;292(2):R875-86. doi:10.1152/ajpregu.00430.2006
585. Brown LD, Hay Jr WW. Impact of placental insufficiency on fetal skeletal muscle growth. *Mol Cell Endocrinol*. 2016;435:69-77. doi:10.1016/j.mce.2016.03.017
586. Regnault TRH, Galan HL, Parker TA, Anthony R V. Placental development in normal and compromised pregnancies - A review. *Placenta*. 2002;23(SUPPL. 1). doi:10.1053/plac.2002.0792
587. Surani MAH, Barton SC, Norris ML. Development of reconstituted mouse eggs suggests imprinting of the genome during gametogenesis. *Nature*. 1984;308(5959):548-550. doi:10.1038/308548a0
588. Barton SC, Surani MAH, Norris ML. Role of paternal and maternal genomes in mouse development. *Nature*. 1984;311(5984):374-376. doi:10.1038/311374a0
589. Barton SC, Adams CA, Norris ML, Surani MAH. Development of gynogenetic and parthenogenetic inner cell mass and trophectoderm tissues in reconstituted blastocysts in the mouse. *J Embryol Exp Morphol*. 1985;VOL. 90:267-285.
590. McGrath J, Solter D. Nucleocytoplasmic interactions in the mouse embryo. *J Embryol Exp Morphol*. 1986;97(SUPPL.):277-290.
591. McGrath J, Solter D. Completion of mouse embryogenesis requires both the maternal and paternal genomes. *Cell*. 1984;37(1):179-183. doi:10.1016/0092-8674(84)90313-1
592. Wang X, Miller DC, Harman R, Antczak DF, Clark AG. Paternally expressed genes predominate in the placenta. *Proc Natl Acad Sci*. 2013;110(26):10705-10710. doi:10.1073/pnas.1308998110
593. Jayasena CN, Radia UK, Figueiredo M, et al. Reduced Testicular Steroidogenesis and Increased Semen Oxidative Stress in Male Partners as Novel Markers of Recurrent Miscarriage. 2019;169:161-169. doi:10.1373/clinchem.2018.289348
594. Murugappan G, Li S, Leonard SA, Winn VD, Druzin ML, Eisenberg ML. Association of preconception paternal health and adverse maternal outcomes among healthy mothers. *Am J Obstet Gynecol MFM*. 2021;3(5). doi:10.1016/j.ajogmf.2021.100384
595. Denomme MM, Parks JC, McCallie BR, McCubbin NI, Schoolcraft WB, Katz-Jaffe MG. Advanced paternal age directly impacts mouse embryonic placental imprinting. *PLoS One*. 2020;15(3):e0229904. doi:10.1371/journal.pone.0229904
596. Ding T, Mokshagundam S, Rinaudo PF, Osteen KG, Bruner-Tran KL. Paternal developmental toxicant exposure is associated with epigenetic modulation of sperm and placental Pgr and Igf2 in a mouse model. *Biol Reprod*. 2018;99(4):864-876. doi:10.1093/biolre/ioy111

597. Pépin A-S, Jazwiec PA, Dumeaux V, Sloboda DM, Kimmins S. Paternal obesity alters the sperm epigenome and is associated with changes in the placental transcriptome and cellular composition. *bioRxiv*. January 2022:2022.08.30.503982. doi:10.1101/2022.08.30.503982
598. Gernand AD, Schulze KJ, Stewart CP, West KPJ, Christian P. Micronutrient deficiencies in pregnancy worldwide: health effects and prevention. *Nat Rev Endocrinol*. 2016;12(5):274-289. doi:10.1038/nrendo.2016.37
599. Braun JM, Messerlian C, Hauser R. Fathers Matter: Why It's Time to Consider the Impact of Paternal Environmental Exposures on Children's Health. *Curr Epidemiol reports*. 2017;4(1):46-55. doi:10.1007/s40471-017-0098-8
600. Donkin I, Barrès R. Sperm epigenetics and influence of environmental factors. *Mol Metab*. 2018;14:1-11. doi:https://doi.org/10.1016/j.molmet.2018.02.006
601. Wu H, Estill MS, Shershebnev A, et al. Preconception urinary phthalate concentrations and sperm DNA methylation profiles among men undergoing IVF treatment: a cross-sectional study. *Hum Reprod*. 2017;32(11):2159-2169. doi:10.1093/humrep/dex283
602. Pilsner JR, Shershebnev A, Wu H, et al. Aging-induced changes in sperm DNA methylation are modified by low dose of perinatal flame retardants. *Epigenomics*. 2021;13(4):285-297. doi:10.2217/epi-2020-0404
603. Kaati G, Bygren LO, Edvinsson S. Cardiovascular and diabetes mortality determined by nutrition during parents' and grandparents' slow growth period. *Eur J Hum Genet*. 2002;10(11):682-688. doi:10.1038/sj.ejhg.5200859
604. Lumey LH, Poppel FWA Van. The Dutch Famine of 1944-45 as a Human Laboratory : Changes in the Early Life Environment and Adult Health. In: Lumey, L. H. and Vaiserman A, ed. *Early Life Nutrition and Adult Health and Development*. Nova Science Publishers, Inc.; 2013:59-76.
605. Dalgaard K, Landgraf K, Heyne S, et al. Trim28 Haploinsufficiency Triggers Bi-stable Epigenetic Obesity. *Cell*. 2016;164(3):353-364. doi:10.1016/j.cell.2015.12.025
606. Cropley JE, Eaton SA, Aiken A, et al. Male-lineage transmission of an acquired metabolic phenotype induced by grand-paternal obesity. *Mol Metab*. 2016;5(8):699-708. doi:10.1016/j.molmet.2016.06.008
607. de Castro Barbosa T, Ingerslev LR, Alm PS, et al. High-fat diet reprograms the epigenome of rat spermatozoa and transgenerationally affects metabolism of the offspring. *Mol Metab*. 2016;5(3):184-197. doi:10.1016/j.molmet.2015.12.002
608. Lambrot R, Siklenka K, Lafleur C, Kimmins S. The genomic distribution of histone H3K4me2 in spermatogonia is highly conserved in sperm. *Biol Reprod*. 2019;100(6):1661-1672. doi:10.1093/biolre/ioz055
609. Lambrot R. Whole genome sequencing of H3 lysine 4 tri-methylation and DNA methylation in human sperm reveals regions of overlap and exclusion linked to fertility, development and epigenetic inheritance. *Cell Rep*. 2021;CELL-REPOR.
610. Stringer JM, Forster SC, Qu Z, et al. Reduced PRC2 function alters male germline epigenetic programming and paternal inheritance. *BMC Biol*. 2018;16(1):1-20. doi:10.1186/s12915-018-0569-5
611. Lesch BJ, Tothova Z, Morgan EA, et al. Intergenerational epigenetic inheritance of cancer susceptibility in mammals. *Elife*. 2019;8:1-29. doi:10.7554/elife.39380

612. Lainez NM, Jonak CR, Nair MG, et al. Diet-induced obesity elicits macrophage infiltration and reduction in spine density in the hypothalami of male but not female mice. *Front Immunol*. 2018;9(SEP):1-16. doi:10.3389/fimmu.2018.01992
613. Ayala JE, Samuel VT, Morton GJ, et al. Standard operating procedures for describing and performing metabolic tests of glucose homeostasis in mice. *DMM Dis Model Mech*. 2010;3(9-10):525-534. doi:10.1242/dmm.006239
614. Hisano M, Erkek S, Dessus-Babus S, Ramos L, Stadler MB, Peters AHFM. Genome-wide chromatin analysis in mature mouse and human spermatozoa. *Nat Protoc*. 2013;8(12):2449-2470. doi:10.1038/nprot.2013.145
615. Lismer A, Lambrot R, Lafleur C, Dumeaux V, Kimmins S. ChIP-seq protocol for sperm cells and embryos to assess environmental impacts and epigenetic inheritance. *STAR Protoc*. 2021;2(2):100602. doi:https://doi.org/10.1016/j.xpro.2021.100602
616. Krueger F. Trim galore. *A wrapper tool around Cutadapt FastQC to consistently apply Qual Adapt trimming to FastQ files*. 2015;516:517.
617. Kim D, Langmead B, Salzberg SL. HISAT: a fast spliced aligner with low memory requirements. *Nat Methods*. 2015;12(4):357-360. doi:10.1038/nmeth.3317
618. Li H, Handsaker B, Wysoker A, et al. The Sequence Alignment/Map format and SAMtools. *Bioinformatics*. 2009;25(16):2078-2079. doi:10.1093/bioinformatics/btp352
619. Pertea M, Pertea GM, Antonescu CM, Chang T-C, Mendell JT, Salzberg SL. StringTie enables improved reconstruction of a transcriptome from RNA-seq reads. *Nat Biotechnol*. 2015;33(3):290-295. doi:10.1038/nbt.3122
620. Bolger AM, Lohse M, Usadel B. Trimmomatic : a flexible trimmer for Illumina sequence data. *Bioinformatics*. 2014;30(15):2114-2120. doi:10.1093/bioinformatics/btu170
621. Salzberg BL and SL. Fast gapped-read alignment with Bowtie 2. *Nat Methods*. 2013;9(4):357-359. doi:10.1038/nmeth.1923.Fast
622. Ramírez F, Ryan DP, Grüning B, et al. deepTools2: a next generation web server for deep-sequencing data analysis. *Nucleic Acids Res*. 2016;44(W1):W160-5. doi:10.1093/nar/gkw257
623. Liu X, Wang C, Liu W, et al. Distinct features of H3K4me3 and H3K27me3 chromatin domains in pre-implantation embryos. *Nature*. 2016;537(7621):558-562. doi:10.1038/nature19362
624. Liu L, Leng L, Liu C, et al. An integrated chromatin accessibility and transcriptome landscape of human pre-implantation embryos. *Nat Commun*. 2019;10(1):364. doi:10.1038/s41467-018-08244-0
625. Shen Y, Yue F, McCleary DF, et al. A map of the cis-regulatory sequences in the mouse genome. *Nature*. 2012;488(7409):116-120. doi:10.1038/nature11243
626. Chu A, Casero D, Thamotharan S, Wadehra M, Cosi A, Devaskar SU. The Placental Transcriptome in Late Gestational Hypoxia Resulting in Murine Intrauterine Growth Restriction Parallels Increased Risk of Adult Cardiometabolic Disease. *Sci Rep*. 2019;9(1):1243. doi:10.1038/s41598-018-37627-y
627. Krueger F, Andrews SR. SNPsplit: Allele-specific splitting of alignments between genomes with known SNP genotypes [version 1; referees: 3 approved]. *F1000Research*. 2016;5:1-15. doi:10.12688/F1000RESEARCH.9037.1

628. Waskom ML. seaborn : statistical data visualization Statement of need. *J Open Source Softw*. 2021;6:1-4. doi:10.21105/joss.03021
629. Harris CR, Millman KJ, van der Walt SJ, et al. Array programming with NumPy. *Nature*. 2020;585(7825):357-362. doi:10.1038/s41586-020-2649-2
630. Mckinney W. Data Structures for Statistical Computing in Python. In: *Proceedings of the 9th Python in Science Conference*. Vol 1. ; 2010:56-61.
631. Hunter JD. Matplotlib: A 2D Graphics Environment. *Comput Sci Eng*. 2007;9(3):90-95. doi:10.1109/MCSE.2007.55
632. Team RC. R: A language and environment for statistical computing. 2018.
633. Love MI, Huber W, Anders S. Moderated estimation of fold change and dispersion for RNA-seq data with DESeq2. *Genome Biol*. 2014;15(12):1-21. doi:10.1186/s13059-014-0550-8
634. Ignatiadis N, Klaus B, Zaugg JB, Huber W. Data-driven hypothesis weighting increases detection power in genome-scale multiple testing. *Nat Methods*. 2016;13(7):577-580. doi:10.1038/nmeth.3885
635. Benjamini Y, Hochberg Y. Controlling the False Discovery Rate: A Practical and Powerful Approach to Multiple Testing. *J R Stat Soc Ser B*. 1995;57(1):289-300. http://www.jstor.org/stable/2346101.
636. Yi L, Pimentel H, Bray NL, Pachter L. Gene-level differential analysis at transcript-level resolution. *Genome Biol*. 2018;19(1):1-11. doi:10.1186/s13059-018-1419-z
637. Ritchie ME, Phipson B, Wu D, et al. limma powers differential expression analyses for RNA-sequencing and microarray studies. *Nucleic Acids Res*. 2015;43(7):e47. doi:10.1093/nar/gkv007
638. Taiyun, Wei, Simko V. R package “corrplot”: Visualization of a Correlation Matrix. 2021. https://github.com/taiyun/corrplot.
639. Kolde R. pheatmap: Pretty Heatmaps. R package. 2019. https://cran.r-project.org/package=pheatmap.
640. Wickham H. *Ggplot2: Elegant Graphics for Data Analysis*. New York: Springer-Verlag; 2016. https://ggplot2.tidyverse.org.
641. Shen L. GeneOverlap : An R package to test and visualize gene overlaps. 2014:1-10.
642. Brionne A, Juanchich A, Hennequet-Antier C. ViSEAGO: A Bioconductor package for clustering biological functions using Gene Ontology and semantic similarity. *BioData Min*. 2019;12(1):1-13. doi:10.1186/s13040-019-0204-1
643. Lun ATL, Smyth GK. csaw: a Bioconductor package for differential binding analysis of ChIP-seq data using sliding windows. *Nucleic Acids Res*. 2016;44(5):e45. doi:10.1093/nar/gkv1191
644. Zhang Y, Parmigiani G, Johnson WE. ComBat-seq: batch effect adjustment for RNA-seq count data. *NAR Genomics Bioinforma*. 2020;2(3). doi:10.1093/nargab/lqaa078
645. Leek JT, Johnson WE, Parker HS, Jaffe AE, Storey JD. The sva package for removing batch effects and other unwanted variation in high-throughput experiments. *Bioinformatics*. 2012;28(6):882-883. doi:10.1093/bioinformatics/bts034
646. Oksanen J, Kindt R, Legendre P, et al. The vegan package. *Community Ecol Packag*. 2007;10(631-637):719.

647. Welch RP, Lee C, Imbriano PM, et al. ChIP-Enrich: gene set enrichment testing for ChIP-seq data. *Nucleic Acids Res*. 2014;42(13):e105-e105. doi:10.1093/nar/gku463
648. Alexa A, Rahnenführer J, Lengauer T. Improved scoring of functional groups from gene expression data by decorrelating GO graph structure. *Bioinformatics*. 2006;22(13):1600-1607. doi:10.1093/bioinformatics/btl140
649. Cavalcante RG, Sartor MA. annotatr: genomic regions in context. *Bioinformatics*. 2017;33(15):2381-2383. doi:10.1093/bioinformatics/btx183
650. Conway JR, Lex A, Gehlenborg N. UpSetR: an R package for the visualization of intersecting sets and their properties. *Bioinformatics*. 2017;33(18):2938-2940. doi:10.1093/bioinformatics/btx364
651. Gel B, Díez-Villanueva A, Serra E, Buschbeck M, Peinado MA, Malinverni R. regioneR: an R/Bioconductor package for the association analysis of genomic regions based on permutation tests. *Bioinformatics*. 2016;32(2):289-291. doi:10.1093/bioinformatics/btv562
652. Pohl A, Beato M. bwtool: a tool for bigWig files. *Bioinformatics*. 2014;30(11):1618-1619. doi:10.1093/bioinformatics/btu056
653. Kim S, Sohn I, Ahn J-I, Lee K-H, Lee YS, Lee YS. Hepatic gene expression profiles in a long-term high-fat diet-induced obesity mouse model. *Gene*. 2004;340(1):99-109. doi:10.1016/j.gene.2004.06.015
654. Fei X, Jiali D, Yajie G, et al. BTG1 ameliorates liver steatosis by decreasing stearoyl-CoA desaturase 1 (SCD1) abundance and altering hepatic lipid metabolism. *Sci Signal*. 2016;9(428):ra50-ra50. doi:10.1126/scisignal.aad8581
655. Støy J, Kampmann U, Mengel A, et al. Reduced CD300LG mRNA tissue expression, increased intramyocellular lipid content and impaired glucose metabolism in healthy male carriers of Arg82Cys in CD300LG: a novel genometabolic cross-link between CD300LG and common metabolic phenotypes. *BMJ open diabetes Res care*. 2015;3(1):e000095. doi:10.1136/bmjdrc-2015-000095
656. Perie L, Verma N, Mueller E. The forkhead box transcription factor FoxP4 regulates thermogenic programs in adipocytes. *J Lipid Res*. 2021;62. doi:10.1016/j.jlr.2021.100102
657. Lacroix M, Linares LK, Rueda-Rincon N, et al. The multifunctional protein E4F1 links P53 to lipid metabolism in adipocytes. *Nat Commun*. 2021;12(1):7037. doi:10.1038/s41467-021-27307-3
658. Lu D, Xia Q, Yang Z, et al. ENO3 promoted the progression of NASH by negatively regulating ferroptosis via elevation of GPX4 expression and lipid accumulation. *Ann Transl Med Vol 9, No 8 (April 2021) Ann Transl Med*. 2021. https://atm.amegroups.com/article/view/68207.
659. Jia X, Zhai T. Integrated Analysis of Multiple Microarray Studies to Identify Novel Gene Signatures in Non-alcoholic Fatty Liver Disease. *Front Endocrinol (Lausanne)*. 2019;10. doi:10.3389/fendo.2019.00599
660. Chu Y, Rosso LG, Huang P, et al. Liver Med23 ablation improves glucose and lipid metabolism through modulating FOXO1 activity. *Cell Res*. 2014;24(10):1250-1265. doi:10.1038/cr.2014.120
661. Iwasaki H. Impaired PRMT1 activity in the liver and pancreas of type 2 diabetic

Goto–Kakizaki rats. *Life Sci*. 2009;85(3):161-166. doi:https://doi.org/10.1016/j.lfs.2009.05.007
662. Choi S, Choi D, Lee Y-K, et al. Depletion of Prmt1 in Adipocytes Impairs Glucose Homeostasis in Diet-Induced Obesity. *Diabetes*. 2021;70(8):1664-1678. doi:10.2337/db20-1050
663. Pacana T, Cazanave S, Verdianelli A, et al. Dysregulated Hepatic Methionine Metabolism Drives Homocysteine Elevation in Diet-Induced Nonalcoholic Fatty Liver Disease. *PLoS One*. 2015;10(8):e0136822. doi:10.1371/journal.pone.0136822
664. Gerdes P, Richardson SR, Mager DL, Faulkner GJ. Transposable elements in the mammalian embryo: pioneers surviving through stealth and service. *Genome Biol*. 2016;17:100. doi:10.1186/s13059-016-0965-5
665. The Jackson Laboratory. Mouse Genome Informatics. http://www.informatics.jax.org. Published 2022.
666. Chu A, Casero D, Thamotharan S, Wadehra M, Cosi A, Devaskar SU. The Placental Transcriptome in Late Gestational Hypoxia Resulting in Murine Intrauterine Growth Restriction Parallels Increased Risk of Adult Cardiometabolic Disease. *Sci Rep*. 2019;9(1):1-15. doi:10.1038/s41598-018-37627-y
667. Naruse M, Ono R, Irie M, et al. Sirh7/Ldoc1 knockout mice exhibit placental P4 overproduction and delayed parturition. *Development*. 2014;141(24):4763-4771. doi:10.1242/dev.114520
668. Henke C, Strissel PL, Schubert M-T, et al. Selective expression of sense and antisense transcripts of the sushi-ichi-related retrotransposon – derived family during mouse placentogenesis. *Retrovirology*. 2015;12(1):9. doi:10.1186/s12977-015-0138-8
669. Shan N, Xiao X, Chen Y, et al. Expression of DAB2IP in human trophoblast and its role in trophoblast invasion. *J Matern neonatal Med Off J Eur Assoc Perinat Med Fed Asia Ocean Perinat Soc Int Soc Perinat Obstet*. 2016;29(3):393-399. doi:10.3109/14767058.2014.1001974
670. Perschbacher KJ, Deng G, Sandgren JA, et al. Reduced mRNA Expression of RGS2 (Regulator of G Protein Signaling-2) in the Placenta Is Associated With Human Preeclampsia and Sufficient to Cause Features of the Disorder in Mice. *Hypertens (Dallas, Tex 1979)*. 2020;75(2):569-579. doi:10.1161/HYPERTENSIONAHA.119.14056
671. Lambrot R, Lafleur C, Kimmins S. The histone demethylase KDM1A is essential for the maintenance and differentiation of spermatogonial stem cells and progenitors. *FASEB J*. 2015;29(11):4402-4416. doi:10.1096/fj.14-267328
672. Maezawa S, Yukawa M, Alavattam KG, Barski A, Namekawa SH. Dynamic reorganization of open chromatin underlies diverse transcriptomes during spermatogenesis. *Nucleic Acids Res*. 2018;46(2):593-608. doi:10.1093/nar/gkx1052
673. Sánchez-Margalet V, Valle M, Ruz FJ, Gascón F, Mateo J, Goberna R. Elevated plasma total homocysteine levels in hyperinsulinemic obese subjects. *J Nutr Biochem*. 2002;13(2):75-79. doi:https://doi.org/10.1016/S0955-2863(01)00197-8
674. Karatela RA, Sainani GS. Plasma homocysteine in obese, overweight and normal weight hypertensives and normotensives. *Indian Heart J*. 2009;61(2):156-159.

675. Morgan HD, Sutherland HGE, Martin DIK, Whitelaw E. Epigenetic inheritance at the agouti locus in the mouse. *Nat Genet*. 1999;23(3):314-318. doi:10.1038/15490
676. Dolinoy DC, Weidman JR, Waterland RA, Jirtle RL. Maternal genistein alters coat color and protects Avy mouse offspring from obesity by modifying the fetal epigenome. *Environ Health Perspect*. 2006;114(4):567-572. doi:10.1289/ehp.8700
677. Anway MD, Cupp AS, Uzumcu M, Skinner MK. Epigenetic Transgenerational Actions of Endocrine Disruptors and Male Fertility. *Science (80-)*. 2005;308(5727):1466 LP - 1469. doi:10.1126/science.1108190
678. Martínez D, Pentinat T, Ribó S, et al. In utero undernutrition in male mice programs liver lipid metabolism in the second-generation offspring involving altered Lxra DNA methylation. *Cell Metab*. 2014;19(6):941-951. doi:10.1016/j.cmet.2014.03.026
679. Carone BR, Fauquier L, Habib N, et al. Paternally-induced transgenerational environmental reprogramming of metabolic gene expression in mammals Benjamin. 2011;143(7):1084-1096. doi:10.1016/j.cell.2010.12.008.Paternally-induced
680. Kerr B, Leiva A, Farías M, et al. Foetoplacental epigenetic changes associated with maternal metabolic dysfunction. *Placenta*. 2018;69:146-152. doi:10.1016/j.placenta.2018.04.006
681. Franzago M, Fraticelli F, Stuppia L, Vitacolonna E. Nutrigenetics , epigenetics and gestational diabetes : consequences in mother and child. *Epigenetics*. 2019;14(3):215-235. doi:10.1080/15592294.2019.1582277
682. Moore T. Genetic conflict, genomic imprinting and establishment of the epigenotype in relation to growth. *Reproduction*. 2001;122(2):185-193. doi:10.1530/rep.0.1220185
683. Rosenfeld CS. Sex-Specific Placental Responses in Fetal Development. *Endocrinology*. 2015;156(10):3422-3434. doi:10.1210/en.2015-1227
684. Naruse K, Tsunemi T, Kawahara N, Kobayashi H. Preliminary evidence of a paternal-maternal genetic conflict on the placenta: Link between imprinting disorder and multi-generational hypertensive disorders. *Placenta*. 2019;84:69-73. doi:https://doi.org/10.1016/j.placenta.2019.02.009
685. Denomme MM, Haywood ME, Parks JC, Schoolcraft WB, Katz-Jaffe MG. The inherited methylome landscape is directly altered with paternal aging and associated with offspring neurodevelopmental disorders. *Aging Cell*. 2020;19(8):e13178. doi:https://doi.org/10.1111/acel.13178
686. Denomme MM, Parks JC, McCallie BR, McCubbin NI, Schoolcraft WB, Katz-Jaffe MG. Advanced paternal age directly impacts mouse embryonic placental imprinting. *PLoS One*. 2020;15(3):1-13. doi:10.1371/journal.pone.0229904
687. Gabory A, Attig L, Junien C. Developmental programming and epigenetics. *Am J Clin Nutr*. 2011;94(suppl_6):1943S-1952S. doi:10.3945/ajcn.110.000927
688. Nelissen ECM, van Montfoort APA, Dumoulin JCM, Evers JLH. Epigenetics and the placenta. *Hum Reprod Update*. 2011;17(3):397-417. doi:10.1093/humupd/dmq052
689. Jazwiec PA, Patterson VS, Ribeiro TA, et al. Paternal obesity results in placental hypoxia and sex-specific impairments in placental vascularization and offspring

metabolic function. *bioRxiv*. January 2021:2021.03.27.437284. doi:10.1101/2021.03.27.437284
690. Leavey K, Wilson SL, Bainbridge SA, Robinson WP, Cox BJ. Epigenetic regulation of placental gene expression in transcriptional subtypes of preeclampsia. *Clin Epigenetics*. 2018;10(1):28. doi:10.1186/s13148-018-0463-6
691. Sun N, Chen H, Ma Y, Pang W, Wang X, Zhang Q. H3K4me3-Mediated Upregulation of LncRNA-HEIPP in Preeclampsia Placenta Affects Invasion of Trophoblast Cells. 2020;11(December):1-11. doi:10.3389/fgene.2020.559478
692. Meister S, Hahn L, Beyer S, et al. Epigenetic modification via H3K4me3 and H3K9ac in human placenta is reduced in preeclampsia. *J Reprod Immunol*. 2021;145:103287. doi:https://doi.org/10.1016/j.jri.2021.103287
693. Eriksson JG, Kajantie E, Osmond C, Thornburg K, Barker DJP. Boys live dangerously in the womb. *Am J Hum Biol Off J Hum Biol Counc*. 2010;22(3):330-335. doi:10.1002/ajhb.20995
694. Gupte AA, Pownall HJ, Hamilton DJ. Estrogen : An Emerging Regulator of Insulin Action and Mitochondrial Function. 2015;2015.
695. Barratt CLR, De Jonge CJ, Anderson RA, et al. A global approach to addressing the policy, research and social challenges of male reproductive health. *Hum Reprod open*. 2021;2021(1):hoab009. doi:10.1093/hropen/hoab009
696. Mitchell M, Strick R, Strissel PL, et al. Gene expression and epigenetic aberrations in F1-placentas fathered by obese males. *Mol Reprod Dev*. 2017;84(4):316-328. doi:10.1002/mrd.22784
697. Brosens I, Pijnenborg R, Vercruysse L, Romero R. The “Great Obstetrical Syndromes” are associated with disorders of deep placentation. *Am J Obstet Gynecol*. 2011;204(3):193-201. doi:10.1016/j.ajog.2010.08.009
698. Eriksson JG, Kajantie E, Thornburg K, Osmond C. Prenatal and maternal characteristics and later risk for coronary heart disease among women. *Eur J Prev Cardiol*. 2016;23(4):385-390. doi:10.1177/2047487315595314
699. Mierzynski R, Dluski D, Darmochwal-Kolarz D, et al. Intra-uterine Growth Retardation as a Risk Factor of Postnatal Metabolic Disorders. *Curr Pharm Biotechnol*. 2016;17(7):587-596. doi:10.2174/1389201017666160301104323
700. Crispi F, Bijnens B, Figueras F, et al. Fetal growth restriction results in remodeled and less efficient hearts in children. *Circulation*. 2010;121(22):2427-2436. doi:10.1161/CIRCULATIONAHA.110.937995
701. Cruz-Lemini M, Crispi F, Valenzuela-Alcaraz B, et al. Fetal cardiovascular remodeling persists at 6 months in infants with intrauterine growth restriction. *Ultrasound Obstet Gynecol*. 2016;48(3):349-356. doi:10.1002/uog.15767
702. Sarvari SI, Rodriguez-Lopez M, Nuñez-Garcia M, et al. Persistence of Cardiac Remodeling in Preadolescents With Fetal Growth Restriction. *Circ Cardiovasc Imaging*. 2017;10(1). doi:10.1161/CIRCIMAGING.116.005270
703. Brodszki J, Länne T, Marsál K, Ley D. Impaired vascular growth in late adolescence after intrauterine growth restriction. *Circulation*. 2005;111(20):2623-2628. doi:10.1161/CIRCULATIONAHA.104.490326
704. Morsing E, Liuba P, Fellman V, Maršál K, Brodszki J. Cardiovascular function in children born very preterm after intrauterine growth restriction with severely abnormal umbilical artery blood flow. *Eur J Prev Cardiol*. 2014;21(10):1257-1266.

doi:10.1177/2047487313486044
705. Menendez-Castro C, Rascher W, Hartner A. Intrauterine growth restriction - impact on cardiovascular diseases later in life. *Mol Cell Pediatr*. 2018;5(1):4. doi:10.1186/s40348-018-0082-5
706. Naismith K, Cox B. Human placental gene sets improve analysis of placental pathologies and link trophoblast and cancer invasion genes. *Placenta*. 2021;112:9-15. doi:https://doi.org/10.1016/j.placenta.2021.06.011
707. Ales KL, Druzin ML, Santini DL. Impact of advanced maternal age on the outcome of pregnancy. *Surg Gynecol Obstet*. 1990;171(3):209-216.
708. Wu Y, Chen Y, Shen M, et al. Adverse maternal and neonatal outcomes among singleton pregnancies in women of very advanced maternal age: a retrospective cohort study. *BMC Pregnancy Childbirth*. 2019;19(1):3. doi:10.1186/s12884-018-2147-9
709. Torous VF, Roberts DJ. Placentas From Women of Advanced Maternal Age: An Independent Indication for Pathologic Examination? *Arch Pathol Lab Med*. 2020;144(10):1254-1261. doi:10.5858/arpa.2019-0481-OA
710. Krielessi V, Papantoniou N, Papageorgiou I, et al. Placental Pathology and Blood Pressure's Level in Women with Hypertensive Disorders in Pregnancy. Di Renzo GC, ed. *Obstet Gynecol Int*. 2012;2012:684083. doi:10.1155/2012/684083
711. Mission JF, Marshall NE, Caughey AB. Pregnancy risks associated with obesity. *Obstet Gynecol Clin North Am*. 2015;42(2):335-353. doi:10.1016/j.ogc.2015.01.008
712. Sohlberg S, Stephansson O, Cnattingius S, Wikström A-K. Maternal body mass index, height, and risks of preeclampsia. *Am J Hypertens*. 2012;25(1):120-125. doi:10.1038/ajh.2011.175
713. MacInnis N, Woolcott CG, McDonald S, Kuhle S. Population Attributable Risk Fractions of Maternal Overweight and Obesity for Adverse Perinatal Outcomes. *Sci Rep*. 2016;6:22895. doi:10.1038/srep22895
714. Lutsiv O, Mah J, Beyene J, McDonald SD. The effects of morbid obesity on maternal and neonatal health outcomes: a systematic review and meta-analyses. *Obes Rev an Off J Int Assoc Study Obes*. 2015;16(7):531-546. doi:10.1111/obr.12283
715. Delhaes F, Giza SA, Koreman T, et al. Altered maternal and placental lipid metabolism and fetal fat development in obesity: Current knowledge and advances in non-invasive assessment. *Placenta*. 2018;69(January):118-124. doi:10.1016/j.placenta.2018.05.011
716. Pintican D, Poienar AA, Strilciuc S, Mihu D. Effects of maternal smoking on human placental vascularization: A systematic review. *Taiwan J Obstet Gynecol*. 2019;58(4):454-459. doi:10.1016/j.tjog.2019.05.004
717. Sebastiani G, Borrás-Novell C, Casanova MA, et al. The Effects of Alcohol and Drugs of Abuse on Maternal Nutritional Profile during Pregnancy. *Nutrients*. 2018;10(8):1008. doi:10.3390/nu10081008
718. Rossant J, Cross JC. Placental development: Lessons from mouse mutants. *Nat Rev Genet*. 2001;2(7):538-548. doi:10.1038/35080570
719. Russ AP, Wattler S, Colledge WH, et al. Eomesodermin is required for mouse trophoblast development and mesoderm formation. *Nature*. 2000;404(6773):95-

99. doi:10.1038/35003601
720. Ciruna BG, Rossant J. Expression of the T-box gene Eomesodermin during early mouse development. *Mech Dev*. 1999;81(1-2):199-203. doi:10.1016/s0925-4773(98)00243-3
721. Chawengsaksophak K, James R, Hammond VE, Köntgen F, Beck F. Homeosis and intestinal tumours in Cdx2 mutant mice. *Nature*. 1997;386(6620):84-87. doi:10.1038/386084a0
722. Kunath T, Strumpf D, Rossant J. Early trophoblast determination and stem cell maintenance in the mouse--a review. *Placenta*. 2004;25 Suppl A:S32-8. doi:10.1016/j.placenta.2004.01.015
723. Chen Y, Wang K, Gong YG, Khoo SK, Leach R. Roles of CDX2 and EOMES in human induced trophoblast progenitor cells. *Biochem Biophys Res Commun*. 2013;431(2):197-202. doi:10.1016/j.bbrc.2012.12.135
724. Guillemot F, Nagy A, Auerbach A, Rossant J, Joyner AL. Essential role of Mash-2 in extraembryonic development. *Nature*. 1994;371(6495):333-336. doi:10.1038/371333a0
725. Tanaka M, Gertsenstein M, Rossant J, Nagy A. Mash2 acts cell autonomously in mouse spongiotrophoblast development. *Dev Biol*. 1997;190(1):55-65. doi:10.1006/dbio.1997.8685
726. Threadgill DW, Dlugosz AA, Hansen LA, et al. Targeted Disruption of Mouse EGF Receptor: Effect of Genetic Background on Mutant Phenotype. *Science (80-)*. 1995;269(5221):230-234. http://www.jstor.org/stable/2888447.
727. Sibilia M, Wagner EF. Strain-dependent epithelial defects in mice lacking the EGF receptor. *Science*. 1995;269(5221):234-238. doi:10.1126/science.7618085
728. Guillemot F, Caspary T, Tilghman SM, et al. Genomic imprinting of Mash2, a mouse gene required for trophoblast development. *Nat Genet*. 1995;9(3):235-242. doi:10.1038/ng0395-235
729. Ferguson-Smith AC, Cattanach BM, Barton SC, Beechey C V, Surani MA. Embryological and molecular investigations of parental imprinting on mouse chromosome 7. *Nature*. 1991;351(6328):667-670. doi:10.1038/351667a0
730. McEwen KR, Ferguson-Smith AC. Distinguishing epigenetic marks of developmental and imprinting regulation. *Epigenetics Chromatin*. 2010;3(1):2. doi:10.1186/1756-8935-3-2
731. Dindot S V, Person R, Strivens M, Garcia R, Beaudet AL. Epigenetic profiling at mouse imprinted gene clusters reveals novel epigenetic and genetic features at differentially methylated regions. *Genome Res*. 2009;19(8):1374-1383. doi:10.1101/gr.089185.108
732. Wen B, Wu H, Bjornsson H, Green RD, Irizarry R, Feinberg AP. Overlapping euchromatin/heterochromatin- associated marks are enriched in imprinted gene regions and predict allele-specific modification. *Genome Res*. 2008;18(11):1806-1813. doi:10.1101/gr.067587.108
733. McMinn J, Wei M, Schupf N, et al. Unbalanced placental expression of imprinted genes in human intrauterine growth restriction. *Placenta*. 2006;27(6-7):540-549. doi:10.1016/j.placenta.2005.07.004
734. Monk D. Genomic imprinting in the human placenta. *Am J Obstet Gynecol*. 2015;213(4):S152-S162. doi:10.1016/j.ajog.2015.06.032

735. Zadora J, Singh M, Herse F, et al. Disturbed Placental Imprinting in Preeclampsia Leads to Altered Expression of DLX5, a Human-Specific Early Trophoblast Marker. *Circulation*. 2017;136(19):1824-1839. doi:10.1161/CIRCULATIONAHA.117.028110
736. Lin J, Gu W, Huang H. Effects of Paternal Obesity on Fetal Development and Pregnancy Complications: A Prospective Clinical Cohort Study. *Front Endocrinol (Lausanne)*. 2022;13. doi:10.3389/fendo.2022.826665
737. Aliee H, Theis FJ. AutoGeneS: Automatic gene selection using multi-objective optimization for RNA-seq deconvolution. *Cell Syst*. 2021;12(7):706-715.e4. doi:https://doi.org/10.1016/j.cels.2021.05.006
738. Han X, Wang R, Zhou Y, et al. Mapping the Mouse Cell Atlas by Microwell-Seq. *Cell*. 2018;172(5):1091-1107.e17. doi:10.1016/j.cell.2018.02.001
739. Cuffe JSM, Walton SL, Singh RR, et al. Mid- to late term hypoxia in the mouse alters placental morphology, glucocorticoid regulatory pathways and nutrient transporters in a sex-specific manner. *J Physiol*. 2014;592(14):3127-3141. doi:10.1113/jphysiol.2014.272856
740. Kim D, Langmead B, Salzberg SL. HISAT: a fast spliced aligner with low memory requirements. 2016;12(4):357-360. doi:10.1038/nmeth.3317.HISAT
741. Van Rossum, Guido; Drake FL. *Python 3 Reference Manual*. Scotts Valley, CA: CreateSpace; 2009.
742. Ferrari S, Cribari-Neto F. Beta Regression for Modelling Rates and Proportions. *J Appl Stat*. 2004;31(7):799-815. doi:10.1080/0266476042000214501
743. Lawrence M, Gentleman R, Carey V. rtracklayer: an R package for interfacing with genome browsers. *Bioinformatics*. 2009;25(14):1841-1842. doi:10.1093/bioinformatics/btp328
744. Heintzman ND, Stuart RK, Hon G, et al. Distinct and predictive chromatin signatures of transcriptional promoters and enhancers in the human genome. *Nat Genet*. 2007;39(3):311-318. doi:10.1038/ng1966
745. Jaffe AE, Murakami P, Lee H, et al. Bump hunting to identify differentially methylated regions in epigenetic epidemiology studies. *Int J Epidemiol*. 2012;41(1):200-209. doi:10.1093/ije/dyr238
746. Aryee MJ, Jaffe AE, Corrada-Bravo H, et al. Minfi: a flexible and comprehensive Bioconductor package for the analysis of Infinium DNA methylation microarrays. *Bioinformatics*. 2014;30(10):1363-1369. doi:10.1093/bioinformatics/btu049
747. Heinz S, Benner C, Spann N, et al. Simple combinations of lineage-determining transcription factors prime cis-regulatory elements required for macrophage and B cell identities. *Mol Cell*. 2010;38(4):576-589. doi:10.1016/j.molcel.2010.05.004
748. Love MI, Huber W, Anders S. Moderated estimation of fold change and dispersion for RNA-seq data with DESeq2. *Genome Biol*. 2014;15(12):550. doi:10.1186/s13059-014-0550-8
749. Yi L, Pimentel H, Bray NL, Pachter L. Gene-level differential analysis at transcript-level resolution. *Genome Biol*. 2018;19(1):1-24. doi:10.1186/s13059-018-1419-z
750. Love MI, Huber W, Anders S. Moderated estimation of fold change and dispersion for RNA-seq data with DESeq2. *Genome Biol*. 2014;15(12):1-21. doi:10.1186/s13059-014-0550-8
751. Van Rossum G. The Python Library Reference, release 3.8.2. 2020.

752. Wolf FA, Angerer P, Theis FJ. SCANPY: large-scale single-cell gene expression data analysis. *Genome Biol*. 2018;19(1):15. doi:10.1186/s13059-017-1382-0
753. Virtanen P, Gommers R, Oliphant TE, et al. SciPy 1.0: fundamental algorithms for scientific computing in Python. *Nat Methods*. 2020;17(3):261-272. doi:10.1038/s41592-019-0686-2
754. Pedregosa F, Varoquaux G, Gramfort A, et al. Scikit-Learn: Machine Learning in Python. *J Mach Learn Res*. 2011;12(null):2825–2830.
755. Kadakia R, Josefson J. The Relationship of Insulin-Like Growth Factor 2 to Fetal Growth and Adiposity. *Horm Res Paediatr*. 2016;85(2):75-82. doi:10.1159/000443500
756. St-Pierre J, Hivert M-F, Perron P, et al. IGF2 DNA methylation is a modulator of newborn's fetal growth and development. *Epigenetics*. 2012;7(10):1125-1132. doi:10.4161/epi.21855
757. Livingstone C, Borai A. Insulin-like growth factor-II: its role in metabolic and endocrine disease. *Clin Endocrinol (Oxf)*. 2014;80(6):773-781. doi:10.1111/cen.12446
758. Cano-Rodriguez D, Gjaltema RAF, Jilderda LJ, et al. Writing of H3K4Me3 overcomes epigenetic silencing in a sustained but context-dependent manner. *Nat Commun*. 2016;7(1):12284. doi:10.1038/ncomms12284
759. Lauberth SM, Nakayama T, Wu X, et al. H3K4me3 interactions with TAF3 regulate preinitiation complex assembly and selective gene activation. *Cell*. 2013;152(5):1021-1036. doi:10.1016/j.cell.2013.01.052
760. Jung YH, Kremsky I, Gold HB, et al. Maintenance of CTCF- and Transcription Factor-Mediated Interactions from the Gametes to the Early Mouse Embryo. *Mol Cell*. 2019;75(1):154-171.e5. doi:10.1016/j.molcel.2019.04.014
761. Dura M, Teissandier A, Armand M, et al. DNMT3A-dependent DNA methylation is required for spermatogonial stem cells to commit to spermatogenesis. *Nat Genet*. 2022;54(4):469-480. doi:10.1038/s41588-022-01040-z
762. Yin Y, Morgunova E, Jolma A, et al. Impact of cytosine methylation on DNA binding specificities of human transcription factors. *Science*. 2017;356(6337). doi:10.1126/science.aaj2239
763. Lea AJ, Vockley CM, Johnston RA, et al. Genome-wide quantification of the effects of DNA methylation on human gene regulation. Ponting CP, Weigel D, Aerts S, eds. *Elife*. 2018;7:e37513. doi:10.7554/eLife.37513
764. Domcke S, Bardet AF, Adrian Ginno P, Hartl D, Burger L, Schübeler D. Competition between DNA methylation and transcription factors determines binding of NRF1. *Nature*. 2015;528(7583):575-579. doi:10.1038/nature16462
765. Tang H, Pan L, Xiong Y, et al. Down-regulation of the Sp1 transcription factor by an increase of microRNA-4497 in human placenta is associated with early recurrent miscarriage. *Reprod Biol Endocrinol*. 2021;19(1):21. doi:10.1186/s12958-021-00701-8
766. Hemberger M, Hanna CW, Dean W. Mechanisms of early placental development in mouse and humans. *Nat Rev Genet*. 2020;21(1):27-43. doi:10.1038/s41576-019-0169-4
767. Glavas MM, Lee AY, Miao I, et al. Developmental Timing of High-Fat Diet Exposure Impacts Glucose Homeostasis in Mice in a Sex-Specific Manner.

Diabetes. 2021;70(12):2771-2784. doi:10.2337/db21-0310
768. McPherson NO, Bell VG, Zander-Fox DL, et al. When two obese parents are worse than one! Impacts on embryo and fetal development. *Am J Physiol Metab*. 2015;309(6):E568-E581. doi:10.1152/ajpendo.00230.2015
769. Tramunt B, Smati S, Grandgeorge N, et al. Sex differences in metabolic regulation and diabetes susceptibility. *Diabetologia*. 2020;63(3):453-461. doi:10.1007/s00125-019-05040-3
770. Sandovici I, Fernandez-Twinn DS, Hufnagel A, Constância M, Ozanne SE. Sex differences in the intergenerational inheritance of metabolic traits. *Nat Metab*. 2022. doi:10.1038/s42255-022-00570-4
771. Wood AJ, Oakey RJ. Genomic imprinting in mammals: emerging themes and established theories. *PLoS Genet*. 2006;2(11):e147. doi:10.1371/journal.pgen.0020147
772. Moore T, Haig D. Genomic imprinting in mammalian development: a parental tug-of-war. *Trends Genet*. 1991;7(2):45-49. doi:10.1016/0168-9525(91)90230-N
773. Bressan FF, De Bem THC, Perecin F, et al. Unearthing the Roles of Imprinted Genes in the Placenta. *Placenta*. 2009;30(10):823-834. doi:10.1016/j.placenta.2009.07.007
774. Haig D, Graham C. Genomic imprinting and the strange case of the insulin-like growth factor II receptor. *Cell*. 1991;64(6):1045-1046. doi:10.1016/0092-8674(91)90256-x
775. Li Y, Salamonsen LA, Hyett J, Costa F da S, Nie G. Maternal HtrA3 optimizes placental development to influence offspring birth weight and subsequent white fat gain in adulthood. *Sci Rep*. 2017;7(1):4627. doi:10.1038/s41598-017-04867-3
776. Kappil MA, Green BB, Armstrong DA, et al. Placental expression profile of imprinted genes impacts birth weight. *Epigenetics*. 2015;10(9):842-849. doi:10.1080/15592294.2015.1073881
777. Bryant D, Seda M, Peskett E, et al. Diverse species-specific phenotypic consequences of loss of function sorting nexin 14 mutations. *Sci Rep*. 2020;10(1):13763. doi:10.1038/s41598-020-70797-2
778. Glaser J, Iranzo J, Borensztein M, et al. The imprinted Zdbf2 gene finely tunes control of feeding and growth in neonates. Brickman JM, Isales C, Ward A, Chamberlain S, Kelsey G, eds. *Elife*. 2022;11:e65641. doi:10.7554/eLife.65641
779. Vaughan OR, Maksym K, Silva E, et al. Placenta-specific Slc38a2/SNAT2 knockdown causes fetal growth restriction in mice. *Clin Sci (Lond)*. 2021;135(17):2049-2066. doi:10.1042/CS20210575
780. Gasperowicz M, Surmann-Schmitt C, Hamada Y, Otto F, Cross JC. The transcriptional co-repressor TLE3 regulates development of trophoblast giant cells lining maternal blood spaces in the mouse placenta. *Dev Biol*. 2013;382(1):1-14. doi:https://doi.org/10.1016/j.ydbio.2013.08.005
781. Lane M, Mcpherson NO, Fullston T, et al. Oxidative Stress in Mouse Sperm Impairs Embryo Development , Fetal Growth and Alters Adiposity and Glucose Regulation in Female Offspring. *PLoS One*. 2014;9(7):1-9. doi:10.1371/journal.pone.0100832
782. Milosevic-Stevanovic J, Krstic M, Radovic-Janosevic D, Popovic J, Tasic M, Stojnev S. Number of decidual natural killer cells & macrophages in pre-

eclampsia. *Indian J Med Res*. 2016;144(6):823-830. doi:10.4103/ijmr.IJMR_776_15
783. Williams PJ, Bulmer JN, Searle RF, Innes BA, Robson SC. Altered decidual leucocyte populations in the placental bed in pre-eclampsia and foetal growth restriction: a comparison with late normal pregnancy. *Reproduction*. 2009;138(1):177-184. doi:10.1530/REP-09-0007
784. Bachmayer N, Rafik Hamad R, Liszka L, Bremme K, Sverremark-Ekström E. Aberrant uterine natural killer (NK)-cell expression and altered placental and serum levels of the NK-cell promoting cytokine interleukin-12 in pre-eclampsia. *Am J Reprod Immunol*. 2006;56(5-6):292-301. doi:10.1111/j.1600-0897.2006.00429.x
785. Du M, Wang W, Huang L, et al. Natural killer cells in the pathogenesis of preeclampsia: a double-edged sword. *J Matern neonatal Med Off J Eur Assoc Perinat Med Fed Asia Ocean Perinat Soc Int Soc Perinat Obstet*. 2022;35(6):1028-1035. doi:10.1080/14767058.2020.1740675
786. Aneman I, Pienaar D, Suvakov S, Simic TP, Garovic VD, McClements L. Mechanisms of Key Innate Immune Cells in Early- and Late-Onset Preeclampsia. *Front Immunol*. 2020;11:1864. doi:10.3389/fimmu.2020.01864
787. de Castro Barbosa T, Ingerslev LR, Alm PS, et al. High-fat diet reprograms the epigenome of rat spermatozoa and transgenerationally affects metabolism of the offspring. *Mol Metab*. 2016;5(3):184-197. doi:10.1016/j.molmet.2015.12.002
788. Chambers TJG, Morgan MD, Heger AH, Sharpe RM, Drake AJ. High-fat diet disrupts metabolism in two generations of rats in a parent-of-origin specific manner. *Sci Rep*. 2016;6:1-11. doi:10.1038/srep31857
789. Andescavage NN, Limperopoulos C. Placental abnormalities in congenital heart disease. *Transl Pediatr*. 2021;10(8):2148-2156. doi:10.21037/tp-20-347
790. Thornburg KL, Marshall N. The placenta is the center of the chronic disease universe. *Am J Obstet Gynecol*. 2015;213(4 Suppl):S14-S20. doi:10.1016/j.ajog.2015.08.030
791. Thornburg KL, Kolahi K, Pierce M, Valent A, Drake R, Louey S. Biological features of placental programming. *Placenta*. 2016;48 Suppl 1(Suppl 1):S47-S53. doi:10.1016/j.placenta.2016.10.012
792. Ueda M, Tsuchiya KJ, Yaguchi C, et al. Placental pathology predicts infantile neurodevelopment. *Sci Rep*. 2022;12(1):2578. doi:10.1038/s41598-022-06300-w
793. Parrettini S, Caroli A, Torlone E. Nutrition and Metabolic Adaptations in Physiological and Complicated Pregnancy: Focus on Obesity and Gestational Diabetes. *Front Endocrinol (Lausanne)*. 2020;11. doi:10.3389/fendo.2020.611929
794. Prasad MS, Charney RM, García-Castro MI. Specification and formation of the neural crest: Perspectives on lineage segregation. *Genesis*. 2019;57(1):e23276. doi:10.1002/dvg.23276
795. Silva JF, Serakides R. Intrauterine trophoblast migration: A comparative view of humans and rodents. *Cell Adh Migr*. 2016;10(1-2):88-110. doi:10.1080/19336918.2015.1120397
796. O'Tierney-Ginn PF, Lash GE. Beyond pregnancy: modulation of trophoblast invasion and its consequences for fetal growth and long-term children's health. *J Reprod Immunol*. 2014;104-105:37-42.

doi:https://doi.org/10.1016/j.jri.2014.04.002
797. Barrientos G, Pussetto M, Rose M, Staff AC, Blois SM, Toblli JE. Defective trophoblast invasion underlies fetal growth restriction and preeclampsia-like symptoms in the stroke-prone spontaneously hypertensive rat. *Mol Hum Reprod*. 2017;23(7):509-519. doi:10.1093/molehr/gax024
798. Duzyj CM, Buhimschi IA, Laky CA, et al. Extravillous trophoblast invasion in placenta accreta is associated with differential local expression of angiogenic and growth factors: a cross-sectional study. *BJOG*. 2018;125(11):1441-1448. doi:10.1111/1471-0528.15176
799. S. WC, June N, Adrian T, et al. Pravastatin ameliorates placental vascular defects, fetal growth, and cardiac function in a model of glucocorticoid excess. *Proc Natl Acad Sci*. 2016;113(22):6265-6270. doi:10.1073/pnas.1520356113
800. Shnorhavorian M, Schwartz SM, Stansfeld B, Sadler-Riggleman I, Beck D, Skinner MK. Differential DNA Methylation Regions in Adult Human Sperm following Adolescent Chemotherapy: Potential for Epigenetic Inheritance. *PLoS One*. 2017;12(2):e0170085. doi:10.1371/journal.pone.0170085
801. Denham J, O'Brien BJ, Harvey JT, Charchar FJ. Genome-wide sperm DNA methylation changes after 3 months of exercise training in humans. *Epigenomics*. 2015;7(5):717-731. doi:10.2217/epi.15.29
802. Tunc O, Tremellen K. Oxidative DNA damage impairs global sperm DNA methylation in infertile men. *J Assist Reprod Genet*. 2009;26(9-10):537-544. doi:10.1007/s10815-009-9346-2
803. Marczylo EL, Amoako AA, Konje JC, Gant TW, Marczylo TH. Smoking induces differential miRNA expression in human spermatozoa: a potential transgenerational epigenetic concern? *Epigenetics*. 2012;7(5):432-439. doi:10.4161/epi.19794
804. Soubry A, Hoyo C, Butt CM, et al. Human exposure to flame-retardants is associated with aberrant DNA methylation at imprinted genes in sperm. *Environ Epigenetics*. 2017;3(1):dvx003. doi:10.1093/eep/dvx003
805. Ouko LA, Shantikumar K, Knezovich J, Haycock P, Schnugh DJ, Ramsay M. Effect of alcohol consumption on CpG methylation in the differentially methylated regions of H19 and IG-DMR in male gametes: implications for fetal alcohol spectrum disorders. *Alcohol Clin Exp Res*. 2009;33(9):1615-1627. doi:10.1111/j.1530-0277.2009.00993.x
806. Lismer A, Shao X, Dumargne MC, et al. Exposure of Greenlandic Inuit and South African VhaVenda men to the persistent DDT metabolite is associated with an altered sperm epigenome at regions implicated in paternal epigenetic transmission and developmental disease – a cross-sectional study. *bioRxiv*. January 2022:2022.08.15.504029. doi:10.1101/2022.08.15.504029
807. García-Tevijano ER, Berasain C, Rodríguez JA, et al. Hyperhomocysteinemia in liver cirrhosis: mechanisms and role in vascular and hepatic fibrosis. *Hypertens (Dallas, Tex 1979)*. 2001;38(5):1217-1221. doi:10.1161/hy1101.099499
808. Stead LM, Brosnan JT, Brosnan ME, Vance DE, Jacobs RL. Is it time to reevaluate methyl balance in humans? *Am J Clin Nutr*. 2006;83(1):5-10. doi:10.1093/ajcn/83.1.5
809. Bedford MT. Arginine methylation at a glance. *J Cell Sci*. 2007;120(Pt 24):4243-

4246. doi:10.1242/jcs.019885
810. Mato JM, Lu SC. Role of S-adenosyl-L-methionine in liver health and injury. *Hepatology*. 2007;45(5):1306-1312. doi:10.1002/hep.21650
811. Williams KT, Schalinske KL. Homocysteine metabolism and its relation to health and disease. *Biofactors*. 2010;36(1):19-24. doi:10.1002/biof.71
812. Clare CE, Brassington AH, Kwong WY, Sinclair KD. One-Carbon Metabolism: Linking Nutritional Biochemistry to Epigenetic Programming of Long-Term Development. *Annu Rev Anim Biosci*. 2019;7(1):263-287. doi:10.1146/annurev-animal-020518-115206
813. Zhang N. Role of methionine on epigenetic modification of DNA methylation and gene expression in animals. *Anim Nutr (Zhongguo xu mu shou yi xue hui)*. 2018;4(1):11-16. doi:10.1016/j.aninu.2017.08.009
814. Mattocks DAL, Mentch SJ, Shneyder J, et al. Short term methionine restriction increases hepatic global DNA methylation in adult but not young male C57BL/6J mice. *Exp Gerontol*. 2017;88:1-8. doi:10.1016/j.exger.2016.12.003
815. Shyh-Chang N, Locasale JW, Lyssiotis CA, et al. Influence of threonine metabolism on S-adenosylmethionine and histone methylation. *Science*. 2013;339(6116):222-226. doi:10.1126/science.1226603
816. Haws SA, Yu D, Cryns VL, Lamming DW, Denu Correspondence JM. Methyl-Metabolite Depletion Elicits Adaptive Responses to Support Heterochromatin Stability and Epigenetic Persistence. *Mol Cell*. 2020;78:1-14. doi:10.1016/j.molcel.2020.03.004
817. Sperber H, Mathieu J, Wang Y, et al. The metabolome regulates the epigenetic landscape during naive-to-primed human embryonic stem cell transition. *Nat Cell Biol*. 2015;17(12):1523-1535. doi:10.1038/ncb3264
818. Roy DG, Chen J, Mamane V, et al. Methionine Metabolism Shapes T Helper Cell Responses through Regulation of Epigenetic Reprogramming. *Cell Metab*. 2020;31(2):250-266.e9. doi:10.1016/j.cmet.2020.01.006
819. Sinclair L V, Howden AJ, Brenes A, et al. Antigen receptor control of methionine metabolism in T cells. *Elife*. 2019;8. doi:10.7554/eLife.44210
820. Ding W, Higgins DP, Yadav DK, Godbole AA, Pukkila-Worley R, Walker AK. Stress-responsive and metabolic gene regulation are altered in low S-adenosylmethionine. *PLoS Genet*. 2018;14(11):e1007812. doi:10.1371/journal.pgen.1007812
821. Mentch SJ, Mehrmohamadi M, Huang L, et al. Histone Methylation Dynamics and Gene Regulation Occur through the Sensing of One-Carbon Metabolism. *Cell Metab*. 2015;22(5):861-873. doi:10.1016/j.cmet.2015.08.024
822. Dai Z, Mentch SJ, Gao X, Nichenametla SN, Locasale JW. Methionine metabolism influences genomic architecture and gene expression through H3K4me3 peak width. *Nat Commun*. 2018;9(1):1955. doi:10.1038/s41467-018-04426-y
823. Shiraki N, Shiraki Y, Tsuyama T, et al. Methionine metabolism regulates maintenance and differentiation of human pluripotent stem cells. *Cell Metab*. 2014;19(5):780-794. doi:10.1016/j.cmet.2014.03.017
824. Hirsch S, Poniachick J, Avendaño M, et al. Serum folate and homocysteine levels in obese females with non-alcoholic fatty liver. *Nutrition*. 2005;21(2):137-141.

doi:10.1016/j.nut.2004.03.022
825. Vayá A, Ejarque I, Tembl J, Corella D, Laiz B. Hyperhomocysteinemia, obesity and cryptogenic stroke. *Clin Hemorheol Microcirc*. 2011;47(1):53-58. doi:10.3233/CH-2010-1365
826. Narin F, Atabek ME, Karakukcu M, et al. The association of plasma homocysteine levels with serum leptin and apolipoprotein B levels in childhood obesity. *Ann Saudi Med*. 2005;25(3):209-214. doi:10.5144/0256-4947.2005.209
827. Yun KU, Ryu CS, Oh JM, et al. Plasma homocysteine level and hepatic sulfur amino acid metabolism in mice fed a high-fat diet. *Eur J Nutr*. 2013;52(1):127-134. doi:10.1007/s00394-011-0294-0
828. Kim YI, Miller JW, da Costa KA, et al. Severe folate deficiency causes secondary depletion of choline and phosphocholine in rat liver. *J Nutr*. 1994;124(11):2197-2203. doi:10.1093/jn/124.11.2197
829. da Silva RP, Kelly KB, Al Rajabi A, Jacobs RL. Novel insights on interactions between folate and lipid metabolism. *BioFactors*. 2014;40(3):277-283. doi:10.1002/biof.1154
830. Champier J, Claustrat F, Nazaret N, Fèvre Montange M, Claustrat B. Folate depletion changes gene expression of fatty acid metabolism, DNA synthesis, and circadian cycle in male mice. *Nutr Res*. 2012;32(2):124-132. doi:10.1016/j.nutres.2011.12.012
831. Akesson B, Fehling C, Jägerstad M, Stenram U. Effect of experimental folate deficiency on lipid metabolism in liver and brain. *Br J Nutr*. 1982;47(3):505-520. doi:10.1079/bjn19820063
832. Jacobs RL, Lingrell S, Zhao Y, Francis GA, Vance DE. Hepatic CTP:phosphocholine cytidylyltransferase-alpha is a critical predictor of plasma high density lipoprotein and very low density lipoprotein. *J Biol Chem*. 2008;283(4):2147-2155. doi:10.1074/jbc.M706628200
833. Zhao Y, Su B, Jacobs RL, et al. Lack of phosphatidylethanolamine N-methyltransferase alters plasma VLDL phospholipids and attenuates atherosclerosis in mice. *Arterioscler Thromb Vasc Biol*. 2009;29(9):1349-1355. doi:10.1161/ATVBAHA.109.188672
834. Vance DE. Physiological roles of phosphatidylethanolamine N-methyltransferase. *Biochim Biophys Acta*. 2013;1831(3):626-632. doi:10.1016/j.bbalip.2012.07.017
835. Cole LK, Vance JE, Vance DE. Phosphatidylcholine biosynthesis and lipoprotein metabolism. *Biochim Biophys Acta - Mol Cell Biol Lipids*. 2012;1821(5):754-761. doi:10.1016/j.bbalip.2011.09.009
836. Kanno K, Wu MK, Scapa EF, Roderick SL, Cohen DE. Structure and function of phosphatidylcholine transfer protein (PC-TP)/StarD2. *Biochim Biophys Acta*. 2007;1771(6):654-662. doi:10.1016/j.bbalip.2007.04.003
837. Wright MM, Howe AG, Zaremberg V. Cell membranes and apoptosis: role of cardiolipin, phosphatidylcholine, and anticancer lipid analogues. *Biochem Cell Biol*. 2004;82(1):18-26. doi:10.1139/o03-092
838. Murín R, Vidomanová E, Kowtharapu BS, Hatok J, Dobrota D. Role of S-adenosylmethionine cycle in carcinogenesis. *Gen Physiol Biophys*. 2017;36(5):513-520. doi:10.4149/gpb_2017031
839. Tremellen K. Oxidative stress and male infertility--a clinical perspective. *Hum*

Reprod Update. 2008;14(3):243-258. doi:10.1093/humupd/dmn004
840. Loft S, Kold-Jensen T, Hjollund NH, et al. Oxidative DNA damage in human sperm influences time to pregnancy. *Hum Reprod*. 2003;18(6):1265-1272. doi:10.1093/humrep/deg202
841. Spanò M, Bonde JP, Hjøllund HI, Kolstad HA, Cordelli E, Leter G. Sperm chromatin damage impairs human fertility. The Danish First Pregnancy Planner Study Team. *Fertil Steril*. 2000;73(1):43-50. doi:10.1016/s0015-0282(99)00462-8
842. Benchaib M, Braun V, Lornage J, et al. Sperm DNA fragmentation decreases the pregnancy rate in an assisted reproductive technique. *Hum Reprod*. 2003;18(5):1023-1028. doi:10.1093/humrep/deg228
843. Larson KL, DeJonge CJ, Barnes AM, Jost LK, Evenson DP. Sperm chromatin structure assay parameters as predictors of failed pregnancy following assisted reproductive techniques. *Hum Reprod*. 2000;15(8):1717-1722. doi:10.1093/humrep/15.8.1717
844. Bungum M, Humaidan P, Spano M, Jepson K, Bungum L, Giwercman A. The predictive value of sperm chromatin structure assay (SCSA) parameters for the outcome of intrauterine insemination, IVF and ICSI. *Hum Reprod*. 2004;19(6):1401-1408. doi:10.1093/humrep/deh280
845. Virro MR, Larson-Cook KL, Evenson DP. Sperm chromatin structure assay (SCSA) parameters are related to fertilization, blastocyst development, and ongoing pregnancy in in vitro fertilization and intracytoplasmic sperm injection cycles. *Fertil Steril*. 2004;81(5):1289-1295. doi:10.1016/j.fertnstert.2003.09.063
846. Borini A, Tarozzi N, Bizzaro D, et al. Sperm DNA fragmentation: paternal effect on early post-implantation embryo development in ART. *Hum Reprod*. 2006;21(11):2876-2881. doi:10.1093/humrep/del251
847. McPherson NO, Shehadeh H, Fullston T, Zander-Fox DL, Lane M. Dietary Micronutrient Supplementation for 12 Days in Obese Male Mice Restores Sperm Oxidative Stress. *Nutrients*. 2019;11(9):2196. doi:10.3390/nu11092196
848. J. Fujii, Y. Iuchi, S. Matsuki and TI. Cooperative function of antioxidant and redox systems against oxidative stress in male reproductive tissues. *Asian J Androl*. 2003;5(3):231-242.
849. Cadet J, Wagner JR. DNA base damage by reactive oxygen species, oxidizing agents, and UV radiation. *Cold Spring Harb Perspect Biol*. 2013;5(2). doi:10.1101/cshperspect.a012559
850. Isoda T, Nakatsu Y, Yamauchi K, et al. Abnormality in Wnt signaling is causatively associated with oxidative stress-induced intestinal tumorigenesis in MUTYH-null mice. *Int J Biol Sci*. 2014;10(8):940-947. doi:10.7150/ijbs.9241
851. Nakabeppu Y. Cellular levels of 8-oxoguanine in either DNA or the nucleotide pool play pivotal roles in carcinogenesis and survival of cancer cells. *Int J Mol Sci*. 2014;15(7):12543-12557. doi:10.3390/ijms150712543
852. Viel A, Bruselles A, Meccia E, et al. A Specific Mutational Signature Associated with DNA 8-Oxoguanine Persistence in MUTYH-defective Colorectal Cancer. *EBioMedicine*. 2017;20:39-49. doi:10.1016/j.ebiom.2017.04.022
853. Wells PG, McCallum GP, Chen CS, et al. Oxidative stress in developmental origins of disease: teratogenesis, neurodevelopmental deficits, and cancer. *Toxicol Sci*. 2009;108(1):4-18. doi:10.1093/toxsci/kfn263

854. Bosshard M, Markkanen E, van Loon B. Base excision repair in physiology and pathology of the central nervous system. *Int J Mol Sci*. 2012;13(12):16172-16222. doi:10.3390/ijms131216172
855. Hahm JY, Park J, Jang E-S, Chi SW. 8-Oxoguanine: from oxidative damage to epigenetic and epitranscriptional modification. *Exp Mol Med*. 2022;54(10):1626-1642. doi:10.1038/s12276-022-00822-z
856. Antoniali G, Lirussi L, D'Ambrosio C, et al. SIRT1 gene expression upon genotoxic damage is regulated by APE1 through nCaRE-promoter elements. *Mol Biol Cell*. 2014;25(4):532-547. doi:10.1091/mbc.E13-05-0286
857. Perillo B, Ombra MN, Bertoni A, et al. DNA oxidation as triggered by H3K9me2 demethylation drives estrogen-induced gene expression. *Science*. 2008;319(5860):202-206. doi:10.1126/science.1147674
858. Pan L, Zhu B, Hao W, et al. Oxidized Guanine Base Lesions Function in 8-Oxoguanine DNA Glycosylase-1-mediated Epigenetic Regulation of Nuclear Factor κB-driven Gene Expression. *J Biol Chem*. 2016;291(49):25553-25566. doi:10.1074/jbc.M116.751453
859. Pastukh V, Roberts JT, Clark DW, et al. An oxidative DNA "damage" and repair mechanism localized in the VEGF promoter is important for hypoxia-induced VEGF mRNA expression. *Am J Physiol Lung Cell Mol Physiol*. 2015;309(11):L1367-75. doi:10.1152/ajplung.00236.2015
860. Schäfer G, Cramer T, Suske G, Kemmner W, Wiedenmann B, Höcker M. Oxidative stress regulates vascular endothelial growth factor-A gene transcription through Sp1- and Sp3-dependent activation of two proximal GC-rich promoter elements. *J Biol Chem*. 2003;278(10):8190-8198. doi:10.1074/jbc.M211999200
861. Amente S, Bertoni A, Morano A, Lania L, Avvedimento E V, Majello B. LSD1-mediated demethylation of histone H3 lysine 4 triggers Myc-induced transcription. *Oncogene*. 2010;29(25):3691-3702. doi:10.1038/onc.2010.120
862. Yang S, Zhang J, Zhang Y, et al. KDM1A triggers androgen-induced miRNA transcription via H3K4me2 demethylation and DNA oxidation. *Prostate*. 2015;75(9):936-946. doi:10.1002/pros.22977
863. Weitzman SA, Turk PW, Milkowski DH, Kozlowski K. Free radical adducts induce alterations in DNA cytosine methylation. *Proc Natl Acad Sci U S A*. 1994;91(4):1261-1264. doi:10.1073/pnas.91.4.1261
864. Turk PW, Laayoun A, Smith SS, Weitzman SA. DNA adduct 8-hydroxyl-2'-deoxyguanosine (8-hydroxyguanine) affects function of human DNA methyltransferase. *Carcinogenesis*. 1995;16(5):1253-1255. doi:10.1093/carcin/16.5.1253
865. Maltseva D V, Baykov AA, Jeltsch A, Gromova ES. Impact of 7,8-dihydro-8-oxoguanine on methylation of the CpG site by Dnmt3a. *Biochemistry*. 2009;48(6):1361-1368. doi:10.1021/bi801947f
866. Valinluck V, Tsai H-H, Rogstad DK, Burdzy A, Bird A, Sowers LC. Oxidative damage to methyl-CpG sequences inhibits the binding of the methyl-CpG binding domain (MBD) of methyl-CpG binding protein 2 (MeCP2). *Nucleic Acids Res*. 2004;32(14):4100-4108. doi:10.1093/nar/gkh739
867. Zhou X, Zhuang Z, Wang W, et al. OGG1 is essential in oxidative stress induced DNA demethylation. *Cell Signal*. 2016;28(9):1163-1171.

doi:10.1016/j.cellsig.2016.05.021
868. Wu J, Mckeague M, Sturla SJ. Nucleotide-Resolution Genome-Wide Mapping of Oxidative DNA Damage by Click-Code-Seq. *J Am Chem Soc*. 2018;140:9783-9787. doi:10.1021/jacs.8b03715
869. Brueckner L, Zhao PA, van Schaik T, et al. Local rewiring of genome–nuclear lamina interactions by transcription. *EMBO J*. 2020;39(6):e103159. doi:https://doi.org/10.15252/embj.2019103159
870. Yoshihara M, Jiang L, Akatsuka S, Suyama M, Toyokuni S. Genome-wide profiling of 8-oxoguanine reveals its association with spatial positioning in nucleus. *DNA Res an Int J rapid Publ reports genes genomes*. 2014;21(6):603-612. doi:10.1093/dnares/dsu023
871. Xavier MJ, Nixon B, Roman SD, Scott RJ, Drevet JR, Aitken RJ. Paternal impacts on development: identification of genomic regions vulnerable to oxidative DNA damage in human spermatozoa. *Hum Reprod*. 2019;34(10):1876-1890. doi:10.1093/humrep/dez153
872. Xavier MJ, Nixon B, Roman SD, Aitken RJ. Improved methods of DNA extraction from human spermatozoa that mitigate experimentally-induced oxidative DNA damage. *PLoS One*. 2018;13(3):e0195003-e0195003. doi:10.1371/journal.pone.0195003
873. Lambert SA, Jolma A, Campitelli LF, et al. The Human Transcription Factors. *Cell*. 2018;172(4):650-665. doi:10.1016/j.cell.2018.01.029
874. Héberlé É, Bardet AF. Sensitivity of transcription factors to DNA methylation. *Essays Biochem*. 2019;63(6):727-741. doi:10.1042/EBC20190033
875. Plaschka C, Nozawa K, Cramer P. Mediator Architecture and RNA Polymerase II Interaction. *J Mol Biol*. 2016;428(12):2569-2574. doi:10.1016/j.jmb.2016.01.028
876. Slattery M, Zhou T, Yang L, Dantas Machado AC, Gordân R, Rohs R. Absence of a simple code: how transcription factors read the genome. *Trends Biochem Sci*. 2014;39(9):381-399. doi:10.1016/j.tibs.2014.07.002
877. Bell O, Tiwari VK, Thomä NH, Schübeler D. Determinants and dynamics of genome accessibility. *Nat Rev Genet*. 2011;12(8):554-564. doi:10.1038/nrg3017
878. Aytes A, Mitrofanova A, Kinkade CW, et al. ETV4 promotes metastasis in response to activation of PI3-kinase and Ras signaling in a mouse model of advanced prostate cancer. *Proc Natl Acad Sci U S A*. 2013;110(37):E3506-15. doi:10.1073/pnas.1303558110
879. Tyagi N, Deshmukh SK, Srivastava SK, et al. ETV4 Facilitates Cell-Cycle Progression in Pancreatic Cells through Transcriptional Regulation of Cyclin D1. *Mol Cancer Res*. 2018;16(2):187-196. doi:10.1158/1541-7786.MCR-17-0219
880. Dumortier M, Ladam F, Damour I, et al. ETV4 transcription factor and MMP13 metalloprotease are interplaying actors of breast tumorigenesis. *Breast Cancer Res*. 2018;20(1):73. doi:10.1186/s13058-018-0992-0
881. Xiao J, Yang S, Shen P, et al. Phosphorylation of ETV4 at Ser73 by ERK kinase could block ETV4 ubiquitination degradation in colorectal cancer. *Biochem Biophys Res Commun*. 2017;486(4):1062-1068. doi:https://doi.org/10.1016/j.bbrc.2017.03.163
882. Oh S, Shin S, Janknecht R. ETV1, 4 and 5: An oncogenic subfamily of ETS transcription factors. *Biochim Biophys Acta - Rev Cancer*. 2012;1826(1):1-12.

doi:https://doi.org/10.1016/j.bbcan.2012.02.002
883. Rodriguez AC, Vahrenkamp JM, Berrett KC, et al. ETV4 Is Necessary for Estrogen Signaling and Growth in Endometrial Cancer Cells. *Cancer Res*. 2020;80(6):1234-1245. doi:10.1158/0008-5472.CAN-19-1382
884. Singsuksawat E, Thuwajit C, Charngkaew K, Thuwajit P. Increased ETV4 expression correlates with estrogen-enhanced proliferation and invasiveness of cholangiocarcinoma cells. *Cancer Cell Int*. 2018;18:25. doi:10.1186/s12935-018-0525-z
885. Marchand GB, Carreau A-M, Weisnagel SJ, et al. Increased body fat mass explains the positive association between circulating estradiol and insulin resistance in postmenopausal women. *Am J Physiol Metab*. 2017;314(5):E448-E456. doi:10.1152/ajpendo.00293.2017
886. Oh H, Coburn SB, Matthews CE, et al. Anthropometric measures and serum estrogen metabolism in postmenopausal women: the Women's Health Initiative Observational Study. *Breast Cancer Res*. 2017;19(1):28. doi:10.1186/s13058-017-0810-0
887. Currie SL, Doane JJ, Evans KS, et al. ETV4 and AP1 Transcription Factors Form Multivalent Interactions with three Sites on the MED25 Activator-Interacting Domain. *J Mol Biol*. 2017;429(20):2975-2995. doi:https://doi.org/10.1016/j.jmb.2017.06.024
888. Jeronimo C, Robert F. The Mediator Complex: At the Nexus of RNA Polymerase II Transcription. *Trends Cell Biol*. 2017;27(10):765-783. doi:10.1016/j.tcb.2017.07.001
889. Englert NA, Luo G, Goldstein JA, Surapureddi S. Epigenetic modification of histone 3 lysine 27: mediator subunit MED25 is required for the dissociation of polycomb repressive complex 2 from the promoter of cytochrome P450 2C9. *J Biol Chem*. 2015;290(4):2264-2278. doi:10.1074/jbc.M114.579474
890. Niopek K, Üstünel BE, Seitz S, et al. A Hepatic GAbp-AMPK Axis Links Inflammatory Signaling to Systemic Vascular Damage. *Cell Rep*. 2017;20(6):1422-1434. doi:https://doi.org/10.1016/j.celrep.2017.07.023
891. Goto S, Takahashi M, Yasutsune N, et al. Identification of GA-Binding Protein Transcription Factor Alpha Subunit (GABPA) as a Novel Bookmarking Factor. *Int J Mol Sci*. 2019;20(5):1093. doi:10.3390/ijms20051093
892. Wu H, Xiao Y, Zhang S, et al. The Ets transcription factor GABP is a component of the hippo pathway essential for growth and antioxidant defense. *Cell Rep*. 2013;3(5):1663-1677. doi:10.1016/j.celrep.2013.04.020
893. Hollenhorst PC, Jones DA, Graves BJ. Expression profiles frame the promoter specificity dilemma of the ETS family of transcription factors. *Nucleic Acids Res*. 2004;32(18):5693-5702. doi:10.1093/nar/gkh906
894. Liu F, Walmsley M, Rodaway A, Patient R. Fli1 Acts at the Top of the Transcriptional Network Driving Blood and Endothelial Development. *Curr Biol*. 2008;18(16):1234-1240. doi:https://doi.org/10.1016/j.cub.2008.07.048
895. Ferdous A, Singh S, Luo Y, et al. Fli1 Promotes Vascular Morphogenesis by Regulating Endothelial Potential of Multipotent Myogenic Progenitors. *Circ Res*. 2021;129(10):949-964. doi:10.1161/CIRCRESAHA.121.318986
896. Dejosez M, Levine SS, Frampton GM, et al. Ronin/Hcf-1 binds to a

hyperconserved enhancer element and regulates genes involved in the growth of embryonic stem cells. *Genes Dev*. 2010;24(14):1479-1484. doi:10.1101/gad.1935210
897. Fujita J, Freire P, Coarfa C, et al. Ronin Governs Early Heart Development by Controlling Core Gene Expression Programs. *Cell Rep*. 2017;21(6):1562-1573. doi:https://doi.org/10.1016/j.celrep.2017.10.036
898. Policarpi C, Munafò M, Tsagkris S, Carlini V, Hackett JA. Systematic Epigenome Editing Captures the Context-dependent Instructive Function of Chromatin Modifications. *bioRxiv*. January 2022:2022.09.04.506519. doi:10.1101/2022.09.04.506519
899. Ryu H, Lee J, Zaman K, et al. Sp1 and Sp3 are oxidative stress-inducible, antideath transcription factors in cortical neurons. *J Neurosci*. 2003;23(9):3597-3606. doi:10.1523/JNEUROSCI.23-09-03597.2003
900. Wei-Guo Z, Kanur S, Zunyan D, et al. Methylation of Adjacent CpG Sites Affects Sp1/Sp3 Binding and Activity in the p21Cip1 Promoter. *Mol Cell Biol*. 2003;23(12):4056-4065. doi:10.1128/MCB.23.12.4056-4065.2003
901. Tan NY, Khachigian LM. Sp1 phosphorylation and its regulation of gene transcription. *Mol Cell Biol*. 2009;29(10):2483-2488. doi:10.1128/MCB.01828-08
902. Swift ML, Beishline K, Azizkhan-Clifford J. Sp1-dependent recruitment of the histone acetylase p300 to DSBs facilitates chromatin remodeling and recruitment of the NHEJ repair factor Ku70. *DNA Repair (Amst)*. 2021;105:103171. doi:https://doi.org/10.1016/j.dnarep.2021.103171
903. Deshane J, Kim J, Bolisetty S, Hock TD, Hill-Kapturczak N, Agarwal A. Sp1 regulates chromatin looping between an intronic enhancer and distal promoter of the human heme oxygenase-1 gene in renal cells. *J Biol Chem*. 2010;285(22):16476-16486. doi:10.1074/jbc.M109.058586
904. Hao N, Xin H, Shi X, et al. Paternal reprogramming-escape histone H3K4me3 marks located within promoters of RNA splicing genes. *Bioinformatics*. 2021;37(8):1039-1044. doi:10.1093/bioinformatics/btaa920
905. Bromfield JJ, Schjenken JE, Chin PY, Care AS, Jasper MJ, Robertson SA. Maternal tract factors contribute to paternal seminal fluid impact on metabolic phenotype in offspring. *Proc Natl Acad Sci U S A*. 2014;111(6):2200-2205. doi:10.1073/pnas.1305609111
906. Robertson SA. Seminal plasma and male factor signalling in the female reproductive tract. *Cell Tissue Res*. 2005;322(1):43-52. doi:10.1007/s00441-005-1127-3
907. Wong CL, Lee KH, Lo KM, et al. Ablation of paternal accessory sex glands imparts physical and behavioural abnormalities to the progeny: An in vivo study in the golden hamster. *Theriogenology*. 2007;68(4):654-662. doi:https://doi.org/10.1016/j.theriogenology.2007.04.062
908. Lane M, Robker RL, Robertson SA. Parenting from before conception. *Science (80-)*. 2014;345(6198):756-760. doi:10.1126/science.1254400
909. Schjenken JE, Moldenhauer LM, Sharkey DJ, et al. High-fat Diet Alters Male Seminal Plasma Composition to Impair Female Immune Adaptation for Pregnancy in Mice. *Endocrinology*. 2021;162(10). doi:10.1210/endocr/bqab123
910. Binder NK, Sheedy JR, Hannan NJ, Gardner DK. Male obesity is associated with

changed spermatozoa Cox4i1 mRNA level and altered seminal vesicle fluid composition in a mouse model. *Mol Hum Reprod*. 2015;21(5):424-434. doi:10.1093/molehr/gav010
911. Thomas S, Kratzsch D, Schaab M, et al. Seminal plasma adipokine levels are correlated with functional characteristics of spermatozoa. *Fertil Steril*. 2013;99(5):1256-1263.e3. doi:10.1016/j.fertnstert.2012.12.022
912. Lotti F, Corona G, Colpi GM, et al. Elevated body mass index correlates with higher seminal plasma interleukin 8 levels and ultrasonographic abnormalities of the prostate in men attending an andrology clinic for infertility. *J Endocrinol Invest*. 2011;34(10):e336-e342. doi:10.3275/7855
913. Martini AC, Tissera A, Estofán D, et al. Overweight and seminal quality: a study of 794 patients. *Fertil Steril*. 2010;94(5):1739-1743. doi:10.1016/j.fertnstert.2009.11.017
914. Eisenberg ML, Kim S, Chen Z, Sundaram R, Schisterman EF, Buck Louis GM. The relationship between male BMI and waist circumference on semen quality: data from the LIFE study. *Hum Reprod*. 2014;29(2):193-200. doi:10.1093/humrep/det428
915. Murphy PJ, Guo J, Jenkins TG, et al. NRF2 loss recapitulates heritable impacts of paternal cigarette smoke exposure. *PLoS Genet*. 2020;16(6):e1008756. doi:10.1371/journal.pgen.1008756
916. Simon MM, Greenaway S, White JK, et al. A comparative phenotypic and genomic analysis of C57BL/6J and C57BL/6N mouse strains. *Genome Biol*. 2013;14(7):1-22. doi:10.1186/gb-2013-14-7-r82
917. Li J, Wu H, Liu Y, Yang L. High fat diet induced obesity model using four strainsof mice: Kunming, C57BL/6, BALB/c and ICR. *Exp Anim*. 2020;69(3):326-335. doi:10.1538/expanim.19-0148
918. Mekada K, Abe K, Murakami A, et al. Genetic Differences among C57BL/6 Substrains. *Exp Anim*. 2009;58(2):141-149. doi:10.1538/expanim.58.141
919. Enríquez JA. Mind your mouse strain. *Nat Metab*. 2019;1(January):5-7. doi:10.1038/s42255-018-0018-3
920. Montgomery MK, Hallahan NL, Brown SH, et al. Mouse strain-dependent variation in obesity and glucose homeostasis in response to high-fat feeding. *Diabetologia*. 2013;56(5):1129-1139. doi:10.1007/s00125-013-2846-8
921. Reynolds TH, Dalton A, Calzini L, Tuluca A, Hoyte D, Ives SJ. The impact of age and sex on body composition and glucose sensitivity in C57BL/6J mice. *Physiol Rep*. 2019;7(3):e13995-e13995. doi:10.14814/phy2.13995
922. Hu S, Wang L, Yang D, et al. Dietary Fat, but Not Protein or Carbohydrate, Regulates Energy Intake and Causes Adiposity in Mice. *Cell Metab*. 2018:415-431. doi:10.1016/j.cmet.2018.06.010
923. Ayala JE, Samuel VT, Morton GJ, et al. Standard operating procedures for describing and performing metabolic tests of glucose homeostasis in mice. *Dis Model Mech*. 2010;3(9-10):525-534. doi:10.1242/dmm.006239
924. Kleinert M, Clemmensen C, Hofmann SM, et al. Animal models of obesity and diabetes mellitus. *Nat Rev Endocrinol*. 2018;14(3):140-162. doi:10.1038/nrendo.2017.161
925. NCD Risk Factor Collaboration (NCD-RisC). Trends in adult body-mass index in

200 countries from 1975 to 2014: a pooled analysis of 1698 population-based measurement studies with 19·2 million participants. *Lancet (London, England)*. 2016;387(10026):1377-1396. doi:10.1016/S0140-6736(16)30054-X
926. Kautzky-Willer A, Harreiter J, Pacini G. Sex and Gender Differences in Risk, Pathophysiology and Complications of Type 2 Diabetes Mellitus. *Endocr Rev*. 2016;37(3):278-316. doi:10.1210/er.2015-1137
927. Lee M-J, Wu Y, Fried SK. Adipose tissue heterogeneity: implication of depot differences in adipose tissue for obesity complications. *Mol Aspects Med*. 2013;34(1):1-11. doi:10.1016/j.mam.2012.10.001
928. Clegg DJ, Riedy CA, Smith KAB, Benoit SC, Woods SC. Differential sensitivity to central leptin and insulin in male and female rats. *Diabetes*. 2003;52(3):682-687. doi:10.2337/diabetes.52.3.682
929. Macotela Y, Boucher J, Tran TT, Kahn CR. Sex and depot differences in adipocyte insulin sensitivity and glucose metabolism. *Diabetes*. 2009;58(4):803-812. doi:10.2337/db08-1054
930. Jeffery E, Wing A, Holtrup B, et al. The Adipose Tissue Microenvironment Regulates Depot-Specific Adipogenesis in Obesity. *Cell Metab*. 2016;24(1):142-150. doi:10.1016/j.cmet.2016.05.012
931. Stubbins RE, Holcomb VB, Hong J, Núñez NP. Estrogen modulates abdominal adiposity and protects female mice from obesity and impaired glucose tolerance. *Eur J Nutr*. 2012;51(7):861-870. doi:10.1007/s00394-011-0266-4
932. Clegg DJ, Brown LM, Woods SC, Benoit SC. Gonadal hormones determine sensitivity to central leptin and insulin. *Diabetes*. 2006;55(4):978-987. doi:10.2337/diabetes.55.04.06.db05-1339
933. Gegenhuber B, Wu M V, Bronstein R, Tollkuhn J. Gene regulation by gonadal hormone receptors underlies brain sex differences. *Nature*. 2022;606(7912):153-159. doi:10.1038/s41586-022-04686-1
934. Krause WC, Rodriguez R, Gegenhuber B, et al. Oestrogen engages brain MC4R signalling to drive physical activity in female mice. *Nature*. 2021;599(7883):131-135. doi:10.1038/s41586-021-04010-3
935. Gao A, Su J, Liu R, et al. Sexual dimorphism in glucose metabolism is shaped by androgen-driven gut microbiome. *Nat Commun*. 2021;12(1):7080. doi:10.1038/s41467-021-27187-7
936. Beck D, Sadler-Riggleman I, Skinner MK. Generational comparisons (F1 versus F3) of vinclozolin induced epigenetic transgenerational inheritance of sperm differential DNA methylation regions (epimutations) using MeDIP-Seq. *Environ epigenetics*. 2017;3(3). doi:10.1093/eep/dvx016
937. Klosin A, Casas E, Hidalgo-Carcedo C, Vavouri T, Lehner B. Transgenerational transmission of environmental information in *C. elegans*. *Science (80-)*. 2017;356(6335):320-323. doi:10.1126/science.aah6412
938. Ni JZ, Kalinava N, Chen E, Huang A, Trinh T, Gu SG. A transgenerational role of the germline nuclear RNAi pathway in repressing heat stress-induced transcriptional activation in C. elegans. *Epigenetics Chromatin*. 2016;9(1):3. doi:10.1186/s13072-016-0052-x
939. Preguiça I, Alves A, Nunes S, et al. Diet-induced rodent models of obesity-related metabolic disorders—A guide to a translational perspective. *Obes Rev*.

2020;21(12):e13081. doi:https://doi.org/10.1111/obr.13081
940. Hintze KJ, Benninghoff AD, Cho CE, Ward RE. Modeling the Western Diet for Preclinical Investigations. *Adv Nutr*. 2018;9(3):263-271. doi:10.1093/advances/nmy002
941. US Department of Agriculture ARS. Nutrient intakes from food and beverages: mean amounts consumed per individual, by gender and age. *What We Eat Am 2014*. 2011.
942. Lau JKC, Zhang X, Yu J. Animal models of non-alcoholic fatty liver disease: current perspectives and recent advances. *J Pathol*. 2017;241(1):36-44. doi:10.1002/path.4829
943. Rothwell NJ, Stock MJ. The cafeteria diet as a tool for studies of thermogenesis. *J Nutr*. 1988;118(8):925-928. doi:10.1093/jn/118.8.925
944. Moore BJ. The cafeteria diet--an inappropriate tool for studies of thermogenesis. *J Nutr*. 1987;117(2):227-231. doi:10.1093/jn/117.2.227
945. Ibrahim SH, Hirsova P, Malhi H, Gores GJ. Animal Models of Nonalcoholic Steatohepatitis: Eat, Delete, and Inflame. *Dig Dis Sci*. 2016;61(5):1325-1336. doi:10.1007/s10620-015-3977-1
946. Stott NL, Marino JS. High Fat Rodent Models of Type 2 Diabetes: From Rodent to Human. *Nutrients*. 2020;12(12):3650. doi:10.3390/nu12123650
947. Small L, Ehrlich A, Iversen J, et al. Comparative analysis of oral and intraperitoneal glucose tolerance tests in mice. *Mol Metab*. 2022;57:101440. doi:10.1016/j.molmet.2022.101440
948. Benedé-Ubieto R, Estévez-Vázquez O, Ramadori P, Cubero FJ, Nevzorova YA. Guidelines and Considerations for Metabolic Tolerance Tests in Mice. *Diabetes Metab Syndr Obes*. 2020;13:439-450. doi:10.2147/DMSO.S234665
949. Gargiulo S, Gramanzini M, Megna R, et al. Evaluation of growth patterns and body composition in c57bl/6j mice using dual energy x-ray absorptiometry. *Biomed Res Int*. 2014;2014. doi:10.1155/2014/253067
950. Liang W, Menke AL, Driessen A, et al. Establishment of a general NAFLD scoring system for rodent models and comparison to human liver pathology. *PLoS One*. 2014;9(12):1-17. doi:10.1371/journal.pone.0115922
951. MacParland SA, Liu JC, Ma X-Z, et al. Single cell RNA sequencing of human liver reveals distinct intrahepatic macrophage populations. *Nat Commun*. 2018;9(1):4383. doi:10.1038/s41467-018-06318-7
952. Alvarez M, Benhammou JN, Darci-Maher N, et al. Human liver single nucleus and single cell RNA sequencing identify a hepatocellular carcinoma-associated cell-type affecting survival. *Genome Med*. 2022;14(1):50. doi:10.1186/s13073-022-01055-5
953. Hildebrandt F, Andersson A, Saarenpää S, et al. Spatial Transcriptomics to define transcriptional patterns of zonation and structural components in the mouse liver. *Nat Commun*. 2021;12(1):7046. doi:10.1038/s41467-021-27354-w
954. Shah RN, Grzybowski AT, Cornett EM, et al. Examining the Roles of H3K4 Methylation States with Systematically Characterized Antibodies. *Mol Cell*. 2018;72(1):162-177.e7. doi:10.1016/j.molcel.2018.08.015
955. Kaya-Okur HS, Wu SJ, Codomo CA, et al. CUT&Tag for efficient epigenomic profiling of small samples and single cells. *Nat Commun*. 2019;10(1):1930.

doi:10.1038/s41467-019-09982-5
956. Skene PJ, Henikoff JG, Henikoff S. Targeted in situ genome-wide profiling with high efficiency for low cell numbers. *Nat Protoc*. 2018;13(5):1006-1019. doi:10.1038/nprot.2018.015
957. Wang M, Zhang Y. Tn5 transposase-based epigenomic profiling methods are prone to open chromatin bias. *bioRxiv*. January 2021:2021.07.09.451758. doi:10.1101/2021.07.09.451758
958. Ma X, Fan Y, Xiao W, Ding X, Hu W, Xia Y. Glufosinate-Ammonium Induced Aberrant Histone Modifications in Mouse Sperm Are Concordant With Transcriptome in Preimplantation Embryos. *Front Physiol*. 2021;12:819856. doi:10.3389/fphys.2021.819856
959. Gopalan S, Wang Y, Harper NW, Garber M, Fazzio TG. Simultaneous profiling of multiple chromatin proteins in the same cells. *Mol Cell*. 2021. doi:https://doi.org/10.1016/j.molcel.2021.09.019
960. Gopalan S, Fazzio TG. Multi-CUT&Tag to simultaneously profile multiple chromatin factors. *STAR Protoc*. 2022;3(1):101100. doi:10.1016/j.xpro.2021.101100
961. Pique-Regi R, Romero R, Tarca AL, et al. Single cell transcriptional signatures of the human placenta in term and preterm parturition. *Elife*. 2019;8:1-22. doi:10.7554/eLife.52004
962. Nelson AC, Mould AW, Bikoff EK, Robertson EJ. Single-cell RNA-seq reveals cell type-specific transcriptional signatures at the maternal-foetal interface during pregnancy. *Nat Commun*. 2016;7. doi:10.1038/ncomms11414
963. Marsh B, Blelloch R. Single nuclei RNA-seq of mouse placental labyrinth development. *Elife*. 2020;9:1-27. doi:10.7554/eLife.60266
964. Liu Y, Fan X, Wang R, et al. Single-cell RNA-seq reveals the diversity of trophoblast subtypes and patterns of differentiation in the human placenta. *Cell Res*. 2018;28(8):819-832. doi:10.1038/s41422-018-0066-y
965. Campbell KA, Colacino JA, Puttabyatappa M, et al. Placental gene expression-based cell type deconvolution: Cell proportions drive preeclampsia gene expression differences. *bioRxiv*. 2021:2021.07.29.454041. https://www.biorxiv.org/content/10.1101/2021.07.29.454041v2%0Ahttps://www.biorxiv.org/content/10.1101/2021.07.29.454041v2.abstract.
966. Zhou X, Xu Y, Ren S, et al. Single-cell RNA-seq revealed diverse cell types in the mouse placenta at mid-gestation. *Exp Cell Res*. 2021;405(2):112715. doi:https://doi.org/10.1016/j.yexcr.2021.112715
967. Garcia-Flores V, Xu Y, Pusod E, Romero R, Pique-Regi R, Gomez-Lopez N. Preparation of single-cell suspensions from the human placenta. *Nat Protoc*. 2022. doi:10.1038/s41596-022-00772-w
968. Soares MJ, Varberg KM, Iqbal K. Hemochorial placentation: development, function, and adaptations†. *Biol Reprod*. 2018;99(1):196-211. doi:10.1093/biolre/ioy049
969. Burton GJ, Watson AL, Hempstock J, Skepper JN, Jauniaux E. Uterine glands provide histiotrophic nutrition for the human fetus during the first trimester of pregnancy. *J Clin Endocrinol Metab*. 2002;87(6):2954-2959. doi:10.1210/jcem.87.6.8563

970. Burton GJ, Jauniaux E, Watson AL. Maternal arterial connections to the placental intervillous space during the first trimester of human pregnancy: the Boyd collection revisited. *Am J Obstet Gynecol*. 1999;181(3):718-724. doi:10.1016/s0002-9378(99)70518-1
971. Knöfler M, Haider S, Saleh L, Pollheimer J, Gamage TKJB, James J. Human placenta and trophoblast development: key molecular mechanisms and model systems. *Cell Mol Life Sci*. 2019;76(18):3479-3496. doi:10.1007/s00018-019-03104-6
972. James JL, Carter AM, Chamley LW. Human placentation from nidation to 5 weeks of gestation. Part I: What do we know about formative placental development following implantation? *Placenta*. 2012;33(5):327-334. doi:10.1016/j.placenta.2012.01.020
973. Hu D, Cross JC. Development and function of trophoblast giant cells in the rodent placenta. *Int J Dev Biol*. 2010;54(2-3):341-354. doi:10.1387/ijdb.082768dh
974. Weier JF, Weier H-UG, Jung CJ, et al. Human cytotrophoblasts acquire aneuploidies as they differentiate to an invasive phenotype. *Dev Biol*. 2005;279(2):420-432. doi:10.1016/j.ydbio.2004.12.035
975. Kunath T, Yamanaka Y, Detmar J, et al. Developmental differences in the expression of FGF receptors between human and mouse embryos. *Placenta*. 2014;35(12):1079-1088. doi:10.1016/j.placenta.2014.09.008
976. Latos PA, Goncalves A, Oxley D, Mohammed H, Turro E, Hemberger M. Fgf and Esrrb integrate epigenetic and transcriptional networks that regulate self-renewal of trophoblast stem cells. *Nat Commun*. 2015;6:7776. doi:10.1038/ncomms8776
977. Adachi K, Nikaido I, Ohta H, et al. Context-dependent wiring of Sox2 regulatory networks for self-renewal of embryonic and trophoblast stem cells. *Mol Cell*. 2013;52(3):380-392. doi:10.1016/j.molcel.2013.09.002
978. Soncin F, Khater M, To C, et al. Comparative analysis of mouse and human placentae across gestation reveals species-specific regulators of placental development. *Development*. 2018;145(2). doi:10.1242/dev.156273
979. Blakeley P, Fogarty NME, del Valle I, et al. Defining the three cell lineages of the human blastocyst by single-cell RNA-seq. *Development*. 2015;142(18):3151-3165. doi:10.1242/dev.123547
980. Okae H, Toh H, Sato T, et al. Derivation of Human Trophoblast Stem Cells. *Cell Stem Cell*. 2018;22(1):50-63.e6. doi:10.1016/j.stem.2017.11.004
981. McPherson NO, Owens JA, Fullston T, Lane M. Preconception diet or exercise intervention in obese fathers normalizes sperm microRNA profile and metabolic syndrome in female offspring. *Am J Physiol Endocrinol Metab*. 2015;308(9):E805-21. doi:10.1152/ajpendo.00013.2015
982. McPherson NO, Bakos HW, Owens JA, Setchell BP, Lane M. Improving metabolic health in obese male mice via diet and exercise restores embryo development and fetal growth. *PLoS One*. 2013;8(8):e71459. doi:10.1371/journal.pone.0071459
983. Zheng J, Alves-Wagner AB, Stanford KI, et al. Maternal and paternal exercise regulate offspring metabolic health and beta cell phenotype. *BMJ open diabetes Res care*. 2020;8(1). doi:10.1136/bmjdrc-2019-000890
984. Billah MM, Khatiwada S, Morris MJ, Maloney CA. Effects of paternal overnutrition

and interventions on future generations. *Int J Obes*. 2022;46(5):901-917. doi:10.1038/s41366-021-01042-7
985. Gu B, Lee MG. Histone H3 lysine 4 methyltransferases and demethylases in self-renewal anddifferentiation of stem cells. *Cell Biosci*. 2013;3(1):39. doi:10.1186/2045-3701-3-39
986. Guo H, Zhu P, Guo F, et al. Profiling DNA methylome landscapes of mammalian cells with single-cell reduced-representation bisulfite sequencing. *Nat Protoc*. 2015;10(5):645-659. doi:10.1038/nprot.2015.039
987. Zhu P, Guo H, Ren Y, et al. Single-cell DNA methylome sequencing of human preimplantation embryos. *Nat Genet*. 2018;50(1):12-19. doi:10.1038/s41588-017-0007-6
988. Andersen E, Clark S, Ingerslev L, Lundell L, Reik W, Barrès R. Single-cell bisulfite sequencing of spermatozoa from lean and obese humans reveals potential for the transmission of epimutations. *bioRxiv*. January 2021:2021.07.09.451752. doi:10.1101/2021.07.09.451752
989. P E de Souza C, Andronescu M, Masud T, et al. Epiclomal: Probabilistic clustering of sparse single-cell DNA methylation data. *PLoS Comput Biol*. 2020;16(9):e1008270. doi:10.1371/journal.pcbi.1008270
990. Liu Y, Siejka-Zielińska P, Velikova G, et al. Bisulfite-free direct detection of 5-methylcytosine and 5-hydroxymethylcytosine at base resolution. *Nat Biotechnol*. 2019;37(4):424-429. doi:10.1038/s41587-019-0041-2
991. D'Errico JN, Fournier SB, Stapleton PA. Considering Intrauterine Location in a Model of Fetal Growth Restriction After Maternal Titanium Dioxide Nanoparticle Inhalation. *Front Toxicol*. 2021;3. doi:10.3389/ftox.2021.643804
992. Keane TM, Goodstadt L, Danecek P, et al. Mouse genomic variation and its effect on phenotypes and gene regulation. *Nature*. 2011;477(7364):289-294. doi:10.1038/nature10413
993. Petropoulos S, Edsgärd D, Reinius B, et al. Single-Cell RNA-Seq Reveals Lineage and X Chromosome Dynamics in Human Preimplantation Embryos. *Cell*. 2016;165(4):1012-1026. doi:10.1016/j.cell.2016.03.023